P
Univ.
I

NEW SERIES No. 84 JANUARY 1, 1925

UNIVERSITY OF IOWA STUDIES

LIBRARY
Exchange
AUG 20 1925
UNIVERSITY OF TORONTO

STUDIES IN PHYSICS

VOLUME II NUMBER 3

CONTRIBUTIONS FROM THE PHYSICAL LABORATORY

PUBLISHED BY THE UNIVERSITY, IOWA CITY, IOWA

Issued semi-monthly throughout the year. Entered at the post office at Iowa City as second class mail matter. Acceptance for mailing at special rate of postage provided for in Section 1103, Act of October 3, 1917, authorized on July 3, 1918.

75-4

Digitized by the Internet Archive
in 2008 with funding from
Microsoft Corporation

http://www.archive.org/details/studiesinphysnew84iowauoft

UNIVERSITY OF IOWA STUDIES IN PHYSICS

GEORGE WALTER STEWART, *Editor*

CONTINUATION OF CONTRIBUTIONS FROM THE PHYSICAL LABORATORY OF THE STATE UNIVERSITY OF IOWA

VOLUME II NUMBER 3

CONTRIBUTIONS FROM THE PHYSICAL LABORATORY

PUBLISHED BY THE UNIVERSITY, IOWA CITY

CONTENTS

1. *A new tone generator* C. W. Hewlett
   Reprinted from The Physical Review, N. S., Vol. XIX, No. 1, 1922.

2. *The crystelliptometer, an instrument for the polariscopic analysis of very slender beams of light* Le Roy D. Weld
   Reprinted from the Journal of the Optical Society of America and Review of Scientific Instruments, Vol. VI, No. 1, 1922.

3. *On the optical constants of selenium in the form of isolated crystals* L. P. Sieg
   Reprinted from the Journal of the Optical Society of America and Review of Scientific Instruments, Vol. VI, 1922.

4. *The path of a rigid electron which moves in a magnetic field of constant strength rotating with constant angular velocity* E. O. Hulburt
   Reprinted from The Physical Review, N. S., Vol. XIX, No. 4, 1922.

5. *Minimum sound energy for audition for tones of high frequency* C. E. Lane
   Reprinted from The Physical Review, N. S., Vol. XIX, No. 5, 1922.

6. *The broadening of the Balmer lines of hydrogen with pressure* E. O. Hulburt
   Reprinted from The Astrophysical Journal, Vol. LV, No. 5, 1922.

7. *Hall effect and specific resistance of silver films* G. R. Wait
   Reprinted from The Physical Review, N. S., Vol. XIX, No. 6, 1922.

8. *The simple rigidity of a drawn tungsten wire at incandescent temperatures* William Schriever
   Reprinted from The Physical Review, Vol. XX, No. 1, 1922, p. 96.

9. *The optical constants of isolated tellurium crystals* George Dewey Van Dyke
   Reprinted from the Journal of the Optical Society of America and Review of Scientific Instruments, Vol. VI, No. 9, 1922.

10. *An experimental study of the scattering of approximately homogeneous x-rays by powdered crystalline carbon, metallic lithium, and liquid benzene, mesitylene, and octane* C. W. Hewlett
    Reprinted from The Physical Review, S. S., Vol. XX, No. 6, 1922.

11. *A telephone receiver and transmitter* C. W. Hewlett
    Reprinted from the Journal of the Optical Society of America and Review of Scientific Instruments, Vol. VI, No. 10, 1922.

12. *Acoustic wave filters* G. W. Stewart
    Reprinted from The Physical Review, S. S., Vol. XX, No. 6, 1922.

13. *Hall effect and specific resistance of evaporated films of silver, copper and iron* J. C. Steinberg

Reprinted from The Physical Review, Vol. XXI, No. 1, 1923.

14. *Note on the principal reflecting powers of tellurium* L. P. Sieg

Reprinted from the Journal of the Optical Society of America and Review of Scientific Instruments, Vol. VII, No. 2, 1923.

15. *A simple prism spectrograph* E. O. Hulburt

Reprinted from the Journal of the Optical Society of America and Review of Scientific Instruments, Vol. VII, No. 2, 1923.

16. *The deflection of a stream of electrons by electromagnetic radiation* E. O. Hulburt

Reprinted from The Physical Review, Vol. XXI, No. 6, 1923.

17. *The distribution of intensity in the broadened Balmer lines of hydrogen* E. O. Hulburt

Reprinted from The Physical Review, Vol. XXII, No. 1, 1923.

18. *The torques and forces between short cylindrical coils carrying alternating currents of radio frequency* W. A. Parlin

Reprinted from The Physical Review, Vol. XXII, No. 2, 1923, pp. 193–197.

19. *Magnetic and natural rotatory dispersion in absorbing media* E. O. Hulburt

Reprinted from The Physical Review, Vol. XXII, No. 2, 1923, pp. 180–187.

20. *On super-regeneration* E. O. Hulburt

Reprinted from the Proceedings of the Institute of Radio Engineers, Vol. XI, 1923.

21. *Standards of capacity particularly for radio frequency currents* J. B. Dempster
E. O. Hulburt

Reprinted from the Proceedings of the Institute of Radio Engineers, Vol. XI, 1923, p. 399.

22. *A variable single band acoustic wave filter* G. W. Stewart

Reprinted from The Physical Review, Vol. XXII, No. 5, 1923, pp. 502–505.

23. *The effect of the material composing the sides of deep slits on the intrinsic intensity of light transmitted through the slits* Clarence R. Smith

Reprinted from the Journal of the Optical Society of America and Review of Scientific Instruments, Vol. VII, No. 12, 1923.

24. *Acoustic wave filters: attenuation and phase factors*
G. W. STEWART
Reprinted from THE PHYSICAL REVIEW, Vol. XXIII, No. 4, 1924, pp. 520–524.

25. *Predicted transmission curves of acoustic wave filters*
H. B. PEACOCK
Reprinted from THE PHYSICAL REVIEW, Vol. XXIII, No. 4, 1924, pp. 525–527.

26. *On the breadth of the hydrogen lines in stellar spectra*
E. O. HULBURT
Reprinted from THE ASTROPHYSICAL JOURNAL, Vol. LIX, No. 3, 1924.

27. *A simple audiofrequency mechanical alternator* C. J. LAPP
Reprinted from the JOURNAL OF THE OPTICAL SOCIETY OF AMERICA AND REVIEW OF SCIENTIFIC INSTRUMENTS, Vol. VIII, No. 5, 1924.

28. *A quartz spectrograph for wave lengths to 1850 A*
E. O. HULBURT
Reprinted from the JOURNAL OF THE OPTICAL SOCIETY OF AMERICA AND REVIEW OF SCIENTIFIC INSTRUMENTS, Vol. VIII, No. 5, 1924.

29. *The Balmer absorption series of hydrogen* E. O. HULBURT
Reprinted from THE PHYSICAL REVIEW, Vol. XXIII, No. 5, 1924, pp. 593–597.

30. *The K and L absorption and emission spectra of tungsten*
C. B. CROFUTT
Reprinted from THE PHYSICAL REVIEW, Vol. XXIV, No. 1, 1924, pp. 9–15.

31. *The absorption lines in the spectrum of the metallic spark in water* E. O. HULBURT
Reprinted from THE PHYSICAL REVIEW, Vol. XXIV, No. 2, 1924, pp. 129–133.

32. *Effect of temperature on the regular reflection of x-rays from aluminum foil* E. H. COLLINS
Reprinted from THE PHYSICAL REVIEW, Vol. XXIV, No. 2, 1924, pp. 152–157.

33. *The intrinsic intensity and polarization of light after passage through deep slits* L. P. SIEG
Reprinted from the JOURNAL OF THE OPTICAL SOCIETY OF AMERICA AND REVIEW OF SCIENTIFIC INSTRUMENTS, Vol. IX, No. 3, 1924.

34. *Acoustic wave filters in series* G. W. STEWART
Reprinted from the JOURNAL OF THE OPTICAL SOCIETY OF AMERICA AND REVIEW OF SCIENTIFIC INSTRUMENTS, Vol. IX, No. 5, 1924.

35. *Magnetic properties of thin films of ferromagnetic metals produced by the evaporation method* A. J. SORENSEN
Reprinted from THE PHYSICAL REVIEW, Vol. XXIV, No. 6, 1924, pp. 658–665.

A NEW TONE GENERATOR

By C. W. Hewlett.

[Reprinted from The Physical Review, N.S., Vol. XIX, No. 1, January, 1922.]

A NEW TONE GENERATOR.

By C. W. Hewlett.

Synopsis.

New Pure Tone Generator and Receiver of Sounds.—(1) *Construction and operation.* The instrument consists of a thin, non-magnetic, metallic diaphragm between two flat coils through which a constant direct current I_0 flows in such a way as to produce a radial magnetic field in the diaphragm; then when a simple harmonic alternating current I of the frequency $\omega/2\pi$ is superposed upon the direct current, circular currents are induced in the diaphragm, which thereupon is acted upon by a simple harmonic electrodynamic force and vibrates with the frequency of the alternating current. For low frequencies the electrodynamic force is approximately proportional to $\omega I_0 I \sin(\omega t + \theta)$ and the amplitude of vibration is approximately proportional to $I_0 I/\omega$. The absence of overtones is due to the absence of ferromagnetic material, and to the fact that the radial magnetic field is constant. The aperiodicity of the diaphragm renders the calculation of the performance of the instrument practicable, and eliminates distortion, due to resonance, in the wave form of the emitted sound when the instrument is excited by a complex alternating current. When used as a generator of pure tones, the coils were connected in the circuit of a thermionic oscillator whose frequency could be varied from 500 to 25,000 vibrations per second. When used as a receiver of sound, the current generated in the coils by the motion of the diaphragm is fed into a thermionic amplifier. (2) *Quantitative study of the performance.* The distribution of the magnetic field between the coils was determined experimentally; the diaphragm current equations were deduced and solved for a particular case; the forces on various parts of the diaphragm were calculated, and thence the amplitude of vibration and the sound energy output. With an aluminum diaphragm 0.0025 cm. thick and 10 cm. in diameter, a direct current of 1 ampere, an alternating current of 0.085 ampere, and a frequency of $10^5/2\pi$, these were respectively 7×10^{-7} cm., and 9 ergs per second. By increasing both direct and alternating currents five-fold, the output could be increased over six hundred-fold. Measurements of the amplitude for various frequencies agreed well with the calculated values. (3) *Applications of the instrument.* Since it gives a pure tone of constant and measurable pitch and intensity over a wide range, it would serve as a *precision source of sound*, useful both for research and lecture purposes. When used as a *telephone receiver and transmitter*, actual tests have shown that the reproduction of sound is remarkably faithful.

Introduction.

In a previous publication[1] the author gave a brief description of a new instrument for generating simple harmonic sound waves. The following is a quantitative description and study of the instrument and its performance, together with a discussion of some of its applications.

[1] Phys. Rev., 17, p. 257, 1921.

I. Specifications for the Construction of the Tone Generator, and Description of a Method of Operation.

The instrument described below was used successfully at frequencies from 500 to 25,000 vib./sec. For lower frequencies the instrument should be wound with a larger number of turns, while for higher frequencies a smaller number of turns of coarser wire should be used.

Figure 1 is a section and elevation. The frame is made of hard fiber,

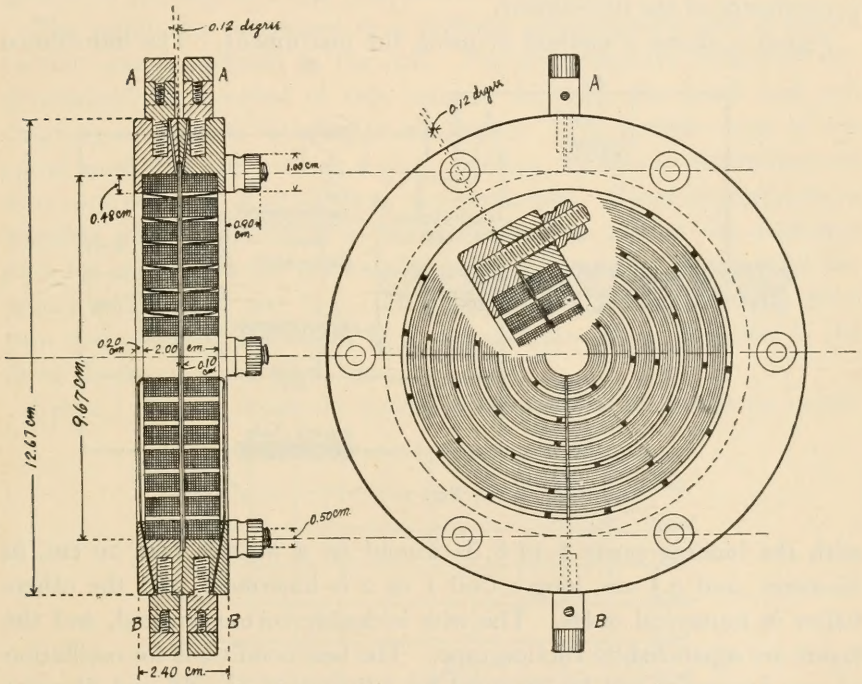

Fig. 1.

and the clamps and binding posts of brass. Each section of the pancake coils contains 98 turns of No. 22 wire, wound in 7 layers. The inside diameter of the innermost section is 1.11 cm., while that of the others is obtained by adding 1.27 cm. successively. These sections were wound on forms, shellaced, baked, and then bound at intervals with silk threads (not shown in figure). The sections mounted concentrically, are held in position by hard wood plugs. The sections of each coil are connected so that the direction of winding is continuous. The frame was turned after completing the coils, and the latter were glued in place with shellac. The taper on the clamping surfaces stretches the diaphragm enough to prevent appreciable sagging.

Any kind of metallic diaphragm will work; the author uses sheet aluminum 0.0025 cm. in thickness. Of the non-magnetic metals, alumi-

num gives the best results. An iron diaphragm gives more intense sounds at low frequencies for a given electrical input, although it will not emit a pure tone even when the instrument is excited by a simple harmonic alternating current. The diaphragm should be thin, as increasing the thickness decreases the intensity of sound emitted for a given electrical input, particularly for high frequencies. The reasons for the above may be drawn from the quantitative discussion of the performance of the instrument.

Figure 2 shows a method of using the instrument. The inductance

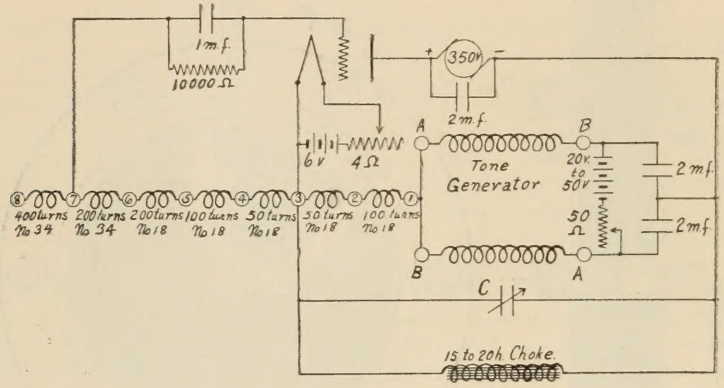

Fig. 2.

with the binding posts 1 to 8, is wound on a wooden core 20 cm. in diameter, and 6.5 cm. long. Coil 1 to 2 is innermost, and the others follow in numerical order. The wire is double cotton covered, and the layers are separated by friction tape. The best conditions for oscillation at any frequency can be obtained by adjustment of grid and filament connections to this inductance. In the actual circuit, *C*, and the choke coil are connected directly to the filament, and a single wire leads from this point to the inductance. The choke coil is home made. *C* consists of two 1 m.f. divided mica condensers, and five oil-filled rotary condensers whose combined maximum capacity is a little greater than the smallest step obtainable with the mica condensers. The other condensers are telephone condensers. The generator may be replaced by a battery, in which case no by-pass condenser is needed. The voltage shown is suitable for the Western Electric 205 B tube. The intensity of the sound from the instrument is controlled by the rheostat in series with the battery furnishing the polarizing current. The frequency of oscillation was measured with an improvised wave meter using a vacuum thermocouple for indicating resonance. If desired the instrument may be operated from a separate generator.

II. Quantitative Investigation of the Performance of the Instrument.

1. *Determination of the Distribution of the Magnetic Field in the Space occupied by the Diaphragm between the Pancake Coils.*—To simplify matters, the field of only one of the coils was investigated. Obviously the field is symmetrical about the coil axis. A flat spiral, of pitch 0.084 cm., consisting of 54 turns of No. 36 wire was wound in a shallow groove on the face of a fiber disc 10 cm. in diameter.

The spiral was connected to a ballistic galvanometer and a known current was established in the coil. The galvanometer deflection was determined for reversal of this current, (*a*) with the spiral and coil coaxially in contact, (*b*) when 1 mm. apart. The outside turns of the spiral were removed two at a time, making the above determinations after each removal, until only two turns remained. These determinations together with a calibration of the galvanometer yielded the necessary data for calculating the normal and radial components of the magnetic induction near the coil face. To simplify the calculation each spiral turn was assumed equivalent to a circular turn whose diameter is the mean diameter of the spiral turn.

Curve I., Fig. 3, shows the normal component of the magnetic induc-

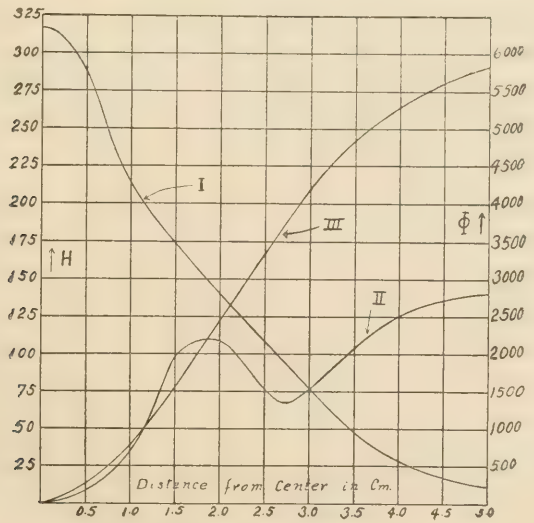

Fig. 3.

tion in C.G.S. units, as a function of the distance from the center, in the space between the two coils, when the latter are separated by a distance of 1 mm., and each carries a current of 1 ampere, their polarity being so adjusted that the unlike faces of the coils are adjacent. In this case

there is no radial component of the magnetic induction in the space between the two coils. Curve III. shows the total flux through a coaxial circle between the two coils as a function of the radius of the circle, for the same conditions of relative positions of the coils, current, and polarity as specified above. Curve II. shows the distribution of the radial component of the magnetic induction when the coils are separated by a distance of 1 mm., and each carries a current of 1 ampere, their polarity being so adjusted that the like faces of the coils are adjacent. In this case there is no normal component in the space between the two coils.

2. *Calculation of the Current Induced in, and Electromagnetic Forces Acting on the Diaphragm.*—The current in the diaphragm will flow in circles coaxial with the coils. The path of each current element will have a different resistance and self inductance, a different mutual inductance with the other paths, and will be acted upon by a different induced e.m.f. The current density and phase will therefore vary from one path to the next. The diaphragm was regarded as 8 annular rings each having a width of 0.645 cm., their mean diameters ranging from 0.97 cm. to 10 cm. Each annulus was considered equivalent to a circular wire of circular cross section of the same mass, material and diameter.

Suppose the current in the coils is given by $I_0 \sin \omega t$. The maximum values of the magnetic flux through each annulus was determined from curve III., and from these were calculated the induced e.m.f.'s in the annuli owing to the current in the coils. The total rise of potential around each annulus was then equated to 0, and the resulting eight equations put in the following form:

$$\left.\begin{aligned}
\left(\frac{r_1}{\omega^2} + a_{11}\right) i_1 + a_{12} i_2 + a_{13} i_3 + \cdots + a_{18} i_8 &= b_1 \sin \omega t + \frac{\Phi_1}{\omega} \cos \omega t \\
a_{21} i_1 + \left(\frac{r_2}{\omega^2} + a_{22}\right) i_2 + a_{23} i_3 + \cdots + a_{28} i_8 &= b_2 \sin \omega t + \frac{\Phi_2}{\omega} \cos \omega t \\
\cdots\cdots\cdots

The values of the coefficients were evaluated and the equations solved, giving the currents in the annuli, for a sine wave current whose maximum value in each coil was 0.085 amp., at a frequency given by $\omega = 10^5$. The current in an annulus may be expressed as follows $i_n = I_n \sin(\omega t + \theta_n)$. In the 4th and 5th columns of Table I. are given the values of I_n and θ_n for the successive annuli, beginning at the center. The second, third,

TABLE I.

I.	II.	III.	IV.	V.	VI.	VII.
n	d_n Cm.	$r_n \times 10^3$ Ohms.	I_n Amperes.	θ_n Degrees.	F_n Dynes.	$A_n \times 10^7$ Cm.
1.....	0.97	5.67	1.71	56° 58′	4	0.30
2.....	2.26	12.1	2.33	43° 16′	73	2.36
3.....	3.55	20.7	2.81	41° 58′	345	7.10
4.....	4.84	28.4	3.11	40° 26′	388	5.85
5.....	6.13	35 8	3.32	38° 38′	511	6.08
6.....	7.42	43.3	2.89	43° 19′	768	7.55
7.....	8.71	50.8	2.77	43° 41′	1022	8.56
8.....	10.00	58.3	2.87	42° 52′	1263	9.22

and sixth columns of this table give respectively the diameters and resistances of the annuli, and the maximum values of the electromagnetic force acting on them. The latter are the products of the maximum current in each annulus, its circumference, and the corresponding radial component of the magnetic field for 1 amp. of direct current in each coil. The current in each annulus and the force acting on it are in phase, but the phases of the total instantaneous force and current differ slightly. These latter are given respectively by $f_t = 4423 \sin(\omega t + 41° 30')$, and $i_t = 22 \sin(\omega t + 42° 25')$.

3. *The Amplitude of Vibration of the Diaphragm, and the Amount of Sound Energy it Emits.*—From the above, the forces on the various parts of the diaphragm are nearly in phase; particularly so for those places where the force is large. Consequently, the diaphragm may be considered to vibrate as a whole. It is practically aperiodic for any frequency concerned, so that its elasticity may be neglected. The equation of motion is then

$$m\frac{d^2x}{dt^2} + a\frac{dx}{dt} = F \sin \omega t,$$

where m is the mass of the diaphragm, a is the dissipative factor, and F is the maximum periodic force. The solution of the equation gives for the amplitude of vibration,

$$A = \frac{F}{\omega\sqrt{a^2 + (m\omega^2)}} .$$

The dissipative factor a is made up of two parts; one due to internal friction in the diaphragm, and the other to the emission of sound energy. The former is readily seen to be negligible compared to $m\omega$, while the latter is equal to the product of the velocity of sound, the density of air, and the area of the diaphragm. For $\omega = 10^5$, a^2 is only 0.0025 of $(m\omega)^2$, and consequently it may be neglected. The amplitude then becomes $A = F/m\omega^2$. Substituting $F = 4423$ dynes, $m = 0.60$ gm. and $\omega = 10^5$, the amplitude comes out 7.37×10^{-7} cm. The sound energy emitted from both sides of the diaphragm per second is 9.1 ergs. By increasing both the direct current and the alternating current in the coils five-fold, which is feasible, the amplitude of vibration would be 25, and the energy output 625 times as great; *i.e.*, an output of 5.7×10^3 ergs/sec.

A better idea of the actual performance of the diaphragm is obtained by calculating the amplitudes of the separate annuli. Making the same assumptions as before these amplitudes were found and are given in the seventh column of Table I. An appendix to this paper gives some measurements of the amplitude at various places on the diaphragm.

From the current equations and the preceding discussion it is seen why a thin diaphragm should be used. For high frequencies $r_{n,n}/\omega^2$ is small compared to $a_{n,n}$, so that the currents in the diaphragm, and the forces acting on it are independent of its resistance. Increasing the thickness, therefore, does not appreciably increase the force, so that the increased mass results in a proportionally decreased amplitude of vibration. At low frequencies where r_n/ω^2 is of more importance, a thin diaphragm is still preferable, although the advantage is not so marked.

An iron diaphragm will not execute a simple harmonic motion with a sine wave current in the coils, for the magnetic flux through such a diaphragm will not be proportional to this current.

III. Some Applications of the Instrument.

1. *Precision Source of Sound.*—A practically pure tone can be obtained whose frequency and intensity can be maintained practically constant for an indefinite period, can be varied continuously over a very wide range, and can be determined with considerable accuracy. The practical absence of eddy current and magnetic hysteresis energy losses makes it possible to operate the instrument at very high frequencies. The natural period of the diaphragm is so low that it introduces no irregularities in the response in the region of operation.

Mr. C. E. Lane has recently used this instrument to determine the minimum flux of sound energy for audition at several frequencies, and it is intended that this work shall be carried further in the near future. In this connection it may be mentioned that the instrument may be constructed with one coil, so that one side of the diaphragm is free. This has the advantage that the waves are unbroken in leaving the instrument. The resulting tone is somewhat impure, because the radial component of the magnetic field, having an alternating component, is no longer constant. The impurities consist of the octave and higher partials of the fundamental, and can be eliminated by a sound filter. With a direct current large compared to the alternating current, these impurities are negligible. Above 10,000 vib./sec. the impurities are inaudible unless the fundamental is very intense.

The instrument is suitable for the demonstration of diffraction, interference, and reflection effects. At high frequencies, the sound goes out in a well-defined beam, which makes possible some very striking qualitative demonstrations.

For reproducing speech the instrument promises interesting development. It has been used successfully as a generator and as a receiver of voice currents. The coils were specially designed to suit each of these uses. As a generator, the vibration of the diaphragm induces alternating currents in the coils, and these currents are fed into a thermionic amplifier. The voice spoken into one instrument is reproduced with remarkable faithfulness in another connected in the plate circuit of the amplifier. This is due partly to the absence of eddy current and magnetic hysteresis energy losses, and partly to the aperiodicity of the diaphragm. As a loud-speaking generator of sound, the instrument has been used to address an audience of more than one hundred persons. The distinctness of the words, and the quality of the voice of the instrument approached very closely those of the speaker who operated the generator of voice currents.

For voice frequencies the current equations are much simplified. Only the terms containing r_m/ω^2 and the cosine terms need be retained, so that the diaphragm currents are approximately proportional to the frequency, and are nearly in phase. Consequently, the force acting on the diaphragm, for a given alternating current in the coils, is proportional to the frequency, and the amplitude of vibration is inversely proportional to the frequency. This would cause distortion if the voice currents were of the same wave shape as the sound waves which gave rise to them. But if the same kind of instrument is used as a generator, the wave form of its electromotive force is such that the distortion arising in the receiver results in the production of sound waves of the

same character as the original ones. As a matter of fact, actual trials have shown that the distortion, as perceived by the ear, even when using a carbon granule transmitter, is very small.

IV. Appendix. Measurements of the Amplitude of Vibration of the Diaphragm.

Mr. C. E. Lane, while a graduate student in this laboratory, conducted the experimental work described below. Using an electric micrometer for amplitude measurements, the amplitude of vibration at a definite frequency, of an ordinary telephone receiver, was first shown to be proportional to the current through the receiver, and then the ratio of amplitude to current was determined for several frequencies. The tone generator and telephone receiver were excited by alternating current of the same frequency, and a brass tube, of internal diameter 0.4 cm., leading to a tuned resonator carrying a Rayleigh disc, was placed close to the diaphragms, alternately of the tone generator and the telephone receiver. The current in the latter was adjusted till the deflection of the disc was the same for the two. The amplitude for the telephone receiver was calculated from the amplitude-current ratio, and it was assumed that this also gave the amplitude for the tone generator. In this manner the amplitude was determined at various places on the diaphragm, and its distribution was shown to agree closely with that given in Table I. The root mean square of the amplitude was calculated for the whole diaphragm and compared with the amplitude calculated as outlined in section II. Table II. shows the results of these measurements reduced to the standard condition of 1 ampere of direct current and 0.1 ampere of alternating current in the coils. The measured and calculated amplitude agree within the limits of experimental error.

Table II.

Frequency.	Measured Amplitude.	Calculated Amplitude.
1440	4.64×10^{-5} cm.	4.96×10^{-5} cm.
1600	4.16 "	4.52 "
2200	4.04 "	3.24 "
3700	1.72 "	1.88 "

The writer takes pleasure in acknowledging the assistance rendered by Mr. C. E. Lane and other students in this laboratory, in parts of this work. Credit is also due Mr. J. B. Dempster for suggestions in design and help in the construction of apparatus.

STATE UNIVERSITY OF IOWA,
IOWA CITY, IOWA,
October 5, 1921.

Reprinted from the JOURNAL OF THE OPTICAL SOCIETY OF AMERICA AND REVIEW OF SCIENTIFIC INSTRUMENTS

Vol. VI, No. 1, January, 1922

THE CRYSTELLIPTOMETER

AN INSTRUMENT FOR THE POLARISCOPIC ANALYSIS OF VERY SLENDER BEAMS OF LIGHT

BY
LE ROY D. WELD

I. INTRODUCTORY

The determination of the elements of elliptic vibration of light, which has been transformed from a condition of plane to one of elliptical polarization, is found to reveal so much concerning the optical nature of the agencies effecting the transformation that it becomes a matter of considerable importance to be able to make such measurements with reasonable accuracy. It so happens that the ordinary methods, which are employed for the elliptical analysis, and most of which are too well known to need setting forth here, require a fair breadth of field, and would therefore not easily apply, for example, to a ray passing through a pin-hole.

The research presented in this paper had its origin in a problem suggested to the writer some years ago by Dr. L. P. Sieg, and was begun in 1915. It has been carried out at Coe College by means of apparatus, much of which was kindly loaned for the purpose by the University of Iowa.

Various investigators have attempted to obtain the optical constants of metals and other opaque substances by reflection methods, with indifferent success. It appears certain from the research of Tate[1] that the difficulty has been due, not to lack of precision in the analysis of the elliptically polarized light reflected from the opaque surfaces, but to the variation in surface conditions, brought about by the polishing process, which modified the nature of that light. Thus it was found impossible to prepare two mirrors of the same kind of metal, even by the same process, which would give consistent results, while different measurements, and even different kinds of reflection measurements, *on*

[1] Tate, Phys. Rev., 34, p. 321, 1912.

the same fresh surface, gave good agreement. Dr. Sieg's suggestion was that opaque crystals, with their natural, unpolished facets, might be prepared of such surface purity as to obviate this difficulty, and at the same time furnish material for an interesting experimental research in crystal optics.

Comparatively few large opaque crystals can be obtained in perfect form. Drude[2] made some experiments long since with lead sulphide, and Müller[3] subsequently, with antimony sulphide, freshly exposed by cleavage, employing ordinary polariscopic methods. In 1916 the writer made a preliminary report[4] on the present research, which had already given unmistakable evidence of strong double refraction in minute hexagonal selenium crystals, and at the same meeting,[5] Dr. Sieg reported having found by direct photometric measurements that the selenium crystal has two different reflecting powers in the two principal directions. Mr. C. H. Skinner has given an account[6] of his interesting observations on selenium, using the ordinary Babinet compensator method, from which he concluded that the crystals, like artificially prepared surfaces, have in some respects their individual peculiarities, especially in the longitudinal direction.

The method adopted by the writer was presented to the Physical Society in 1917 but was published only in abstract[7] at that time, the research being then still in progress. It is applicable not only to the polariscopic analysis of light reflected from polished plane surfaces of any sort, however small (such as minute spikelets or flakes of selenium, tellurium, cadmium, etc.), but to light in slender beams from any source. Its application has recently been suggested, for example, to the comparison, from point to point, of the optical properties of metal film-deposits of non-uniform thickness. Furthermore, being a photographic method, it is adaptable to the ultra-violet, and the apparatus was designed with this in view. Its original application to crystal-reflected,

[2] Drude, Ann. d. Physik, 36, p. 532, 1889.
[3] Müller, Neues Jahrbuch für Mineralogie, 17, p. 187, 1903.
[4] Weld, Proc. Iowa Acad. Sci., 1916, p. 233.
[5] Sieg, Proc. Iowa Acad. Sci., 1916, p. 179.
[6] Skinner, Phys. Rev., N.S. 9, p. 148, 1917.
[7] Weld, Phys. Rev., N.S. 11, p. 249, 1918.

elliptically polarized light is what suggested to the writer the name "crystelliptometer" for the distinctive apparatus employed.

II. PRINCIPLE OF THE POLARISCOPIC METHOD

As regards the polariscopic analysis itself, the method employed is a modification of that used by Voigt for the study of polarized ultra-violet. The principle is stated in Voigt's original article[8] and a more detailed account given by Mr. R. S. Minor[9] who applied it to artificially polished mirrors of steel, copper, silver, etc. A non-mathematical statement of the original method will first be given.

Let us have a uniform parallel beam of elliptically polarized monochromatic light; to determine the two elements of the elliptic vibration, which may be taken as the ratio $r = \frac{a}{b}$ of the X to the Y amplitude, and the phase advance ∇ of the X ahead of the Y harmonic component (either positive or negative).[10]

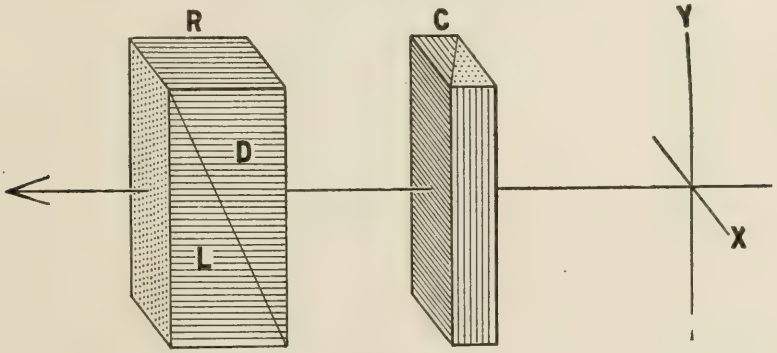

Fig. 1

Cross hairs and quartz wedge systems. XY, reticule. C, compensator. R, rotator

This beam first passes through a pair of quartz wedges similar to a Babinet compensator, except that they are fixed with reference to each other (C, Fig. 1). The edges are, let us say, vertical, that is, parallel to the Y direction. As we now face the oncoming

[8] Voigt, Physik. Zeitschr., 2, p. 203, 1901.

[9] Minor, Ann. d. Physik, 10, p. 581, 1903.

[10] The reason for here using the inverted ∇ instead of the customary Δ will appear later (Sec. VII).

light and move across the emergent beam from left to right, we encounter a steady increase in the phase advance, so that, whereas the light through the center of the compensator has phase difference ∇ (the same as the original light), that at distance x from the center has phase difference $\nabla + sx$, where s is the compensator constant in degrees of phase per millimeter. Periodically, therefore, we shall come to regions of light *plane polarized* at some angle, viz., where $\nabla + sx = 0, \pi, 2\pi, \ldots$.

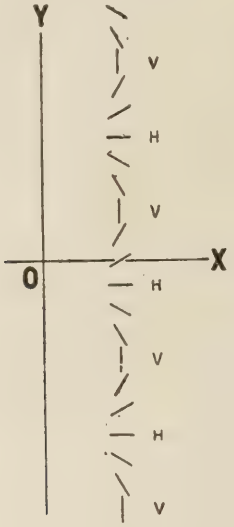

Fig. 2

Showing action of rotator on a strip of plane-polarized light

The next optical member is another pair of wedges, which will be called a *rotator* (R, Fig. 1). This consists of a wedge D of right-handed, and one L of left-handed, quartz, the optic axis of each being along the path of the light. It is easily seen that if the light entering the rotator be plane-polarized, it will suffer a net rotation of plane which will be the greater, the higher the point at which it traverses the two wedges. This rotation may be designated by qy, q being the rotator constant in degrees of azimuth per millimeter.

To an observer facing the light as it comes from the rotator, any one of the periodic vertical ribbons of plane-polarized light from the compensator will have been acted upon by the rotator as

shown in Fig. 2. Therefore as we traverse this emergent beam vertically along any one of these plane-polarized regions, we shall encounter, at intervals, light vibrating vertically, and half way between these, light vibrating horizontally (V and H, Fig. 2).

Finally, let the beam be passed through a Nicol set so as to extinguish, say, the vertical component. Obviously, wherever we had in one of these plane-polarized strips a point of vertical vibration, we shall now have a black spot. The field will then be covered with black spots arranged in a regular pattern of vertical columns and horizontal rows, the exact design of which will depend upon the elements of the original elliptic vibration. Conversely, these elements may be easily deduced from the observed arrangement of the spot-pattern. There is introduced into the

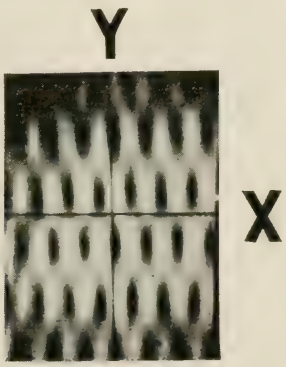

Fig. 3

Spot-pattern for elliptically polarized light reflected from nickel. (Enlarged.)

field a pair of cross hairs corresponding to X and Y axes and coinciding with the neutral lines of rotator and compensator, respectively. This reticule is photographed along with the spot-pattern and the coordinates of the spots determined by subsequent measurements on the plate. Such a spot-pattern, with the cross hairs, is shown, enlarged, in Fig. 3, in which the elliptic polarization was produced by reflection from nickel.

The equations relating to the processes just described, and the practical deduction of the elliptic elements therefrom, will be worked out in subsequent sections of the paper.

III. Adaptation of the Method to Slender Beams

The above procedure, as followed by Voigt and others, obviously requires a beam of light whose cross section is large enough to cover the entire spot-pattern, and hence would not be adapted at all, for example, to light reflected from one facet of a small crystal. The writer's modification of it consists simply in keeping the very slender parallel beam, so reflected, stationary, and moving the whole analyzing system of quartz wedges, cross hairs, Nicol and camera back and forth perpendicularly across it, with

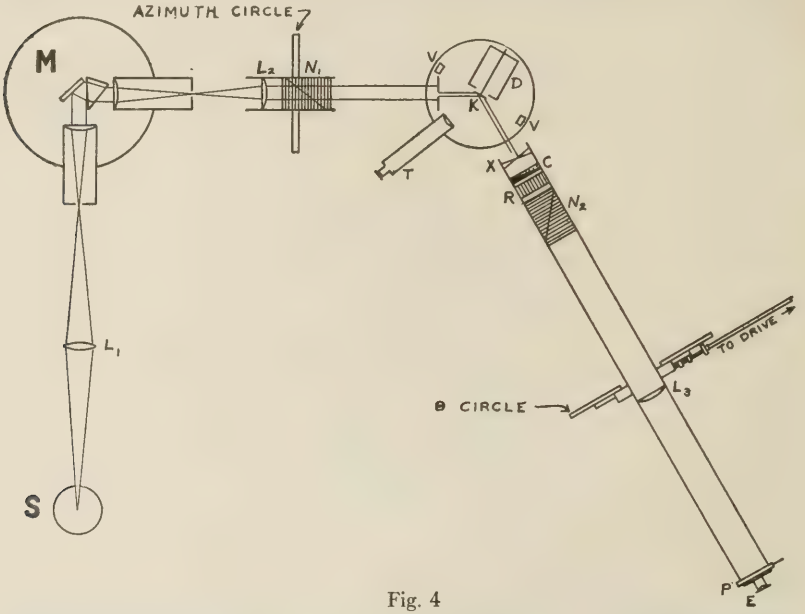

Fig. 4

Diagrammatic layout of apparatus. *S*, source. *M*, monochromator. L_2, N_1, collimator and polarizer. *K*, reflecting surface mounted in front of drum *D*. *X* to *E*, crystelliptometer

a sort of weaving motion, until the whole spot-pattern has been covered. The effect is the same as if the beam had a cross section as large as the field thus traced out. Whenever any point of the analyzing system corresponding to one of the dark spots arrives at the beam, the latter is extinguished thereby, and the spot is left on the plate. In practice it is not necessary to cover the whole pattern, but only the regions of it in which the rows of spots are known approximately to lie; and this fact saves much time.

The assemblage of optical parts, which is given the lateral motion just described, together with its mountings, considered as a single instrument, is what has been referred to as the "crystelliptometer."

The arrangement of the writer's apparatus for the study of crystals is shown in Fig. 4. Light from the source S is focused by the quartz lens L_1 on the inlet slit of the monochromator M, from whose outlet slit the monochromatic light diverges and is collimated by the quartz lens L_2. (In the earlier work, color filters were used instead of the monochromator, and the filtered light focused by L_1 directly upon the slit of the collimator.) The parallel beam from L_2 is plane-polarized in any desired azimuth by N_1, a large polarizing prism with square ends and a glycerine film.

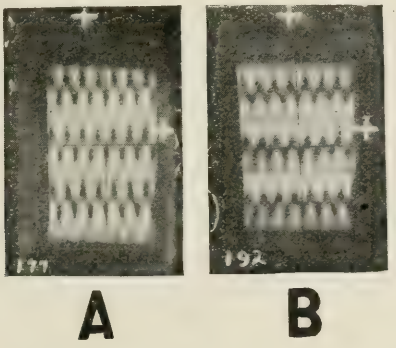

Fig. 5

A, spot-pattern for light reflected for selenium in parallel position. *B*. in perpendicular position

The crystal or other small reflector K is mounted on a spectrometer, by means of whose telescope T and verniers V any desired angle of incidence may be secured. The mounting can be rotated so that it is very easy to exhibit the double refraction of selenium, tellurium, etc., the spot-patterns obtained with axis horizontal and with axis vertical being quite visibly different, as seen in Fig. 5.

The slender reflected beam, in general elliptically polarized, now enters the analyzing system X, C, R, N_2 of the crystelliptometer. X represents the cross hairs, which the writer has found it necessary to place in front of the compensator C. (See Sec. VI.)

The compensator wedges have an angle of 52′, which gives a relative phase change of about 144° per horizontal millimeter with sodium light. R is the rotator, with wedge angle 24°, which gives a rotation in azimuth of about 16° per vertical millimeter with sodium light. The dimensions of the field are about 15 x 30 mm. The wedge system and cross hairs are mounted adjustably in a brass tube which screws upon the tube containing the analyzing prism N_2.

N_2 is a duplicate of N_1, the two being interchangeable. They are rectangular prisms 15 x 30 x 30 mm consisting of Iceland spar wedges separated by glycerine, the angle of incidence on the interface being 65°. The emergent (extraordinary) light vibrates parallel to the 15 mm dimension.

The spot-pattern and cross hairs are photographed together, by means of the quartz lens L_3, upon the plate P. Behind the plate is an eyepiece E, used in adjusting the focus and alignment before the plate is inserted. The plates are 1 x 1½ inch, with emulsion adapted to the wave-length, and are held in a diminutive plate holder.

The whole crystelliptometer, from cross hairs X to eyepiece E, is contained in a tube about 85 cm long, so mounted on two pairs of guides at right angles that it can be given the weaving motion referred to in order to trace out the spot-pattern. This is accomplished by means of two micrometer screws perpendicular to each other. One of these screws is driven by a worm-gear electric motor mechanism so as to move the instrument slowly across, along a line determined by the other screw, the speed varying with the exposure required. Furthermore, the whole tube, with its micrometer mountings, can be rotated about its longitudinal axis through any desired angle, thus varying the relative inclination of the elliptic vibration to be analyzed, with respect to the coordinate axes of the analyzing system. The extinction plane of the analyzer N_2, which coincides with the Y axis, being first vertical, one spot-pattern is produced. On rotating the instrument through an angle θ another is obtained, and so on; without, however, modifying in any way the actual nature of the elliptic light under analysis. The equations used in the subsequent

theory make provision for this arbitrary angle θ, the advantage of which will then appear.

The source of light at first employed was an open Nernst filament, which has later been replaced by a special low-voltage tungsten ribbon lamp. In some preliminary work with ultraviolet, an iron arc was employed.

A general view of the apparatus is shown in Fig. 6.

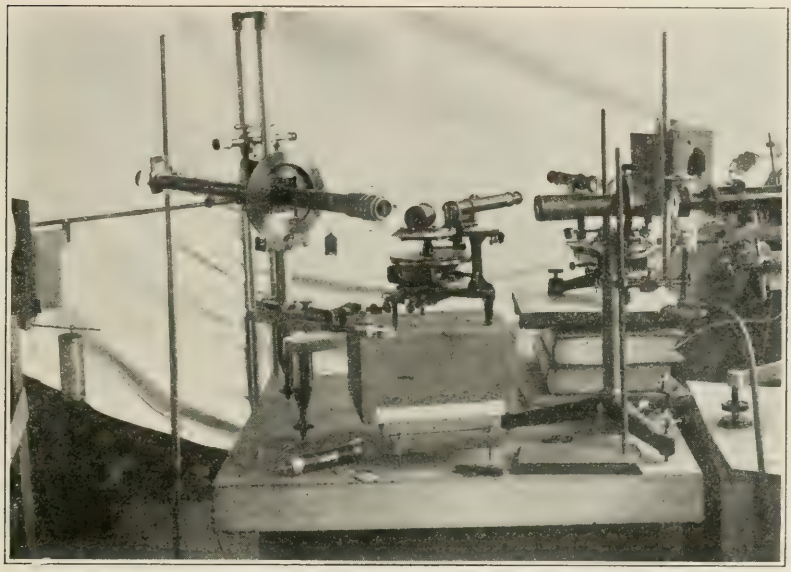

Fig. 6

General view of crystelliptometer and accessory apparatus

The spot-patterns are measured upon a micrometer comparator to one-hundredth of a millimeter. The lenses were removed from the microscope, and a pin-hole and hair-line substituted, a device suggested to the writer by Dr. Elmer Dershem. Not a little of the routine work consists of the p'ate measurements and their reduction. It has been found possible, with good, clear plates, to locate a spot by a single measurement with a probable error of less than one-hundredth of a millimeter. A selenium spot-pattern and the corresponding "comparison plate" (see Sec.VI) are shown

together as A, B in Fig. 7, and another similar pair, with greater wave-length, as C, D.

The quartz lenses and wedges and the Iceland spar wedges for the Nicols, designed by the writer, were made by Hilger of London, as was also the monochromator; the comparator by Gaertner of Chicago. The remainder of the special apparatus, including the driving mechanism, was built at the University of Iowa by Messrs. M. H. Teeuwen and J. B. Dempster, assisted by the writer.

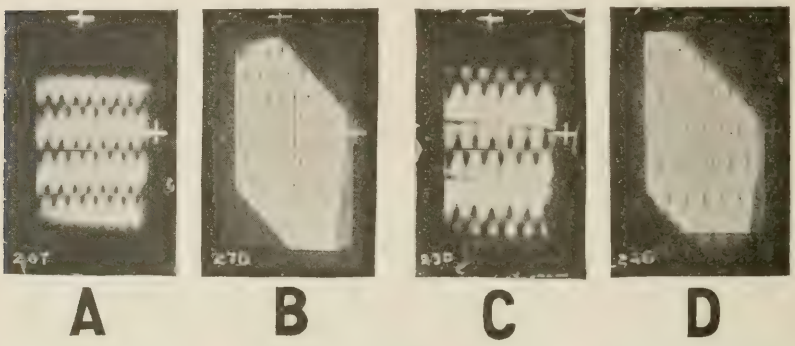

Fig. 7

A, selenium spot-pattern. *B*, corresponding comparison plate. *C*, *D*, same, with greater wave-length. Note the greater spot-intervals

IV. Outline of the Mathematical Theory of the Analyzing System

The mathematical theory of the action of the analyzing system, as used in the writer's method, and of the determination of the elliptic elements, will now be briefly given.[11] In the notation here used, X and Y are components of the vibration displacement of the light, while x and y are coordinates of points of the field with reference to the axes.

[11] This is necessary for the reason that the present method departs in certain essential particulars from the original and gives rise to a different set of equations. Minor did not, for example, rotate the quartz wedge system through the arbitrary angle θ which makes possible the least square adjustment of the observations, and which, as will be easily seen, also provides automatically for any difficulty due to the azimuth of the light under examination happening to be very small, without altering that light in any way.

Let the harmonic components of the elliptic vibration to be analyzed, as viewed by one facing the oncoming waves, be given by the equations

$$X = a \cos(\omega t + \nabla) \quad \ldots\ldots (1)$$
$$Y = b \cos \omega t \quad \ldots\ldots (2)$$

If the analyzing system by now rotated through an angle $+\theta$, these equations are transformed, with reference to the new axes, into

$$X' = a \cos\theta \cos(\omega t + \nabla) + b \sin\theta \cos \omega t \quad \ldots\ldots (3)$$
$$Y' = b \cos\theta \cos \omega t - a \sin\theta \cos(\omega t + \nabla) \quad \ldots\ldots (4)$$

Upon passage through the compensator, the Y-component receives an advance of phase, varying with the abscissa x of the point where it passes through, and equal to sx. (3) and (4) then become

$$X'' = a \cos\theta \cos(\omega t + \nabla) + b \sin\theta \cos \omega t, \quad \ldots\ldots (5)$$
$$Y'' = b \cos\theta \cos(\omega t + sx) - a \sin\theta \cos(\omega t + \nabla + sx) \quad (6)$$

Upon passage through the rotator, there is a simple rotation of the axes of the ellipse, without further change, through an angle qy, which corresponds to a rotation $-qy$ of the coordinate axes, so that the components of the finally emergent light are

$$X''' = a \cos\theta \cos qy \cos(\omega t + \nabla) + b \sin\theta \cos qy \cos \omega t$$
$$- b \cos\theta \sin qy \cos(\omega t + sx) + a \sin\theta \sin qy \cos(\omega t + \nabla + sx). \quad \ldots\ldots (7)$$

Y''' = (a corresponding long expression which we shall not need) $\ldots\ldots (8)$

The light now passes through the Nicol N_2, which shuts off the Y-component all over the field; hence (8) is not needed. Only X''' gets through, and this will vanish, leaving the dark spots, at every point where x and y have such values as to render the expression (7) equal to zero *all the time*, that is, independently of the value of t. To fulfill this condition, dividing (7) by $b \cos\theta$, letting $\frac{a}{b} = r$, expanding the parentheses containing ωt and grouping the terms in $\sin \omega t$ and $\cos \omega t$ separately, we have

$$[-r \tan\theta \sin qy \sin(\nabla + sx) + \sin qy \sin sx$$
$$- r \cos qy \sin \nabla] \sin \omega t$$

$$+[\tan\theta\cos qy+r\cos qy\cos\nabla-\sin qy\cos sx$$
$$+r\tan\theta\sin qy\cos(\nabla+sx)]\cos\omega t=0.$$

That this may be true independently of t, the coefficients must separately vanish, giving

$$-r\tan\theta\sin qy\sin(\nabla+sx)+\sin qy\sin sx-r\cos qy\sin\nabla=0 \quad (9)$$

$$\tan\theta[\cos qy+r\sin qy\cos(\nabla+sx)]+r\cos qy\cos\nabla-\sin qy\cos sx=0 \quad (10)$$

Letting $\tan\theta=m$, expanding the functions of $\nabla+sx$, and collecting, these become

$$[m\sin qy\cos sx+\cos qy]r\sin\nabla+m\sin qy\sin sx.\,r\cos\nabla=\sin qy\sin sx \quad (11)$$

$$m\sin qy\sin sx.\,r\sin\nabla+[m\sin qy\cos sx+\cos qy]r\cos\nabla=\sin qy\cos sx-m\cos qy \quad (12)$$

In these equations, x and y are the measured coordinates of any dark spot, s and q are the compensator and rotator constants, determined from the spot intervals, and m is the tangent of the known angle θ. Hence everything is known except r and ∇. Letting

$$\left.\begin{aligned} m\sin qy\cos sx+\cos qy &= H,\\ m\sin qy\sin sx &= K,\\ \sin qy\sin sx &= L,\\ \sin qy\cos sx-m\cos qy &= P, \end{aligned}\right\} \quad (13)$$

(11) and (12) become

$$H\cdot r\sin\nabla+K\cdot r\cos\nabla=L \quad (14)$$

$$K\cdot r\sin\nabla+H\cdot r\cos\nabla=P \quad (15)$$

the solution of which, as simultaneous equations, gives the required elliptic elements

$$r=\frac{\sqrt{(L^2+P^2)\,(H^2+K^2)-4\,LHPK}}{H^2-K^2} \quad (16)$$

$$\tan\nabla=\frac{LH-PK}{PH-LK} \quad (17)$$

It is thus theoretically possible to deduce the elements from the measured coordinates of any single spot.

V. APPLICATION TO SPOT-PATTERNS

If we place under examination light which is plane-polarized at azimuth 45°, so that $r = 1$ and $\nabla = 0$, it will be seen from the manner of their formation, as described in Sec. II, that the spots will be *symmetrically* arranged with respect to the Y-axis in *equally spaced* horizontal rows. This is the condition of things on the comparison plate, Fig. 7 B (see Sec. VI). Let the distance apart of the spots in the rows be d, and in the vertical columns, (Fig. 8). These are easily measured (see Sec. VI). The compensator constant s is equal to $\frac{360}{d}$, and the rotator constant q equals $\frac{180}{\delta}$, in degrees per millimeter (see Sec. II).

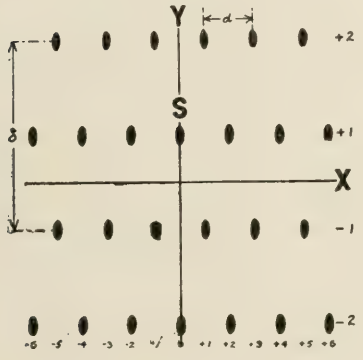

Fig. 8

Diagram of spots on a comparison plate, taken with plane-polarized light at 45° azimuth

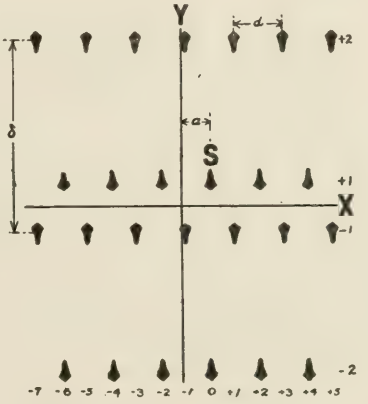

Fig. 9

Diagram of spots on a pattern taken with light elliptically polarized at phase difference 202° and azimuth 29°

If now we introduce by any means a phase difference ∇ between the X- and Y-components, there will be a uniform lateral displacement a of the whole spot system, so that the coordinates of the spot S, which in Fig. 8 are $0, \frac{\delta}{4}$, now become $a, \frac{\delta}{4}$. Then, again, if a change is produced in the azimuth of the incident light, the alternate rows $+1$, -2, etc. will be displaced vertically one way,

and rows $+2$, -1, etc., the other way, through a certain amount a, so that now the coordinates of S are $x=a$, $y=\frac{\delta}{4}+a$ (a being negative). These changes are shown in Fig. 9.[12]

Introducing the above values of s, q, x, and y into (13), and resuming $m=\tan\theta$, we get

$$\left.\begin{aligned} H &= \tan\theta \sin\left[45^\circ+\frac{a}{\delta}180^\circ\right]\cos\left[\frac{a}{d}360^\circ\right]+\cos\left[45^\circ+\frac{a}{\delta}180^\circ\right], \\ K &= \tan\theta \sin\left[45^\circ+\frac{a}{\delta}180^\circ\right]\sin\left[\frac{a}{d}360^\circ\right], \\ L &= \sin\left[45^\circ+\frac{a}{\delta}180^\circ\right]\sin\left[\frac{a}{d}360^\circ\right]. \\ P &= \sin\left[45^\circ+\frac{a}{\delta}180^\circ\right]\cos\left[\frac{a}{d}360^\circ\right]-\tan\theta\cos\left[45^\circ+\frac{a}{\delta}180^\circ\right]. \end{aligned}\right\} \quad (18)$$

While the attention is, indeed, fixed on one particular spot S, Fig. 9, whose coordinates are a and $\frac{\delta}{4}+a$, yet in actual practice it is expedient to make measurements on a number of spots, usually twenty or more, and deduce the position of S from them. Referring to Fig. 9, it is clear that the abscissa of any spot in the nth vertical column (numbered along the bottom of the figure) is

$$x=a+n\frac{d}{2},$$

which gives

$$a=x-\frac{n}{2}d \quad \ldots\ldots\ldots\ldots\ldots\ldots\ldots\ldots (19)$$

By measuring the abscissas of several spots in different rows, thus varying x and n, we obtain as many independent observations upon a.

[12] If the azimuth is made 90°, rows $+1$, $+2$, rows -1, -2, etc., will merge or dove-tail together in pairs forming continuous horizontal dark stripes. If it is made 0, the pairs of rows $+1$, -1, etc., will similarly coincide. This affords a good means of adjusting the quartz wedge system with respect to the previously adjusted analyzing Nicol (see Sec. VI).

Again, the ordinate of any spot in the νth horizontal row (counted upward or downward from the X-axis) may be seen to be

$$y = \pm(-1)^{\nu+1}\ \alpha - \frac{\pm 1 - 2\nu}{4}\ \delta,$$

$$\text{or} \qquad \alpha = \pm(-1)^{\nu+1}\left[y + \frac{\pm 1 - 2\nu}{4}\ \delta\right] \ldots\ldots\ldots\ldots (20)$$

($\pm$ according as the row is above or below the X-axis), and we shall have, therefore, as many observations upon α as there are spots measured.

The averages from these observations on a and α are easily obtained by means of formulas depending upon the particular selection of spots made. If the selection consists of an equal number of vertical columns on each side of the Y-axis and of horizontal rows above and below the X-axis (as should be the case for other reasons), these averaging formulas become quite simple. a, α, d and δ being thus determined from the measurements on the plate, substitution of their values in (18) gives the necessary constants H, K, L, P, appearing in the expressions for r and $\tan \nabla$, Eqs. (16), (17), and the problem is solved so far as is possible from a single experiment.

We may, however, expose other plates with different values of θ, obtained by rotating the crystelliptometer tube about its own axis. This does not alter the elliptic elements, but it gives new values of H, K, L, P. In such case, (14) and (15) may be used as *observation equations* of the first degree with $r \sin \nabla$ and $r \cos \nabla$ as unknowns, and we may obtain as many different pairs of them as there are measured plates, finally adjusting them by the method of least squares. It has been the writer's practice to assign a weight to each measured plate by means of the grading method,[13] each plate characteristic, such as clearness, symmetry of spots, etc., being graded separately.

It should be stated that, *except in cases where the number of spots on a plate available for measurement is too limited for precision*, a

[13] Weld, *A Method of Assigning Weights to Original Observations*, Science, 50, p. 461, 1919.

single plate, with $\theta = 0$, is sufficient, and a vast amount of laborious calculation is thus avoided. For with $\theta = 0$ in (18), the elliptic elements, given by (16) and (17), reduce at once to

$$r = \tan\left[45° + \frac{a}{\delta}180°\right] \quad \ldots\ldots\ldots\ldots\ldots\ldots (21)$$

$$\nabla = \frac{a}{d}360° \quad \ldots\ldots\ldots\ldots\ldots\ldots\ldots\ldots\ldots (22)$$

It is only with light of very large wave-length that the number of spots in the field is likely to be so few as to require the repeated exposures.

VI. Miscellaneous Details and Sources of Error

The general arrangement of the apparatus as employed for the study of opaque crystals was explained in Sec. III. In order to adjust all the parts in proper relation to each other, use is made of a sensitive cathetometer set with reference to the pier on which the apparatus stands. By this means is secured the horizontality of the monochromator, the collimator, the polarized incident beam, the reflected beam from the crystal, and the crystelliptometer tube, taken in the order named. The plane of incidence and reflection is thus strictly horizontal, and the azimuth of polarization, the arbitrary angle θ, and the vibration components X and Y are reckoned with reference to it. The crystal is mounted on the end of a small rod in front of the dark opening into a hollow drum,—a black body, so to speak, which makes a perfectly dead back-ground. The mounting may be turned in a vertical plane, and is provided with a graduated circle, so as to give the crystal any desired angle from 0° to 180° with the plane of reflection. The drum (D, Fig. 4) is placed on a spectrometer prism table for adjusting the angle of incidence, as previously explained.

Considerable trouble has been experienced with the monochromator, inasmuch as no reliance can apparently be placed upon the wave-lengths indicated by it; and furthermore, the wave-length corresponding to any given setting is found to vary from day to day. In all final work it has therefore been customary to

divert the light emerging from the monochromator into a separate grating spectrometer (not shown in Fig. 4) and compare it with the sodium standard just before making each exposure. Another and more serious difficulty with the monochromator is the impurity of the light furnished, especially in the shorter wave-lengths.

The accurate adjustment of the focus of the collimating and camera lenses is a matter of some importance, especially the latter. These quartz lenses are, of course, not achromatic, and the focus must be calibrated for wave-length. In the case of the collimator, it has sufficed to measure the focal length for one wave-length on an optical bench and calibrate the tube from the known dispersion of quartz. But any inaccuracy in the focus of the camera lens will result in displacements of the spot images and resultant errors in the elliptic elements, so that this requires greater precision. The method here employed is one devised by the writer and referred to as the "offset" or "broken prism" method.[14] The proper focus for a given wave-length may be thus obtained with a probable error of only one or two tenths of a millimeter, and it is easy to calibrate the focus tube accordingly.

The need for a special precaution arises from the fact that the spot-pattern in the crystelliptometer appears to be a sort of virtual image lying in a definite plane. It is necessary to get the cross hairs accurately into that plane, otherwise there will be an apparent parallax between cross hairs and spots, and the results will be seriously affected if the light happens to be not strictly parallel to the crystelliptometer axis. Furthermore, the position of this virtual plane is found to vary systematically with the wave-length, so that the adjustment has to be made for each wave-length used. This is accomplished by mounting the cross hairs in a ring having a longitudinal micrometer movement in the tube. The crystelliptometer is turned a little to right and left with respect to the beam of light and the reticule moved forward or backward until the parallax disappears. It has always been found necessary, in the visible spectrum, to place the reticule in front of the compensator, as in Fig. 4.

[14] Weld, *Some Precise Methods of Focusing Lenses*, School Science and Mathematics, 18, p. 547, 1918.

The cross hairs in the writer's instrument are of very fine spun glass, their images representing on the plate the X- and Y-axes of the spot-pattern. The ring in which they are mounted is provided with the usual lateral adjusting screws. It is inevitable that the reticule will get out of adjustment laterally, and for the purpose of determining this error (which would be serious if neglected), what are called *comparison plates* are taken at frequent intervals, using a full-sized beam of parallel, strictly plane-polarized light direct from the polarizing Nicol. The cross hairs are first given approximate adjustment visually, using this light. The comparison plate is then taken and the small errors of cross hair adjustment remaining, amounting to a few thousandths of a millimeter, are determined by measurements upon it and proper allowance made for them in the reduction of other plates. If a symmetrical pattern is selected, the adjustment of the *horizontal* cross hair is really immaterial, as the true X-axis can readily be found as the mean position of the horizontal rows of spots employed in measuring any plate.

Owing, no doubt, to slight inequality of the quartz wedge angles, the cross hair adjustment error is found, like the parallax, to vary systematically with the wave-length, and a new comparison plate must therefore be taken for each wave-length used. It is very difficult, even with the spectrometer test, to keep the wave-length strictly constant through a series of experiments. Curiously enough, the most sensitive, and the final, check on wave-length has been found to be the spot-interval d (Figs. 8, 9), which can be measured with great precision (see below). The greater the wave-length, the farther apart are the spots, both horizontally and vertically, on account of the dependence of both the phase-relation change, and the rotation, in quartz, upon the wave-length. (See Fig. 7.) In practice, it is found advisable to determine, by means of auxiliary comparison plates, the relation of the cross hair error to d for light in each region of the spectrum used, and to deduce the required correction from the measured d on each elliptic plate.

The accurate determination of the spot intervals d and δ for each plate is an essentially vital part of the work. The most

probable value of d can be deduced fr m the plate measurements by forming observation equations from the abscissas of the spots taken by groups in each row, and applying the simple least square adjustment requisite to the case. This is all done very quickly by means of a formula which is the same for all spot-patterns similarly selected. With a symmetrical spot-pattern δ is simply twice the mean absolute ordinate of the spots (without sign). Thus no extra measurements are necessary for d and δ. But it will not do to rely on the comparison plate, or any other one plate, for the spot-intervals corresponding to a supposedly fixed wave-length, as variations of wave-length too slight to have noticeable effect on the ordinary properties of the light, will cause serious errors through this means.

When, as usual, the arbitrary orientation (Sec. IV) is zero, it is seen by Eq. (21) that the ratio r of the two vibration components of the unknown light, which is the tangent of the azimuth, is given in terms of α and δ. These are determined from the y measurements alone. For some reason not certainly explained, it has been found that there is a persistent error in r as deduced from the measurements on the spot-pattern, whose value appears to be a linear function of r itself. The error is eliminated by first finding the uncorrected value of r from the plate measurements, and then taking a correction pattern with plane-polarized light having azimuth set for that value of r (which is thus accurately known). The measurement of this plate, and the comparison of the erroneous value of r deduced therefrom with the true value given by the polarizer azimuth circle, afford the necessary correction, which sometimes amounts to as much as two or three degrees. This must be done for each wave-length used. These azimuth-correction plates, like the comparison plates, are taken with full-sized beam from the polarizer and require only a short exposure.

One more detail of technique is worthy of note. It will be noticed from Fig. 7C, for example, that on some patterns the spots are not symmetrical vertically, but are decidedly triangular or cuneiform, and tend to run together in double rows. This makes it difficult to estimate the Y position of the spot nucleus with certainty in measuring these plates. It will not do to bisect the

spot with the micrometer in this direction. In order to ascertain the location of the nucleus within the spot, the means adopted has been to calculate, theoretically, the geometrical form of the concentric lines of equal intensity surrounding it, taking the constants from actual measurements on typical plates. The form of these lines, derived from an application of the mean value theorem, is

$$\cos(\nabla - sx) = \frac{1 - M - (1 - r^2)\cos^2 qy}{r \sin 2qy} \qquad (23)$$

in which M is a parameter depending on the intensity along the curve in question; for the nucleus, $M = 0$. x and y are the coordinate

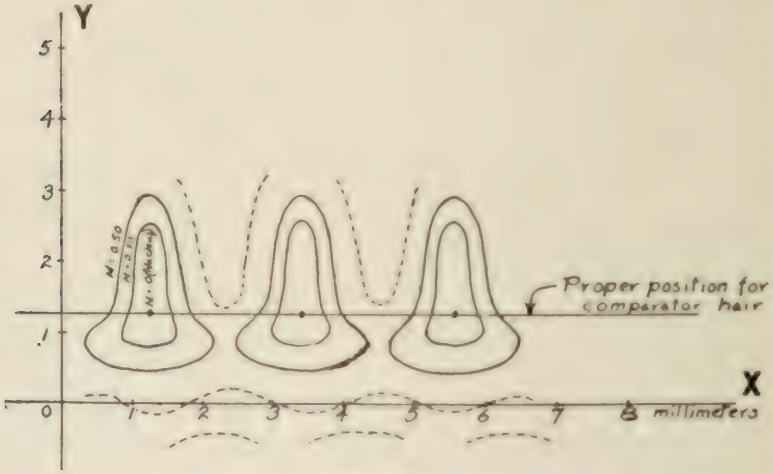

Fig. 10

Lines of equal intensity about the spot of Fig. 5B, greatly enlarged

variables, and the other quantities have the same meanings as in Sec. IV. Fig. 10 shows the nuclei and curves corresponding to $M = 0$, 0.25 and 0.50 on the plate shown in Fig. 5B. With the knowledge afforded by such a figure, it is easy to estimate with some accuracy what point within the spot is to be aimed at in making the measurement. The nucleus appears to represent approximately the center of gravity of the spot area, rather than to bisect its vertical dimension.

VII. TYPICAL APPLICATIONS. REFLECTION FROM SELENIUM CRYSTALS

Among the preliminary tests of the crystelliptometer and the methods of using it set forth in the foregoing sections were the analysis of polarized light rendered elliptical by reflection from nickel and copper mirrors or from crystals of lead sulphide and tellurium, or by passage through sheets of mica; and a tryout of Fresnel's equations for the rotation of plane-polarized light reflected from glass. The only problem, however, upon which serious attack has yet been made by the crystelliptometer method is the experimental part of an extensive research now in progress at the University of Iowa, viz., the optical laws of absorbing crystals. The general theory of this subject was handled with great thoroughness by Drude in his inaugural dissertation[15] many years ago, but until recently the only experimental data upon which tests of the theory might be based have been with reference to certain large crystals of the rhombic system. The unique electro-optical properties of the hexagonal selenium crystal have suggested a revival of the subject, the outgrowth of which is the research in question. The few data given below are the first final results obtained by this method, and will serve to illustrate it. They are summarized from a long series of measurements on many selenium crystals, and involved the taking of nearly three hundred plates. The instrument is now in the hands of other observers whose aim is to accumulate information regarding the optical properties of small crystals of various metallic substances.

Some of the finest crystals of hexagonal selenium ever prepared were kindly put at the writer's disposal by Dr. E. O. Dieterich, who produced them by sublimation at the University of Iowa. They are 2 or 3 cm long and with facets often 0.5 mm in width. From some hundreds of these, about a dozen superb specimens were selected and mounted for use with the crystelliptometer. Selenium has a tendency to twist and warp, and great care had to be exercised to select crystals with plane facets. Even with these it

[15] Drude, Ann. d. Physik, 32, p. 584, 1887.

was usually found expedient to limit the illumination to only one or two millimeters of length, so that an area of one square millimeter or less of reflecting surface was quite typical.

Much of the work was carried on at wave-lengths near the middle of the visible spectrum. The incident light was, in every case, plane-polarized at azimuth 45°. Several crystals were tested in both horizontal and vertical positions at wave-length 0.5μ, and at incidence angles 45° and 60°. At the other wave-lengths the incidence angle was maintained at 60°. The wave-lengths principally used were 0.45μ, 0.50μ, 0.55μ, 0.65μ, and 0.70μ, a range sufficient to give typical results. The wave-length 0.60μ was deferred to a separate research, for the reason that the data obtained by C. H. Skinner[16] and others with selenium contain certain anomalies near this point, while the writer's results are strongly suggestive of what, with a transparent substance, would correspond to an absorption band, in the neighborhood of this wave-length. The matter deserves, therefore, more minute investigation.

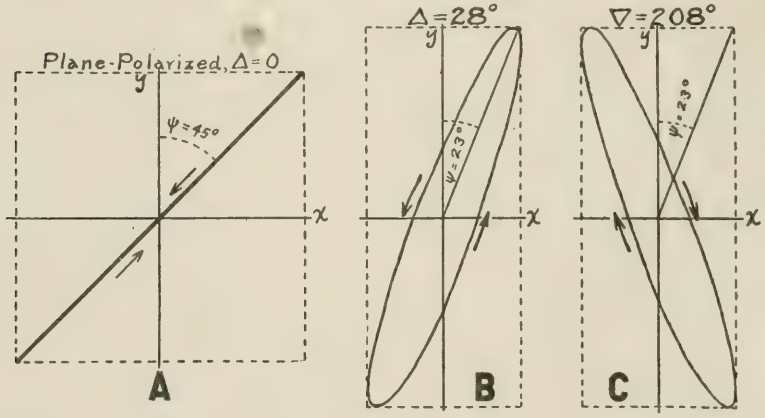

Fig. 11

A, incident vibrations, plane-polarized. *B*, *C*, elliptic vibrations viewed looking *with* and *against* the beam, respectively

Upon experimenting with a number of crystals prepared at different times, it was found that, with one or two exceptions, they gave fairly consistent results, *though all the crystals were several months old when the experiments were begun*. Great care, however,

[16] *Loc. cit.*

had been taken to keep them clean and away from contact with fumes or corrosive gases. It is quite possible that these exceptions were due to surfaces that had in some way become tarnished or contaminated, in spite of the precautions. After the first trials, three crystals were selected which gave the clearest spot-patterns, and subsequent work was confined to these. The data in the accompanying tables are the weighted means of the results obtained at the respective wave-lengths. It should be stated that those corresponding to 0.70μ have small relative weight.

Elliptic Elements for Selenium Crystal at 60° Incidence

Wave-length (Microns)	Crystal Axis Parallel to Incidence Plane		Crystal Axis Perpendicular to Incidence Plane	
	Δ	Ψ	Δ	Ψ
0.45	23° 11′	35° 22′	29° 31′	24° 25′
.50	11 52	34 14	27 54	23 15
.55	4 26	32 27	20 41	24 26
.65	13 54	34 12	21 49	27 7
.70	11 24	31 13	14 38	26 7

The data refer to the light vibrations as they would appear to an observer stationed just behind, or within, the reflecting surface of the crystal. The plane-polarized incident light vibrating as represented in Fig. 11A, the reflected light vibrates elliptically as in B. But as the latter is viewed through the crystelliptometer, the observer, *facing the oncoming reflected beam*, it would of course appear reversed, as in C. The phase difference ∇ of Sec. IV, which is what the crystellipometer analysis gives, applies to Fig. 11C; while the Δ given in the tables below, corresponding to Fig. 11B, is simply ∇ minus 180°. Ψ is the azimuth angle, whose tangent is the amplitude ratio $\frac{a}{b}$ or r of Sec. IV.

Two Incidences at Wave-length 0.5 Micron

Incidence	Axis Parallel				Axis Perpendicular			
	Δ		Ψ		Δ		Ψ	
45°	2°	11′	44°	52′	14°	1′	37°	46′
60°	11	52	34	14	27	54	23	15

The values given in the second table are capable, according to Dr. R. P. Baker, who has recently investigated the application of Drude's theory to hexagonal crystals, of yielding the two sets of optical constants of selenium corresponding to this wave-length. It is expected that this calculation will appear in a subsequent paper along with data from the further experimental work now in progress.

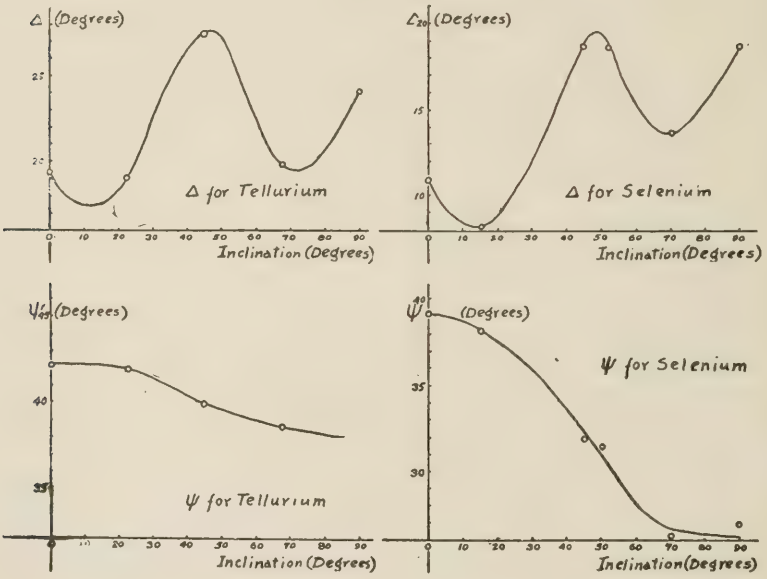

Fig. 12

Variations of Δ and Ψ with inclination of crystal, to plane of incidence, for selenium and tellurium

The above results refer only to the two principal positions of the crystal, namely, with the axis parallel to and perpendicular to the

incidence plane. Incidentally it was thought worth while to study the variations of the elliptic elements with the angle of inclination as the crystal is turned from one position to the other. Typical results are depicted in Fig. 12 with selenium and tellurium. No explanation is immediately apparent for the maxima and minima occurring in both cases in the value of Δ, but it is hoped that the mathematical theory may ultimately yield one. Further experiments of this kind would be desirable.

In conclusion, the writer wishes to pay tribute to the "team work" among the various workers at the University of Iowa who have contributed toward the progress of the research, to one phase of which this paper is devoted. The generous cooperation of the staff of the Physics Department, and especially of Dr. Sieg, who suggested the problem, is very greatly appreciated.

COE COLLEGE, CEDAR RAPIDS, IOWA,
OCTOBER, 1921.

ON THE OPTICAL CONSTANTS OF SELENIUM IN THE FORM OF ISOLATED CRYSTALS

BY
L. P. SIEG

I. INTRODUCTORY

The optical constants of absorbing materials are of considerable interest in view of the information they may contribute toward the solution of the problem of the structure of matter. The optical constants usually referred to are the index of refraction, the coefficient of absorption, and, derived from these, the reflecting power. Many substances have been studied by various observers, and long lists of these constants are to be found in our reference tables. In view of the fact, however, that the crystalline state of matter is the normal and natural state, it would appear that more attention should be centered upon obtaining these constants, as far as possible, for single crystals of the substances. This matter becomes significant if one cites, for example, the metal zinc. The fundamental crystal form of this element is hexagonal, and as such we should certainly not expect it to possess merely one set of optical constants. In this case there should be two sets, and these should differ from each other in some manner not to be predicted without intimate study of an isolated crystal. And yet our tables contain data for the optical constants of zinc, in which only one set is assumed and recorded. This result is of course to be expected when we consider that the usual practice is to take a slab of the material in question, containing countless crystals, oriented in various ways, polish the specimen, and proceed to determine the constants. The results thus obtained can mean little unless perhaps they represent some intermediate value of the true constants.

As a rule the index of refraction and the coefficient of absorption for highly absorbing substances must be determined by some indirect means, because the substances are too dense to transmit

sufficient light for direct measurements. The regular procedure is to reflect plane polarized light, usually at an azimuth of 45° from the surface in question. By virtue of the absorption and conduction possessed by the medium there is a phase difference introduced into the reflected components of the polarized light. From a knowledge of the form of the reflected elliptically polarized light one can calculate the optical constants by well-known formulas.

It was some years ago, with these ideas in mind, that I set Mr. C. H. Skinner[1] the problem of determining the optical constants of a single crystal of selenium. Skinner followed the regular Babinet compensator method, and found, as was expected, that different results were obtained with a given azimuth and incidence, depending upon whether the long axis of the hexagonal crystal was perpendicular or parallel to the plane of incidence. In such a case the ordinary formulas do not serve, but in their stead we must employ some such expressions as those developed by Drude[2] for absorbing crystalline bodies. In fact Drude,[3] and later Müller,[4] tested these expressions for a natural crystal of antimony sulphide. As far as I am aware, however, this method, with the exception of Skinner's work, has not been applied to elementary substances.

The difficulties which Skinner had in employing so small surfaces, led me to the necessity of seeking some better apparatus for this type of work. Dr. L. D. Weld[5] attacked the problem, and succeeded in devising and constructing an elegant apparatus for the work in question. While his chief problem was the development of the apparatus, he succeeded also in obtaining some data for the ellipticity of the light of various wave lengths, reflected from selenium crystals. His paper contains these data but, at the time of publication, as we were not satisfied that we fully understood Drude's[6] expressions, it was thought best not to reduce

[1] Skinner, Phys. Rev., *9*, p. 148; 1917.
[2] Drude, Ann. d. Phys., *32*, p. 584; 1887.
[3] Drude. Ann. d. Phys., 34, p. 489; 1888.
[4] Müller, Neues Yahrb. für Mineral. u.s.w. *17*, p. 187; 1903.
[5] Weld, J. O. S. A. and R. S. I. *6*, p. 67; 1922.
[6] Loc. cit.

the elliptic constants to optical constants, but to publish them as they stood. Since then I have had some opportunity of examining the equations, and further of determining directly the reflecting powers of these crystals. The experimental results, which will be discussed later in the paper, seem to agree better with Skinner's results than with Weld's.

If one accepts Drude's postulates, one has in the derived equations complete expressions for determining the optical constants for any crystal, uniaxial or biaxial. The difficulties[7] arise in the computations since direct application of the experimental data to Drude's equations yields simultaneous equations between complex quantities of high order. Drude[8] and Müller[9] simplified the equations by certain assumptions as to the relative magnitudes of certain terms. It was really to test the validity of these assumptions that the completion of Weld's work was deferred.

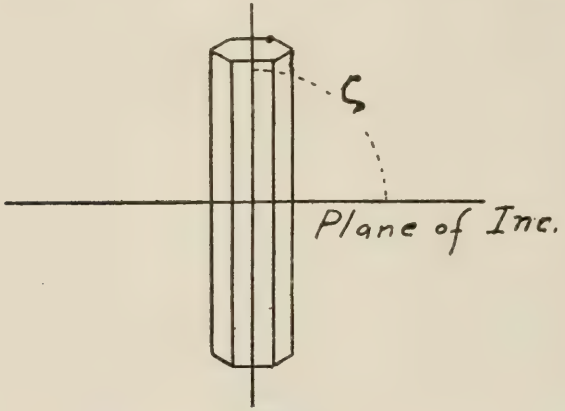

FIG. 1
Orientation of crystal with respect to plane of incidence.

[7] In the Babinet Compensator method as employed by Skinner, no serious difficulties in reducing the results arose, because in that method one adjusts conditions until a phase difference of 90° is introduced. The formulas, for purposes of calculation, are thus vastly simplified. In Weld's apparatus, on the other hand, one obtains a photographic record, and from this calculates the phase differences. It would involve an inordinate labor to repeat observations until a value of 90° for the phase difference were found.

[8] Drude, Ann. d. Phys. *34*, p. 489; 1888.

[9] Müller, Loc. cit.

II. Theoretical

One should consult Drude's[10] classic paper for the full theory and the working equations there developed. Here only the few expressions pertinent to this discussion will be considered. In Fig. 1 suppose we have represented one face of the hexagonal crystal lying perpendicular to the plane of incidence, with the optic axis in this case also perpendicular to the plane of incidence. Let ζ be the angle between the optic axis and the plane of incidence. Denote by R_s and R_p the amplitude of the components of the reflected light perpendicular and parallel respectively to the plane of incidence. Then we have

$$r=\frac{R_s}{R_p}e^{i\Delta}=\tan\Psi\cdot e^{i\Delta} \tag{1}$$

where r is a certain useful function of the angle ψ, the azimuth of the reflected elliptically polarized light, and of Δ, the phase difference introduced upon reflection. If we denote by Φ the angle of incidence, and if further one always uses an azimuth of 45° in the incident plane polarized light, so that the incident components perpendicular and parallel respectively to the plane of incidence are equal, one obtains[11]

$$\left.\begin{aligned} r_1&=\frac{\cos\Phi-\sqrt{\alpha}\,\sqrt{1-\alpha\sin^2\Phi}}{\cos\Phi+\sqrt{\alpha}\,\sqrt{1-\alpha\sin^2\Phi}}\cdot\frac{\sqrt{\gamma}\cos\Phi+\sqrt{1-\gamma\sin^2\Phi}}{\sqrt{\gamma}\cos\Phi-\sqrt{1-\gamma\sin^2\Phi}}\\ r_2&=\frac{\sqrt{\alpha}\cos\Phi+\sqrt{1-\alpha\sin^2\Phi}}{\sqrt{\alpha}\cos\Phi-\sqrt{1-\alpha\sin^2\Phi}}\cdot\frac{\cos\Phi-\sqrt{\gamma}\,\sqrt{1-\alpha\sin^2\Phi}}{\cos\Phi+\sqrt{\gamma}\,\sqrt{1-\alpha\sin^2\Phi}} \end{aligned}\right\} \tag{2}$$

where r_1 and r_2 refer respectively to the first and second principal positions of the crystal, i.e., where the optic axis is in the surface of the crystal in both cases, but in the first it is perpendicular to ($\zeta=90°$), and in the latter it is parallel to ($\zeta=0°$) the plane of incidence. Hereafter the subscripts 1 and 2 shall refer all quantities respectively to these two principal planes. In the above equations α and γ are complex quantities from which one can readily deduce the ordinary optical constants.

[10] Loc. cit. 1887.

[11] Drude, loc. cit. pp. 618-620; 1887.

It is shown by Drude that the following equations (3) are

$$\left.\begin{aligned} R_1 &= \frac{1+r_1}{1-r_1} = \frac{\cos 2\Psi_1}{1-\sin 2\Psi,\cos\Delta_1} + i\,\frac{\sin 2\Psi_1 \sin\Delta_1}{1-\sin 2\Psi,\cos\Delta_1} \\ R_2 &= \frac{1+r_2}{1-r_2} = \frac{\cos 2\Psi_2}{1-\sin 2\Psi_2\cos\Delta_2} + i\,\frac{\sin 2\Psi_2\sin\Delta_2}{1-\sin 2\Psi_2\cos\Delta_2} \end{aligned}\right\} \quad (3)$$

the final working equations for reducing the elliptical constants Ψ and Δ, for a given incidence Φ, to expressions which lead directly to the optical constants. In attempting to solve rigorously the simultaneous equations (3) one meets some difficulties. As Weld points out in his paper,[12] the suggestion was made that if one should take two different angles of incidence one could reduce the order of equations (3) to the second. Weld had, for one wavelength, used incidences both of 60° and of 45°. However, in attempting to employ these data in calculation it soon became evident that the data for 45° were useless, as they by chance yielded certain phase differences which made the errors involved too large for the method to be of service. I then tried the plan of expanding the equations (3) up to and including terms of the third degree, and a satisfactory solution was found. For simplification in equations (2) let us make the following substitutions:

$$\sin^2\Phi = A^2,\ \cos^2\Phi = B^2,\ \sqrt{\alpha} = x,\ \sqrt{\gamma} = y$$

Remembering that $R_1 = \dfrac{1+r_1}{1-r_1}$, and $R_2 = \dfrac{1+r_2}{1-r_2}$, we have after some reductions and simplifications,

$$\left.\begin{aligned} R_1 &= \frac{B^2y - x\sqrt{1-A^2x^2}\,\sqrt{1-A^2y^2}}{Bxy\sqrt{1-x^2A^2} - B\sqrt{1-A^2y^2}} \\ R_2 &= \frac{B^2x - y(1-A^2x^2)}{(xy-1)B\sqrt{1-A^2x^2}} \end{aligned}\right\} \quad (4)$$

Expanding, and assuming tentatively that both x and y are less than unity, we have

$$\sqrt{1-A^2x^2} = 1 - \frac{A^2x^2}{2} - \ldots \quad (5)$$

[12] Weld, loc. cit. p. 90.

together with a similar expression for $\sqrt{1-A^2y^2}$. Putting (5) in (4) we have, carrying only to terms of the third degree,

$$\left.\begin{aligned} R_1 &= -By+\frac{x}{B}-\frac{A^2}{2B}x^3-\frac{A^2B}{2}y^3+\frac{x^2y}{B}-Bxy^2+\ldots \\ R_2 &= -Bx+\frac{y}{B}-\frac{BA^2}{2}x^3+\frac{xy^2}{B}-\frac{A^2+2B^2}{2B^2}\cdot x^2y+\ldots \end{aligned}\right\} \quad (6)$$

No second degree terms appear in (6). While Drude,[13] and later Müller,[14] in their applications of the general expressions to obtain the optical constants of antimony sulphide did not expand the equations in the above manner, the expressions they used were exactly what one would obtain by retaining only the first two terms on the right hand sides of equations (6). I have adopted their plan in reducing Weld's data, the results of which appear later in this paper. I have, however, for two wave-lengths employed equations (6) as they stand. The resulting optical constants so obtained are not very seriously different from those obtained by using the simpler expressions, but still they differ enough to cause one to have some doubt as to the accuracy claimed by both Drude and Müller. The method of approximating to the solution of equations (6) is in general similar to Newton's method of approximation, excepting that here we are dealing with quantities x and y which are complex. In view of all the pitfalls that ordinarily might appear in applying the following method to the complex plane, I feel that it was only by a fortunate chance that any results came at all.

To make clear the method of computation used, actual calculations from data for $\lambda = 0.55\ \mu$, from Weld's[15] paper, will be outlined. Weld[16] gives for this wave-length, where $\Phi = 60°$, the following:

$$\Delta_1 = \pi + 20°41' \qquad \Psi_1 = 24°26'$$
$$\Delta_2 = \pi + 4°\ 26' \qquad \Psi_2 = 32°27'$$

[13] Loc. cit. 1888.

[14] Loc. cit.

[15] Loc. cit.

[16] Weld gives Δ, as 20° 41′, etc., but if the light is viewed as it comes toward an observer, his expression ∇, or $\pi + 20°\ 41'$ must be employed. Drude's equations are developed on this basis.

Applying these data to equations (3) we have

$$\left.\begin{aligned} R_1 &= 0.386 - 0.156\,i \\ R_2 &= 0.223 - 0.037\,i \end{aligned}\right\} \tag{7}$$

Equations (6) become

$$\left.\begin{aligned} .386 - .156\,i &= 2x - y/2 - 3/4\,x^3 - 3/16\,y^3 - xy^2/2 + 2x^2y \ldots \\ .223 - .037\,i &= -x/2 + 2y - 3/16\,x^3 + 2xy^2 - 5/4\,x^2y \ldots \end{aligned}\right\} \tag{8}$$

Employing terms of the first degree only we get the following approximations, using primes to denote approximate values

$$\left.\begin{aligned} x' &= .236 - .088\,i \\ y' &= .170 - .041\,i \end{aligned}\right\} \tag{9}$$

Substituting the values of x' and y' in the terms of (8), which were previously omitted, we have, changing signs

$$\Delta R_1 = -.0038 + .004\,i$$
$$\Delta R_2 = -.0009 - .0026\,i$$

From (8), taking the derivatives

$$-.0038 + .004i = (2 - 9/4\,x^2 - y^2/2 + 4xy)\Delta x + (2x^2 - xy - 9/16y^2 - 1/2)\Delta y$$

$$-.0009 - .0026i = (2y^2 - 5/2\,xy - 9/16\,x^2 - 1/2)\Delta x + (2 + 4xy - 5/4\,x^2)\Delta y$$

or substituting the approximate values x' and y' from (9)

$$-.0038 + .004i = (2.0244 + .0015i)\Delta x + (-.4558 - .0505i)\Delta y$$
$$-.0009 - .0026i = (-.5638 + .0572i)\Delta x + (2.0860 - .0469i)\Delta y$$

whence, solving the above,

$$\Delta x = -.00207 + .00179i,\ \Delta y = -.00092 - .00073i$$

and the next approximations for x and y are

$$\left.\begin{aligned} x &= x' + \Delta x = .234 - .086i \\ y &= y' + \Delta y = .169 - .042i \end{aligned}\right\} \tag{10}$$

No closer approximation is needed, since substitution of the values from (10) in (8) yield the following

$$\left.\begin{aligned} R_1 &= .387 - .155i \\ R_2 &= .222 - .039i \end{aligned}\right\} \tag{11}$$

which are as close to the true values as the errors of experiment warrant.

As simple as the above is in theory, the actual computations, to insure accuracy, is a matter of several hours' work. In view of

this, but especially in view of the very small corrections necessary, this detailed method was used for only one other wave-length, $\lambda = .75\mu$. The full data were reduced by following the simpler course indicated by Drude. In table 1 are recorded the results

TABLE 1
$\Phi = 60°$

$\lambda(\mu)$	$\Delta_1 - \pi$	Ψ_1	$\Delta_2 - \pi$	Ψ_2	α	γ
.45	29°31′	24°25′	23°11′	35°22′	.03421−.06887i	.00318−.04009i
.50	27°54′	23°15′	11°52′	34°14′	.04685−.06168i	.01853−.02566i
.55	20°41′	24°26′	4°26′	32°27′.	.04773−.04156i	.02729−.01378i
.65	21°49′	27° 7′	13°54′	34°12′	.03009−.04382i	.01451−.02530i
.70	14°38′	26° 7′	11°24′	31°13′	.04226−.03180i	.02755−.02321i

following the simpler calculations. For comparison, in table 2 are the results yielded by the more rigorous calculation.

TABLE 2

λ (μ)	α	γ
.55	.0473−.0402i	.0268−.0142i
.70	.0417−.0306i	.0275−.0225i

It remains to calculate the optical constants from these values of α and γ. In Drude's[17] dissertation we have

$$\alpha = a_{11} + ia_{12}$$
$$\beta = a_{21} + ia_{22}$$
$$\gamma = a_{31} + ia_{32}$$

With hexagonal crystals, β becomes equal to α, and so has not entered into our present discussion. Further, we have χ and ϵ which are two auxiliary angles defined by

$$\tan X = \frac{a_{32}}{a_{31}}, \quad \tan \epsilon = \frac{a_{12}}{a_{11}},$$

then the absorption coefficients are given by

$$k_1 = \tan X/2, \qquad k_2 = \tan \epsilon/2,$$

[17] Loc. cit. 1887. There is a change in the use of the letters α, β, and γ in Drude's two papers. Careful reading will obviate any confusion.

and the indices of refraction by

$$n_1^2 = \frac{2\ (\sin X/2)\ (\cos^3 X/2)}{a_{32}},\quad n_2^2 = \frac{2\ (\sin \epsilon/2)\ (\cos^3 \epsilon/2)}{a_{12}},$$

and the reflecting powers by the usual expressions

$$P = \frac{n^2(1+k^2)+1-2n}{n^2(1+k^2)+1+2n},$$

using the subscripts *1* and *2* for the two cases. The results follow in Table 3.

TABLE 3

$\lambda(\mu)$	k_1	n_1	ρ_1	k_2	n_2	ρ_2
.45	.92	3.66	.56	.62	3.06	.39
.50	.51	5.00	.53	.50	3.22	.37
.55	.24	5.56	.50	.37	3.72	.39
.65	.58	5.07	.55	.53	3.84	.44
.70	.36	4.95	.49	.36	4.12	.40
and by the more accurate approximations						
.55	.25	5.57	.51	.37	3.77	.39
.70	.36	4.99	.49	.33	4.18	.42

These data are graphically represented in Figs. 2, 3, and 4.

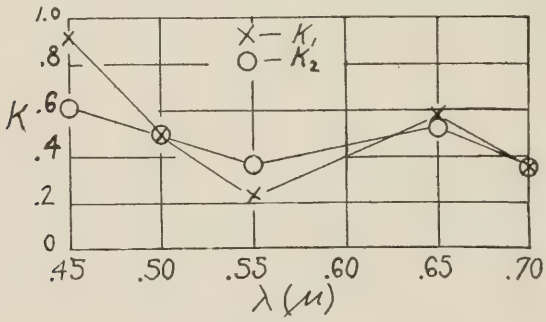

FIG. 2

Variation of the absorption coefficient with the wave-length, in the two principal positions.

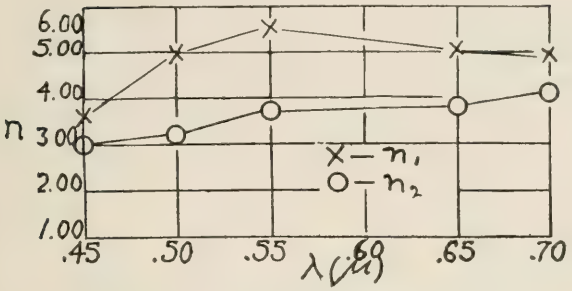

FIG. 3
Variation of the index of refraction with the wave-length in the two principal positions.

III. EXPERIMENTAL DETERMINATION OF THE PRINCIPAL REFLECTING POWERS

Some time ago, following the publication of Skinner's paper, I attempted to check his results by experiment. To measure k and n directly with crystals so small as these is practically out of the question. To use cast selenium as Wood[18] did for the direct determination of n would be begging the whole question. However, the direct measurement of the reflecting powers seemed

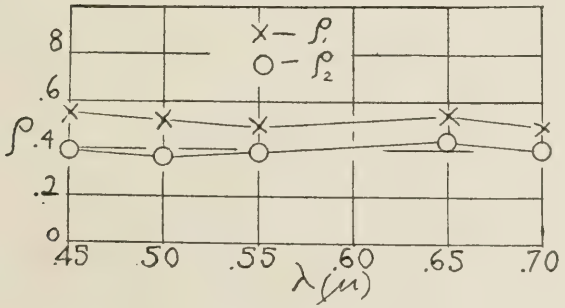

FIG. 4
Variation of the reflecting power with the wave-length in the two principal positions.

feasible and some preliminary results were obtained and published,[19] but they were subject to considerable experimental error, and small reliance was placed in them. Last fall the problem was again attacked, and while it is felt that the results are still far

[18] Wood, Phil. Mag. *3*, p. 612; 1902.
[19] Sieg, Proc. Ia. Acad. Sci. *23*, p. 179; 1916.

from possessing the accuracy which I should like, they are still much more consistent than were the former values. They at least definitely prove the contention concerning the necessity of working with isolated crystals. The arrangement of the apparatus, shown in elevation is sketched in Fig. 5. Light of the desired

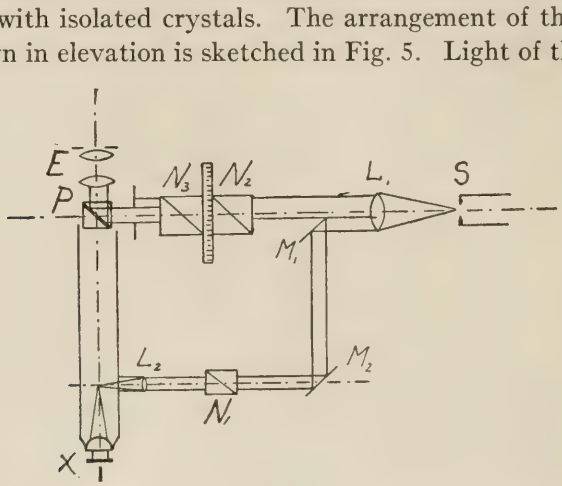

FIG. 5
Arrangement of spectrophotometer for determining the reflecting powers of small surfaces.

wave-length from the slit of the monochromatic illuminator S is made parallel by lens L_1. A portion of this beam is intercepted by mirror M_1, and then made by mirror M_2 to pass through Nicol N_1 to the opaque illuminator of the Saveur type in one of the regular metallographic microscopes of Bausch and Lomb. This plane polarized light with the electric vector horizontal was reflected through the objective system (usually an 8 mm objective was employed), and fell normally on the crystal X. In fact this is a cone of light which falls on the crystal, but the angle of the cone is only about 3°, and so for all practical purposes the incidence is normal. The crystal X is mounted on the stage in a special holder, and can be turned,without loss in centering, or in maintenance of plane, so that its long axis is either parallel or perpendicular to the electric vector of the incident polarized light. The reflected light passes up through the tube and forms a real image of the crystal surface on the interface of the double prism P. This image owes its intensity to the magnitude of the reflecting power of the crystal in the particular position it happens to

occupy. The double prism P consists of two small right angled prisms, one of them silvered with the silver film cut into a grid by removing alternate narrow strips of the silver. That portion of the image passing between the strips is viewed by the eyepiece E. The upper portion of the beam from L_1 passes through the two Nicols, N_2 and N_3, illuminating the silver strips, which are viewed by the same eyepiece E. By adjusting the Nicol N_2 (N_3 set to make the electric vector horizontal) a match in intensity can be made for each wave-length, and for each position of the crystal. With this arrangement, as far as described, only the relative reflecting powers in the two principal positions can be determined. In order to obtain the absolute reflecting powers a piece of glass, backed with silver, is substituted for the crystal at X. The absolute reflecting powers of glass, backed with silver,

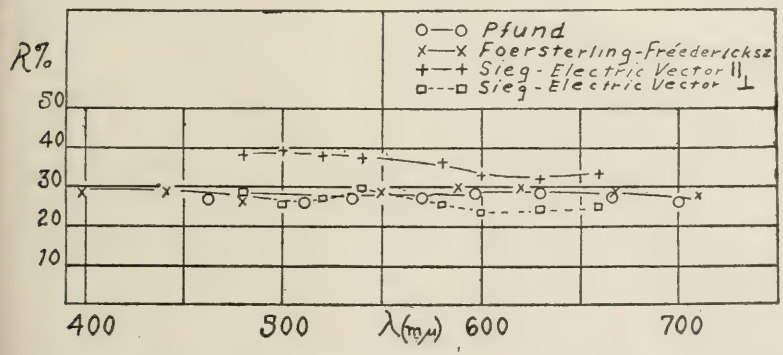

FIG. 6

Experimental determination of the principal reflecting powers of an isolated selenium crystal, compared with previous results on cast selenium plates.

being easily found in physical tables, it becomes a simple matter to translate relative reflecting powers into absolute ones. On account of the loss in light resulting from dividing the beam, and using fairly high magnification, it was not found possible to extend the results very far toward either the red or violet ends of the spectrum. Individual sets of observations were somewhat difficult to repeat with any great accuracy, but by making many different settings, and using several different crystals it is felt that the mean results are correct to 5 to 7 per cent. The extensive original

data will not be presented here. The final mean values are shown in graphical form in Fig. 6. The curves are largely self-explanatory. The data of Foersterling and Freedericksz,[20] and of Pfund[21] are recorded for the sake of comparison with the results of other observers on crystalline selenium in the form of polished plates. The essential point to re-emphasize is that here we have double reflecting powers and that in previous work we have single reflecting powers. That former values are not exactly half way between these double values is of no great moment. An exact mean would imply that the crystals were all lying on their sides, and haphazardly arranged. If any crystals were inclined to the reflecting surface of the plate, then the smaller reflecting power would predominate. In fact recently Grippenberg[22] concludes that in the process of crystallizing selenium plates, most crystals are formed "end on" to the plane surface. This agrees well with the results shown in Fig. 6, as previous values are distinctly below the average position of my results.

It happens that my data agree somewhat better with Skinner's results than with Weld's, but there is no vast difference between them. Weld was chiefly concerned with the development of an accurate instrument for the determination of optical data for small crystals, and his results on selenium were largely intended to be illustrative. They were very accurate, but if one were to make that the chief job, he would have to obtain more data, particularly using various angles of incidence. At that, however, I consider the calculated values from Weld's data as more reliable than the experimental results. I have been pleased enough to find that experiment yielded results of the proper order of magnitude.

UNIVERSITY OF IOWA,
APRIL, 1922

[20] Ann. der Phys. *43*, p. 1227; 1914.
[21] Pfund, Phys. Zeit. *10*, p. 340; 1909.
[22] Grippenberg, Phys. Zeit. *22*, p. 281; 1921.

[Reprinted from THE PHYSICAL REVIEW, N.S., Vol. XIX., No. 4, April, 1922.]

THE PATH OF A RIGID ELECTRON WHICH MOVES IN A MAGNETIC FIELD OF CONSTANT STRENGTH ROTATING WITH CONSTANT ANGULAR VELOCITY.

BY E. O. HULBURT.

SYNOPSIS.

Equations of Motion of a Rigid Electron in a Uniformly Rotating Magnetic Field of constant strength rotating with a frequency $\omega/2\pi$ in the XZ plane, are obtained. The reactions on the motion due to finite size, radiation, and the variation of mass with velocity are neglected. If initially the velocity of the electron has components only along the X-axis or the Z-axis the path of the electron is a wavy curve inside an annular space whose axis is parallel to the Y-axis. If the initial velocity of the electron has components only along the Y-axis the path is a rather complicated type of spiral winding in the general direction of the Y-axis. It is found that a high frequency of rotation of the magnetic field, of the order of 10^6, such as may be produced by means of electron-tube circuits, would not impart a great velocity to the electron.

1. A rigid electron is assumed of mass m and charge e and of size small in comparison with the displacements it undergoes. The electron is subjected to a magnetic field whose components are H_x, H_y and H_z. The reactions on its motion due to the variation of mass with velocity and to radiation both from the electron and from the magnetic field are neglected. Let x, y and z be the positional coördinates of the electron. When electromagnetic units are used, the equations of motion of the electron are, in Newtonian notation,

$$\begin{aligned} \frac{m}{e}\ddot{x} &= H_y\dot{z} - H_z\dot{y}, \\ \frac{m}{e}\ddot{y} &= H_z\dot{x} - H_x\dot{z}, \\ \frac{m}{e}\ddot{z} &= H_x\dot{y} - H_y\dot{x}. \end{aligned} \tag{1}$$

Let H rotate in the XZ plane with a constant angular velocity of frequency $\omega/2\pi$. Then

$$H_x = H\cos\omega t, \qquad H_y = 0, \qquad H_z = H\sin\omega t. \tag{2}$$

Introducing (2) into (1) gives

$$\begin{aligned} \frac{m}{e}\ddot{x} &= -H\dot{y}\sin\omega t, \\ \frac{m}{e}\ddot{y} &= H(\dot{x}\sin\omega t - \dot{z}\cos\omega t), \\ \frac{m}{e}\ddot{z} &= H\dot{y}\cos\omega t. \end{aligned} \tag{3}$$

These equations may be integrated and the constants of integration determined from the initial conditions.

2. Suppose initially that when $t = 0$, $x = y = z = \dot{x} = \dot{y} = 0$ and $\dot{z} = w$. The solutions[1] of (3) are in this case,

$$\begin{aligned} x &= \frac{wH^2e^2}{2\nu m^2}\left[\frac{\cos(\nu+\omega)t}{(\nu+\omega)^2} - \frac{\cos(\nu-\omega)t}{(\nu-\omega)^2}\right] + \frac{2\omega wm^2}{H^2e^2}, \\ y &= \frac{wHe}{\nu^2 m}[\cos\nu t - 1], \\ z &= \frac{wH^2e^2}{2\nu m^2}\left[\frac{\sin(\nu+\omega)t}{(\nu+\omega)^2} + \frac{\sin(\nu-\omega)t}{(\nu-\omega)^2}\right], \end{aligned} \tag{4}$$

where

$$\nu = \sqrt{\frac{H^2e^2}{m^2} + \omega^2}.$$

To reduce to the case of a stationary magnetic field, ω is placed equal to zero in (2) and (4). Then $\nu = He/m$, $H_x = H$, $H_y = H_z = 0$, and (4) becomes

$$\begin{aligned} x &= 0, \\ y &= \frac{wm}{He}\left(\cos\frac{He}{m}t - 1\right), \\ z &= \frac{wm}{He}\sin\frac{He}{m}t. \end{aligned} \tag{5}$$

We see from (5) that the electron moves in a circle in the YZ plane of radius wm/He and with the centre at $(0, -wm/He, 0)$. This is in agreement with formulas given by others.[2]

3. The determination of the path of the electron from equations (4) is facilitated by noticing that

$$\sqrt{\left(x - \frac{2\omega wm^2}{H^2e^2}\right) + z^2} = \frac{wH^2e^2}{2\nu m^2}\sqrt{\frac{1}{(\nu+\omega)^4} + \frac{1}{(\nu-\omega)^4} - \frac{2\cos\nu t}{(\nu^2-\omega^2)^2}}. \tag{6}$$

[1] I am indebted to Dr. E. W. Chittenden of the Mathematics Department for these solutions.

[2] J. J. Thomson, Conduction of Electricity through Gases, page 107, 1906.

This transformed to polar coördinates is

$$\rho = \sqrt{a + b \cos 2\nu t}, \tag{7}$$

where ρ, a and b are determined by identifying (7) with (6). From (7) it follows that at no time does ρ become greater than $\sqrt{a+b}$ or less than $\sqrt{a-b}$. Hence the electron moves always between two coaxial cylindrical surfaces of radii $\sqrt{a+b}$ and $\sqrt{a-b}$, the axis of the surfaces being parallel to the Y-axis. The equation of the axis is

$$x = \frac{2\omega w m^2}{H^2 e^2},$$

$$z = 0.$$

Further, from (4) it is seen that y varies harmonically with the time reaching the extreme values 0 and $-2\omega \times He/\nu^2 m$. Therefore the electron moves always between the two planes $y = 0$ and $y = -2\omega He/\nu^2 m$. With these facts in mind it is found that the electron pursues a wavy orbit inside the annular space as indicated in Fig. 1. The electron does not in general retrace its path during its subsequent excursion through the space to which it is confined.

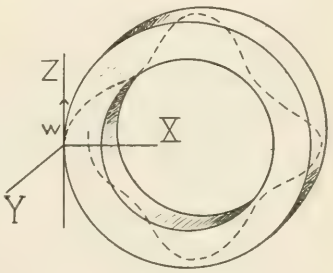

Fig. 1.

The case in which the electron has initial velocity components only along the X-axis is by symmetry the same as the case just discussed, and the path of the electron is of the same form as that of Fig. 1.

4. If the initial conditions are $t = 0$,

$$x = y = z = \dot{x} = \dot{z} = 0, \text{ and } \dot{y} = v,$$

the solutions of (4) are:

$$\begin{aligned}
x &= \frac{vH^3e^3}{2\nu^2m^3}\left[\frac{\sin(\nu+\omega)t}{(\nu+\omega)^2} - \frac{\sin(\nu-\omega)t}{(\nu-\omega)^2}\right] + \frac{vHe}{\nu^2 m}\sin\omega t, \\
y &= \frac{vH^2e^2}{\nu^3m^2}\sin\nu t + \frac{v\omega^2}{\nu^2}t, \\
z &= -\frac{vH^3e^3}{2\nu^2m^3}\left[\frac{\cos(\nu+\omega)t}{(\nu+\omega)^2} + \frac{\cos(\nu-\omega)t}{(\nu-\omega)^2}\right] - \frac{vHe}{\nu^2 m}\cos\omega t + \frac{2vm}{He}.
\end{aligned} \tag{8}$$

The path of the electron is found by transforming equations (8) to a new set of axes X', Y', Z', such that the new coördinates x', y', z', are

related to the old ones x, y, z by the relations

$$x' = x - \frac{vHe}{v^2 m} \sin \omega t,$$

$$y' = y - \frac{v\omega^2}{v^2} t,$$

$$z' = z + \frac{vHe}{v^2 m} \cos \omega t - \frac{2vm}{He}.$$

The new axes remain always respectively parallel to the old ones. The new origin moves on a spiral wound on a cylinder, circumventing the cylinder $\omega/2\pi$ times a second and advancing with a velocity whose Y-component is $v\omega^2/v^2$. The radius of the cylinder is $vHe/v^2 m$; the equation of its axis is

$$x = 0,$$

$$z = \frac{2vm}{He}.$$

With reference to the new axes the path of the electron is of the same form as discussed in section (3). With reference to the old axes the path is a rather complicated type of spiral winding in the general direction of the Y-axis.

5. A special case occurs when ω is large. This is of interest because it is possible by means of electron tube circuits to produce magnetic fields which rotate with frequencies of the order of 10^6, although with the apparatus available at present such fields are relatively weak. If ω is large and if the initial conditions are those of section (2) we find that y, z, $\dot{x}$, $\dot{y}$, $\dot{z}$ are small and x is large. With the initial conditions of (3) and with ω large, x, z, $\dot{x}$, $\dot{z}$ are small, $y \doteq vt$ and $\dot{y} \doteq v$. We see from this that even when the magnetic field rotates at a high frequency the electron does not acquire a very great velocity.

STATE UNIVERSITY OF IOWA,
November, 1921.

MINIMUM SOUND ENERGY FOR AUDITION FOR TONES OF HIGH FREQUENCY.

[Reprinted from THE PHYSICAL REVIEW, N.S., Vol. XIX., No. 5, May, 1922.]

MINIMUM SOUND ENERGY FOR AUDITION FOR TONES OF HIGH FREQUENCY.

BY C. E. LANE.

SYNOPSIS.

Minimum Energy for Audition for Tones above 2000 p.p.s.—Using the new tone generator developed by Hewlett as the source of sound, experiments were carried on at night and out of doors on a platform raised 5 meters above the ground and with the listening ear 150 cm. from the source. The amplitude of vibration of the diaphragm of the generator was calculated from the electrical input, and from it the corresponding sound intensity at the ear of the listener was computed, assuming the amplitude of the sound wave at the diaphragm the same as that of the diaphragm and correcting for the concentration of sound around the axis of symmetry as experimentally determined. No correction for the effect of the listener's head, however, was made. *Sensitivity frequency curves* for eight normal ears, ages 19 to 35 years, are reproduced. The minimum audible intensity was found to remain practically constant at 7×10^{-8} ergs per cm.^{2} for frequencies from 2,000 to 14,000 p.p.s., but above 14,000 the sensitivity decreased more and more rapidly until at between 18,000 and 20,000 p.p.s., depending on the individual, an intensity of 0.1 erg per cm.^{2} was inaudible. *A variation with age* was observed, the upper frequency limit being considerably higher for children and lower for older persons than for normal young adults.

Distribution of Sound Intensity around a Hewlett Tone Generator for 2,000 to 15,000 p.p.s. was determined roughly by studying the minimum amplitude for audition as a function of the angular position of the listener with reference to the axis of symmetry. The sound is largely concentrated in a cone of about 20°, the angle decreasing as the frequency increased, so that for 10,000 p.p.s., for instance, the intensity 150 cm. along the axis was fifty times as great as if the distribution had been spherical.

INTRODUCTION.

THE purpose of this investigation was to determine in absolute units the sensitivity of the ear for tones ranging from 2,000 p.p.s. to the upper limiting audible frequencies. Experiments have been made by many different observers for determining the minimum amount of sound energy for audition but most of these investigations have been concerned with tones of frequencies below 4,000 p.p.s. Little work at the higher frequencies has been done because of the limitations of the apparatus used. In the early work done by Wien[1] and in the recent work of Kranz[2] the ear was shown to reach a maximum sensitivity in the neighborhood of 2,000 p.p.s. At the Chicago meeting of the National Academy of Sciences, November 14, 1921, Fletcher and Wegel presented some results

[1] Archiv. für die gesamte Physiologie, Vol. 97, pp. 1–57, 1903.

[2] PHYS. REV., (2) xvii, 1921, page 384.

which they had obtained for sensitivity of normal ears. These results showed that the ear reached a maximum sensitivity in the neighborhood of 2,000 p.p.s. and then remained constant to 4,000 p.p.s. No attempt was made by them to obtain measurement in absolute units at higher frequencies.

Apparatus and Method.

In this investigation the new tone generator,[1] developed by C. W. Hewlett, was used as a source of sound. The radiating surface of the tone generator consisted of a thin aluminum diaphragm, 10 cm., in diameter, actuated by a flat coil carrying variable polarizing (direct) and alternating currents. One side of the diaphragm was wholly unobstructed for the free passage of sound waves from its surface, while the type of coil used did not greatly affect the passage of sound from the opposite side. Amplitudes of motion of the diaphragm for minimum audible sounds were calculated from the corresponding current input by using Hewlett's theory, adapted to suit the particular arrangement used. At any frequency it can be shown that the amplitude of motion of the diaphragm is proportional to the product of the direct and alternating currents and that the energy radiated is proportional to the square of this product.

The work was done out of doors with the observer on a small platform five meters above the ground and the sound source 1.5 meters from his ear. This arrangement was assumed to reduce reflections from the ground to an amount negligible compared to the energy received directly. It is evident that the ratio of direct energy from the apparatus to reflected energy from the ground, assuming the most unfavorable conditions, would be of the order of magnitude of the ratio of $(2 \times 5)^2 : 1.5^2 = 44 : 1$.

The work was done at night to minimize the interfering effect of noise. The face of the sound source was turned toward the observer and the ear to be tested was turned toward the source. It was found by trial that it was not necessary to close the other ear on account of the sound shadow of the head.

The amplitude of the sound wave was assumed to be the same at the diaphragm surface as that of the diaphragm. The total energy emitted was calculated assuming it to be the same as would be radiated in a plane wave. Therefore, the total amount of sound energy, E_t, given off by one side of the diaphragm per second would be given by—

$$E_t = \tfrac{1}{2} S \rho V A^2 \omega^2.$$

S = area of each side of the diaphragm.

[1] Phys. Rev., (2), xix, p. 52, 1922.

ρ = density of the air.
V = velocity of sound in air.
A = amplitude of vibration of the diaphragm.
ω = 2π times the frequency.

In a simple spherical distribution the energy flux per sq. cm. at a distance of D from the source would be $E_t/2\pi D^2$. This is an average value for energy flux on the surface of a hemisphere of radius D. If R is the ratio of the actual value, J, at the position of the observer's ear to the average value, then

$$J = \frac{E_t R}{2\pi D^2}$$

R was determined for each frequency from the following considerations.

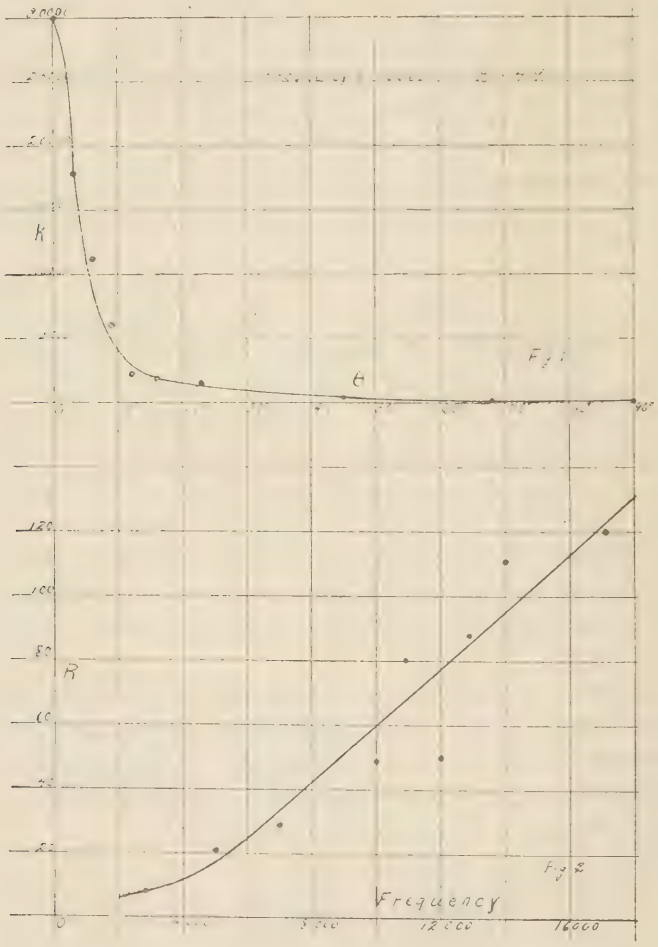

Fig. 1.
Fig. 2.

The sound field was assumed to be symmetrical with respect to the axis of the diaphragm. This axis (horizontal) also passed through the ear of the observer. The relative distribution of energy flux on the surface of a sphere of radius D was determined by calculation from the measurement of minimum audible amplitude of the diaphragm as it was turned about a vertical axis, through its center, through an angle of 180°. Fig. 1 shows energy density so determined at 10,000 p.p.s. plotted in arbitrary units as a function of the angle. Between 90° and 180° it is roughly symmetrical with that between 90° and 0°. It is seen that the major part of the energy from the side of the receiver toward the observer is concentrated within a cone making an angle of 20° at the center of the diaphragm. The assumption that all of the energy radiated from one side of the diaphragm is contained in the corresponding beam indicated in Fig. 1 is justified on the basis of the theory of radiation of a plane wave from a circular aperture. Using this distribution curve and the calculation of the total energy flux, as determined from the tone generator theory, the energy flux per sq. cm. could be calculated at any point on the sphere of radius D. The ratio, R, of the energy flux density at the position of the ear to that which would be obtained in a simple spherical distribution was found to be 49 : 1 at the frequency illustrated in Fig. 1. Fig. 2 is a plot of R as a function of frequency. This shows, as might have been expected, that the energy becomes more and more concentrated in a narrow beam as the frequency increases.

Results and Conclusions.

The value of J was determined at different frequencies for eight normal ears. In order to show the variation in sensitivity of the ears graphically the $\log_{10}(1/J)$ was plotted against frequency. Logarithms were necessary because of the wide variation of sensitivity of the so-called normal ears. The audiograms—sensitivity frequency curves for the ears—thus obtained are shown in Figs. 3, 4, 5 and 6. Figs. 3, 4 and 5 are audiograms for individual ears, Figs. 4 and 5 being the left and right ears of the same individual. Fig. 6 shows the results obtained for eight ears from seven different individuals. Each of the persons from whom the data were obtained was between 19 and 35 years of age. The value of J for a frequency of 2,000 p.p.s. as obtained by taking the mean value of $\log_{10}(1/J)$ for this frequency, was found to be 7×10^{-8} ergs. This is about three times the value given by Kranz, about seven times the value obtained by Fletcher and Wegel[1] and 30,000 times the value given by Wien for the same frequency. But litt'e variation in the ear sensitivity

[1] R. M. S. pressure in dynes per sq. cm. is equal to 6.5 $\sqrt{J}$.

from this was noted until a frequency of 14,000 p.p.s. was reached. As the frequency was increased above 14,000 p.p.s., the sensitivity decreased more and more rapidly. Between 18,000 p.p.s. and 20,000 p.p.s., a frequency was reached for each individual ear at which it was no longer

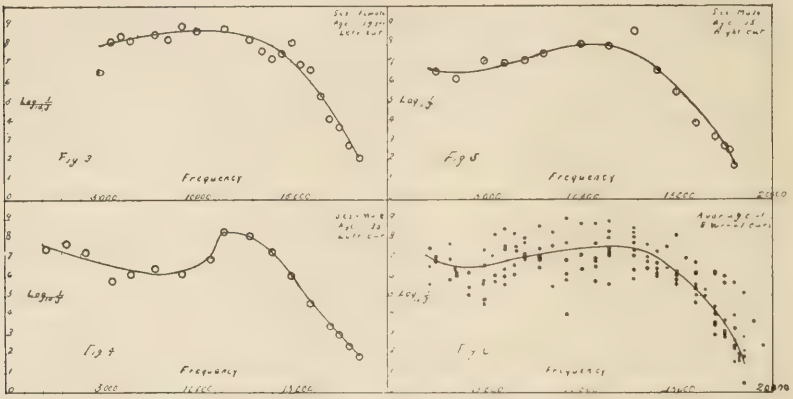

Figs. 3, 4, 5, 6.

possible to produce a tone of sufficient intensity for audition by means of the apparatus used. The mean value for J at a frequency of 18,500 was about .1 erg. If it had been possible to produce tones of greater intensity, no doubt the threshold of audition would have been found at a higher frequency. However, it would appear from the rapid decrease in sensitivity at these high frequencies, it would be necessary to increase the intensity of the tone by a very large amount in order to raise the threshold to a frequency noticeably higher.

Special attention is called to the age of the individuals tested. There is certainly a great variation in ear sensitivity, especially for high frequencies, with the age of the individuals. Some qualitative results were obtained which show that children under fifteen years of age may hear tones as high as 25,000 cycles when the intensity is no greater than for a value of J corresponding to .1 erg. On the other hand, persons past fifty years of age are not able, as a rule, to hear such high frequencies as were heard by the individuals whose ears were tested.

There are a few sources of inaccuracy in the results obtained which should be mentioned. The value of R varies a great deal from the mean value. However, this error is small and may be neglected when we consider the fact that the observational errors for the same frequency and the same individual may themselves vary by as much as 50 per cent. It should also be mentioned here that the work was not done under

perfectly quiet conditions and the very slight disturbance would make the ear appear less sensitive than it actually is. The work was done at night but some noise was present due to the sound of insects. J has been defined as the amount of sound energy necessary for audition flowing per second through a sq. cm. It is evident that the value of J obtained by this method only gives the amount of energy which would flow through a sq. cm. were the head not at the position for which J was calculated. Further, if it may be assumed that the sound is completely absorbed by the head, the figures given for sensitivity represent the energy per sq. cm. flowing into the ear. If the head may be assumed to be a plane reflector the actual energy density at the ear is twice that in the first case. The actual condition is between the two extremes but in all probability nearer the second. However, it will be seen from the figures that a factor of two would involve a negligibly small relative error.

In conclusion I wish to express my appreciation of the assistance rendered during the experimental work by Dr. C. W. Hewlett and other members of the staff of the University of Iowa as well as the suggestions offered in the interpretation of the data by various members of the scientific staff of the Western Electric Company, Inc.

Physics Laboratory,
State University of Iowa,
June, 1921.

Reprinted for private circulation from
THE ASTROPHYSICAL JOURNAL VOL. LV, No. 5, June 1922

THE BROADENING OF THE BALMER LINES OF HYDROGEN WITH PRESSURE

BY E. O. HULBURT

ABSTRACT

Photographic width of the Balmer lines of hydrogen for pressures up to 135 mm.— There is some question as to whether among the possible causes of the widening of lines with pressure, the decrease of mean free path is important. A theoretical calculation of the width to be expected for hydrogen lines if the length of the train of waves emitted is limited by the time between molecular collisions, gives for a temperature of 600° C. and a pressure of 100 mm a width of about 0.04 A, between wave-lengths where the intensity is one-tenth of that at the middle. Experimentally, however, it was found that a pressure of about 100 mm gave photographic images 80 A wide. Purified hydrogen in a capillary discharge tube was excited by condensed discharges and a series of spectrograms were taken for pressures from 0.2 to 135 mm. The exposure time was 30 minutes in each case and the discharge was regulated so that the intensity of the central portion of Hβ was practically the same for all pressures. As shown by Figure 2, Hβ, Hγ, and Hδ behave very much alike. The fact that the actual width is much greater than that computed theoretically indicates that the widening of spectrum lines is probably due to some other cause, perhaps electrical fields.

Introductory.—The former Lord Rayleigh has summarized the causes which interfere with the absolute homogeneity of spectrum lines under five headings:[1] (1) The translatory motion of the radiating particles in the line of sight operating in accordance with Doppler's principle. (2) A possible effect of the rotation of the particles. (3) Disturbance depending on collision with other particles either of the same or of another kind. (4) Gradual dying down of the luminous vibrations as energy is radiated away. (5) Complications arising from the multiplicity of sources in the line of sight. To which is added a sixth cause proposed and investigated by Merton.[2] (6) The effect of an electric field on the radiating particle. The electric field may be that imposed on the electrodes of the tube or may be the field of neighboring atoms as suggested by Stark,[3] or a superposition of the two.

The researches of Fabry and Buisson[4] and Michelson[5] have demonstrated that for pressures of the luminous gas below one

[1] *Philosophical Magazine*, **29**, 274, 1915.
[2] *Proceedings of Royal Society*, **92**, 322, 1915.
[3] *Elektrische Spectralanalyse chemischer Atome*, 1914.
[4] *Journal de Physique*, **2**, 442, 1912.
[5] *Astrophysical Journal*, **2**, 251, 1895.

millimeter of mercury (1) is probably the only cause of broadening of the spectrum line. This cause is, however, impotent to explain the tremendously greater broadening produced in certain lines by the use of either greater pressures or condensed discharges, and therefore recourse must be had to the other causes mentioned. Of these the effects of (2) and (4) must perforce be omitted from discussion, for our present knowledge of atomic constitution and the nature of radiation is insufficient for a successful consideration of the effect of rotation of the luminous particle and of the damping of the vibration as the energy is radiated away. We also neglect (5), for this merely aggravates the effects of the other causes. There remain (3) and (6). From their recent work on the energy distribution in the broadened lines of hydrogen, helium, and lithium by high pressures stimulated by condensed discharges, Merton and Nicholson[1] concluded that cause (6) was all important in producing the broadening and that (2) played no part whatsoever. Their observations were concerned with the *form* of the broadened line and did not touch upon the *magnitude* of the broadening. In view of the novelty of this conclusion it seemed of interest to determine the magnitude of the broadening. The present work was carried out to this end and the photographic widths of Hβ, Hγ, and Hδ of the Balmer series of hydrogen were measured for pressures from 0.2 to 135 mm of mercury. The broadening which might be expected from cause (3) under the conditions of the present experiment was then calculated and was found to be considerably less than the observed broadening. This evidence thus supported the conclusions of Nicholson and Merton in that it threw doubt on the validity of (3) as a cause of the widening.

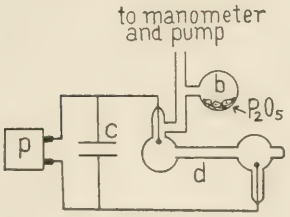

FIG. 1

Experimental.—Hydrogen, prepared from hydrochloric acid and zinc and purified through sodium hydroxide solution and concentrated sulphuric acid, was passed into the end-on discharge tube *d*, Figure 1, made of glass with aluminum electrodes arranged out of line with the

[1] *Philosophical Transactions*, Vol. 216, 459, 1916.

PLATE VII

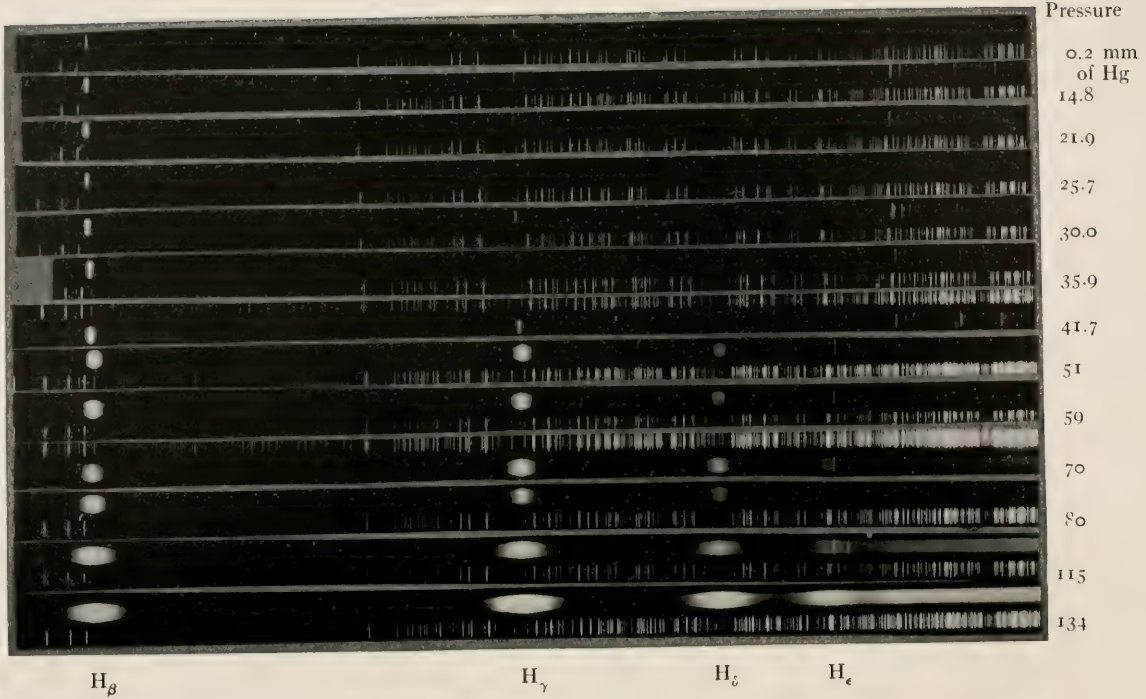
Pressure
0.2 mm of Hg
14.8
21.9
25.7
30.0
35.9
41.7
51
59
70
80
115
134
H_β
H_γ
H_δ
H_ϵ

capillary. The capillary was 10 cm long and 5 mm in diameter. A bulb *b* with phosphorous pentoxide was sealed to the tube. The tube was connected by glass tubing about a meter in length to a bulb of perhaps 200 c.c. capacity and a mercury manometer. The total capacity of the discharge tube and glass system, perhaps 300 c.c., was filled with hydrogen at various pressures and no change in pressure was observed when the discharge was run continuously for an hour. The condenser *c*, Figure 1, of capacity of about 0.01 μ F, which discharged through the tube, was charged by the 25,000 volt transformer *p*. The spectra were photographed in the first order of a concave grating of 2 meters radius of curvature and ruled 14,435 lines to the inch, the dispersion being about 8.8 A per mm.

Spectra of hydrogen were taken for a series of pressures from 0.2 to 135 mm. These are shown in Plate VII with the iron arc comparison spectrum. The tube was maintained rigidly in position throughout the series and the time of exposure was 30 minutes for each spectrogram. In order to obtain conditions for the various pressures that might be compared the procedure was as follows: A glass prism spectroscope was trained on the hydrogen tube so that Hβ could be observed visually at the same time that the spectrum was being photographed. A small region at the center of the line was isolated by the second slit of the prism-spectroscope and observed by a low-power eyepiece. A comparison line was reflected into the field of view of the eyepiece obtained by illuminating a portion of the first slit with the light from a tungsten lamp filtered through a greenish-blue filter. The intensity of the comparison line was maintained constant, and by adjusting the power consumed in the hydrogen tube the intensity of the central portion of Hβ was kept approximately constant for each pressure. It is worthy of remark that the condensed discharge through the hydrogen tube was at all times an oscillatory one, the frequency as measured by a wave-meter being 0.28×10^6 alternations a second. For this reason the electrical power consumed in the tube could not be determined in a simple manner by electrical methods.

The widths in angstrom units of Hβ, Hγ, and Hδ were measured from the photographs of Plate VII, and were plotted in Figure 2

as ordinates against pressures in mm of mercury as abscissae. The measurement of the width was made simply by judging the points on the edges of the lines on the plates where the blackening became slight and measuring between these points. This was manifestly inaccurate but was deemed sufficiently precise for the purpose in hand. The last two points on each of the curves were too high, for at these two highest pressures it was not possible to

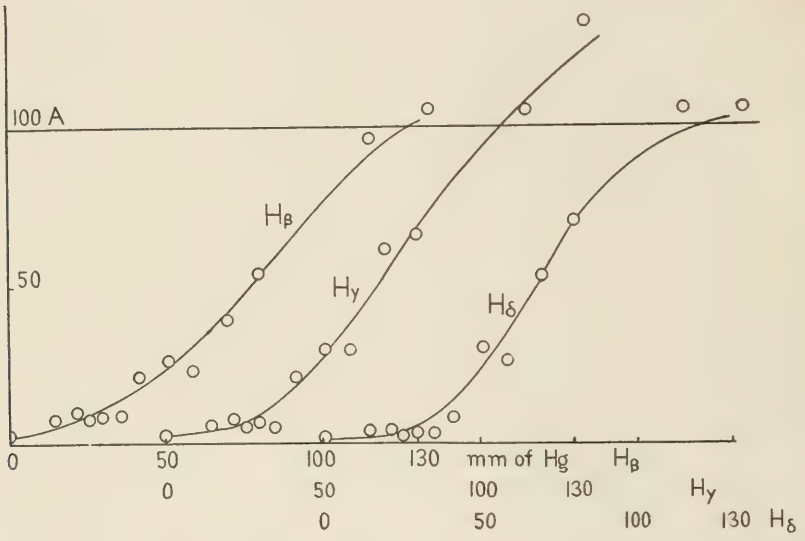

FIG. 2

reduce the intensity of the center of Hβ to the intensity used at the lower pressures and still maintain sufficient voltage to render the gas luminous.

Theoretical.—The third cause of widening mentioned in the introduction is the disturbance of the free vibration of the radiating particle due to encounters with other bodies. The simplest supposition open to us is that an entirely fresh start is made at each collision, so that we have to deal with a series of regular vibrations of finite length. The problem thus arising has been treated by Godfrey[1] and Schönrock.[2] The Fourier analysis of the limited

[1] *Philosophical Transactions*, **195**, 329, 1899.

[2] *Annalen der Physik*, **22**, 209, 1907.

train of waves of length r gives for the intensity of various parts of the spectrum line

$$I = I_0 \frac{\sin^2 \pi r\left(\frac{1}{\lambda_0} - \frac{1}{\lambda}\right)}{\left(\frac{1}{\lambda_0} - \frac{1}{\lambda}\right)^2} \tag{1}$$

where I_0 and λ_0 are the intensity and wave-length respectively of the center of the spectrum line and I and λ are the respective quantities in any part of the line. r is the length of the train of waves in cms. λ_0 is the wave-length which would be dominant if r were infinitely long.

We calculate r from the Kinetic Theory of Gases,[1] to be

$$r = \frac{c}{4\nu\sigma^2}\sqrt{\frac{m}{\pi RT}} \tag{2}$$

where ν is the number of molecules per unit volume at the pressure and temperature in question, σ is the diameter of the sphere of molecular action from the Kinetic Theory standpoint, m is the mass of the molecule, c is the velocity of light *in vacuo* and R is the gas constant.

Substituting (2) in (1) gives

$$I = I_0 \frac{\sin^2 \frac{\pi c}{4\nu\sigma^2}\sqrt{\frac{m}{\pi RT}}\left(\frac{1}{\lambda_0} - \frac{1}{\lambda}\right)}{\left(\frac{1}{\lambda_0} - \frac{1}{\lambda}\right)^2} \tag{3}$$

Formulae (2) and (3) assume slightly different forms depending on the methods used in averaging the velocities of the gas particles. These have been discussed by Tait,[2] Rayleigh,[3] and Godfrey,[4] and it seems that the various methods yield expressions which differ from (2) and (3) by not more than 10 per cent. This difference is small enough to be ignored in the present case.

[1] Jeans, *Dynamical Theory of Gases*, p. 32.

[2] *Transactions Royal Society of Edinburgh*, **33**, 74, 1886.

[3] *Proceedings Royal Society, A*, **76**, 440, 1905. [4] *Loc. cit.*

Comparison of theory and experiment.—By giving values to ν corresponding to the various pressures I was determined by means of (3) as a function of λ for each pressure, and from this the width of the spectrum line was calculated for each pressure. At a temperature 0° C. and 760 mm pressure ν was taken to be 4×10^{19}. The diameter of a hydrogen molecule was 2×10^{-8} cm. We assume that the gas was always at the temperature 600° C. $c=3\times10^{10}$, $R=9.3\times10^{-17}$, and $m=2.25\times10^{-24}$ grams. Introducing these values into (3) leads to

$$I=I_0\frac{\sin^2 \dfrac{10634\,p}{\left(\dfrac{1}{\lambda_0}-\dfrac{1}{\lambda}\right)}}{\left(\dfrac{1}{\lambda_0}-\dfrac{1}{\lambda}\right)^2}, \qquad (4)$$

where p is the pressure of the hydrogen in mm of mercury. When I was computed from (5) for pressures within the range of the present measurements, curves of the type shown in Figure 3 were obtained. The width of the line increased with increase of pressure but was very narrow in all cases. For example, Figure 3 gives a curve for $\lambda_0=5000$ A and $p=100$ mm of mercury, and the width of the line represented by the curve is less than 0.04 A. In short, the broadening with pressure to be expected from the collision theory, or cause (3), is smaller by a different order of magnitude than that observed in the Balmer lines of hydrogen. In order to make the calculation agree approximately with the experimental measurements as far as the actual magnitude of the broadening is concerned, the number of equation (5) should be about 75 instead of 10634. The calculation was made on the basis

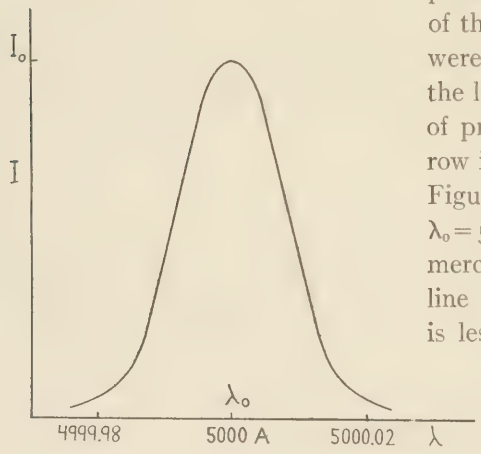

FIG. 3

of molecular hydrogen. Many researches, however, point to the fact that a disruptive discharge breaks the hydrogen molecule into its component atoms. If, then, we use values referring to the atoms, that is, employ a value for ν twice as great and for σ and m one-half as great as the molecular values previously substituted in (3), we find the number of equation (4) to be larger by the square root of two. This would make the calculated width of the line still smaller.

Discussion.—The discrepancy between theory and experiment is probably not to be found in experimental errors, approximate though the measurements were, or in a wrong assumption of the temperature of the gas. The discrepancy should rather be attributed to more fundamental errors of assumption, and in the light of the present experiment and the experiments of Merton and Nicholson (*loc. cit.*) we are ready to abandon cause (3) as inadequate and to turn to cause (6) as a possible explanation, as suggested by Merton (*loc. cit.*).

If the principal cause of the widening be attributed to the influence of an electric field on the radiating particle we may well inquire whether the electric field is the one imposed on the tube or is due to neighboring particles. Careful experiment on the separate influences of pressure and intensity of the discharge on the broadening combined with the known data of the Stark effect might differentiate between the two actions if they both exist. If the broadening is due to the electric field of neighboring particles we again return to the idea of collision. The effect of the collision upon the radiating particle, however, would be not merely a disturbance of the radiating centers by a mechanical shock but a profound momentary influence of an intense electric field.

STATE UNIVERSITY OF IOWA
IOWA CITY, IOWA
April 1922

[Reprinted from The Physical Review, N.S., Vol. XIX, No. 6, June, 1922.]

HALL EFFECT AND SPECIFIC RESISTANCE OF SILVER FILMS.

By G. R. Wait.

Synopsis.

Hall Effect and Specific Resistance of Silver Films, 200 to 20 μμ. Thick.—In agreement with previous results, the specific resistance increased more and more rapidly with decreasing thickness, becoming infinite for about 20 μμ. On the other hand the Hall coefficient was found to be the same in the films as in the bulk metal. The thicknesses were computed from the weight of silver in each film, assuming the density that of the bulk metal. The films were obtained by chemical deposition.

Theory of Electrical Conduction in Thin Films.—After discussing various proposed theories in the light of the above results, it is concluded that these and other facts are in harmony with the simple conception that the film consists of granules, each having the properties of the bulk metal, and that conduction occurs only along strings of granules in contact.

Brashear Method of Depositing Silver Films.—Exceptionally hard films whose resistance, instead of decreasing, increased slightly with time, were obtained by using about four times the amount of sodium hydroxide specified.

Historical.

Miss Stone[1] in 1898 found that the specific resistance of thin silver films was greater than that of bulk metal, and that it increased with decreasing thickness of the film down to a thickness between 50 μμ and 60 μμ, where it almost suddenly became very great. Other workers in the field of films, since that time, have obtained similar results. Among the contributions to this field may be mentioned the work of Vincent,[2] Longden,[3] Patterson,[4] Reide,[5] Swann,[6] Pogany[7], Weber and Oosterhuis,[8] and King.[9]

Moreau[10] made an investigation of the Hall effect in silver and nickel films. He found that the coefficient of the Hall effect in the films was not constant for various thicknesses, being much greater than the value in bulk metal for the smaller thicknesses and decreasing to smaller values than that in bulk metal at a thickness greater than about 60 μμ.

[1] Phys. Rev., (1), vi, p. 1, 1898.
[2] Ann. d. Chim. et Phys., 7, p. 421, 1900.
[3] Phys. Rev., (1), xi, p. 40 and p. 84, 1900.
[4] Phil. Mag., 4, p. 652, 1902.
[5] Ann. d. Physik, 6, p. 881, 1914.
[6] Phil. Mag., 28, p. 467, 1914.
[7] Phys. Zeitsch., 15, p. 563, 1914.
[8] K. Akad. Amsterd. Proc., 19, p. 597, 1917.
[9] Phys. Rev., (2), x, p. 291, 1917.
[10] Journ. de Physique, 10, p. 478, 1901.

EXPERIMENTAL METHODS.

Deposition of Films.—The resistance of films, obtained by the Brashear[1] method of chemical deposition, decreased with time, a phenomenon experienced by other investigators. By increasing to about four times the amount of sodium hydroxide specified in this method, exceptionally hard films were obtained, their resistances increasing slightly with time, occasioned probably by a combination of the film with gases of the air. Cleanliness of the glass surface and purity of chemicals were extremely important in the production of satisfactory films.

Determination of Thickness.—The thickness of a film was determined from the weight of the silver composing it and, as a check, from the weight of silver iodide after the film was transformed. The densities of silver and silver iodide were assumed to be those of bulk silver and ordinary silver iodide respectively. Determinations of thickness by the two methods of weighing were used only after they had been proved superior to the Newton ring method by a rather extensive investigation.

Measurement of Resistance.—The resistance of the films was measured as soon as possible after they were dry, or usually a few minutes after being removed from the solution. In order to determine the contact resistance between the electrode and the film, four electrodes were placed upon the film. Let a, b, c, d represent the four electrodes, c and b being placed very near to each other at one end of the film and a and d near each other at the opposite end; then using the measurements of resistances between a and b, a and c, a and d, b and c, b and d, c and d, six equations were formed from which two independent values of the film's resistance were found.

Measurement of the Hall Effect.—The films were cut into the shape shown in Fig. 1, the electrodes for the primary current being connected at A and B, while those for the measurement of the Hall effect were connected at C and D. The latter electrodes could be shifted accurately by removing some of the film at one or both of the narrow necks. The equipotential points could thus be easily found and permanently retained.

The film under investigation was placed in a holder made of insulating fiber (Fig. 2) upon which had been fastened three electrodes and a groove

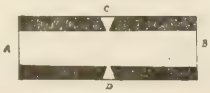

Fig. 1.

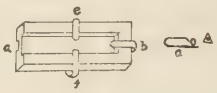

Fig. 2.

for the fourth. The electrodes were made of spring phosphor bronze

[1] Astrophys. Journal I, p. 252, 1898.

and shaped as shown in Fig. 2. In order to secure the best contact between the electrode and the film, the point *o* of the electrode was fitted into a small dent of a triangular piece of copper whose underside had been made plane. This triangular piece of copper was placed upon the film with a small piece of aluminum foil separating the two. The above holder and design of electrodes were used in the measurements of the resistance as well as the Hall effect.

The experimental arrangement for the measurement of the Hall effect consisted of a double potentiometer and is shown in Fig. 3, A, B, C, and D are resistance boxes, the resistances in B and in C being large in comparison with the resistances in A and in D, respectively. The drop across the box D was so adjusted that it was just equal to the Hall effect. G_1 is a Leeds and Northrup galvanometer having a sensitiveness of about 10^{-8} volts per mm. scale deflection. B_2 is a storage cell furnishing the primary current for F. A_1 is an ammeter for the measurement of this current, which was varied (by altering R) from approximately 0.0015 to 0.03 ampere, the thicker films permitting the larger currents.

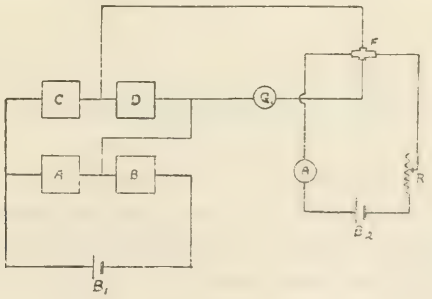

Fig. 3.

Since the Hall effect was measured by taking the drop in potential across D necessary to prevent a deflection of the galvanometer G_1, then $E = -\frac{A V \frac{1}{2} (D_1 - D_2)}{(A + B)(C + D)}$, where E is the value of the Hall effect in c.g.s. units, D_1 and D_2 are the values of D necessary to prevent a deflection of G_1 with the magnetic field in opposite directions, A, B and C are the resistances shown and V s the potential difference of the cell B_1, measured in c.g.s. units.

The magnetic field was furnished by a large electro-magnet, the faces of whose pole pieces were four centimeters in diameter and one centimeter apart. The field strength was measured by means of a bismuth spiral calibrated for this purpose. The measurement of the field for different currents through the magnet over a duration of five years using

two different spirals gave differences of only 0.8 per cent. The fields used were from 5,000 to 12,000 lines per cm.[2]

TABLE I.

Film	ϵ.	E/HI.	R	Residuals.	Film	ϵ.	E/HI.	R	Residuals.
42	21	320	805	30	9	40	216	20.7	19
34	21	...	$3 \times 10''$	..	33	43	164	3.5	2
28	22	...	$3 \times 10''$	.	37	46	188	8.3	..
36	23	321	200	..	27	47	118	3.9	6
41	28	325	9.7	3	31	50	138	3.8	4
33	29	314	10.8	9	7	51	143	12	11
35	31	284	5.8	17	4	51	170	8.8	7
23	33	295	8.5	6	30	54	185	5	11
32	36	232	8.6	2	40	89	108	2.8	2
18	38	182	10	13	29	109	74	3.7	5
26	38	202	9.4	18	10	182	47	2.6	7
43	40	212	9.3	8					

EXPERIMENTAL RESULTS.

In Table I. are given the results of the present investigation. In column one is given the film number; in column two, its thickness in millimicrons, the mean of the thickness obtained upon the basis of the weight of the silver and its weight after it had been transformed into silver iodide. The third column gives E, the Hall e.m.f. divided by the product of the magnetic field H, in e.m.u. and the primary current I in c.g.s.u. In most instances four different strengths of the magnetic field were used, in which case there were four values for $E\,HI$; the one given in column three is the mean of the four. The mean residual for each film is recorded in column five. A particular residual was obtained by taking the differences between the mean $E\,HI$ and the $E\,HI$ for that particular field and current. Column four contains the resistance in 10^{-6} ohms per cm.[3] of each film. For two films the Hall effect is not given, this being due to the fact that it was not possible to obtain measurements of the effect for films having such high resistances. Although considerable data have been obtained by various investigators upon the variation of specific resistance of films with their thickness, and also som data upon coefficients of the Hall effect, the author, is not aware that the two phenomena have ever been studied for the same film. It is important, if results upon the two phenomena be used in conjunction with each other, that they be obtained from the same film. This would be even more important for films that change with time.

Specific Resistance.—In Fig. 4 is plotted ρ, the specific resistance, against

ϵ, the thickness of the films. It will be seen that for films having the greater thickness the ρ is very little greater than its value in bulk silver, and seems to approach asymptotically to that value. The value of ρ gradually increases toward decreasing thickness until about 50 $\mu\mu$ is reached, when it increases much more rapidly. It will be seen that the value of ρ seems to approach ∞ in the neigh- borhood of 20 $\mu\mu$.

Hall Effect.—As is well known, the Hall e.m.f., E, is given by the rela-

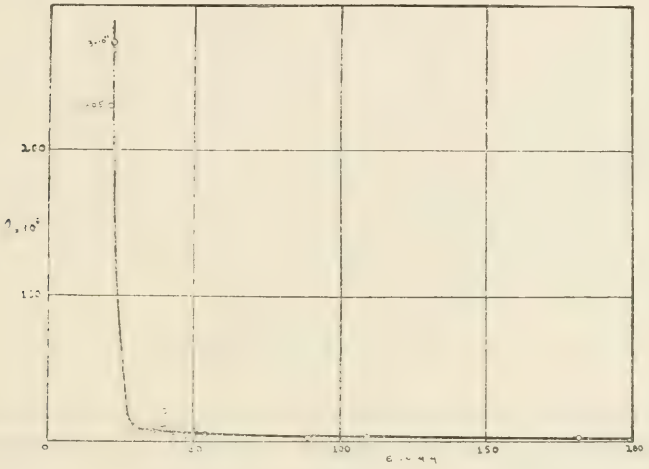

Fig. 4.

tion $E = (HI/\epsilon)\alpha$ wherein α is the Hall coefficient. In numerous tests with silver films herein described, E was found to be proportional to H and I. The values of E/HI for various values of ϵ, given in Table I., are

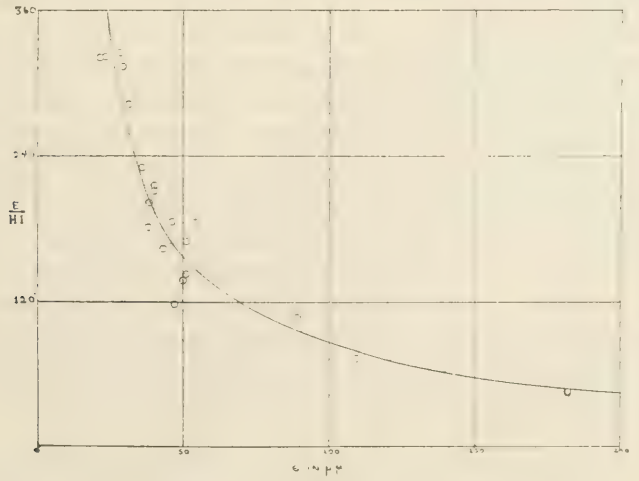

Fig. 5.

plotted in Fig. 5 in which is drawn a hyperbola with $\alpha = 0.00084$, the accepted value of the Hall coefficient in silver. It will be seen that the curve fairly represents their mean. Thus the value of α, the Hall coefficient, in the films is the same as in bulk silver and is constant for all thicknesses investigated greater than 23 $\mu\mu$.

Theoretical Considerations.

Assuming that there is a diffusion of negative electrons through the spaces between the atoms, that the electrical properties of the metal arise entirely in the average motion impressed by external circumstances on the swarm of electrons which are otherwise moving about quite freely in the spaces between the atoms, and that the distribution of velocities among them at any instant is precisely that specified by Maxwell's law, the electron theory of the Hall effect leads to the following well-known result for the electric field in the z-direction at right angles to the direction of current density in the y-direction J_y, and to the magnetic field of intensity H in the x-direction:

$$E_z = -\frac{3\pi}{8Nec} HJ_y.$$

E_z is the electric field of uniform intensity produced in the z-direction, the current density, J_z, being supposed zero; N is the number of free electrons per unit volume, e the charge on the electron, and c the ratio of units. This result is in accord with experiments in a large number of cases. Without further assumptions it is not possible to apply the result of the theoretical investigation to a thin film wherein the material is supposed to consist of granules not in the intimate contact obtaining in bulk form.

Let us assume that J_y' is constant through the xz cross-section of any granule and that the packing of granules is sufficiently close to warrant the approximate statement that the current through the film cross-section is carried by the granules and not by gaps. Consider the xz cross-section. We are concerned with a gross result rather than what occurs in the individual granule, and consequently we are induced to idealize the location of these granules in order to simplify our own thinking. Let us assume that we have a layer of similar granules of thickness Δx. All of them may not be carrying current and in those that do, the current densities are not the same. The total difference of potential across this film will be $\Sigma E_z' \cdot \Delta z$ where Δz is the approximate width of the granules, and $\Delta x . \Delta z$ is the area of the granule in cross-section. But,

$$\Sigma E_z' \Delta z = -\frac{3\pi}{8Nec} H \Sigma J_y' \Delta z = -\frac{3\pi}{8Nec} H \Sigma J_y' \frac{\Delta x \cdot \Delta z}{\Delta x}$$

or

$$E = -\frac{3\pi}{8\,Nec} HJ,$$

where J is the current per unit thickness.

In the expression for E_z, the value of current density J_y was introduced by assuming that in the granule $J_y = \sigma E_y$, where σ is the conductivity determined by the same assumptions as to electrons, and E_z is the electric field. In applying this theory to the granule, we have thus assumed consistently that the theory applies to the granules the same as to the bulk metal. Our conclusion is that the coefficient should be constant irrespective of the specific resistance or thickness of the film, and that it should be the same as in bulk metal. Both of these points are verified by experiment as already shown. The assumptions seem therefore to be in agreement with the experimental facts, and the author will assume the correctness of this simple theory of thin films, namely that they are composed of granules having the property of bulk metal and of conducting gaps which give resistance only.

J. J. Thomson[1] explained the variation of specific resistance of films with thickness by assuming that the mean free path of the conducting electron was less in the film than in the bulk metal. The curve drawn based upon such an assumption, however, is not so steep as the experimental curve. Patterson suggests that this may be due to a gradation in the density of electrons from the inner part of the film toward the outer boundaries. Swann[2] assumed that the mean free path of the conducting electron varied with temperature the same in the film as it does in bulk metal. By measuring the specific resistance of platinum films over a wide range of temperature he obtained results which show that Thomson's explanation is not in agreement with experimental facts. The present investigation furnishes direct information regarding Patterson's suggestion pertaining to the change in the number of conducting electrons per unit volume. From Patterson's assumptions alone, the thinner films should show the greater value for the coefficient and its value should approach that in bulk metal as the thickness is increased. Instead of this, however, the Hall coefficient is always constant, having the same value as in bulk metal.

Moreau[3] explained his results for the Hall effect in films by means of Vincent's transition layer theory. The results of the present investigation, however, are not in accord with Moreau's results nor with Vincent's theory. Now Vincent was able to explain the rapid increase in specific

[1] Phil. Mag. (4), p. 675, 1902.
[2] Loc. cit.
[3] Phil. Mag. (4), p. 675, 1902.

resistance upon the assumption that the specific resistance of the film of metal between the transition layers was that of ordinary metal, while the resistance of the layers was constant and quite great. Obviously, the Hall coefficient, which depends upon the number of conducting electrons per cm.^{3} would therefore change at the thicknesses where the increase in specific resistance is so marked. No such change was detected experimentally.

Swann,[1] found the three following interesting facts: (*a*) Thick films underwent an increase in resistance with increase in temperature, (*b*) thin films underwent a decrease in resistance with increase in temperature, and (*c*) films having a thickness between these had an apparent zero temperature coefficient of resistance over most of its range. Now, the change in a film's resistance, when its temperature is increased slightly, will depend at least upon the three following factors: (1) Expansion of the glass, upon which the film is deposited. (2) Expansion of metal composing the groups bringing them into more intimate contact. (3) The regular temperature coefficient of the metal. For very thin films the effect of (2) will be to decrease the resistance, as the temperature is increased; for thicker films this effect may be very small as may be seen from the following considerations. In the case of very thin films it was seen that a very small addition of groups produced a great decrease in the resistance, but that the addition of the same number of groups to a thick film decreased the resistance very much less. Similarly an expansion of groups might be expected to produce a great change of resistance in the case of thin films, and a small change in the case of the thicker ones. The above considerations make possible an explanation of the so-called temperature coefficients, and permits the simple assumption that the addition of groups have the effect of decreasing the number of conducting paths through the film, by combining many that are already present and making them straighter and wider.

The general conclusion is that the experiments herein recorded and all others in thin films are in harmony with the simple theory here proposed, namely that we are dealing with granules which have the same electrical properties as bulk metal and with conducting gaps.

The author wishes to express his appreciation to the Physics Department of the State University of Iowa for valuable assistance received, and especially to Professor G. W. Stewart under whose direction this work was carried on, and whose encouragement and criticisms made the work possible.

PHYSICAL LABORATORY, STATE UNIVERSITY OF IOWA.

[1] Phil. Mag. (4), p. 675, 1902.

THE SIMPLE RIGIDITY OF A DRAWN TUNGSTEN WIRE AT INCANDESCENT TEMPERATURES

By William Schriever

Abstract

Rigidity of a 10-mil drawn tungsten wire to 2000°K.—To avoid errors due to end effects, two lengths of the same wire were mounted in series and heated by the same current so that the middle portions of both were at the same temperature. The apparatus was placed in an evacuated tube; the torque was applied magnetically and measured by the twist in a cold fine tungsten wire. The rotations of the mirrors attached to the ends of the heated wires were noted within a few seconds after application of the torque, since at the higher temperatures even a twist of 0.1° per cm exceeded the elastic limit. On the three successive runs made, the rigidity increased progressively due to the crystal growth in the temperature range above 1600°K. For the recrystallized or equiaxed wire the values of the modulus obtained on the third run are: 21.7 at 300°K, 21.0 at 1030°K and 3.4 at 1985°K, all times 10^{11} dynes/cm^2.

Introduction

UP to the present time, as far as is known to the writer, the simple rigidity of a drawn tungsten wire at incandescent temperatures has not been determined.

Koch and Dannecker[1] seem to have made the first determination of the simple rigidity of a metal at temperatures which approach the melting point of the material; they made observations on wires of some twenty-two elements and alloys using the usual torsion-pendulum method. They allowed for the changes in periods caused by the temperature gradients along the wires, by making several assumptions and approximations together with graphical interpolations and extrapolations—a very indirect method.

When the temperatures desired are not too high the whole apparatus may be heated in some sort of an oven and the temperature gradients in the wires, the "end-effects," thereby avoided. Since an apparatus which could be heated to 2000°K did not seem feasible, the following simple method of allowing for the end-effects was devised. The same torque was applied to two different lengths of the same piece of electrically heated wire whose central portions were at the same temperature. When the angle of twist of the shorter was subtracted from that of the

[1] Koch and Dannecker, Ann. der Phy. **47**, 197-227, 1915

longer the difference was the angle of twist produced by that torque in a uniformly heated wire of a length equal to the difference of the lengths of the two wires. This scheme necessitated using a static method for making the simple rigidity determinations. Since glowing tungsten is oxidized in the open air or in the presence of water vapour, the wires and attached apparatus were enclosed in an evacuated vessel.

Streintz[2] and Meissner[3] have found that the simple rigidities of all the metals which they investigated are independent of the manner of heating. While it is possible, it is not probable that tungsten wire would show a difference. In fact Dodge[4] has found that Young's modulus of tungsten wire is independent of the method of heating between 0° and 1000°C. The writer has thus far not attempted to check this point for higher temperatures experimentally.

Apparatus and Procedure

A schematic drawing of the wires and attached apparatus, all of which was enclosed in a large glass tube, is shown in Fig. 1. The short length and the long length of the tungsten wire on which the simple rigidity determinations were to be made are shown at L_1 and L_2 respectively. L_3 is a relatively fine tungsten wire attached by means of a clamp to the lower end of L_2, the axes of the wires being in the same straight line; L_3 was never heated and was used to measure the torque applied to L_1 and L_2. The top end of L_1 was clamped securely in the end of the vertical round brass rod to which were attached the soft iron cross-bar *Fe* and the mirror M_1. An electro-magnet acting through the glass tube on the iron cross-bar made it possible to rotate the rod and therefore to twist the series of wires.

The lower end of L_3 was held securely in a clamp to which were attached the mirror M_4 and the weight W; the clamp had a rectangular cross section and could thus slide up and down, as the wires changed in length due to thermal changes, but could not turn. The weight of the clamp and W (170g) served to hold the wires taut.

To the clamp which held together L_2 and L_3 was attached the mirror M_3 and an inverted U of iron wire which dipped into the mercury in the annular iron mercury-cup *Hg*. The mercury-cup and the parts of the brass frame were so insulated that the heating current flowed in at P_1, down R_1 to *Hg*, up L_2 and L_1, and out at P_2. L_1 and L_2 were one continuous piece of tungsten wire separated into two segments by a brass clamp to which was attached the mirror M_2.

[2] Streintz, Pogg. Ann. **150**, 368-380, 1873
[3] Meissner, Ann. der Phys. Beibl. **34**, 756, 1910
[4] Dodge, Phys. Rev. **11**, 311, 1918

Each mirror was made by depositing a film of platinum on a cover-glass by an evaporation method, covering the film side with another cover-glass, and mounting the two in a light copper frame. Silvered mirrors put together in the same manner were tried first, but the mercury vapor soon caused them to lose their reflecting power almost completely, while the platinized mirrors seemed to be in perfect condition after several months of exposure to mercury vapor. The asbestos tape which was wound around the three cross-heads to make the frame fit the glass tube snugly, had previously been heated to 350° C in a tube attached to a vacuum pump, in order to get rid of the organic matter which would otherwise discolor the glass tube of the final apparatus and thus make optical temperature measurements inaccurate.

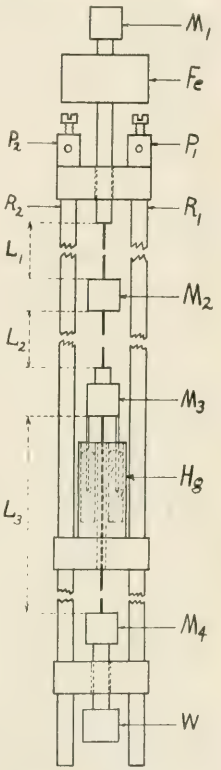

Fig. 1. Torsion system for determining the rigidity.

After the frame had been placed in the tube and the mirrors were in proper adjustment, annealed coiled copper leads were pulled out of side-arms and made fast in the binding posts P_1 and P_2. The top of the large tube was then closed by sealing on a cap to which was attached a pump connection. A side-tube of small diameter was sealed into the large tube so that mercury could be let into the mercury-cup through it. This apparatus was placed in a long electrically heated oven from which protruded the pump connection and the small side-tube to which was attached a bulb containing sufficient clean air-free mercury. A drying-tube containing phosphorus pentoxide was placed in the pump-line. The vacuum pump was operated for about eight hours during which time the oven was maintained at a temperature slightly above 325° C. After a side discharge-tube had indicated an x-ray vacuum for three hours, the apparatus was sealed off. As soon as the apparatus was cool enough to be handled, it was removed from the oven, set in a vertical position and the mercury cup filled. The side-tube was sealed off at once thus leaving the wires in a sealed glass tube.

The scales on which the angles of twist of the mirrors M_1, and M_2 and M_3 were observed, were complete circles 360 cm in circumference, while the scale for M_4 was a short arc having the same radius. For each mirror was provided an illuminated wire and a lens for focusing its image

on its scale. Thus for each degree of twist of a mirror the image of the wire moved along the scale 2 cm.

The method of measuring the d ameters of the wires has already been reported.[5] L_1, L_2 was a piece of 10-mil drawn tungsten wire of lot B24-3822 of the Nela Research Laboratory; L_3 was a piece of 6-mil tungsten wire of the same lot. Their diameters were respectively $252.3 \pm 0.3\mu$ and $156.72 \pm 0.16\mu$ and their lengths 11.91 cm, 26.62 cm and 25.03 cm at room temperature. The heating current for the 10-mil wire was furnished by large lead storage cells and was regulated by varying the number of cells and by three variable rheostats in parallel; it was measured by means of a 0.01 ohm standard resistance in conjunction with a Leeds and, Northrup potentiometer. The temperatures of the wires were measured with a Holborn-Kurlbaum type optical pyrometer; corrections were made for the absorption of the enclosing glass tube. The pyrometer used and the methods emp'oyed have already been described.[6]

The length of L_1 was such that its mid-point was at the same temperature as the mid-point of the longer section L_2 when the same heating current passed through both. Another piece of 10-mil tungsten wire 17.6 cm long, mounted in the same frame, was heated by constant currents so that its mid-point assumed the following temperatures: 1065, 1200, 1338 and 1492°K. For each mid-point temperature the temperatures of various points along the wire were obtained. The curves in Fig. 2 showing the temperature as a function of the distance along the wire measured from the top clamp, gave the information necessary to determine the minimum length for L_1.

The 10-mil tungsten wire was next heated to about 1600°K for just a few seconds in order to get rid of most of the graphite coating which always remains on a tungsten wire when its drawing is completed. Then a constant current of 4.200 amperes was passed through the wire and the brightness temperatures of the mid-points of L_1 and L_2 were found to be 1123 and 1119°K respectively. The lower section of the wire had been polished somewhat before mounting it, and consequently its graphite coating was more completely removed by the first heat ng; this may help to account for the observed 4° difference. At any rate the change in the simple rigidity caused by a 4° change in temperature could not have been detected since it was less than the experimental error.

The lengths of all the wires were measured and checked several times during the process of making the rigidity determinations; the measurements were always made at room temperature. The length of $(L_2 - L_1)$ at

[5] Schriever, Proc. Iowa Acad. Sci. **24**, 235-240, 1917
[6] Schriever, Proc. Iowa Acad. Sci. **28**, 69-82, 1921

a higher temperature was obtained by adding the expansion caused by he heating, the expansion being calculated by using the first term of Worthing's expansion formula.[7] Allowance was also made for the expansion of the diameter of the wire. The effects of the two expansions tended to balance in the final calculations, and if they had been neglected the error would have been small.

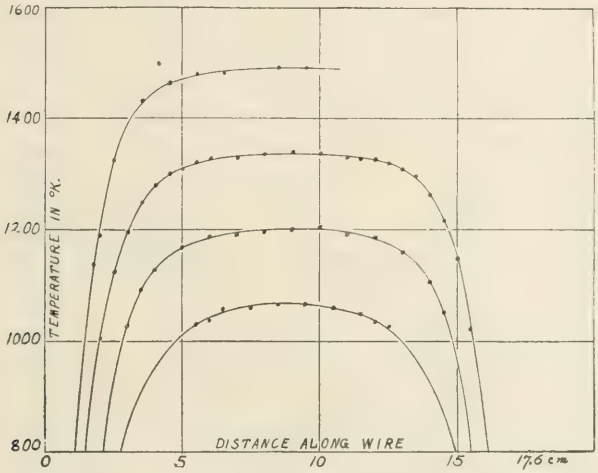

Fig. 2. Temperature distributions along a ten-mil heated tungsten filament.

After the wires L_1 and L_2 had been heated to a definite known temperature, the iron cross-bar, *Fe* in Fig. 1, was twisted through a small angle and the positions of the images reflected from the four mirrors on the four circular scales were recorded. The cross-bar was then twisted still further in the same direction and the final positions of the images were recorded. The cross-bar was then twisted back to the neutral position and the whole operation was repeated. From six to eight such sets of observations were made at each temperature. The temperature was kept constant by taking pyrometer readings at the beginning, after the third set of observations, and after the sixth set of observations, and making slight adjustments in the heating-current rheostats when necessary. At the higher temperatures the temperature was checked. and adjusted if necessary, after each set of observations. The temperature determinations were certainly correct to within 5°.

The temperature distribution along the wire at the top of L_1 was very approx mately like that at the bottom of L_2, and that of the bottom end

[7] Worthing, Phys. Rev. **10**, 638, 1917

of L_1 like that at the top end of L_2. The twists in L_1 and L_2 may each be considered to have been made up of two twists, first, a twist in the end-sections in which there were temperature gradients, and second, a twist in the center section all of which was at a uniform temperature. Therefore the difference of the total twists in L_1 and L_2 gave the twist in a section of the wire of length (L_2-L_1), the temperature of all of which was that of the mid-point of either wire. Let α, β, γ, and δ be the angles turned through by the mages reflected from M_1, M_2, M_3 and M_4 respectively. Then $(\alpha-\beta)=\varphi_1$ was twice the twist in L_1; $(\beta-\gamma)=\varphi_2$ was twice the twist in L_2; and $(\gamma-\delta)=\varphi_3$ was twice the twist in L_3. Therefore $(\varphi_2-\varphi_1)$ was twice the twist in a uniformly heated section of wire of length (L_2-L_1); φ_3 was twice the twist in a length L_3 of the cold wire. $\varphi_3/(\varphi_2-\varphi_1)$ obviously should be a constant for twists which do not exceed the elastic limit. The average value of this ratio for each six to eight sets of observations taken at a constant temperature was determined and its probable error calculated. $(\varphi_2-\varphi_1)$ was kept small; it was always of the order of 0.1 degrees per centimeter.

The mirrors M_2, M_3 and M_4 were displaced from the axis of rotation 0.27, 0.38 and 0.23 cm respectively. Therefore the observed angles of deflection were not twice the angles through which the mirrors were turned. Corrections for M_2 and M_3 were calculated and applied in determining the correct va'ues of β and γ for each set of observations. The deflections of M_4 never exceeded one degree and in most cases were too small to be observed.

The torque required to twist a wire of radius R and length L through an angle θ is

$$T=\tfrac{1}{2}\pi\eta\theta R^4/L$$

where η is the modulus of simple rigidity of the wire. In the apparatus employed in this work the same torque acted on the cold and hot wires. Therefore we have

$$\eta_h=\frac{\theta_c}{\theta_h}\left(\frac{R_c}{R_h}\right)^4\frac{L_h}{L_c}\ \eta_c$$

where the subscripts h and c refer to the hot and cold wires respectively. L_h/R_h^4 was calculated for each temperature, due allowance being made for the expansion as explained above. $R_c^4\eta_c/L_c$, a constant for the apparatus, was found to be 215.9 ± 0.8.* θ_c/θ_h is obviously the average $\varphi_3/(\varphi_2-\varphi_1)$, the determination of which has already been explained.

Moduli of rigidity, as given in tables of physical constants, have, in general, been obtained from angles of twist which were not great enough to

* The value of $\eta_c=14.34\pm0.04\times10^{11}$ dynes per cm^2 was obtained from Dr. L. P. Sieg; he used a static method on a piece of the 6-mil wire taken from the same spool.

cause the elastic limit of the material to be passed. In this work on tungsten the angles of twist were less than 0.1 degree per centimeter and yet, at the higher temperatures, this was considerably beyond the elastic limit. This was shown by the fact that, after the final twist was given, the mirrors M_2 and M_3 turned slowly back toward the original positions. Twists which would not strain the wire beyond the elastic limit at the highest temperatures, could not be measured accurately enough with this apparatus. In order to obtain consistent and fairly accurate results the following method of taking scale readings was used. Two card sliders to indicate the position of the beam of light reflected from a mirror, were placed on each circular scale. Four of the sliders were set at the

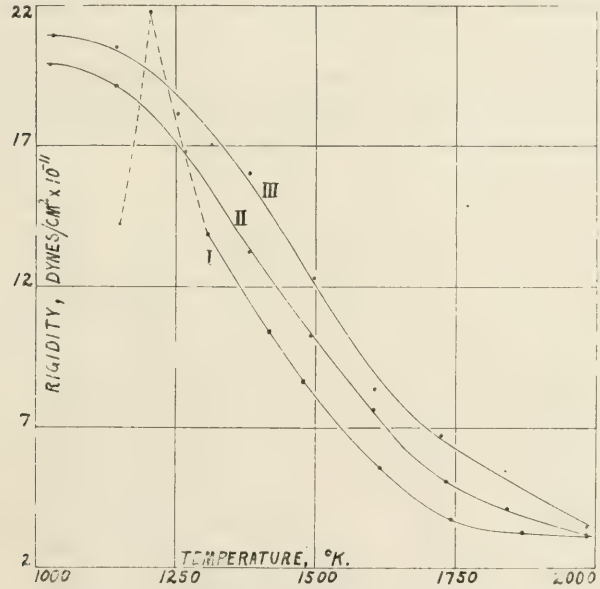

Fig. 3. Rigidity as a function of temperature for three successive runs.

initial positions of the reflected beams on the four scales. The final twist was given and the other four sliders were adjusted in the following order: first for M_3, second for M_2, third for M_4, and last for M_1. The wire was then twisted back to the initial position and the positions of the sliders were recorded. M_1 and M_4 did not change their positions, and M_2 twisted back only very slowly relative to the rate of M_3; this will explain the order of making the slider adjustments. The second slider for M_3 was in position in about two seconds after the final twist was given. The variations in the value of $\varphi_3/(\varphi_2-\varphi_1)$ for a given set at the higher temperatures, are probably largely due to the inaccuracy of the settings of the second slider for M_3.

The wire was heated for about an hour at each of the nine different temperatures of the first series, and about three quarters of an hour at each temperature of the second series. The last series was taken more rapidly; each temperature was maintained for about thirty-five minutes.

The probable error of the modulus of rigidity for each temperature was calculated from the probable error of the mean of $\varphi_3/(\varphi_2-\varphi_1)$, that of the constant of the cold wire, and that of the radius of the hot wire. The probable errors of the length-measurements were neglected since they were relatively small compared to those of the fourth powers of the radii.

Results

Curves showing the modulus of rigidity of the 10-mil drawn tungsten wire as a function of the temperature, are shown in Fig. 3. The data for each curve were obtained at a series of increasing temperatures; the curves were obtained in the order indicated by the numbers. A recapitulation of the results is shown in Table I.

Table I

Set No.	Length of hot section (cm)	R_h^4 (10^{11}cm^4)	$\Omega = 215.9L/R^4$ (10^{-10})	$\Gamma = \frac{\varphi_3}{\varphi_2-\varphi_1}$	Brightness temperature	True Temperature	$\eta_h = \Omega\Gamma$ (10^{-11} dynes/cm^2)
			Series I				
1	14.73	2576 ± 16	12.33 ± .10	11.55 ± .09	1094°K	1150°K	14.23 ± .16
2	.74	2576	.33	17.72 .43	1144	1205	21.80 .52
3	.75	2585	.33	11.28 .20	1238	1308	13.88 .25
4	.76	2585	.32	8.46 .13	1336	1418	10.41 .16
5	.77	2592	.32	7.04 .12	1389	1479	8.66 .15
6	.78	2592	.32	4.53 .23	1506	1615	5.57 .27
7	.79	2602	.29	3.01 .15	1618	1743	3.70 .18
8	.80	2608	.25	2.62 .13	1727	1870	3.22 .16
9	.81	2615	.21	2.54 .06	1823	1985	3.10 .08
			Series II				
10	14.75	2569 ± 16	12.41 ± .10	16.08 ± .06	985	1025	19.92 ± .16
11	.76	2576	.36	15.46 .25	1089	1143	19.15 .32
12	.76	2576	.36	13.57 .08	1191	1268	16.81 .16
13	.77	2585	.31	10.73 .09	1301	1380	13.21 .14
14	.78	2592	.32	8.35 .12	1401	1492	10.27 .16
15	.79	2592	.33	6.19 .03	1499	1605	7.61 .07
16	.80	2602	.30	4.15 .04	1610	1734	5.10 .06
17	.82	2608	.28	3.30 .02	1704	1843	4.06 .03
18	.86	2615	.28	2.58 .05	1823	1985	3.17 .06
			Series III				
19	14.75	2538 ± 16	12.54 ± .10	17.39 ± .14	——	296	21.73 ± .22
20	.80	2569	.45	16.84 .11	988	1030	20.98 .21
21	.81	2576	.40	16.55 .18	1089	1143	20.51 .27
22	.82	2576	.40	14.66 .14	1187	1252	18.17 .22
23	.83	2585	.38	12.94 .20	1301	1380	16.05 .27
24	.84	2592	.38	9.94 .11	1405	1497	12.31 .16
25	.85	2592	.38	6.72 .18	1499	1605	8.34 .22
26	.87	2602	.36	5.40 .15	1603	1726	6.70 .18
27	.89	2608	.31	4.45 .11	1702	1841	5.48 .13
28	.91	2615	.30	2.78 .07	1823	1985	3.42 .09

Some qualitative determinations of the simple rigidity of a 10-mil drawn tungsten wire 30.5 cm long were obtained previously.[8] No corrections were made for the end-effects but, since each temperature was calculated from the total amount of expansion, the error in the rigidity calculation tended to balance the error in the temperature calculation in such a way that the curves are more nearly correct than one might at first thought expect. The curves which were obtained are shown in Fig. 4. The data for Curve I was obtained by starting at room temperature; at the higher temperatures the elastic limit was passed so easily that observations became very inaccurate. The wire was then heated to about 2000° K for 100 minutes, allowed to cool to room temperature, and the observations for Curve II were started. Observations for Curve III were started at the highest temperature used for Curve II and completed at room temperature. A shorter length of the wire taken from the same spool gave curves having the same general shapes as those of Fig. 4, the irregularities occurring at the same temperatures.

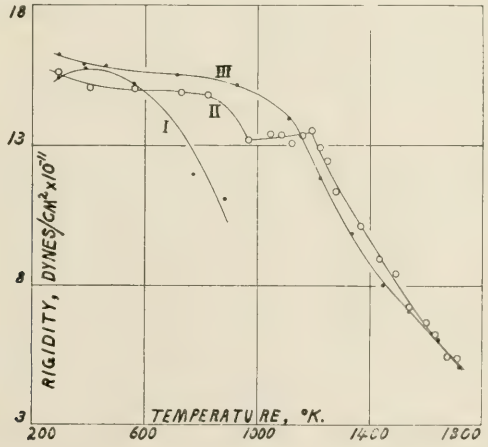

Fig. 4. Results of some preliminary measurements.

Jeffries' work[9] on the change of crystal structure of tungsten wire by heat treatments at various temperatures makes it possible to interpret the shapes of the Curves in Figs. 3 and 4. Dr. L. P. Sieg found the value 13.99×10^{11} dynes/cm^2 for the rigidity of the wire at room temperature; the wire had been given no heat-treatment other than that which it received when it was drawn. In the present research the temperature at which the apparatus was baked out never exceeded 330°C, and the very short heating at 1600°K (to remove the graphite film) certainly changed the structure very little. The first rigidity determination was

[8] Schriever, Master's Thesis in Uni. of Iowa Library

[9] Jeffries, Trans. Am. Inst. Mining Eng. 1037-1092, 1918

made at 1150°K (Curve I of Fig. 3); the value was $14.2 \pm 0.3 \times 10^{11}$ dynes cm^2 which, within the experimental error, is the same as found by Dr. Sieg at room temperature. The structural changes caused by the heating at 1600°K and especially by the heat treatment at 1150°K during the process of making the first rigidity determination, will account for the constancy of the rigidity from room temperature to 1150°K for the first heating. If observations starting at room temperature had been taken, a rapid falling off of the rigidity would have been observed before a temperature of about 1100°K was reached, as was shown by the wire giving Curve I of Fig. 4.

Heat treatment at 1150 to 1300°K will cause the structure of a new wire to change rapidly. The wire (Curve I of Fig. 3) was held at 1150°K for slightly more than two hours, at 1250° for an hour, and at 1308° for about an hour. Although these temperatures are below the five-minute equiaxing or recrystallization temperature, namely 1600°K, the long exposures at these temperatures probably allowed crystallization to take place. This evidently was the case because the rigidity at 1308°K was only a little less than it was at 1150°K. From 1300 to 1700°K the curve is almost linear which indicates that no radical change in the structure took place. Above 1700°, the region of rapid grain growth, the slope of the curve decreases rapidly. Unless the crystal grains enlarged a great deal it would be difficult to explain the relatively small decrease in rigidity between 1740 and 1985°K for the first heating of the wire to such high temperatures. The fact that large crystal grains were formed would also account for the high value of the rigidity at 1025°K (first point of Curve II, Fig. 3) and again at 1030°K in the third series of measurements. Since the change of slope near the lower end of each curve is less rapid in each succeeding curve, it seems probable that, after the grain-growth is completed, the rigidity will decrease regularly with temperature-increase, and that the curves obtained thereafter will not show a decrease of slope at the higher temperatures.

If the scale readings for the final positions of M_3 at the higher temperatures had been made less rapidly, the deflections for this mirror would have been smaller, and smaller values for the modulus of rigidity would have resulted. Consequently the change of slope near the lower end of each curve cannot be due to the yielding of the wire. Thus this decreased rate of falling off of the rigidity with temperature-increase must be real and, in all probability, due to the rapid grain-growth at the higher temperatures.

It is known that the modulus of rigidity when calculated from small twists, is greater than when calculated from large twists. This effect

was observed in this research, and for this reason the twist per centimeter was kept approximately constant.

It is observed that Curve III of Fig. 4 lies below Curve II for temperatures above 1175°K. This peculiar result was probably due to the wire having formed a crystal structure which made an exceptionally rigid wire but one which was not stable at the highest temperature. The second point for Curve I of Fig. 3 is probably incorrectly located although the data do not indicate this for they are consistent among themselves.

Since in mall tungsten wires a single crystal grain may occupy a very large part of the cross-section of the wire,[9] the modulus of rigidity determined from such a wire may be quite different from that obta'ned from observations made on a relatively large wire. An increase of rigidity with decrease in size of wire has been observed in the case of freshly drawn tungsten wires.[10] The results given in this article may therefore be different from those which a bar of the metal would yield even if the bar had the same grain-size as the wire. Wires smaller than the one used wou'd undoubtedly give still different values for the modulus of rigidity. The determination of the change of the rigidity with the size of the wire would make very interesting work but the labor involved would be very great.

In conclusion I wish to express my appreciation to Professor L. P. Sieg for his many valuable suggestions and keen interest in this work; and to the Director of the Nela Research Laboratory who, through Dr. A. G. Worthing, so kindly furnished the tungsten and sealing-in wires, the calibrated standard amp and the pyrometer lamp. I am also indebted to J. B. Dempster and M. Teeuween for much valuable information regarding workshop methods, and to J. C. Steinberg who generously helped me prepare the platinum-coated mirrors with his evaporation apparatus.

PHYSICAL LABORATORY,
STATE UNIVERSITY OF IOWA,
June 6, 1923.[11]

[10] Sieg, Proc. Iowa Acad. Sci. **24**, 207, 1917

[11] This work was completed in July, 1921. Present address is University of Oklahoma, Norman, Oklahoma.

THE OPTICAL CONSTANTS OF ISOLATED TELLURIUM CRYSTALS

By George Dewey Van Dyke

This paper is a brief report on one phase of an extended research which is being conducted by Dr. L. P. Sieg of the State University of Iowa, on the optical properties of small metallic crystals. The information obtained from such investigations should reveal much in regard to the crystalline structure of the pure metal and possibly throw some light on the atomic structure of metals in general.

Skinner[1] has published results on the optical constants of a selenium crystal, finding the crystal doubly refracting, the index when the principal axis of the crystal is parallel to the plane of incidence being higher than that of any other known element. Skinner employed the ordinary polarimetric method of determining the elliptic constants. Weld[2] has made a fairly extensive study of the elliptic constants of light reflected from a small selenium crystal using the "Crystelliptometer," a special apparatus designed by himself. The same apparatus was used by the writer in obtaining the optical constants of tellurium crystals. The crystals were made by sublimation at the State University of Iowa, by Dr. A. R. Fortsch.

Drude[3] has developed the theory of metallic reflection for crystalline bodies.

Let Φ_1, Δ_1, Ψ_1, be respectively, the angle of incidence, phase difference, and azimuth when the principal crystal axis is parallel to the plane of incidence;

Φ_2, Δ_2, Ψ_2 be, respectively, the angle of incidence, phase difference, and azimuth when the principal axis of the crystal is perpendicular to the plane of incidence, and

n_1, n_2, k_1, k_2, ρ_1, ρ_2, be the indices of refraction, absorption coefficients, and coefficients of reflection, respectively, for the

[1] Skinner, Phys. Rev., N. S., *9*, p. 148; 1917.

[2] Weld, *Journal of the Optical Society of America*, *6*, p. 67; 1922.

[3] Drude, Ann. d. Physik, *34*, p. 529; *32*, p. 616, 1887; *35*, p. 518; 1888.

two principal positions of the crystal axis, n_1, referring, for example, to the index of refraction when the electric vector agrees with the principal axis.

Then

$$\frac{\sqrt{\alpha}}{\cos\phi_1}-\sqrt{\gamma}\cos\phi_1=\frac{\cos 2\Psi_1+i\sin 2\Psi_1\sin\Delta_1}{1-\sin 2\Psi_1\cos\Delta_1}$$

$$\frac{\sqrt{\gamma}}{\cos\phi_2}-\sqrt{\alpha}\cos\phi_2=\frac{\cos 2\Psi_2+i\sin 2\Psi_2\sin\Delta_2}{1-\sin 2\Psi_2\cos\Delta_2}$$

where α and λ are auxiliary complex constants employed in determining the final optical constants. The letter i represents $\sqrt{-1}$.

Let the values of α and γ as given by the above equations be

$$\alpha=a_{11}+i\,a_{12} \qquad\qquad \gamma=a_{31}+i\,a_{32}$$

Then if we define X by $\tan X=\frac{a_{12}}{a_{11}}$,

and E by $\tan E=\frac{a_{32}}{a_{31}}$, we have

$$k_1=\tan\frac{X}{2}, \qquad\qquad k_2=\tan\frac{E}{2},$$

$$n_1^2=\frac{2\sin\frac{X}{2}\cos^3\frac{X}{2}}{a_{12}}, \qquad\qquad n_2^2=\frac{2\sin\frac{E}{2}\cos^3\frac{E}{2}}{a_{32}}$$

$$\rho_1=\frac{n_1^2(1+k_1^2)+1-2n_1}{n_1^2(1+k_1^2)+1+2n_1}, \text{ and} \qquad\qquad \rho_2=\frac{n_2^2(1+k_2^2)+1-2n_2}{n_2^2(1+k_2^2)+1+2n_2}$$

It should be noted that the values of α and γ do not depend upon the angles of incidence, hence for each wave-length we are able to determine α and γ for several angles of incidence and average the results.

The optical constants for five different wave-lengths in the visible spectrum were obtained. The results of the investigation (c. f. Figs. 1, 2, and 3) show that a crystal of tellurium is doubly refracting, the index of refraction being higher in the horizontal than in the vertical position. The reflecting power of the crystal

Table of Elliptic Constants

λ ($\mu\mu$)	Φ	Δ_1	$2\Psi_1$	Δ_2	$2\Psi_2$
437	60°	141°30′	74°	136°	66°48′
437	65°	126°6′	73°48′	119°24′	64°12′
437	70°	108°54′	72°12′	103°54′	60°36′
437	75°	89°42′	69°48′	78°54′	61°
450	60°	127°30′	69°12′	120°24′	63°24′
450	65°	117°12′	68°48′	113°36′	61°12′
450	70°	99°30′	66°24′	86°30′	62°48′
508	60°	136°30′	73°36′	133°24′	61°12′
508	65°	122°6′	67°24′	119°48′	58°24′
508	70°	108°36′	62°24′	105°	56°
508	75°	84°12′	61°48′	76°36′	55°12′
590	60°	137°36′	71°	133°	67°
590	65°	132°12′	65°12′	117°18′	60°24′
590	70°	108°6′	64°48′	100°36′	57°12′
590	75°	89°18′	59°24′	80°6′	54°24′
650	60°	127°54′	68°48′	115°12′	57°24′
650	65°	115°30′	65°	102°24′	55°48′
650	70°	102°24′	62°	92°42′	55°36′

Averages of Crystal Constants

λ	α	γ
437	$.0528+.0503i$	$.0513+.0811i$
450	$.0751+.0918i$	$.0800+.1232i$
508	$.0493+.0738i$	$.0391+.0967i$
590	$.0416+.0688i$	$.0426+.0896i$
650	$.0659+.1034i$	$.0641+.1532i$

Table of Optical Constants

	Crystal Axis Horizontal			Crystal Axis Vertical		
λ	n_1	κ_1	ρ_1	n_2	κ_2	ρ_2
437	3.44	.399	.33	2.52	.551	.30
450	2.62	.466	.28	2.29	.543	.26
508	2.96	.535	.31	2.57	.672	.30
590	3.07	.563	.34	2.68	.632	.30
650	2.50	.548	.29	2.05	.666	.27

varies very little for the two positions and for the various wave-lengths used, a fact verified by Sieg[4] by direct measurement of the reflecting power. The curve obtained from plotting the index of refraction against the wave-length shows a distinct

[4] Unpublished results.

minimum and maximum over the range investigated. This characteristic is also shown in Skinner's[5] results for selenium,

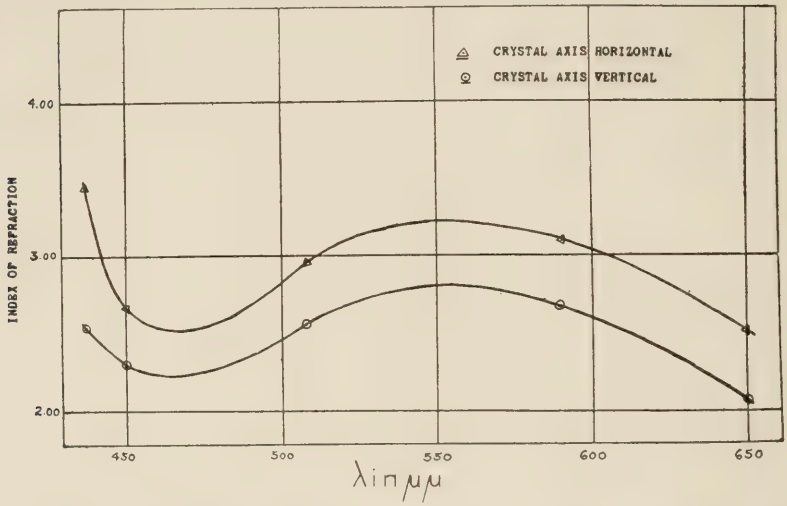

FIG. 1. *Principal indices of refraction of an isolated tellurium crystal for various wave-lengths.*

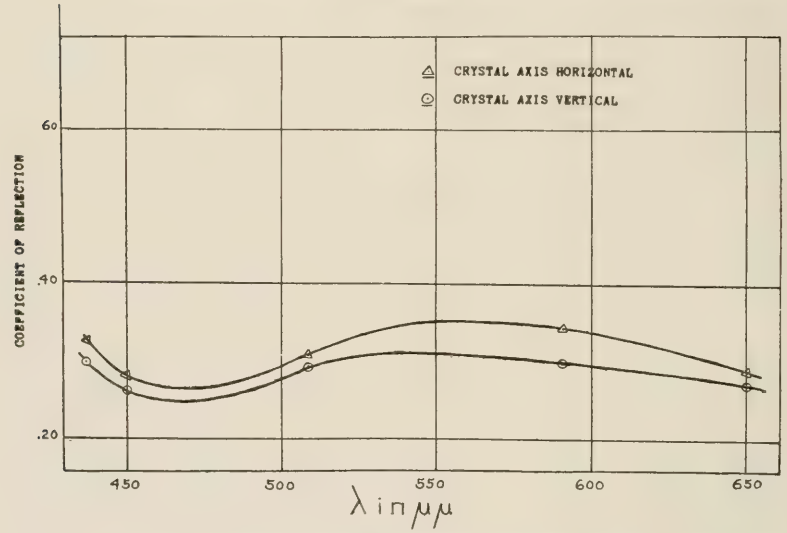

FIG. 2. *Principal reflecting powers of an isolated tellurium crystal for various wave-lengths.*

[5] Loc. cit.

although to a far less degree. The peculiarity found in the index in the horizontal position was not evident in tellurium, the two indices following almost similar curves.

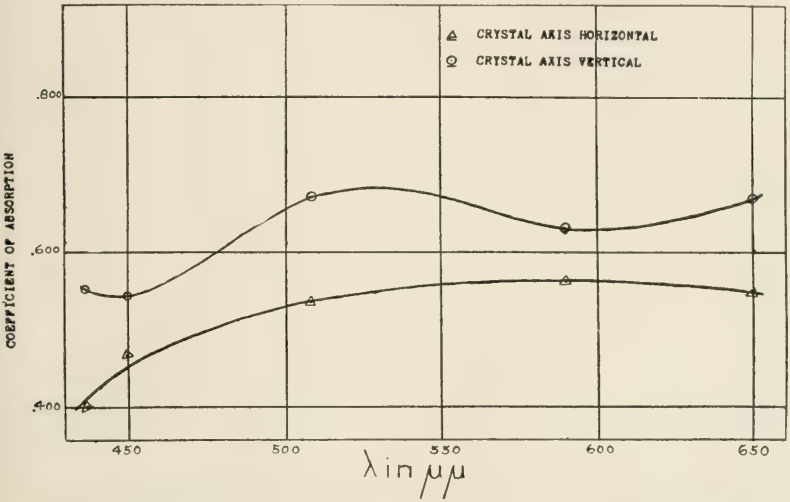

FIG. 3. *Variation in the coefficients of absorption of a crystal of tellurium with a variation in the wave-length.*

The above problem was suggested to me by Professor L. P. Sieg, to whom I wish to express my appreciation.

STATE UNIVERSITY OF IOWA,
AUGUST, 1922.

SCATTERING OF X-RAYS.

[Reprinted from The Physical Review, S.S., Vol. XX., No. 6, December, 1922.]

AN EXPERIMENTAL STUDY OF THE SCATTERING OF APPROXIMATELY HOMOGENEOUS X-RAYS BY POWDERED CRYSTALLINE CARBON, METALLIC LITHIUM, AND LIQUID BENZENE, MESITYLENE, AND OCTANE.

By C. W. Hewlett.

Synopsis.

Scattering and Absorption of Homogeneous X-Rays by Carbon (Diamond and Graphite), Metallic Lithium, and the Liquids Benzene, Mesitylene and Octane.— 1. *Scattering curves.* The intensity of the radiation scattered by the substance contained in a small capsule placed at the center of the spectrometer was measured by the ionization method for angles from 2° to 165°. While a ZrO_2 screen was used to isolate the K_α line of Mo (0.712 Å.), some radiation of λ 0.445 Å. was apparently also present. For diamond, graphite and lithium, the maxima agree in position and relative intensity with those found by A. W. Hull by the photographic method. The curves for the liquids, however, are remarkable in that each shows one maximum; 8.5° for benzene, 6.5° for mesitylene and 8.1° for octane, with indications of others unresolved, suggesting that the liquids have a crystal structure. For very small angles the scattering is zero for the solids, and approaches zero for the liquids. 2. *Mass-scattering coefficients* were obtained by integrating the area under the curves, or by experimentally integrating the ionization for all angles of scattering. The coefficients for carbon (diamond and graphite), 0.200, and for lithium, 0.168, agree with Thomson's theoretical values. For benzene, mesitylene, and octane, however, the values 0.238, 0.244, and 0.262 respectively are about ten per cent. larger than those predicted by theory, and give too large specific values for carbon and hydrogen, 0.22 and 0.46 instead of 0.20 and 0.40 respectively. The results are probably accurate to three per cent. 3. *True mass-absorption coefficients*, obtained from the total absorption, the scattering and the density, are found for the solids to be in accord with the theoretical expression $KN^3\lambda^3$, the mean value of K being 4.38×10^{-3}.

Evidence of crystal structure of liquids seems to have been found in the scattering curves for benzene, mesitylene and octane, as suggested above, and the spacings of the planes of atoms responsible for the principal maximum are benzene 4.8 Å., mesitylene 6.3 Å., and octane 5.0 Å.

Introduction.

THE experiments described in the following report are the outgrowth of a former series of experiments made by the writer[1] in which the mass absorption and mass-scattering coefficients of homogeneous x-rays were studied for several substances as a function of the wavelength of the x-rays. The definitions of these coefficients, and a discussion of the expression $KN^3\lambda^3 + (\sigma/\rho)$ which has been proposed to give the value of the total mass absorption coefficient of x-rays of wave-

[1] Phys. Rev., N. S., 17, 1921, p. 284.

length λ in an element whose atomic number is N, is given in the paper referred to above. In this former work the total mass-absorption coefficient was measured by determining the intensity of a beam of homogeneous x-rays before and after passing through a screen of the absorbing element. The mass-scattering coefficient deduced from the above equation was found to depart from the theoretical value deduced by J. J. Thomson,[1] and the value of K to depend on the scattering element. Moreover the curves were not found to be linear with λ^3 as they should have been in the region investigated according to theoretical considerations. In particular there seemed to be something anomalous in the behavior of carbon in the neighborhood of wave-length 0.75 Å. which is near the K_α line of molybdenum 0.712 Å. The scattering of hydrogen calculated from the experiments on water and liquid oxygen, and the absorption coefficient of lithium could not be interpreted in the light of theory. It therefore seemed advisable to measure the mass scattering, and the true mass-absorption coefficients for certain elements and wave-lengths independently of one another. The present work, of which a preliminary report[2] was made last November before the American Physical Society, consists of measurements of the scattered x-rays as a function of the angle of scattering from graphite, diamond, lithium, and three liquid compounds of carbon and hydrogen. The radiation falling on the scattering material was the x-radiation from a molybdenum anode tube excited at about 30 kv. The radiation was filtered through a screen of zirconium oxide which absorbed very greatly all the radiation except that in the neighborhood of the K_α line of molybdenum.

The general results of the measurements have been expressed in two ways. The intensity of scattering has been plotted as a function of the angle of scattering, and the mass-scattering coefficients and the true mass-absorption coefficients have been tabulated together with other data from which they were directly deduced.

The matter is presented in the following order:

I. Description of Apparatus and Mounting of the Scattering Material.
II. Procedure in the Experiments.
III. Procedure in Calculating the Mass Scattering and the True Mass-Absorption Coefficients.
IV. Sources of Error.
V. Results and Discussion.
VI. Appendix; a Detailed Consideration of a Point arising in III.

[1] Conduction of Electricity through Gases, 2nd edition, p. 325.

[2] Phys. Rev., N. S., 19, 1922, p. 265.

Description of Apparatus and Mounting of Scattering Material.—The Coolidge tube was mounted on sulphur insulators in a lead-covered wooden box about 2 ft. x 2 ft. x 3 ft. The tube was supplied by a 35 kv. oil-insulated transformer which in turn was supplied by a motor generator set. Regulation of voltage and frequency were obtained by rheostats inserted in the field circuits of the motor generator. A D'Arsonval type milliammeter was inserted in the secondary of the transformer at its midpoint which was grounded. All of the high potential apparatus was enclosed in a wire netting cage and the door into this cage could not be opened without opening the primary circuit of the transformer.

The x-ray spectrometer was constructed in this laboratory, and angular settings could be made with an accuracy within 2′ of arc. The ionization chamber was mounted on wheels so that it could rotate about the axis of the spectrometer. The scattering material was mounted in a small celluloid capsule whose axis coincided with that of the spectrometer. The small table holding the scattering material was caused to rotate continuously about the axis of the spectrometer.

The ionization chamber was 1 foot long. The outside brass cylinder was 4 inches in diameter and was earthed. The inside cylinder was $3\frac{3}{4}$ inches in diameter, and was kept charged to a potential of about 250 volts by a battery of dry cells. A horizontal electrode insulated by amber was placed in this inner cylinder about half way between its axis and surface. A fine wire was soldered to this electrode and then passed along the axis of a brass tube leading from the ionization chamber to a point in the axis of the spectrometer about 6 inches above the scattering material. From this point the wire passed down the axis of another tube to one pair of quadrants of an electrometer. The movable and fixed tubes were connected by end pieces, one of which could rotate inside the other. The wire joining the electrode to the electrometer was insulated by amber throughout and was completely shielded, all of the shielding being connected together by soldered wires and grounded. The opening in the ionization chamber was 1.50 cm. in diameter, was situated in the horizontal plane passing through the x-ray beam and scattering material and the distance of this opening from the scattering material was 35.5 cm. The electrodes in the ionization chamber were so placed that none of the x-rays from the scattering material could strike them. A lead screen was placed about half way between the scattering material and the opening in the ionization chamber. An opening in this screen was made just large enough to allow every part of the scattering material to send x-rays to every part of the opening. A lead hood was placed over the space between the ionization chamber and this screen to cut off

possible radiation from other objects than those in the neighborhood of the axis of the ionization chamber. In order to cut off all unnecessary direct x-radiation there were two lead slits between the box and the scattering material, the one nearest the scattering material being about 10 cm. distant.

The other pair of quadrants of the electrometer were connected to the case of the electrometer and to earth. An earthing key was connected through a resistance of about 1,000 ohms to earth. This resistance was connected to a potentiometer so that the key could be charged to any desired potential or earthed at will. This key dipped into a mercury cup connected to the electrode in the ionization chamber. The electrometer needle was charged to a potential of 100 volts, and the sensitivity ranged from 1,000 to 5,000 divisions per volt in the different parts of the work.

The scattering material was mounted in thin cylinders of circular cross section, which were made by cutting sheet celluloid of 1 mil thickness into strips from $\frac{1}{8}$ to $\frac{3}{8}$ inch in width and wrapping them helically on a brass or steel rod, allowing each turn a narrow lap on the preceding one. This helix was then secured at each end and the helical seam cemented with collodion. These capsules were found to absorb less than one per cent. of the x-rays falling on them. Two sizes of capsules with internal diameters of $\frac{3}{16}$ and $\frac{1}{4}$ inch were used.

The material called artificial graphite was a highly purified carbon which was obtained in compressed cakes. It was finely powdered by filing, and the powder packed into the capsule. The natural graphite was originally in chunks. This material was forced through a sieve of 50 meshes to the inch, and then packed into a capsule. The diamond was in the form of five splints. These splints were very thin and their cross-sectional area ranged from 0.010 to 0.001 sq. cm. The lithium, from a very old exhibition sample, of German manufacture, was squirted through a die into a rod of the required dimensions, and immediately enclosed in one of the celluloid capsules. Fortunately none of the three liquids used in these experiments attacked the capsules.

II. Procedure in the Experiments.

Method of obtaining the data for plotting the curves. The beam of x-rays, which had a rectangular cross section, was adjusted so as to cover the whole width of the capsule of scattering material and to project a short distance on either side. The cross section of the beam in the vicinity of the scattering material was approximately 0.8 cm. square, but this was varied slightly from time to time when different size capsules were used.

The x-ray tube was operated at a potential of about 30 kv. at 60.7 cycles per sec. and the current read on a D'Arsonval type milliammeter was 4 m.a. These conditions of operation were maintained constant to within 1 per cent. throughout the work. A zirconium oxide screen, which reduced the K_α line to about 60 per cent. of its intensity without the screen, and reduced the K_β line to about 6 per cent. of the intensity of K_α line, was placed in the path of the radiation as it emerged from the box containing the tube.

The ionization chamber was set at as small an angle as could be done without allowing any of the direct beam to enter it, the electrometer was charged, the earth connection broken, and the time required for the electrometer deflection to change from one of two definite values to the other was determined. An empty capsule of the same construction as the one containing the scattering material was then substituted for the full capsule, and the time required for the same change in deflection determined. Deducing the rates of deflection, and subtracting that due to the empty from that due to the full capsule, the rate of deflection due to the scattering material was obtained, and this was taken as a measure of the intensity of the scattered radiation entering the ionization chamber. If the intensity was so great that the rate of deflection was no longer an accurate measure of its intensity, the following method was adopted. A lead screen was placed between the scattering material and the ionization chamber, the electrometer charged, the earth connection broken, and the deflection noted. The lead screen was then removed for a definite interval of time and then replaced. When the deflection became constant its value was again noted. Whenever necessary, account was taken of the rate of deflection with the lead screen in place. In this way the intensity was determined from point to point, the steps in most cases being less than the angle subtended by the opening in the ionization chamber at the scattering material, particularly in the region of a pronounced maximum. When once the position of the principal maximum of scattering was known, measurements were made frequently at this setting, to check the constancy of operation. Finally the intensity at the various angles was expressed as percentages of the intensity at the principal maximum.

In order to calculate from the scattering curve the fraction of the incident energy which was scattered it was necessary to know the ratio between the flux of radiation into the ionization chamber at some particular setting and the flux of energy falling on the scattering material; and in addition, the total mass-absorption coefficient of the radiation in the scattering material. These quantities were usually determined at

the beginning and at the end of each series of measurements of the intensity. Two methods were used in determining the above ratio and the total mass absorption coefficient.

In the first method a thin lead sheet through which had been bored a circular hole about 0.10 cm. in diameter was placed immediately behind the capsule so that the beam of x-rays through the hole passed through the axis of the capsule. A lead disc mounted on the axle of a small electric motor was placed between the capsule and the ionization chamber with its face perpendicular to the beam of x-rays. The axis of the ionization chamber was set to coincide with that of the beam of x-rays. There was a narrow radial slit in the disc so that when the disc was in rotation the small beam passing through the circular hole entered the ionization chamber for a short interval once during each revolution of the disc. By this means it was found possible to secure a conveniently measurable fraction of the energy flux falling on the capsule. This fraction of the energy flux was calculated from the cross section of the x-ray beam striking the capsule when unobstructed by the lead sheet, the area of the hole, and the angular width of the slit in the lead disc. The cross section of the x-ray beam falling on the capsule was deduced from an x-ray shadow picture made by the x-ray beam on a photographic film placed perpendicular to the x-ray beam and in contact with the full capsule, the beam passing first through the capsule, then striking the film. The width of the shadow of the capsule checked with the diameter of the capsule. The diameter of the hole was measured with a micrometer microscope. The total mass-absorption coefficient of the radiation in the scattering material was determined from measurements of the energy flux through the small hole and rotating disc, determined alternately when the x-rays passed through the full and the empty capsule.

There are two objections to the method outlined above; namely, a flash of x-rays entering the ionization chamber is not representative of the average intensity of the beam, but is a very small section of the radiation emitted during one cycle of the alternating current. The number of these flashes received by the chamber during a determination is very large, however, and unless the disc should have a speed bearing a simple relation to the frequency of the alternating current from the transformer, this consideration should not lead to undesirable results. On the other hand, the thin lead screen with the small hole had to be adjusted very accurately perpendicular to the x-ray beam, for it had a thickness comparable with the diameter of the hole. This consideration led to the adoption of another method for determining the total mass-absorption coefficient and the ratio of the energy flux falling on the capsule to that entering the ionization chamber at a definite setting.

The following method was designed to allow the total energy flux falling on the capsule to pass into the ionization chamber for the time of one complete cycle of the alternating current from the transformer. A lead disc carrying an angular slit of adjustable width was mounted on a horizontal axle, so that in rotating, the beam of x-rays was allowed to pass through the slit when the latter was vertical. This disc and axle was controlled by a stiff steel helical spring in the same manner as the balance wheel of a watch. Two stops with trigger action were arranged so that one of them could hold the disc displaced from its vertical position by a definite amount, and upon release, the other stop would catch and hold the disc at the end of its first swing. By successive adjustments of the stiffness of the spring, the width of the slit, and the height of the stops, the time for the slit to sweep across a point in the x-ray beam was made equal to the period of the alternating current to within 1 per cent. In order to determine when the adjustment was completed, the face of the disc was covered with a thin film of smoke and a vibrating reed operated by the alternating current supplying the transformer traced a curve on the disc as it swung. The disc was mounted close to the box containing the tube, where the cross section of the beam was a minimum. Obviously it makes no difference what part of the cycle the exposure begins if it lasts one complete cycle.

A lead slit open at the lower end and having a width equal to that of the capsule was placed on the capsule when making measurements of the direct beam, so that only the portion of the beam striking the capsule could pass on to the ionization chamber. The opening in the ionization chamber was large enough to receive all of the radiation which passed through the capsule, and the exact position of the chamber was secured with the aid of a fluorescent screen.

The procedure was as follows: with the empty capsule in place the lead disc was secured by one of the stops. The electrometer was charged, the earth connection broken, and the electrometer deflection noted. The stop was tripped, allowing the disc to swing. The deflection of the electrometer changed rapidly, and became constant again in about one minute, at which time its value was again noted. From the change in deflection the charge given to the insulated system was computed, and this was taken as a measure of the radiation falling on the capsule during one cycle. The full capsule was then substituted for the empty one, and the procedure repeated, from which was computed the radiation transmitted through the scattering material during one cycle. A number of such determinations were made at each experiment, those with the empty and full capsules being distributed in such a manner that the mean

values of each corresponded to the same epoch. The intensity of the scattered radiation for the principal maximum of the scattering material was next determined in the manner already described.

By multiplying the ordinates of a scattering curve by the sine of the angle of scattering, and by a factor to take account of the size of the angular opening of the ionization chamber measured from the scattering material, a new curve was obtained, the area under which gave the total amount of scattered radiation in terms of the radiation falling on the scattering material. This procedure rests upon the assumption that an element of the scattering material containing a large number of small crystals would scatter radiation equally in all directions making a given angle with the direction of the direct beam.

The following method was devised so that the procedure of calculation from the scattering curve just described would be done automatically by the method of measuring the scattering. Having first measured the intensity of the direct beam through the empty and full capsules, the ionization chamber was set close to the direct beam. With a lead screen in front of the chamber the electrometer was charged, the earth connection broken, and the deflection noted. At a definite instant, which was recorded beforehand, the lead screen was removed and the ionization chamber moved along from degree to degree, leaving it on each degree for an interval of time proportional to $\sin\theta$, where θ was the angular setting of the chamber from the direct beam. The schedule for moving the chamber was prepared beforehand, and was so designed that the amount of radiation entering the ionization chamber during its tour around the circle was equal to the total amount of radiation scattered in 1 second.

The total charge taken by the electrometer during its tour around the circle was then proportional to the total x-rays scattered during 1 second. This total charge was deduced from the total change in deflection of the electrometer. This procedure was carried through for the empty capsule and for the full capsule in such a manner that the results for each corresponded to the same epoch. At the end, the intensity of the direct beam was again measured through the empty and full capsules.

III. Procedure in Calculating the Mass-Scattering Coefficient and the True Mass-Absorption Coefficient.

1. Calculation of the total mass-absorption coefficient $(\mu + \sigma)/\rho$. The densities of the materials in the capsules were determined, in the case of the solids, by dividing the mass of the material packed in the capsule by the volume of the capsule; in the case of the liquids by finding the loss in weight of a sinker of known volume when suspended in them.

When the small hole and rotating disc were used for measuring the total mass-absorption coefficient, this quantity was given by the expression

$$d = \epsilon^{-\frac{\mu+\sigma}{\rho} \cdot t},$$

where t is the average length of path of the x-rays through the scattering material, and d is the ratio of the intensity of the beam through the full capsule to that through the empty capsule.

When one cycle of the x-rays falling on the capsule was allowed to enter the ionization chamber the total mass-absorption coefficient was calculated from the following expression:

$$d = 1 - \frac{\pi}{4} b + \frac{1}{3} b^2 - \frac{\pi}{32} b^3 + \frac{1}{45} b^4 - \cdots,$$

where

$$b = \frac{\mu + \sigma}{\rho} D.$$

D is the diameter of the capsule.

2. Calculation of the fraction of the x-rays falling on the scattering material that was scattered. When using the scattering curves the first procedure was to multiply the ordinates of the scattering curve by the factor

$$\frac{2 \sin \delta}{1 - \cos \delta} \sin \theta,$$

where δ is half the plane angle subtended at the scattering material by the opening in the ionization chamber, and θ is the angle from the direct beam at which the scattering was measured. The area under this new curve was then found, using 2δ as the unit abscissa and 100 per cent. as the unit ordinate. This area is equal to the total measured scattered x-rays in terms of that measured at the angle of maximum scattering. The number for the total measured x-rays was then corrected by estimation for the scattering between 165° and 180° inaccessible to the ionization chamber. This correction usually amounted to 1 or 2 per cent. of the total measured x-rays. Next the correction for absorption in the scattering material (see appendix) was applied, giving the total scattered x-rays in terms of that measured at the angle of maximum scattering. Finally, this number was divided by the ratio of the energy flux falling on the scattering material to that entering the ionization chamber at the angle of maximum scattering, giving the fraction of incident x-rays that was scattered.

When the scattering was measured by rotating the ionization chamber

from degree to degree the total measured scattered x-rays for the empty capsule were subtracted from that for the full capsule, and the corrections for the region inaccessible to the ionization chamber and for the absorption in the scattering material were applied. This gave the total x-rays scattered in 1 second which was then divided by the x-rays falling on the scattering material in 1 second.

3. Calculation of the mass-scattering and the true mass-absorption coefficients. When one cycle of the radiation falling on the capsule was allowed to enter the ionization chamber, the amount of the direct beam taken out by the scattering material is given directly by $1 - d$. When the small hole and rotating disc was used the fraction of the direct beam of x-rays taken out by the scattering material was calculated from the expression

$$\frac{\pi}{4}b - \frac{1}{3}b^2 + \frac{\pi}{32}b^3 - \frac{1}{45}b^4 + \cdots,$$

where

$$b = \frac{\mu + \sigma}{\rho} D.$$

Let this fraction be denoted by T, while S denotes the fraction of the incident beam scattered. Then since scattering and absorption take place together

$$\frac{S}{T} = \frac{\sigma}{\mu + \sigma},$$

so that the mass-scattering coefficient is given by

$$\frac{\sigma}{\rho} = \frac{S}{T} \cdot \frac{\mu + \sigma}{\rho}.$$

Each of the three quantities on the right were measured so that σ/ρ could be calculated. The true mass-absorption coefficient was then obtained by subtracting the mass-scattering coefficient from the total mass-absorption coefficient.

IV. Sources of Error.

1. On account of the finite size of the scattering material there is some indefiniteness as to its centroid. The volume of the scattering material was about 0.10 cm.^{3} and 0.20 cm.^{3} for the smaller and larger capsules respectively.

2. The x-rays were not parallel at the scattering material, so that the total mass-absorption coefficients as calculated would be slightly in error. The distance from the source of x-rays to the scattering material was 1 meter.

3. Saturation voltage in the ionization chamber was secured by trial, and then twice that voltage allowed as a factor of safety.

4. The electrometer scale was not absolutely uniform, but the proper corrections were applied wherever necessary.

5. The variation of voltage, frequency, and thermionic current through the tube would introduce serious errors in work of this kind if not carefully controlled. All of these were carefully regulated by hand, frequently one person giving this his entire attention.

6. Variation in the effective amount of methyl bromide in the ionization chamber during a series of experiments. Although this was at times rather large, standardizing measurements were made at the beginning and end of each series, and frequently during the series, so that it was possible to allow by interpolation for uniform changes such as the above.

7. Non-uniformity of the density of the scattering material in the capsules. In the case of the liquids this consideration does not enter, and in the case of the diamond splints it is safe to conclude that the effect is negligible. With the two kinds of graphite every precaution was taken to insure uniformity of distribution by careful packing, and the observations were made allowing the x-rays to fall on different sections of the capsule. In the case of the lithium there is a possibility (hardly probable) of blow holes. These blow holes might even be filled with some of the oil in which the lithium had been kept.

8. The adjustment of the small hole behind the scattering material in the one method for measuring the absorption coefficient and the adjustment of the slit on the scattering material in the other method were made with great care as a small displacement of these limiting devices would lead to a relatively large error in the results.

All of these main sources of error and several other minor ones have been carefully considered and it is estimated that the final results are not in error by more than 3 per cent. on account of them.

V. Results and Discussion.

Table I. gives the results on the mass-scattering and the true mass-absorption coefficients of the substances given in the first column. The second column gives the method used in the determination, the number in brackets showing the number of separate determinations from which the values in a given line were deduced.

Method *A* signifies that the calculations were made from the scattering curve for the material. The comparison with the direct beam of x-rays in these calculations was determined by allowing one cycle of the x-rays

falling on the capsule to enter the ionization chamber. In method *B* the ionization chamber was moved from degree to degree allowing the charge on the electrometer to accumulate. The comparison with the direct beam of x-rays in these calculations was determined by the small hole and rotating disc method. Method *C* differed from method *B* in that the comparison with the direct beam was as in method *A*. The third column gives the percentage *S*, of the x-rays falling on the scattering material, which was scattered. The fourth column gives the fraction *F*, of the x-rays falling on the scattering material, which was removed by the combined processes of absorption and scattering. The fifth, sixth, and seventh columns give the total mass-absorption coefficient, the mass-scattering coefficient, and the true mass-absorption coefficient respectively. The eighth column gives the means of the mass-scattering coefficient for each substance. The ninth column gives the value of *K* calculated from the expression $\mu'/\rho = KN^3\lambda^3$ where μ/ρ is the true mass-absorption coefficient.

A comparison of the position of the maxima in the scattering curves for the solid substances shows good agreement with those obtained by Hull [1] using the photographic method. The relative intensities of the

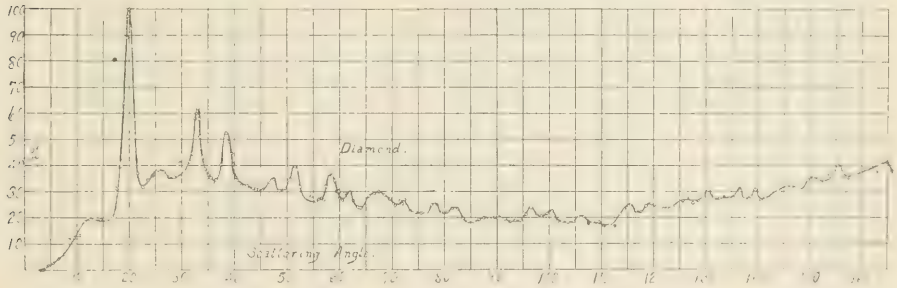

Fig. 1.

various maxima agree as well as might be expected considering the degree of uncertainty that lies in estimating relative intensities from blackening of photographic plates.

A novel point of interest shown by the curves and previously reported by the writer[2] is that for the solid substances the scattering becomes zero for very small angles from the direct beam, and approaches zero for the liquids. A special experiment was carried out to check this fact. A lead slit about 3 mm. wide was placed over the opening in the ionization chamber and it was found that at 2° from the direct beam the liquids

[1] Phys. Rev., N. S., 10, 1917, p. 661.
[2] Phys. Rev., N. S., 17, 1921, p. 284.

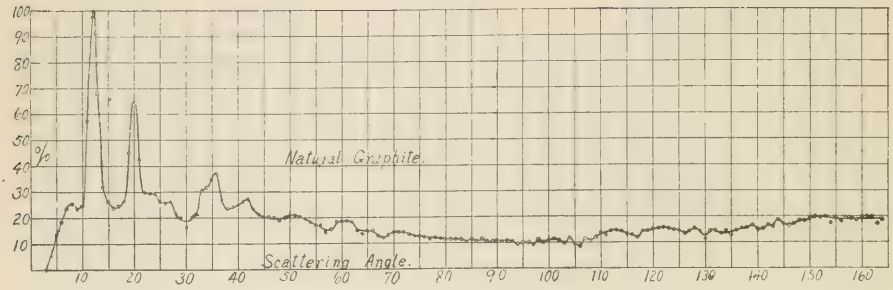

Fig. 2.

scattered less than 10 per cent. as much as at the angle of maximum

TABLE I.

1.	2.	3.	4.	5.	6.	7.	8.	9.
Substance.	Method.	S%.	F%.	$\frac{\mu+\sigma}{\rho}$.	$\frac{\sigma}{\rho}$.	$\frac{\mu}{\rho}$.	Mean $\frac{\sigma}{\rho}$.	K.
Diamond Splints.....	$A(1)$	11.86	26.1	.428	.195	.233		4.40×10^{-3}
Diamond Splints.....	$B(10)$	12.16	31.7	.515	.198	.317	.199	4.44
Diamond Splints.....	$C(2)$	12.19	29.6	.497	.205	.292		4.33
Natural Graphite.....	$A(1)$	6.55	18.6	.553	.195	.358		4.53
Artificial Graphite....	$A(1)$	6.33	17.4	.551	.200	.351	.201	4.33
Artificial Graphite....	$B(7)$	6.49	17.4	.551	.206	.345		4.26
Artificial Graphite....	$C(3)$	6.35	15.2	.477	.199	.278		4.35
Metallic Lithium.....	$A(1)$	4.21	5.78	.217	.158	.059	.168	4.36
Metallic Lithium.....	$C(4)$	4.14	4.80	.206	.178	.028		
Benzene.....	$A(1)$	9.28	18.6	.478	.238	.240		
Benzene.....	$B(3)$	6.90	14.7	.497	.233	.264	.238	
Benzene.....	$C(3)$	6.69	13.8	.468	.227	.240		
Benzene.....	$C(1)$	9.70	21.6	.567	.255	.312		
Mesitylene.....	$A(1)$	9.39	18.4	.478	.244	.234		
Mesitylene.....	$B(2)$	6.83	14.4	.489	.232	.257	.244	
Mesitylene.....	$C(2)$	7.02	12.8	.431	.236	.195		
Mesitylene.....	$C(1)$	9.89	21.3	.564	.262	.302		
Octane.....	$A(1)$	8.05	15.5	.496	.258	.238	.262	
Octane.....	$C(1)$	8.29	16.3	.524	.266	.258		

scattering, while for graphite and diamond the scattering was zero at angles of 5° and 6° respectively. Since this fact was published, A. H. Compton[1] has given a theoretical discussion in which he has shown that the scattering would be expected to become zero for small angles in the case of crystalline material. A quantitative explanation of this behavior for the liquids is as yet not forthcoming. It will be noticed that there is a prominent maximum which occurs for the solid substances at a smaller

[1] Not yet published.

angle than the principal maximum which corresponds to a wave-length 0.712 Å. Assuming that this maximum at the smaller angle is due to

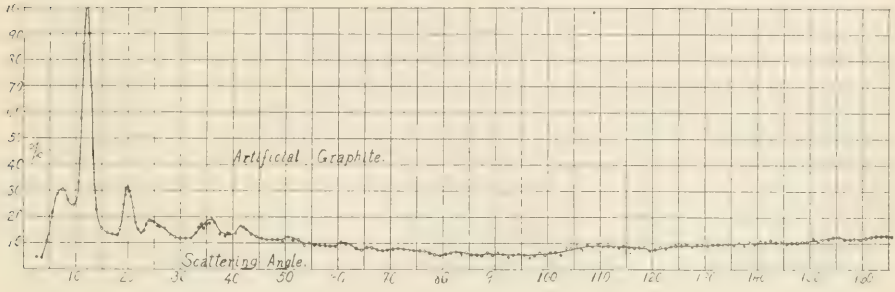

Fig. 3.

the short wave-length radiation which gets through the Zr filter, the effective wave-length was calculated from the data on diamond graphite and lithium supposing that this maximum was due to reflection from the set of planes giving the principal maximum in each case. This gave the effective wave-length of this radiation as 0.446, 0.441, and 0.449 Å.,

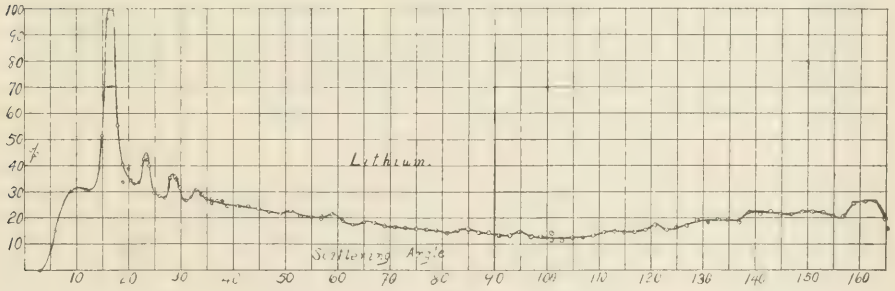

Fig. 4.

for the three substances in the order named. The mean value for this wave-length is then 0.445 Å. This explains the appearance of the maximum occurring in the neighborhood of 25° in the curve for diamond, for this is the correct position for second-order reflection of wave-length 0.445 Å. from the 111 planes.

The appearance of a very pronounced maximum at a small angle for each of the liquids investigated points very strongly toward the view that these liquids have something of a crystal structure. These maxima occur at rather small angles, and consequently the maxima due to the first two or three orders of reflection for the wave-length 0.445 Å. would overlap the first two due to the wave-length 0.712 Å. It will be seen

that this idea readily lends itself to explain the relatively complicated structure of the maxima, and the slightly irregular course of the scattering

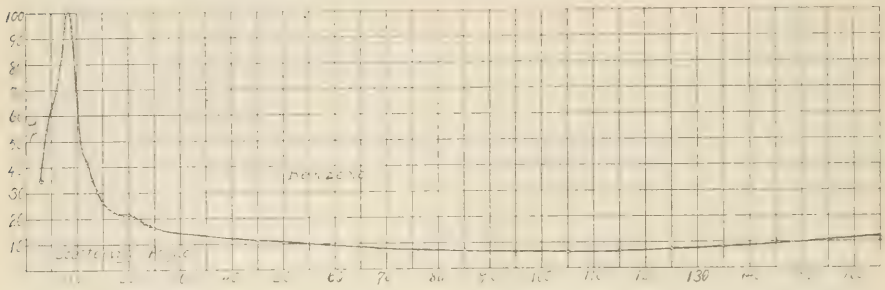

Fig. 5.

curves for the liquids between 10° and 25° scattering angle. The capsules containing the liquids from which these curves were obtained were 0.25 inch in diameter, so that the overlapping would be greater than with the smaller capsules (0.187 inch in diameter) which were used for graphite and diamond. The scattering curves for these liquids for the first 25° have been studied very carefully, using capsules 0.187 inch in diameter, and a slit 3 mm. wide across the opening in the ionization chamber. With this arrangement the complicated structure of the maxima shown in the curves in this paper have been resolved into separate maxima, and the position of the principal maximum due to

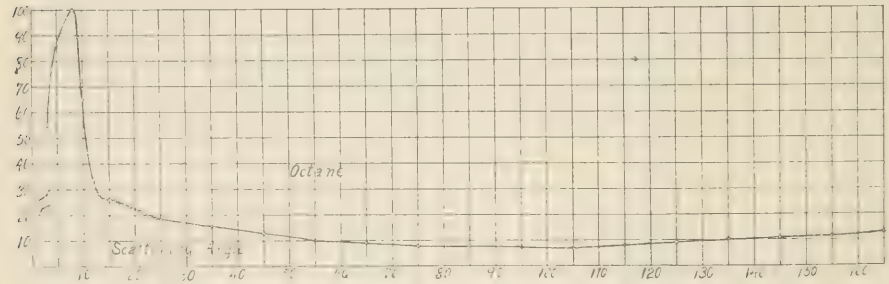

Fig. 6.

wave-length 0.712 Å. found as follows: benzene 8°.5, mesitylene 6°.5, octane 8°.1. The distances between the planes of atoms responsible for these maxima are as follows: benzene 4.8 Å., mesitylene 6.3 Å., octane 5.0 Å.

Very little information can be drawn from the curves in regard to the intensity of reflection from the crystal planes in the successive orders, for the number of sets of planes coöperating at a given angle of scattering

in the case of powdered crystals is too great. Since there are an infinite number of sets of planes in any given crystal lattice, the number of coöperating sets at any given angle of scattering would be very great, and would be greater the smaller the individual crystals of the material. This point is illustrated by a comparison of the curves for natural and artificial graphite. The artificial graphite was more finely powdered than the natural graphite, and the maxima for the latter stand out more prominently than for the former. The curves indicate, however, that the reflections in the successive orders decrease at least as rapidly as the inverse square of the order of reflection.

It should be mentioned that the shape of the scattering curves depends to some extent on the dimensions of the scattering material and the opening in the ionization chamber; the changes in the curves becoming more abrupt the smaller these dimensions. The relative heights of the maxima and minima would also be slightly dependent on these considerations. The radiation falling on the scattering material contains, besides the K_α line of molybdenum, an appreciable amount of shorter wave-length radiation, which fact in itself complicates the interpretation of the curves to a certain extent. With different thicknesses of filtering material the scattering curves would be different. The more homogeneous the radiation the more prominent, and the sharper would be the maxima of the curves. But even with constant filter thickness, dimensions of apparatus, and conditions of tube operation, there is still a factor

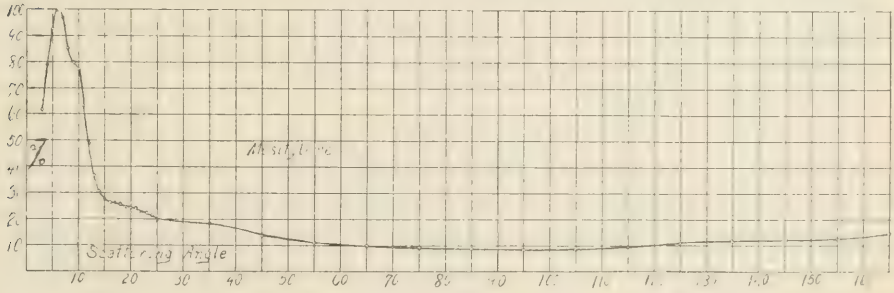

Fig. 7.

which affects the experimental scattering curves. The ionization chamber is not long enough to absorb all the radiation which enters it; especially is this true for the short wave-length radiation. When the ionization chamber had been freshly filled with methyl-bromide gas the short wave-length radiation was absorbed to a much greater extent by the gas than a few days later when the gas had become less susceptible to ionization. The longer wave-length radiation of the K_α line was

absorbed almost to the same extent when the chamber was freshly filled, and for a few days thereafter. It may readily be seen that the experimental scattering curve, with a given distribution of radiation falling on the scattering material, will depend upon the density of methyl-bromide gas in the ionization chamber; the maxima will be sharper and more pronounced, the less the density of the gas. For the sake of uniformity and in order to have large ionization currents which could be measured with accuracy, the curves shown in this paper were determined in the interval between freshly filling the ionization chamber and a time when the ionization current had fallen to half value with a constant intensity of x-rays. In the other part of the work where the ionization chamber was rotated continuously so as to automatically integrate the scattered radiation, the density of the gas in the ionization chamber varied widely. It is noticeable in this connection that although the total and true mass-absorption coefficients varied through a wide range for a given substance the mass-scattering coefficient was nearly constant. This is to be explained by the variation in the amount of methyl-bromide gas in the ionization chamber. Since there is both short and long wave-length radiation present the ionization chamber will give a relatively greater importance to the short wave-length radiation when freshly filled than some time later, so that the effective wave-length for ionization will be shorter the greater the density of methyl bromide in the chamber. According to theoretical considerations the mass-scattering coefficient is independent of the wave-length (over certain regions of wave-length this is not true) while the true mass-absorption coefficient in this region of wave-length should be proportional to the cube of the wave-length.

In order to test the above proportionality, the factor of proportionality was calculated for diamond, graphite, and lithium from the equation $\mu_\rho \rho = KN^3\lambda^3$. The value of λ to be substituted in this equation was determined for diamond and graphite by reading off from the absorption curve for carbon previously published by the writer the wave-length corresponding to the value for the total mass-absorption coefficient. The value of the wave-length for lithium was taken to be the same as that for natural graphite as the conditions of operation were about the same in the two cases. It is noticeable that K is nearly the same for diamond, graphite, and lithium, its mean value being 4.38×10^{-3}. This contradicts the writer's former work on lithium where K and the absorption coefficient were found to be abnormally high. The lithium used in the former experiments must have been impure. At least it is known that potassium chloride was mixed with the lithium chloride in the electrolytic separation of the lithium.

From the data given in the table it is seen that the mass-scattering coefficient for carbon agrees with the theoretical value calculated by J. J. Thomson,[1] the average values for graphite and for diamond agreeing with one another and with the theoretical value, 0.200, within the limit of experimental error. The mass-scattering coefficient is thus seen to be independent of the crystal structure. The mean value for lithium 0.168 comes within 3.5 per cent. of the theoretical value 0.174. The mass-scattering coefficients found for the liquids varied somewhat erratically, moreover they are greater than the theoretical values assuming the mass-scattering coefficient of carbon and hydrogen to be 0.200 and 0.399 respectively. The theoretical values for benzene, mesitylene, and octane are 0.215, 0.220, and 0.231 respectively, while the means of the experimental values are 0.238, 0.244, and 0.248 respectively. Assuming that these experimental mass-scattering coefficients are each made up of two parts, one due to carbon and one due to hydrogen, each part in proportion to the mass of carbon and hydrogen present respectively, the mass-scattering coefficients of carbon and hydrogen were calculated to be 0.228 and 0.375 respectively. The value thus found for hydrogen comes within 6 per cent. of the theoretical value 0.399, while the value for carbon is 14 per cent. higher than the value found for graphite and diamond. The mass-scattering coefficients of the three liquids found by method *A* furnish probably a more just basis for determining the separate coefficients for carbon and hydrogen than the above calculation, for the three curves were determined simultaneously point for point. The three equations for the three substances are:

For benzene	$12C + H = 3.100,$
For mesitylene	$9C + H = 2.440,$
For octane	$16C + 3H = 4.893,$

where C and H represent the mass-scattering coefficients of carbon and hydrogen respectively. These equations give three independent values for C and H.

	C.	H.
	0.220	0.488
	0.221	0.441
	0.220	0.460
Means,	0.220	0.463

It is seen that both the values of C and H are considerably larger than the theoretical values. If these liquids contained very small percentages of some element of moderately large atomic weight, such as bromine,

[1] Conduction of Electricity through Gases, 2nd edition, p. 325.

some of the absorbed x-rays reëmitted as characteristic x-radiation would be of sufficient penetrating power to reach the ionization chamber where it would add to the effect of the scattered radiation. At least this hypothesis is plausible in the case of the octane, for bromine was one of the constituents of one of the compounds from which it was prepared. The origin of the benzene and mesitylene is not known, but their boiling points and densities indicate that they are relatively pure. One might look for some such effect as proposed above by the method devised by A. H. Compton.[2] This was tried at the angle of maximum scattering for benzene with a negative result.

VI. Appendix. Correction for Absorption of the Scattered Radiation within the Scattering Material.

Attempts to arrive at a complete solution of this problem have not succeeded.

Making the usual assumption of exponential absorption of the x-rays, let $(\mu + \sigma)$ be the linear absorption coefficient, where μ represents that part of the coefficient due to true absorption, and σ that due to scattering. Let us suppose that the distance of the source of x-rays from the scattering material is great enough so that the x-rays are parallel in passing through. This condition is sufficiently fulfilled in the present work. It may then be shown that of a beam of x-rays striking a circular cylinder of material perpendicular to its axis, a fraction is scattered per unit solid angle in the direction making an angle θ with the beam, given by the following expression:

$$S_\theta = f(\theta)\left(1 - \frac{4}{3\pi}a + \frac{1}{8}a^2 - \frac{4}{45\pi}a^3 + \frac{1}{192}a^4 - \cdots\right),$$

where $a = (\mu + \sigma)D$ and D is the diameter of the cylinder $f(\theta)$ is a factor depending on the crystal structure, expressing the angular distribution of the scattered radiation. Not all of this scattered radiation gets out of the scattering material because it is absorbed and scattered on its way out. If it assumed that none of S_θ which is rescattered gets out, we arrive at the following expression for the fraction of the original beam getting out of the cylinder per unit solid angle in the direction making an angle θ with the beam

$$S_\theta' = f(\theta)\int_{-R}^{+R}\int_{-\sqrt{R^2-x^2}}^{+\sqrt{R^2-x^2}} \epsilon^{-(\mu+\sigma)\left[y+\sqrt{R^2-y^2}+\sqrt{R^2-x\sin\theta+y\cos\theta)^2-(x\cos\theta+y\sin\theta)^2}\right]}\,dxdy,$$

where R is the radius of the cylinder. The origin of coördinates is taken

[2] Phys. Rev., N. S., 18, 1921, p. 96.

on the axis of the cylinder. The above assumption is not justifiable, and consequently S_θ' given above is too small. The first four terms of the expansion in powers of a, of the above integral, which were found for me by Prof. E. W. Chittenden, of the department of mathematics at this university, are as follows:

$$S_\theta' = f(\theta)\left[1 - \frac{8}{3\pi}a + \frac{1}{4}\left(1 - \frac{\cos\theta}{4} + \frac{\gamma(\pi-\gamma)}{2\pi\sin\gamma} + \frac{\pi-2\gamma}{4\pi}\cos\gamma + \frac{\sin\gamma}{\pi}\right)a^2 - \frac{24}{45\pi}\left(1 - \frac{7}{22}\cos\theta + \frac{1}{22}\cos^2\theta - \frac{1}{22}\cos^3\theta + \frac{1}{22}\cos^4\theta\right)a^3\right],$$

$$a = (\mu + \sigma)D$$

and

$$\gamma = \theta \quad \text{if} \quad 0 \leqq \theta \leqq \frac{\pi}{2},$$

$$\gamma = -\theta \quad \text{if} \quad -\frac{\pi}{2} \leqq \theta \leqq 0,$$

$$\gamma = \pi - \theta \quad \text{if} \quad \frac{\pi}{2} < \theta \leqq \pi,$$

$$\pi = \pi + \theta \quad \text{if} \quad -\pi \leqq \theta < -\frac{\pi}{2}.$$

The ratio S_θ/S_θ' gives the correction factor for a given angle θ, that is the number by which the measured scattered radiation must be multiplied to give the actual amount scattered. This factor will be too large, however, because, as mentioned above, S_θ' is too small. The diamond splints being the substance requiring the largest correction factor, calculations were made for it for nine values of θ from 0 to π. The factor has its largest value 1.228 at 0 and continuously decreases to its smallest value 1.200 at π, the value 1.216 at $\pi/2$ being almost the mean of the other two.

Now we may get another estimate of the correction factor by assuming that all of the originally scattered radiation which is rescattered gets out. With this assumption the fraction of the original beam getting out of the cylinder per unit solid angle in the direction making an angle θ with the beam is given by the following expression:

$$S_\theta'' = f(\theta)$$

$$\times \int_{-R}^{+R} \int_{-\sqrt{R^2-x^2}}^{+\sqrt{R^2-x^2}} \epsilon^{-\mu\left[x + \sqrt{R^2-y^2} + \sqrt{R^2-(x\sin\theta + y\cos\theta)^2} - x\cos\theta + y\sin\theta\right] - \sigma\sqrt{R^2-y^2}} dxdy.$$

Since the previous integral when solved varied so little with the angle θ it was deemed sufficient to solve the above expression for $\theta = 0$. Now

this expression will give too large a value for the scattered radiation getting out of the cylinder, and too small a value for the correction factor for some of the rescattered radiation will be absorbed. The above integral when solved for $\theta = 0$ gives

$$S_\theta'' = f(\theta)\left(1 - \frac{4}{3\pi}\frac{b^2 - a^2}{b - a} + \frac{1}{8}\frac{b^3 - a^3}{b - a} - \frac{4}{45\pi}\frac{b^4 - a^4}{b - a} + \cdots\right),$$

where $a = \mu D$; $b = (\mu + \sigma)D$.

The values of S_θ/S_θ' and S_θ/S_θ'' for $\theta = 0$ for the diamond capsule were respectively 1.228 and 1.130. The mean value of this is 1.179, and since the value 1.228 for $\theta = 0$ was about 1 per cent. larger than the mean value, the value 1.17 was taken as the average correction factor for the diamond capsule. In the case of the other materials the difference between the two estimates of the correction factor were much smaller. For instance for the artificial graphite the two values were 1.11 and 1.07, giving a mean value of 1.09.

The writer takes pleasure in recording the following acknowledgments: To Tiffany and Co. of New York City for lending the diamond splints; to Prof. L. C. Raiford for the mesitylene; to Mr. John R. Couture for the benzene and octane; to Prof. P. A. Bond for the lithium; to Dr. A. W. Hull for the graphite and zirconium-oxide filter used in this investigation; to Mr. J. B. Dempster for much help in the construction and design of the apparatus; to Miss Marcella Lindeman, Mr. Joseph L. Fiala, Mr. Harlan Porter and other students in this laboratory for help in taking observations.

STATE UNIVERSITY OF IOWA,
IOWA CITY, IOWA,
June 9, 1922.

Reprinted from the Journal of the Optical Society of America and Review of Scientific Instruments
Vol. VI, No. 10, December, 1922

A TELEPHONE RECEIVER AND TRANSMITTER

By C. W. Hewlett

In previous publications [Phys. Rev., *17*, p. 257, 1921; and *19*, p. 52, 1922] the writer has described an instrument which lends itself to the reception and generation of voice currents. It consists of two coaxial pancake coils held by an insulating frame a short distance apart on either side of an electrically conducting diaphragm. Figs. 1 to 4 inclusive show reproductions of photographs of two of these instruments.

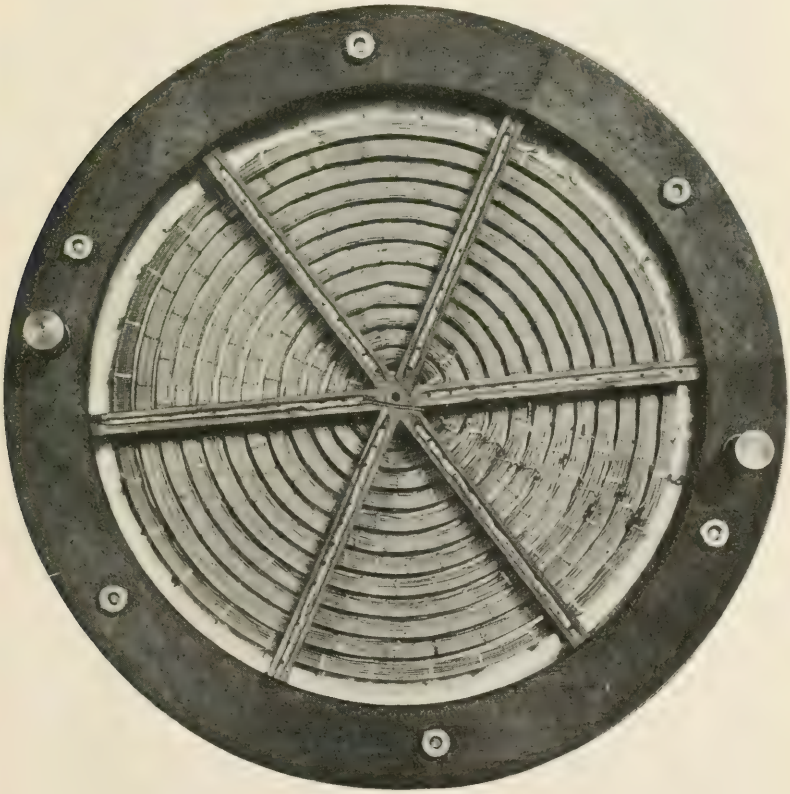

Fig. 1

In order to use the instrument a direct current is sent through the coils in such a way that their magnetic fields oppose, the result being a radial magnetic field in the space occupied by the diaphragm between the coils. Fig. 5 shows an arrangement of circuits for using two of the instruments, one as a generator, and the other as a receiver of voice currents. In practice the circuit is somewhat simplified since one or two batteries can be used to supply all the currents. If generators are used instead of batteries, filters are necessary. LLLL are the coils, and DD the diaphragms of the voice current generator and receiver. AA are two amplifying tubes; *CC*, coupling condensers; *rr*, grid leaks; and *RR*, coupling resistances. C_1 is an output condenser coupling the second tube with the receiver of voice currents.

The generator of voice currents, shown on the left, functions as follows: Sound waves, striking *D*, cause it to vibrate across the radial magnetic field. This generates voice currents in the diaphragm which in turn induce voice electromotive forces in the coils *LL*. The induced electromotive forces in the two coils are in multiple supplying the grid-filament circuit of the first tube. The condensers *CC* should have an impedance small compared to the grid-filament resistance for all frequencies concerned. The twice amplified voice current is fed through the condenser C_1 to the receiver of voice current where it induces voice current in the diaphragm. The reaction between the voice current in the diaphragm and the radial magnetic field causes the diaphragm to vibrate and produce sound waves of the same character as the original ones striking the diaphragm of the generator of voice currents.

To avoid diaphragm resonance, which is one of the chief factors giving rise to distortion in the usual telephone apparatus, the diaphragm is thin and is held without tension between the coils. Calculation shows that the amplitude of motion of the diaphragm is nearly independent of its thickness, but increases with increase of its conductivity and decrease of its density. An aluminum diaphragm from 1 to 2.5 mils thick has been found suitable. Electrical resonance has been found to be of no importance for telephonic purposes, as with the low-inductance instruments

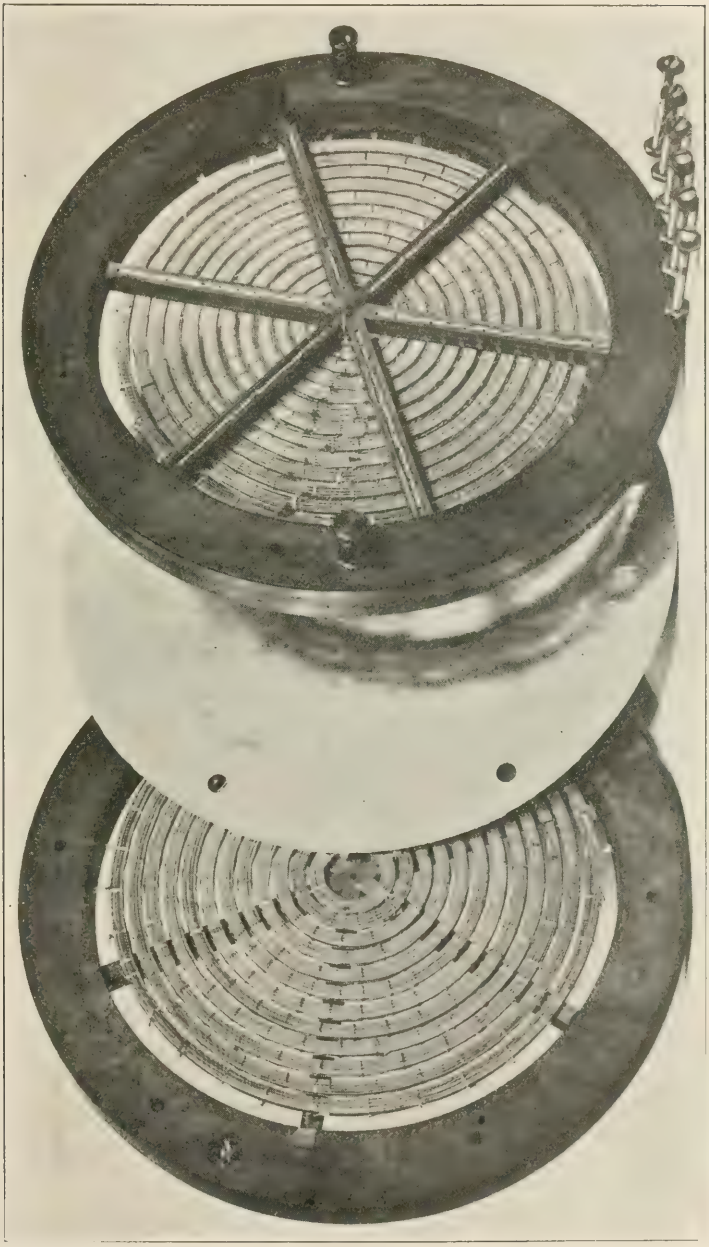

FIG. 2

the frequencies of electrical resonance are usually above audibility, while with the high inductance instruments the resistance is usually so large that there are no sharp resonance peaks.

Another point of advantage in this type of instrument when used as a receiver of voice currents is that the diaphragm is acted upon fairly uniformly over its surface by the varying force due to the interaction between the voice current in the diaphragm and the radial magnetic field. This is unfavorable to the production of resonance as the diaphragm is urged to and fro somewhat

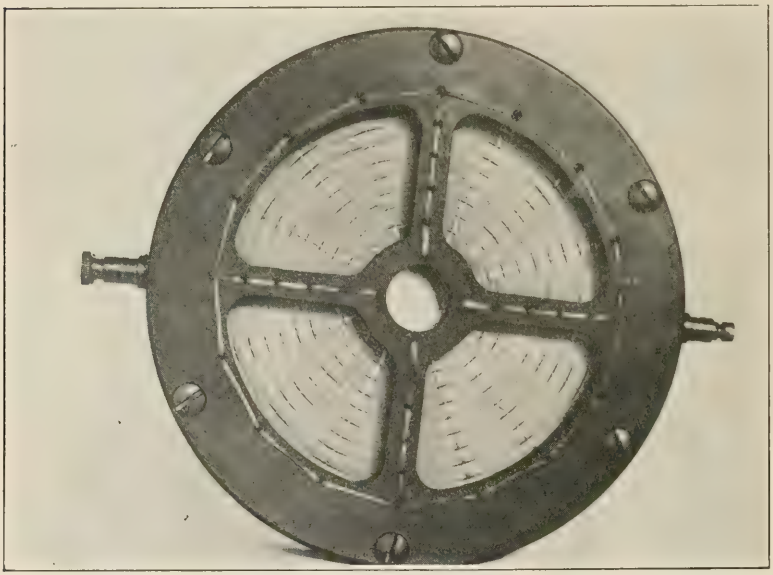

Fig. 3

like a piston. Calculation shows that the magnitude of the electrodynamic forces acting on the diaphragm is large compared to the reaction of the air due to the emission of sound waves.

In the ordinary forms of telephone apparatus there is a certain amount of distorsion which arises from the magnetic behavior of the iron used in its structure. The instrument described in this paper is free from this defect.

On account of being able to use a large diaphragm which is acted upon fairly uniformly over its whole surface, the use of a

horn for intensifying the sound is of less advantage than in the usual forms of speakers. The use of a horn while greatly intensifying the sound always introduces distorsion due to resonance in the horn. The quality of the speech given by this instrument is remarkably like that spoken into the voice current generator when a properly designed amplifier connects the two.

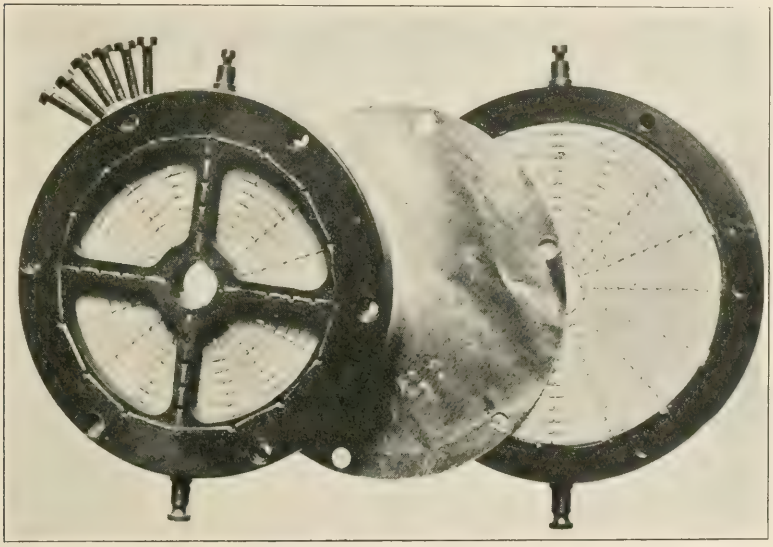

FIG. 4

The pancake coils of the instrument shown in figures 1 and 2 are each composed of twelve annular coils. Each annular coil is composed of eight layers five turns wide of No. 22 A. W. G. single silk covered copper wire, bound at intervals with silk thread. The outside diameter of each pancake is 7.5 inches. The resistance of each pancake is 8 ohms and the inductance 16 millihenuries. The diaphragm is 2.5 mil sheet aluminum, and is spaced 30 mils from each coil. The frame is of laminated walnut. This instrument is used as a speaker on receiver of voice currents. When excited by a direct current of 1.5 amperes and a voice current of 0.1 ampere it produces speech that is comfortably audible at all points in a room 20 ft. square. Another instrument wound

with No. 34 A.W.G. double silk covered wire containing nine times as many turns, but with otherwise the same geometry and construction as the above is frequently used as a generator of voice currents. Each pancake has a resistance of 1200 ohms and an inductance of 1.2 heuries. This instrument may also be used as a speaker if the output of the amplifier has a high impedance.

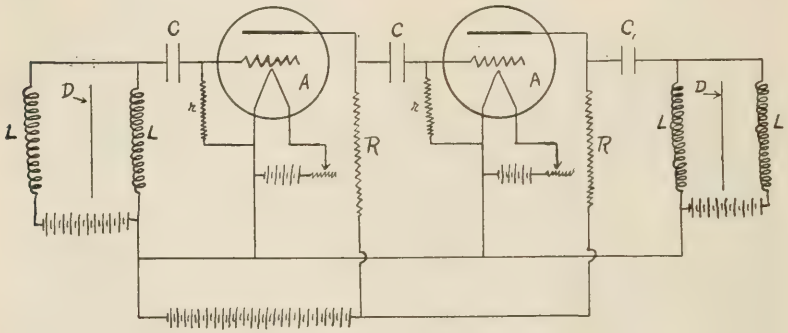

FIG. 5

The instrument shown in Figs. 3 and 4 consists of two compact pancake coils. Each wound of 3300 turns of No. 34 A.W.G. double silk covered wire. The coils are not impregnated, but are woven together with silk threads and are attached in the same manner to the hard fiber framework supporting them. Each pancake is 4 inches in diameter, is 0.2 inch thick, has a resistance of 540 ohms, and an inductance of 0.5 heury. The diaphragm is 1 mil sheet aluminum and is spaced 30 mils from the coils. The performance of this instrument differs only in magnitude from that shown in figures 1 and 2. It appears that the coils do not much cut off the sound waves to or from the diaphragm.

In case the amplifier used has an output impedance much different from that of the speaker at voice frequencies, it may be best to sacrifice quality of reproduction to a certain extent in order to obtain more intensity. This may be done by using a transformer as shown in figure 6. P and S are the primary and secondary of a transformer. The impedances of P and S are designed to fit the output of the amplifier and the coils LL of the speaker respectively. B is a direct current supply for polarizing the coils.

It is possible by the use of choke coils and condensers inserted at the proper places to use the plate current of the amplifier tube as the polarizing current of the speaker, provided this plate current is large enough. This has not been found very useful, however, on account of the large choke coils required. A high impedance head set has been used in which the plate current of a

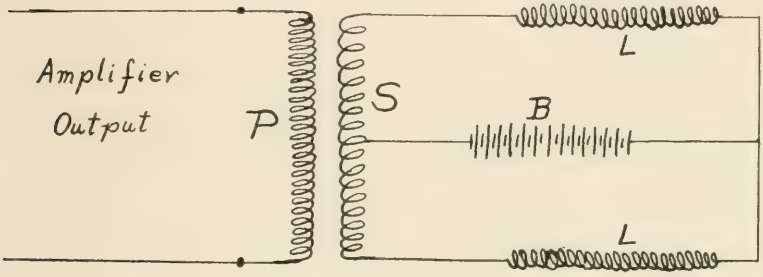

FIG. 6

single amplifier passing through the two halves of the instrument in series (one half held at each ear, and each half having a diaphragm) is sufficient to polarize the instrument. When the two halves are separated in this way, the choke coils and condensers mentioned above are of no use, and to avoid appreciable distorsion the variations of the plate current during amplification must be small.

Compared to other forms of receivers and transmitters, particularly the microphone and ordinary magnetic receiver, the instrument described above is very insensitive, but it gives an excellent quality of reproduction of speech and music.

The writer takes pleasure in acknowledging the help in the construction of these instruments and in the experimental work in connection with them rendered by Messrs. J. B. Dempster and Harlan Porter.

STATE UNIVERSITY OF IOWA,
IOWA CITY, IOWA,
JULY 20, 1922.

ACOUSTIC WAVE FILTERS.

[Reprinted from The Physical Review, S.S., Vol. XX., No. 6, December, 1922.]

ACOUSTIC WAVE FILTERS.

By G. W. Stewart.

Synopsis.

Acoustic Wave Filters Composed of a Series of Like Sections.—(1) *Theory.* Taking the impedance of any part of an acoustic circuit to be equal to the complex ratio of the applied pressure difference to the rate of change of volume displacement, it is shown that, neglecting dissipative forces, it is possible to construct a filter having limiting frequency values of no attenuation determined by the formulæ $Z_1/Z_2 = 0$ and $Z_1/Z_2 = -4$, where Z_1 is the impedance of the transmitting conduit circuit and Z_2 of each branch of each section. The impedance of any section depends on the inertance M of dimensions mass per unit area squared, and the capacitance C which has the dimensions of stiffness per unit area squared. If M and C are in parallel, $Z = iM\omega/(1 - MC\omega^2)$, whereas if they are in series, $Z = i(M\omega - 1/C\omega)$. For instance, in the case of a closed chamber or resonator, M and C are in series and are equal to ρ/C and $V/\rho a^2$ respectively where ρ is the density of the medium, c is the conductivity of the mouth, a the velocity of sound and V the volume. Formulæ are derived for various assumed cases. On account of the uncertainty as to whether a tube may be considered as having the equivalent inertness and capacitance connected in parallel or in series, the application of these formulæ to actual cases is somewhat empirical. (2) *Construction and test of filters of three types.* Low-frequency-pass filters were made, for example, by two concentric cylinders joined by walls equally spaced and perpendicular to the axis. Each chamber thus formed had a row of apertures in the inner cylinder which served as the transmission tube. In one case the volume of each chamber was 6.5 cm.^{3}, the radius of the inner tube 1.2 cm. the length between apertures, 1.6 cm. A chamber and one such length of the inner tube is called a section. Four such sections were found to transmit 90 per cent. of the sound from zero to approximately 3,200 d.v. where the attenuation became very high, resulting in zero transmission up to about 4,600 d.v. where transmission again appeared, Other similar filters of different dimensions attenuated through wider or narrower ranges. The lower limit of attenuation was found to correspond within 8 per cent. with the formula: $f = (1/\pi)(M_1C_2 + 4M_2C_2)^{-1/2}$. The upper limit was not predicted theoretically. High-frequency pass filters were made with a straight tube for transmission and short side tubes, for example, 0.5 cm. long and 0.28 cm. in diameter, opening through a hole with conductivity 0.08 into a tube 10 cm. long and 1 cm. in diameter. Six sections of such a filter would transmit about 90 per cent. of sounds above 800 but would refuse transmission to sounds of lower frequency. As would be expected, the cut off is not sharp. Filters with other dimensions were found to have an upper limit of attenuation varying from 450 to 2,300 d.v., agreeing with the formula $f = (1/2\pi)(1/4M_2C_1 + 1/M_1C_2)^{1/2}$, within about 13 per cent., on the average. The single-band filters made were a combination of the other two types, having side tubes leading to chambers of considerable volume. For instance, three sections each 5 cm. long and 0.5 cm. in diameter, with side tubes of the same size and 2.2 cm. long leading to a volume of 28 cm.^{2}, transmitted between 270 and 370 d.v. The frequencies of the edges of the band of small attenuation are determined by the following formulae,

$$2\pi f = [M_2C_2(1 + M_2'/M_2)]^{-\frac{1}{2}} \text{ and}$$

$$2\pi f = [M_2C_2(1 + 4M_2'/M_1)^{-1}(1 + M_2'/M_2 + 4M_2'/M_1)]^{-\frac{1}{2}}.$$ Such filters

exhibit the same variations from theoretical performance as would be expected from a combination of the other two types. However, the agreement of each type with theory is sufficient to enable filters to be designed to fulfill set conditions. The *attenuation secured* with only four sections is very great, the transmission being certainly less than 10^{-7} in the attenuated region, while it may rise to 90 per cent. in unattenuated regions. *Possible applications* of these simple filters in laboratory work and in connection with specking devices, are briefly suggested.

I. General Introduction.

THE selective transmission of an acoustic wave of a given frequency is well known. A Helmholtz resonator with a small ear opening is such a filter. Cylindrical tubes such as shown in Fig. 1 will also serve as filters, (*a*) transmitting chiefly the resonating frequencies of *cd* and (*b*) giving poor transmission especially for the resonating frequencies of *cd*. The acoustic wave filters which this article describes

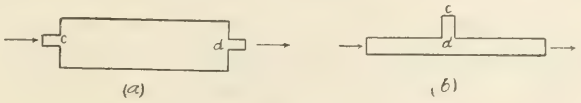

Fig. 1.

are different in principle and in performance in that they do not depend upon resonance itself, but upon the interaction between recurrent similar sections of a transmission "line," these sections containing the elements upon which free vibrations are to depend, and having over-all dimensions that are small in comparison with a wave-length of the sound.

These new filters are remarkable in that selected groups of frequencies, extending over a large range, can be eliminated in the transmission. Up to the present time, three kinds have been constructed and tested. The low frequency pass filter will give approximately zero transmission at all frequencies above, and a fairly good transmission below a certain predetermined frequency. The high-frequency filter will transmit above a minimum frequency. The single-band filter will transmit a group of frequencies. In all cases, the frequency limits are ascertained approximately by calculation from the dimensions so that the filters may be designed to fit specifications. In these filters, the cutoffs are not sharp and the performances are not exactly as just stated, but, as will be shown, the explanation is found in the fact that the experimental conditions only approximate the theoretical.

II. Theory.

A. General.

An exact theoretical discussion of the acoustic wave filter may be possible, but certainly there is much to be gained in securing a theory

which, though only approximate, will aid in understanding the operation of the filters and in developing new designs. The well-known electric wave filters suggested to the writer the possibility of analogous effects in acoustics. Naturally, the theory[1] of the electric filters has been of much assistance.

Certain limitations will be imposed in our discussion. We will assume that the length of any selected section of an acoustic "line" or conductor is so small in comparison with a wave-length that no change in phase occurs therein. We will consider only sinusoidal waves. The term "acoustic impedance" will be used. Its absolute value is the ratio of the maximum pressure difference applied to the maximum rate of change of volume displacement. When complex notation is used for simplicity, as in alternating electric current theory, the acoustic impedance is the complex ratio of the pressure difference applied and the rate of change of volume displacement. The mathematical procedure will be based upon three hypotheses which are obviously reasonable approximations. They are: (1) the rate of volume displacement in any selected portion of the line, with a harmonically varying applied difference of pressure, can always be expressed by $Ie^{i\omega t}$ where I is complex; (2) the product of acoustic impedance and rate of volume displacement in any selected portion of the line equals the difference of pressure applied; (3) the algebraic sum of the volume displacements at any junction of lines is zero. By acoustic "line" is meant a bounded region of fluid or solid, forming a tube or channel and capable of transmitting sound waves in the direction of the tube or channel only.

We will consider an acoustic wave filter consisting of equal acoustic impedances in series, divided into sections by acoustic impedances in what might be termed shunt branches. In Fig. 2, let a sound wave of a

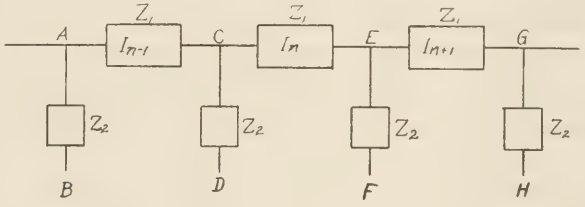

Fig. 2.

frequency $\omega/2\pi$ be transmitted through the line AG, a portion of an infinite line, containing a series of equal impedances, Z_1. Let each branch line AB, CD, EF, GH, etc., contain an impedance Z_2 and terminate in a

[1] U. S. Patent 1,227,113 by George A. Campbell. Chapter XVI. of Pierce's "Electrical Oscillations and Electric Waves," 1920.

volume of gas otherwise at rest, so that there is a common constant pressure at or near these termini. Let $I_n e^{i\omega t}$, etc., represent the rates of change of volume displacement in the corresponding lines, I_n being a complex quantity, and let the positive direction be from A to G. From the three conditions stated in the foregoing paragraph the following equation may be secured:

$$Z_2(I_{n-1} - I_n) = Z_2(I_n - I_{n+1}) + Z_1 I_n$$

or

$$I_{n+1} - \left(2 + \frac{Z_1}{Z_2}\right) I_n + I_{n-1} = 0. \tag{1}$$

This equation does not require an infinite line, but we will for convenience impose that condition. We may then write, using ΔP as the complex pressure difference over a branch,

$$\Delta P_{CD} = I_n(Z_1 + Z_\infty)$$

and

$$\Delta P_{EF} = I_{n+1}(Z_1 + Z_\infty),$$

wherein Z_∞ is the impedance of the infinite network to the right in the figure and has the same value in both equations.[1] Substituting the values,

$$\Delta P_{CD} = Z_2(I_{n-1} - I_n),$$
$$\Delta P_{EF} = Z_2(I_n - I_{n+1})$$

and dividing we have,

$$\frac{I_{n+1}}{I_n} = \frac{I_n - I_{n+1}}{I_{n-1} - I_n}$$

or

$$\frac{I_{n+1}}{I_n} = \frac{I_n}{I_{n-1}}. \tag{2}$$

Let us call the ratio of these successive I's, e^Y, where Y is unknown but in general is complex. Substitute in (1), and we have,

$$e^Y + e^{-Y} = 2 + \frac{Z_1}{Z_2}$$

or

$$\cosh Y = 1 + \tfrac{1}{2}\frac{Z_1}{Z_2}. \tag{3}$$

[1] The filter through its branches terminates in the undisturbed medium. The pressure at E can be expressed by $I_n Z_\infty$. From the equation of motion of a portion of a vibrating medium having a sinusoidal impressed force, and possessing mass, stiffness and dissipation, it can readily be shown that the impedance Z is a function of mass, stiffness, the dissipative factor and frequency only. In as much as these factors are the same for our Z_∞, whether taken from E or from G or any junction point, the assumption of identity of the Z_∞'s is justified.

If Y is a pure imaginary the rates of volume displacement in two adjacent sections differ only in phase. If Y is not a pure imaginary the rate of volume displacement is diminished in transmission, obviously the diminution occurring away from the input end. If Y is a pure imaginary, since $\cosh ix = \cos x$

$$+ 1 > \left(1 + \tfrac{1}{2}\frac{Z_1}{Z_2}\right) > - 1 \tag{4}$$

and hence the limiting values of no attenuation are determined by the following:

$$\frac{Z_1}{Z_2} = 0, \tag{5}$$

$$\frac{Z_1}{Z_2} = - 4. \tag{6}$$

We can find the limiting values of no attenuation in a filter by utilizing the actual values of Z_1 and Z_2. It would therefore appear that an acoustic wave filter can be constructed, the only uncertainty being the manner of constructing Z_1 and Z_2. In order to determine upon the practical development of the filter, idealized conditions will first be discussed.

B. Inertance and Capacitance in Parallel.

Consider two idealized diaphragms, a and b, supposed to move as a whole, the former having mass, m_a, and not stiffness, and the latter stiffness, f_b, and not mass. Let them have areas S_a and S_b and displacements ξ_a and ξ_b and let them be connected in parallel as branches of an acoustic line so that they are subject to the same fluid pressure differences, $Pe^{i\omega t}$. Then,

$$m_a \frac{d^2\xi}{dt^2} = S_a P e^{i\omega t} \qquad \text{and} \qquad f_b \xi_b = S_b P e^{i\omega t},$$

the latter being merely the definition of f_b.

If we are concerned with the total volume displacement of the gas at the diaphragms, X_a and X_b, these equations become:

$$\frac{m_a}{S_a^2}\frac{d^2X_a}{dt^2} = Pe^{i\omega t} \qquad \text{and} \qquad \frac{f_b X_b}{S_b^2} = Pe^{i\omega t}. \tag{7}$$

We wish to obtain an expression for dX/dt or the rate of change of volume displacement in the main line at the junction of these two branches. By integration we find,

$$\frac{m_a}{S_a^2}\frac{dX_a}{dt} = \frac{P}{i\omega}e^{i\omega t} \tag{8}$$

the constant of integration vanishing since we are dealing with a variation in dX/dt caused by P and vanishing with P. By differentiation we obtain,

$$f_b \frac{dX_b}{dt} \Big/ S_b^2 = i\omega P e^{i\omega t}. \tag{9}$$

But we know that at the junction of the branches the algebraic sum of the rate of volume displacements must be zero, or

$$\frac{dX_a}{dt} + \frac{dX_b}{dt} = \frac{dX}{dt}. \tag{10}$$

Substituting the values of dX_a/dt and dX_b/dt just found, we obtain,

$$\frac{dX}{dt} = Pe^{i\omega t}\left(\frac{1 - MC\omega^2}{iM\omega}\right), \tag{11}$$

wherein

$$M = \frac{m_a}{S_a^2} \quad \text{and} \quad \frac{1}{C} = \frac{f_b}{S_b^2}. \tag{12}$$

We will call M the *inertance*, C the *capacitance*, both defined by (12) and (7). We thus have for the impedance of the combination of the two circuits in parallel,

$$Z = \frac{iM\omega}{1 - MC\omega^2}. \tag{13}$$

Let us now assume that our impedances Z_1 and Z_2 are each composed of two such branches in parallel. The branch having mass, m_a, will vanish when $m_a = \infty$ or $M = \infty$ and the branch having stiffness, f_b, will vanish when $f_b = \infty$ or $C = 0$.

If we apply condition (5) to Z_1 and Z_2 as just determined in (13) and we have as a limiting frequency, f_1:

$$\omega^2 = \frac{1}{M_2C_2} \quad \text{or} \quad f_1 = \frac{1}{2\pi}\sqrt{\frac{1}{M_2C_2}}. \tag{14}$$

If we apply condition (6), we have:

$$\omega^2 = \frac{M_1 + 4M_2}{M_1M_2(4C_1 + C_2)} \quad \text{or} \quad f_2 = \frac{1}{2\pi}\sqrt{\frac{M_1 + 4M_2}{M_1M_2(4C_1 + C_2)}}. \tag{15}$$

In (14) and (15) the subscripts of M and C correspond to those adopted for the Z's. These frequencies f_1 and f_2 are those that limit the range in which there is no attenuation. It is to be observed that the range of no attenuation is one in which $\left(1 + \frac{1}{2}\frac{Z_1}{Z_2}\right)$ can change from $+1$ to -1.

But, from (13), Z_1/Z_2 is a continuous function of ω or $2\pi f$ and hence there is a continuous frequency range wherein there is no attenuation. A filter in which Z_1 and Z_2 each consists of an inertance and capacitance in parallel is thus possible.

C. Inertance and Capacitance in Series.

Consider each Z_1 and Z_2 to be an inertance and capacitance in series. The current must be the same throughout Z_1 or Z_2. Let P_1 be the pressure difference over the inertance, M_1, and P_2, over the capacitance, C_1. Then, from (7) and (8)

$$\frac{P_1}{i\omega M_1} = I = \frac{P_2}{\frac{1}{C_1 i\omega}}.$$

Hence

$$\frac{P_1 + P_2}{i\omega M_1 + \frac{1}{iC_1\omega}} = I$$

or

$$Z_1 = i\left(M_1\omega - \frac{1}{C_1\omega}\right). \tag{16}$$

If we now ascertain the limits of no attenuation, we have from (5),

$$f_1 = \frac{1}{2\pi}\sqrt{\frac{1}{M_1C_1}} \tag{17}$$

and from (6)

$$f_2 = \frac{1}{2\pi}\sqrt{\frac{C_2 + 4C_1}{C_1C_2(M_1 + 4M_2)}}. \tag{18}$$

Again we have the possibility of a filter.

A special and yet a common case of inertance and capacity in series is one wherein M_1 is the inertance of an orifice entering a chamber and C_1 is the capacitance of the chamber. The condition for resonance, or $Z = 0$, occurs as shown by (16) when,

$$M_1\omega = \frac{1}{C_1\omega} \qquad \text{or} \qquad f = \frac{1}{2\pi}\sqrt{\frac{1}{M_1C_1}}. \tag{19}$$

But in orifices which are short compared with their diameters we cannot use for M_1 the mass divided by the square of the area, for this expression neglects the end effects of the channel. The well-known formula for the vibration of such a system is,[1] neglecting dissipation[2]

[1] Rayleigh, Theory of Sound, Vol. II., p. 195.

[2] Insertion of dissipation seems to lead to difficulties which are avoided by this approximation.

$$\frac{\rho}{c}\ddot{X} + \frac{\rho a^2}{V}X = Pe^{i\omega t} \tag{20}$$

from the solution of which we get,

$$\dot{X} = \frac{Pe^{i\omega t}}{i\rho\left(\frac{\omega}{c} - \frac{a^2}{V\omega}\right)}. \tag{21}$$

In these equations ρ is the density, c is the "conductivity" of the channel, a the velocity of sound and V the volume of the chamber.

It is evident that the new value of Z_1 viz.,

$$Z = i\rho\left(\frac{\omega}{c} - \frac{a^2}{V\omega}\right), \tag{22}$$

differs from (16) only by the apparent substitution of ρ/C for M_1 and $V/\rho a^2$ for C_1.

D. Inertance and Capacitance of a Tube.

In order to assist in constructing a filter, we will now discuss the nature of a column of gas, which we must use as Z_1 in our conducting line.[1]

Assume an acoustic plane simple harmonic wave passing along a tube in the direction of x. Let ξ be the displacement of a particle from its mean position; ρ the density, a the velocity of sound, and p the excess pressure over the mean.

Then

$$\rho\frac{\partial^2\xi}{\partial t^2} = -\frac{\partial p}{\partial x} \tag{23}$$

(an exact equation) and for small vibrations,[2]

$$\frac{\partial^2\xi}{\partial t^2} = a^2\frac{\partial^2\xi}{\partial x^2}. \tag{24}$$

From (23) and (24)

$$\rho a^2\frac{\partial^2\xi}{\partial x^2} = -\frac{\partial p}{\partial x}. \tag{25}$$

The integration of (25), since

$$\frac{\partial\xi}{\partial x} = 0$$

at all times when $p = 0$, gives

$$\rho a^2\frac{\partial\xi}{\partial x} = -p. \tag{26}$$

[1] Similar discussions occur in Drysdale, Jl. of Inst. Elec. Engs., July, 1920, Vol. 58, p. 591, and Kennelly and Kurowaka, Proc. Am. Acad., Feb., 1921, Vol. 56, No. 1, p. 29.

[2] Lamb's Hydrodynamics, 1916, p. 474.

We may write (26) as follows:

$$\rho a^2 \frac{\partial \xi}{\partial x} \frac{\Delta x}{\Delta x} = - p$$

and if we represent the volume in a length Δx by ∇V, we have,

$$\rho a^2 \frac{\Delta V}{V} = - p$$

or $\rho a^2 = - E$ where E is the modulus of elasticity of volume. Since the compression is due to p and not to changes of pressure along the line, the stiffness can be considered as analogous to stiffness in the walls of the tube upon which the pressure difference p acts. Our tube possesses inertance and capacitance as we know, but the above shows that these are not the equivalent of inertance and capacitance connected either in parallel or in series. Indeed, the capacitance can be thought of as between the inside and outside of the tube instead of along the tube.

Inasmuch as we must use tubes in a practical construction it is essential that we consider whether or not a tube can be used for either Z_1, or Z_2, arranged as in the preceding theory. Consideration shows that Z_1 cannot accurately be composed of a tube, for Z_1 is wholly in the line and not between the line and the outside. Hence we must ascertain whether or not such a substitution would be a sufficient approximation. In short, can we consider a tube as having the equivalent of inertance and capacitance connected in parallel or in series, or may we consider it as having inertance only or as capacitance only?

Assume that any tube we may use will be short as compared with a wave-length. Consider the gas to move as a whole. Then the δp is due to inertance. Or consider the gas to be stationary acting as a cushion. Then δp is due to capacitance. In both cases we have neglected the change of phase along the tube. Whichever case is the better approximation will depend upon the service the tube is rendering, or, in other words, will depend upon the adjacent construction or the composition of the filter. It might appear that the tube can be approximated by lumping the capacitance. This cannot be done at the center of the section for the general theory does not permit of a side branch other than Z_2. It cannot be lumped at Z_2 as can be shown by comparison of the resulting theory with experiment. The assumption of M_1 and C_1 in series does not appear reasonable for the total pressure over the section certainly acts on M_1. We are therefore forced to the policy of using M_1 and C_1 in parallel in the line with the understanding that experiment will determine empirically whether M_1 or C_1 or both shall be used in the

computations. As will subsequently be shown, experiments thus far seem to demand the introduction of C_1 in only one of the three types of filters. Thus the somewhat arbitrary manner of introducing C_1 in parallel is minimized. It is fair to say that, in this one case, the assumption seems not without a theoretical justification. It is thus observed that at the outset we are driven to an approximation which demands an empirical selection of formulæ.

III. Construction of Filters.

A. General Limitations.

If we are to construct an acoustic filter that will have good transmission we must avoid any changes in the nature of the medium and in the diameter of the transmitting conduit or conductor. If the filter is to have good attenuation, similar conditions would hold for the branch lines. For first experiments, then, a single medium and a transmitting line of constant cross section are chosen. These selections suggest, from the standpoint of convenience, the use of air and the use of a cylindrical tube as the boundary of the transmission line.

The only limitation to our application is that there be a series of like sections with Z_1 in the main line and Z_2 in the side branch. With no limitation placed upon the constitution of Z_1 or of Z_2, an infinite number of designs may be possible. But, as already stated, considerations lead to the selection of a cylindrical tube containing air as the transmission line. The impedance of a short section of such a line cannot be accurately expressed by an equivalent M_1 and C_1 connected either in series or parallel. We will assume M_1 and C_1 in parallel, for thereby we can make $M_1 = \infty$ or $C_1 = 0$ or remove them from consideration without obstructing the transmission of the line. But even with these limitations the number of filters is infinite, for Z_2 can be formed, theoretically, in any manner one chooses.

B. Low Frequency, High Frequency, and Single Band Pass Filters.

In order to determine the construction of low frequency and high frequency pass and single band filters in as simple a manner as possible, an additional provisional limitation will be made, viz., to filters in which Z_2 consists of an equivalent M_2 and C_2 connected either in series or parallel. We shall then have four quantities M_1, M_2, C_1 and C_2. If either M_1 or M_2 is absent, *i.e.*, removed from consideration, its value is infinity. Under similar conditions the value of a capacitance is zero. We have then to ascertain the possible combinations of

$$M_1 = \infty, \qquad M_2 = \infty, \qquad C_1 = 0, \qquad C_2 = 0.$$

Taken singly there are four combinations in pairs, six in triplets, four with one only, and one with none, making a total of fifteen possible combinations. If we remove those combinations which remove the *line* or the branches entirely, we have left nine designated as follows:

1. All present,
2. $M_1 = \infty$,
3. $M_2 = \infty$,
4. $C_1 = 0$,
5. $C_2 = 0$,
6. $M_1 = M_2 = \infty$,
7. $M_1 = \infty$, $C_2 = 0$,
8. $M_2 = \infty$, $C_1 = 0$,
9. $C_1 = 0$, $C_2 = 0$.

By the preceding, our values of acoustical impedances are limited to the following:

In the transmission line,

$$Z_1 = \frac{iM_1\omega}{1 - M_1C_1\omega^2}. \qquad (13)\text{ bis}$$

In the branch,

$$Z_2 = \frac{iM_2\omega}{1 - M_2C_2\omega^2} \qquad (13)\text{ tris}$$

or

$$Z_2 = i\left(M_2\omega - \frac{1}{C_2\omega}\right). \qquad (16)\text{ bis}$$

If the limits of no attenuation are now ascertained by the application of equations (5) and (6) we find the values in Table I. for the nine cases, each having the possibility of Z_2 in parallel or in series.

The explanation of most of the blanks in the fourth and fifth columns is that, assuming M_2 and C_2 to be in series, our original arrangement of Z_2 providing for the same pressure in common at the termini, requires the following:

1. There must always be an M_2 at the junction point, for otherwise there could be no $\dot{X}$ and hence no use of the side branch. Hence M_2 is at the junction point and C_2 is next in the branch.

2. M_2 cannot be infinity, for if infinity, the side branch would not be used at all.

3. C_2 cannot be zero for this would prevent any value of $\dot{X}$ and therefore any use of the side branch. Thus six of the nine cases are eliminated from consideration leaving only cases 1, 2 and 4. Case 1 leads to the possibility of an imaginary frequency and introduces two values of f_2,

TABLE I.

Case.	Parallel.		Series.	
	f_1.	f_2.	f_1.	f_2.
1	$\frac{1}{2\pi}\sqrt{\frac{1}{M_2C_2}}$	$\frac{1}{2\pi}\sqrt{\frac{M_1+4M_2}{M_1M_2(4C_1+C_2)}}$	0	
2	$\frac{1}{2\pi}\sqrt{\frac{1}{M_2C_2}}$	$\frac{1}{2\pi}\sqrt{\frac{1}{M_2(4C_1+C_2)}}$	∞	$\frac{1}{2\pi}\sqrt{\frac{C_2+4C_1}{4M_2C_1C_2}}$
3	0	$\frac{1}{2\pi}\sqrt{\frac{4}{M_1(4C_1+C_2)}}$		
4	$\frac{1}{2\pi}\sqrt{\frac{1}{M_2C_2}}$	$\frac{1}{2\pi}\sqrt{\frac{M_1+4M_2}{M_1M_2C_2}}$	0	$\frac{1}{2\pi}\sqrt{\frac{4}{C_2(M_1+4M_2)}}$
5	∞	$\frac{1}{2\pi}\sqrt{\frac{M_1+4M_2}{4M_1M_2C_2}}$		
6	0	0		
7	∞	$\frac{1}{2\pi}\sqrt{\frac{1}{4M_2C_1}}$		
8	0	$\frac{1}{2\pi}\sqrt{\frac{4}{M_1C_2}}$		
9	∞	∞		

which are not found in experience. Knowing that the assumption of C_1 in parallel with M_1 is arbitrary, we are justified in acknowledging the incorrectness of the assumption in this case and omitting the formulæ from consideration.

These considerations lead to the development of the three following types of filters:

1. Low-frequency pass filters; case 3, parallel; case 4, series; and case 8, parallel.

2. High-frequency pass filters; case 2, series; case 5, parallel; case 7, parallel.

3. Single-band pass filters; case 1, parallel; case 2, parallel; case 4, parallel.

Conditions of construction suggest that an additional formula for the single-band filter be determined. The three cases in which we have a

single-band filter as above stated, are those in which we have M_2 and C_2 in parallel. But in actual construction it is impractical to have truly a C_2 without an orifice into a volume and in this orifice we have an M_2' in series with C_2. A simple construction is thus suggested of taking *Case I* and adding an M_2' as an orifice into C_2. The impedance of the orifice and C_2 will be, according to (16)

$$Z_2' = i\left(M_2'\omega - \frac{1}{C_2\omega}\right).$$

This impedance is in parallel with the inertance M_2, the impedance of which is,

$$Z_2'' = i\omega M_2.$$

As readily follows from the definition of impedance and the fact that the sum of the two currents is the resultant branch current, the combined impedance, Z_2, is determined from the following relation,

$$\frac{1}{Z_2} = \frac{1}{iM_2\omega} + \frac{1}{i\left(M_2'\omega - \frac{1}{C_2\omega}\right)}$$

or

$$Z_2 = i\frac{M_2\omega\left(M_2'\omega - \frac{1}{C_2\omega}\right)}{M_2\omega + M_2'\omega - \frac{1}{C_2\omega}} = i\frac{M_2\omega(M_2'C_2\omega^2 - 1)}{M_2C_2\omega^2 + M_2'C_2\omega^2 - 1}. \qquad (27)$$

According to equation (13) if we make C_1 arbitrarily zero for the sake of simplicity, we have

$$Z_1 = iM_1\omega. \qquad (28)$$

If we now use the values of (27) and (28) for the conditions (5) and (6) we will have, respectively,

$$f_1 = \frac{1}{2\pi}\sqrt{\frac{1}{C_2(M_2 + M_2')}}, \qquad (29)$$

$$f_2 = \frac{1}{2\pi}\sqrt{\frac{M_1 + 4M_2}{C_2(M_1M_2 + M_1M_2' + 4M_2M_2')}}. \qquad (30)$$

C. Computation of Inertance and Capacity.

By comparison of (23) with (7) we see that the inertance for a straight tube, assumed to move as a whole, is,

$$M = \frac{m}{S^2} = \frac{\rho lS}{S^2} = \rho\frac{l}{S}. \qquad (31)$$

In the case of an orifice, M, as already shown, is expressed by ρ/c where c is the conductivity. The expression for c in terms of the radius, R, and length, l, of the channel is[1]

$$c = \frac{\pi R^2}{l + \frac{\pi R}{2}}. \tag{32}$$

With l large in comparison with $\pi R/2$, this reduces to S/l and $M = \rho(l/S)$ as already stated.

As shown in the discussion of (22) we should substitute $V/\rho a^2$ for C_1. Therefore our equations for substitution are:

$$M = \frac{\rho}{c} = \frac{\rho\left(l + \frac{\pi R}{2}\right)}{\pi R^2} \tag{33}$$

and

$$C = \frac{V}{\rho a^2}. \tag{34}$$

D. Form of the Filters.

(*a*) *Low-Frequency Pass Filter.*—In a preceding section we found at least three formulæ for a low-frequency pass filter. They are as follows:

$$f_1 = 0, \qquad f_2 = \frac{1}{\pi}\sqrt{\frac{1}{M_1(4C_1 + C_2)}} = \frac{1}{\pi}\sqrt{\frac{1}{M_1C_2 + 4M_1C_1}}, \tag{A}$$

requiring that C_2 be the only portion of the branch;

$$f_1 = 0, \qquad f_2 = \frac{1}{\pi}\sqrt{\frac{1}{C_2(M_1 + 4M_2)}} = \frac{1}{\pi}\sqrt{\frac{1}{M_1C_2 + 4M_2C_2}}, \tag{B}$$

requiring that M_2 and C_2 be connected in series and that C_1 be zero;

$$f_1 = 0, \qquad f_2 = \frac{1}{\pi}\sqrt{\frac{1}{M_1C_2}}, \tag{C}$$

requiring that C_2 be the only portion of the branch and that C_1 be zero.

All these formulas are dimensionally correct and there is no conclusive evidence showing that one is superior to another save by actual experiment. Attention may be called, however, to the difficulty of constructing a C_2 without an M_2 in series. With C_2 only the most favorable cross-section of construction would be similar to Fig. 3. But there would be an M_2 and the justification for neglecting it would be raised.

Fig. 3.

[1] Rayleigh, Theory of Sound, Vol. II., p. 181.

If the construction is made as in Fig. 4, the M_2 is better defined and can be determined from equation (33). These considerations point to the use of (*B*).

Fig 4.

(*b*) *High-Frequency Pass Filter.* — We previously found three simple cases of a high-frequency pass filter. The formulæ are as follows:

$$f_1 = \infty, \qquad f_2 = \frac{1}{2\pi}\sqrt{\frac{C_2 + 4C_1}{4M_2C_1C_2}} = \frac{1}{2\pi} = \sqrt{\frac{1}{4M_2C_1} + \frac{1}{MC_{22}}} \qquad (D)$$

requiring that $M_1 = \infty$;

$$f_1 = \infty, \qquad f_2 = \frac{1}{2\pi}\sqrt{\frac{M_1 + 4M_2}{4M_1M_2C_1}} = \frac{1}{2\pi}\sqrt{\frac{1}{4M_2C_1} + \frac{1}{M_1C_2}} \qquad (E)$$

requiring that $C_2 = 0$;

$$f_1 = \infty, \qquad f_2 = \frac{1}{2\pi}\sqrt{\frac{1}{4M_2C_1}}, \qquad (F)$$

requiring that $M_1 = \infty$ and $C_2 = 0$. Formula (*E*) and (*F*) indicate that it might be possible to construct such a filter with a straight tube and side branches consisting of M_2 only, or consisting of orifices. This plan has been followed in the filters herein described.

(*c*) *Single-Band Filter.*—We previously found four simple single-band filters. The formulæ are as follows:

$$f_1 = \frac{1}{2\pi}\sqrt{\frac{1}{M_2C_2}}, \qquad f_2 = \frac{1}{2\pi}\sqrt{\frac{M_1 + 4M_2}{M_1M_2(4C_1 + C_2)}}$$

$$= \frac{1}{2\pi}\sqrt{\frac{1}{M_2C_2}\left[\frac{1 + 4\dfrac{M_2}{M_1}}{1 + 4\dfrac{C_1}{C_2}}\right]}, \qquad (H)$$

requiring that all of the four elements remain in consideration;

$$f_1 = \frac{1}{2\pi}\sqrt{\frac{1}{M_2C_2}}, \qquad f_2 = \frac{1}{2\pi}\sqrt{\frac{1}{M_2(4C_1 + C_2)}}$$

$$= \frac{1}{2\pi}\sqrt{\frac{1}{M_2C_2}\left[\frac{1}{1 + 4\dfrac{C_1}{C_2}}\right]}, \qquad (I)$$

requiring that $M_1 = \infty$;

$$f_1 = \frac{1}{2\pi}\sqrt{\frac{1}{M_2C_2}}, \qquad f_2 = \frac{1}{2\pi}\sqrt{\frac{M_1 + 4M_2}{4M_1M_2C_2}}$$

$$= \frac{1}{2\pi}\sqrt{\frac{1}{M_2C_2}\left[\frac{1}{4} + \frac{4M_2}{M_1}\right]}, \qquad (J)$$

requiring that $C_1 = 0$. The fourth pair of values requiring that $C_1 = 0$ is found in equations (29) and (30) or

$$f_1 = \frac{1}{2\pi}\sqrt{\frac{1}{M_2C_2}\left[\frac{1}{1+\frac{M_2'}{M_2}}\right]}, \quad f_2 = \frac{1}{2\pi}\sqrt{\frac{1}{M_2C_2}\left[\frac{1+4\frac{M_2}{M_1}}{1+\frac{M_2'}{M_2}+\frac{4M_2'}{M_1}}\right]}. \quad (K)$$

E. Empirical Character of Formulæ.

We are prevented from securing accurate formulæ by the following circumstances:

1. Our dimensions cannot be vanishingly small as compared to a wave-length and therefore appreciable phase differences occur in any section or branch.

2. We cannot get an accurate expression for the impedance of a short tube because our theory assumes that this impedance is strictly in the line, whereas a tube has distributed capacitance virtually between itself and the undisturbed surrounding medium.

3. One hypothesis upon which the theory is based assumes that the junction points are really points, *i.e.*, there can be no accumulation there.

In respect to these circumstances stated, it is fair to say that the accuracy of the approximations cannot be estimated save by experiment. It is allowable, therefore, to take the position that we are to seek, in the case of each construction, that pair of formulæ which seems best to agree with experiment. In other words, the formulæ are somewhat empirical, though their manner of derivation gives a reason for their forms. This attitude of empiricism does not, then, hide the nature of the phenomena but rather decides as to the best approximation.

IV. Comparison of Theory and Experiment.

A. Measurement of Transmission.

An apparatus, Fig. 5, similar to that used by Drs. Gray and Roebuck, but not described in print, gave sufficiently accurate measurements of

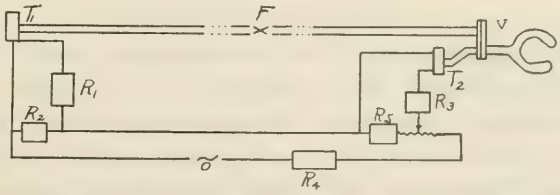

Fig. 5.

the transmission of the filters. T_1 and T_2 are similar telephone receivrse, V is a valve connecting a pair of stethoscope binaurals to either T_2 or

the tube which connects to the filter F and T_1, the resistance boxes are marked by the R's, and the source of sinusoidal currents is an oscillator loaned by the Western Electric Company. The circuits of the latter consist of an oscillating circuit, an amplifier, an electrical low-frequency pass filter of two sections, a resistance R_4, and inductances and capacities by means of which it was possible to get fairly pure tones from 90 to 1,500 vibrations and tones up to 5,000 without the use of a filter. R_2 was small in comparison with R_1 and the latter about ten times the impedance of T_1 for a frequency of 1,000 cycles. R_5 was never greater than one tenth the impedance of T_2 and R_3. The brass tubing on either side of F was .557 cm. in internal diameter and 2.5 meters long. The method pursued was to adjust the values of the R's so that, without the acoustic filter present, the values of R_5 required to produce the same intensity at the stethoscope with either acoustic connection, were not in excess of the limit above stated. Each filter had its conducting tube of approximately the same diameter as the tubes from F_1 to T_1 and V. Settings of R_5 were recorded for the various frequencies with and without F, in the latter case a tube of the same length and internal diameter being substituted for F. The transmitted intensities were assumed proportional to the square of R_5. Thus the percentage transmission of F at a certain frequency would be the ratio between the squares of R_5 with F and with its substitute tube. Obviously, the tubes in the apparatus have resonance and this will greatly reduce the accuracy of the transmission values. For frequencies lower than 2,000, pieces of hair felt were inserted every 15 cm. or so to increase the viscosity and reduce resonance. Improved readings were then obtained. The curves herewith presented must be examined with the understanding that resonance does exist. Since our immediate object was merely to get an estimate of the filtering action rather than an accurate measure of transmission, no effort at further refinement was considered. Experiments showed that even with the felt present, variations of 10 per cent. to 20 per cent. apparent transmission with frequency might occur.

B. Low-Frequency Pass Filters.

The general construction of the low-frequency pass filters and the experimental transmission curve is shown in Fig. 6. The accompanying Table II. gives the dimensions, the computations and certain experimental facts concerning a number of low-frequency filters. In this Table l, r, and V refer to the length of section, internal radius and volume respectively. The subscript 1 refers to the conducting line or tube and the subscript 2 to the branches or in the case of the form here used, to

the surrounding tube. The value f_m is the value of the frequency at which the transmission is 50 per cent. of the "unattenuated" transmission of the filter. Inasmuch as the beginning of attenuation cannot be sharp, this mean value is perhaps the fairest selection of an experimental value. The computations indicated by the letters, A, B, and C were made according to the formulæ so marked in the preceding theory. These formulæ when expressed in terms of the dimensions become, after

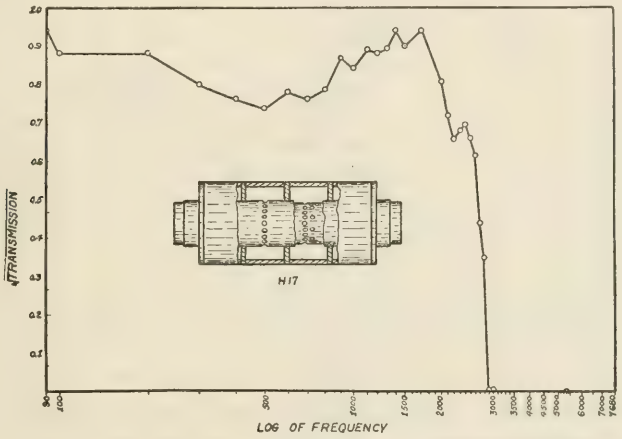

Fig. 6.

substitution in accord with (31), (33) and (34), respectively, (A'), (B') and (C') as follows:

$$f_1 = 0, \qquad f_2 = \frac{a}{\pi}\sqrt{\frac{S_1}{l_1 V_2}\left[\frac{1}{1 + 4\dfrac{l_1 S_1}{V_2}}\right]}, \tag{A'}$$

$$f_1 = 0, \qquad f_2 = \frac{a}{\pi}\sqrt{\frac{S_1}{l_1 V_2}\left[\frac{1}{1 + 4\dfrac{S_1}{c l_1}}\right]}, \tag{B'}$$

$$f_1 = 0, \qquad f_2 = \frac{a}{\pi}\sqrt{\frac{S_1}{l_1 V_2}}. \tag{C'}$$

It is evident that the formula (B') is to be preferred since it gives approximately the experimental values of f_m and also explains satisfactorily the variation of the frequency limit of attenuation with the conductivity of the orifices leading from the transmission conduit to the volume in the branch.

Attention should be directed to several other facts shown in the table. The percentage transmission in the "unattenuated" region given in column "T," seems to depend upon the ratio between r_2 and r_1, the

TABLE II.

No.	No. of Sections.	l_1 cm.	r_1 cm.	r_2 cm.	V_{2_3} cm.	f_m d.v.	$f_2(A')$ d.v.	$f_2(B')$ d.v.	$f_2(C')$ d.v.	No. of Apertures.	T %.	*Faf*	
												f	%.
2	3	2.66	.243	1.71	21.6	450	595	462	624	2	.20	5,250	708
3	5	5.0	.243	1.71	43.1	230	308	291	321	4	.36	3,100	933
13	4	4.0	1.42	2.57	44.4	920	1,140	880	2,075	6	.80	3,300	106
15	4	1.67	.75	1.42	5.94	2,200	2,670	2,710	4,620	16	.80	5,150	106
15	4	1.67	.75	1.42	5.94	1,700	2,670	2,120	4,620	8		2,900	38
16	4	1.67	.75	1.15	2.62	3,200	2,965	4,085	6,960	16		6,200	55
16	4	1.67	.75	1.15	2.62	2,500	2,965	3,200	6,960	8		4,000	29
17	4	1.67	.75	1.30	4.36	2,700	2,800	3,175	5,400	16	.65	5,200	66
17	4	1.67	.75	1.30	4.36	2,200	2,800	2,480	5,400	8		3,000	25
*R*1	3	1.58	1.19	1.82	7.1	2,700	3,080	2,840	6,885	8	.90	3,500	9.4
*R*2	4	1.58	1.19	1.82	7.1	2,750	3,080	2,840	6,885	8	.72	4,000	25
*R*3	4	1.32	1.19	1.82	5.87	3,350	3,700	3,170	8,300	8	.72	4,750	18.7
*R*4	4	1.45	1.19	1.82	6.48	3,025	3,370	3,010	7,520	8	.90	4,600	65
*R*5	6	2.58	1.19	1.82	11.82	2,000	1,890	2,095	4,180	8	.90	3,000	25
*R*6	6	1.58	1.19	1.82	7.1	2,700	3,080	2,700	6,885	4	.90	4,750	44
*R*6	6	1.58	1.19	1.82	7.1	2,075	3,080	2,100	6,885	4	.72	3,100	24

number of sections constant, the greater the ratio the less the transmission. In the last two columns labeled "*Faf*," the one under "f" refers to the first audible frequency above the cut-off, and under "%" the ratio between the range of inaudibility and the actual cut-off. Here we note that while filters in which r_2/r_1 is large have inferior transmission, yet they have a surprisingly great range of frequencies above the cut-off where the filter operates successfully. In filters 2 and 3 this range is at least over ten times the cut-off frequency. As the ratio of r_2/r_1 becomes smaller, this cut-off range decreases but the transmission in the "unattenuated" region improves. It is impossible to select, without specifications and trial, the most successful design for a given frequency cut-off, for success depends upon both the range of cut-off and upon the percentage of transmission in the unattenuated region desired. The remarkable feature is that the high attenuation in the region above the theoretical lower limit, f_2, is ever as great as ten times this limit. In fact, in the case of No. 2, that frequency having a wave-length of approximately the length of a section is highly attenuated. The performance is better than one would hope. Attention is directed to *R* 1, a tube about 6 cm. long and 2.4 cm. in diameter yet capable of having an attenuation producing inaudible transmission for a considerable range above the cut-off. Such a performance is a surprise to one accustomed to the difficulty in preventing the passage of sound through holes and channels.

C. *High-Frequency Pass Filters.*

We previously have mentioned three possible simple cases of a high-frequency pass filter but two of these seemed to consist merely of a straight tube with side branches each having an M_2 or orifices, only. The cross-section of such a filter and its transmission is shown in Fig. 7.

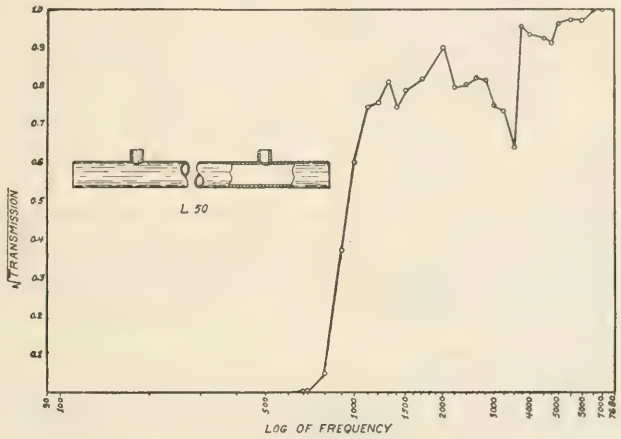

Fig. 7.

If we substitute in the formulæ, (E) and (F) in accord with (33) and (34), we obtain the following:

$$f_1 = \infty, \qquad f_2 = \frac{a}{2\pi}\sqrt{\frac{c}{4V_1}\left(1 + \frac{4S_1}{l_1 c}\right)}, \tag{E'}$$

$$f_1 = \infty, \qquad f_2 = \frac{a}{2\pi}\sqrt{\frac{c}{4V_1}}, \tag{F'}$$

wherein c is the conductivity of the orifice as defined in (32).

Data of several filters of differing dimensions are given in Table III. The last column found in Table II. is here omitted because these filters gave transmission up to the highest frequency tried—5,000–7,000 d.v. The experimental results are therefore strictly in accord with the limits of attenuation set by the theory from f_2 to zero. A reason is doubtless that the less the frequency the more nearly the experimental conditions meet those assumed in the theory.

The general conclusion is that the formula (E') is very satisfactory. It is to be noted that in (E) we have used C_1. This is the only case of the three where experiment has indicated that C_1 should be used. As stated in the discussion of the theory, the assumption of C_1 in parallel with M_1 is arbitrary. A justification may now be seen in the following fact. The branch lines, M_2, are short. Thus there is a much greater

TABLE III.

No.	No. of Sections.	l_1 cm.	r_1 cm.	l_2 cm.	r_2 cm.	c.	f_m.	$f_2(E')$.	$f_2(F')$.	T.
15 II....	8	2.5	.243	0.5	.115	.061	2,300	2,400	988	.75
19.....	4	5.0	.243	0.5	.115	.061	1,500	1,300	699	.60
22.....	8	2.5	.243	0.5	.152	.099	2,200	2,520	1,262	.50
1,2,3,4..	8	4.0	.483	1.22	.278	.146	1,500	1,490	610	.75
50.....	12	5.0	.483	0.5	.139	.0845	920	1,170	415	.85
50.....	6	10.0	.483	0.5	.139	.0845	810	620	293	.90
50.....	4	15.0	.483	0.5	.139	.0845	525	436	240	.90
50.....	3	20.0	.483	0.5	.139	.0845	450	344	207	.90

pressure gradient in M_2 than in the conduit or conducting line itself. The particle velocity in M_2 is therefore much greater than in the conduit. If the particle velocity in the line were actually at rest, the conduit would serve as a capacitance for M_2. Thus, the existence of an effective capacitance is not surprising.

Attention should be called to the fact that experiment showed that as M_2 was made longer or very narrow, introducing viscosity, the cut-off became less sharp.

D. Single-Band Filters.

We have already presented four pairs of formulæ for single-band filters. If we now have a filter of the construction shown in Fig. 8 and denote

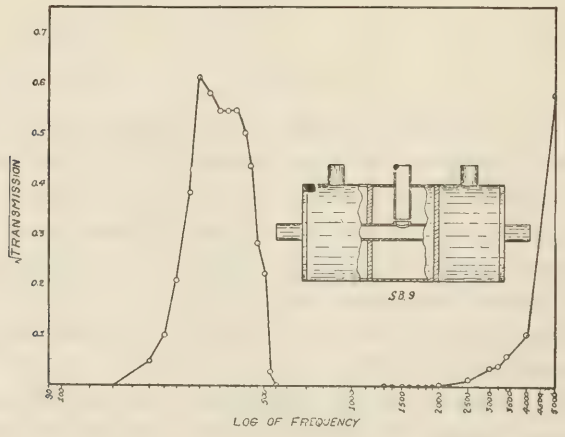

Fig. 8.

by l_2, S_2 the length and area of the side tube and by c the conductivity of the holes from the side branch into the chamber V_2, these four formulæ

may be written after substitution according to (33) and (34) as follows:

$$f_1 = \frac{a}{2\pi}\sqrt{\frac{S_2}{{}_2lV_2}}, \qquad f_2 = \frac{a}{2\pi}\sqrt{\frac{S_2}{l_2V_2}\left[\frac{1 + 4\dfrac{l_2S_1}{l_1S_2}}{1 + 4\dfrac{l_1S_1}{V_2}}\right]}, \qquad (H')$$

$$f_1 = \frac{a}{2\pi}\sqrt{\frac{S_2}{l_2V_2}}, \qquad f_2 = \frac{a}{2\pi}\sqrt{\frac{S_2}{l_2V_2}\left[\frac{1}{1 + 4\dfrac{l_1S_1}{V_2}}\right]}, \qquad (I')$$

$$f_1 = \frac{a}{2\pi}\sqrt{\frac{S_2}{l_2V_2}}, \qquad f_2 = \frac{a}{2\pi}\sqrt{\frac{S_2}{l_2V_2}\left(1 + 4\frac{l_2S_1}{l_1S_2}\right)}, \qquad (J')$$

$$f_1 = \frac{a}{2\pi}\sqrt{\frac{cS_2}{V_2(l_2c + S_2)}}, \qquad f_2 = \frac{a}{2\pi}\sqrt{\frac{S_2}{l_2V_2}\left[\frac{1 + 4\dfrac{l_2S_1}{l_1S_2}}{1 + \dfrac{S_2}{l_2c} + \dfrac{4S_1}{cl_1}}\right]}. \qquad (K')$$

Fig. 8 also shows the transmission curve of one of the filters, *SB*9, with which the range of highly attenuated frequencies above f_2 is relatively small. The two-column "*Faf*" in Table IV. is similar to that in Table II. The reasons for the lack of attenuation in these high frequencies are doubtless the same as in the case of the low-frequency pass filters described in a previous section. For, as will be observed, the single-band filter may be looked upon as a combination of the two other types. The experimental results show the (K') formulæ to be the most satisfactory.

V. Discussion and Conclusions.

The high attenuation secured with but few sections was not anticipated. General experience in acoustics increases the remarkableness of the action of the filters. The agreement with the theory is, in view of the assumptions made, fairly satisfactory for it is possible to construct filters that meet specifications.

The physical action considered herein is clearly not dissipation but interference. With a source transmitting energy through a filter, the action of the latter is to prevent the emission of energy from the source in these frequencies for which there is attenuation. There is dissipation, or at least a decrease in transmission in the filters, extending over the unattenuated region and this seems to be the greater, in the case of the low-frequency-pass filter, the greater the ratio of r_2 and r_1.

The extent of the usefulness of the filter will be determined by experience. Its simplicity and cheapness of construction make it a serviceable

TABLE IV.

No.	No. of Sections.	l_1 cm.	r_1 cm.	l_2 cm.	r_2 cm.	V_2 cm.^{3}	c	Observed.		Computed.						T %.	Faf	
								f_1	f_2	$f_1(H'I'J')$	$f_2(H')$	$f_2(I')$	$f_2(J')$	$f_1(K')$	$f_2(K')$			%.
1	3	5.0	.243	2.33	.243	42.7	0.69	190	260	236	380	227	400	224	346	.12	3,000	900
2	3	2.66	.243	2.33	.243	21.19	0.69	275	375	304	680	322	710	318	575	.26	3,000	500
3	3	5.0	.243	2.20	.243	28.02	0.69	270	370	300	468	282	499	283	430	.23	2,200	389
4	3	2.66	.243	1.70	.243	14.81	0.69	430	520	470	830	441	882	436	707	.28	3,125	400
5	3	5.0	.243	3.35	.243	28.02	0.69	190	270	242	439	228	466	234	410	.28	2,100	425
6	3	2.66	.243	2.80	.243	14.81	0.69	350	500	366	782	344	835	349	680	.29	3,000	400
7	3	1.17	.243	1.20	.243	5.74	0.69	700	1,300	836	1,875	835	2,030	810	1,380	.54	3,200	129
9	3	2.66	.243	2.40	.243	22.7	.455	285	475	319	648	306	685	295	506	.37	1,300	106
10	4	1.77	1.12	0.5	.278	14.4	.58	600	1,250	1,407	2,255	960	3,590	1,080	1,530	.56	1,800	33

device. In the laboratory it can be used in the elimination of undesirable components in a sound wave, and for certain types of sound analysis. In the latter case its advantage over a resonating device is its selection of a band of adjustable width. Its possible fields of usefulness in practical instruments may be merely mentioned. In the rendition of records on the phonograph and in the wireless telephone many undesirable frequencies can be removed. In wireless telegraphy an acoustic filter makes possible the simultaneous reception of an indefinite number of messages with the same antenna. In connection with a megaphone on a loud-speaking device, the filter has also an application. The introduction of this new filtering phenomenon may in time affect the design of musical instruments. Although the future use of the acoustic filter cannot be foreseen, there is one fundamental fact to be recognized, namely, that an aerial wave is used in audition and that a modification of this wave by a strictly acoustical method wherein the air is the medium, gives an opportunity for the energy to flow directly from the filter to the ear without any transformation which would introduce undesirable modifications. These acoustic filters have a great acoustic interest and the investigation of them, both theoretical and experimental, is being continued.

Physical Laboratory,
State University of Iowa.

[Reprinted from The Physical Review, Vol. 21, No. 1, January, 1923.]

HALL EFFECT AND SPECIFIC RESISTANCE OF EVAPORATED FILMS OF SILVER, COPPER AND IRON.

By J. C. Steinberg.

Abstract.

Specific resistance and Hall coefficient of evaporated films, 20 to 200 $\mu\mu$ thick.—The specific resistances of films of *silver, copper and iron* were found to be from 15 to 57 times the values for the bulk metals, being respectively 24.3, 29.7 and 506 instead of 1.6, 1.8 and 8.8. The Hall coefficients of films of silver and copper, two diamagnetic metals, were respectively 41 and 11 per cent. *less* than the bulk values, while for the iron films the coefficient was + 42.5 as compared with + 6.6 for bulk iron, an *increase* of over 500 per cent. For the silver and copper films the Hall effect is proportional to the field throughout, but for iron films the proportionality extends only to 10,000 gausses, whereas the limit for bulk iron is 20,000 gausses. This indicates that the *maximum intensity of magnetization in iron films* is only half as great as that attainable in pure bulk iron.

Structure of evaporated metal films.—X-ray analysis showed that films of silver and iron and probably other metals have the same crystal structure as the bulk metals, but the crystal grains are too fine to distinguish with a microscope.

Effect of extreme fineness of crystal structure on certain physical properties of metals.—The increase of *specific resistance* is probably due to the multiplication of the number of contacts between grains. The *Hall coefficient* is practically independent of the structure except as it affects the magnetic condition of the crystals. The *intensity of magnetization* in iron crystals seems to be limited by the demagnetizing action of the poles of the crystals, which is greater the smaller the crystal grains.

Method of producing uniform metallic films by evaporation.—This involves moving a heated filament uniformly over the surface to be coated, at a distance less than the mean free path in a high vacuum. The films are hard and bright and resist corrosion.

Introduction.

THIS work extends an investigation on chemically deposited silver films by G. R. Wait[1] to films obtained by evaporation. For a discussion of the various film phenomena, and references of historical interest, the reader is referred to Wait's publication. Wait concludes that his results as well as the results of others are consistent with the conception that the film consists of granules, each granule having the properties of the bulk metal.

Evaporated films were employed in order to learn more of the nature of these granules. The Hall effect and the specific resistance were measured in films whose thicknesses varied from 20 to 200 $\mu\mu$. The

[1] G. R. Wait, "Hall Effect and Specific Resistance of Silver Films," Phys. Rev., 19, 615, 1922.

films were examined under a microscope for traces of structure, and also subjected to x-ray analysis.

Experimental Method.

The essential features of the evaporation method of obtaining a film consist in drawing an electrically heated filament of the metal back and forth over a microscope slide in vacuum. Both glass and quartz slides were used. The particles of metal given off by the hot filament adhere to the microscope slide, giving a uniform film.

The details of the evaporation apparatus are shown in Fig. 1. Two

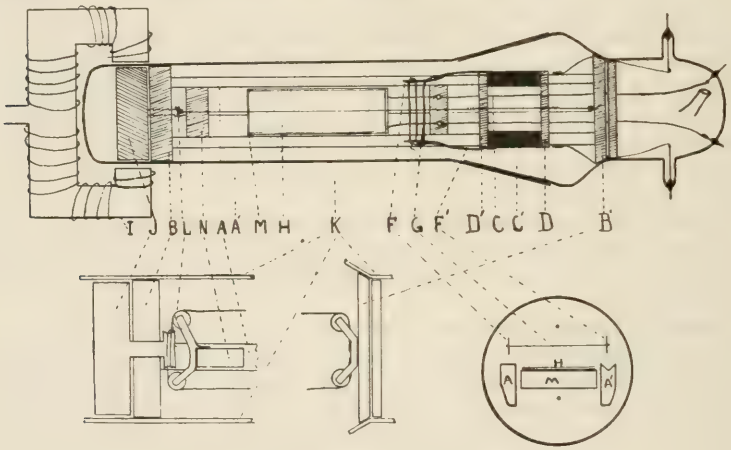

Fig. 1.

brass tracks AA' are fitted into the cylindrical fibre plugs BB'. Ground to fit the tracks are two brass blocks CC', which, held rigid by the fibre straps DD', constitute the carriage. The mica strips FF' serve to support the wire G connected across the blocks. The electro-magnet I turns around the pyrex tube K. Inside the tube, the iron core J turns with the magnet. By means of a small capstan L, the carriage is drawn along the tracks. The electro-magnet, which was designed by Dr. G. R. Wait and Mr. J. B. Dempster, is so constructed that it reverses its direction of rotation every three revolutions, and turns with constant angular velocity. Thus the carriage moves uniformly back and forth along the tracks. M is a small heating element to drive occluded vapors from the microscope slide H, prior to evaporation. Current is furnished the wire by means of leads connected to the brass tracks.

The tube was connected to a Knipp mercury vapor pump, with a Gaede mercury pump and a water aspirator as fore-pumps. The pumps which were very rapid were kept in operation during evaporation. Pre-

cautions were taken to insure the pressure being reduced to such a value that the maximum distance of the wire from the glass slide would be less than the mean free path of the gas molecules. The required pressure was .001 mm. mercury. As a rough indication, the pressure was reduced sufficiently to enable a spark to jump a one and one half inch air gap in parallel with the electrodes of an attached discharge tube.

It was found necessary to give a new wire a preliminary evaporation before desirable films could be obtained. In practice the wire was maintained at its evaporation temperature several hours before taking a film. When this precaution was not observed, the films obtained were found to be erratic in behavior and not constant with time. Etching the wire prior to evaporation did not eliminate the effect to any marked extent. Metals of very good purity were used, and the evaporated metals were probably very pure.

For microscopic examination a Bausch and Lomb metallurgical microscope was employed. X-ray analysis was made by means of a method described by Hull.[1] The apparatus used for the work was kindly loaned by Dr. C. W. Hewlett, and a description of its method of operation may be found in his publication.[2] The metals were evaporated under the same conditions as the films, and scraped from the surfaces upon which they were deposited. They were then finely powdered, and suitably mounted in a homogeneous beam of x-rays from a molybdenum target. A filter of zirconium powder .037 cm. thick reduced the spectrum to approximately a single line, of wave-length .712 A.U. The angular deviations of the lines were determined by observing the rate of discharge of an ionization chamber.

Hall effect and specific resistance were measured in a manner similar to that described by Wait.[3] Thickness was determined by weighing, assuming the density to be that of the bulk metal. This assumption is justified on the grounds that any sensible change in density would not account quantitatively for the magnitude of the observed effects.

Results.

The Hall effect in a film is given by the relation,

$$E = \frac{RHI}{\epsilon},$$

where E is the Hall e.m.f., R, the Hall coefficient, H the magnetic field, I the current through the film, and ϵ the thickness of the film. E, H, I,

[1] Phys. Rev., 10, p. 661, 1917.
[2] C. W. Hewlett, Phys. Rev., 20, 688, 1922.
[3] Wait, loc. cit.

and ϵ are determined experimentally and R computed. The values given in Table I. were obtained during the investigation when not otherwise indicated.

TABLE I.

Metal.	$R \times 10^5$ (e.m.u.).	$\rho \times 10^{-3}$). (e.m.u.
Taken from		
Bulk Silver (pure)—Smithsonian Tables	−88.0	1.6
Chem. Dep. Silver	−86.4	2.7
Evaporated Silver	−52.0	24 3
Bulk Copper (pure)—Smithsonian Tables	−56.0	1.8
Evaporated Copper	−50.0	29.7
Bulk Iron (pure)—A. W. Smith[1]	+ 660	8.8
Evaporated Iron	+4250	506.4

Evaporated Silver Films.

The Hall coefficient in evaporated silver is negative and independent of the thickness. The value given in Table I. is the average of the values obtained from a large number of films whose thicknesses varied from 20 to 200 $\mu\mu$. In Fig. 2, experimental values of E/HI are plotted against ϵ. The curve drawn through the points is a graph of the equation $E/HI = R/\epsilon$, where R has the average value obtained from the films.

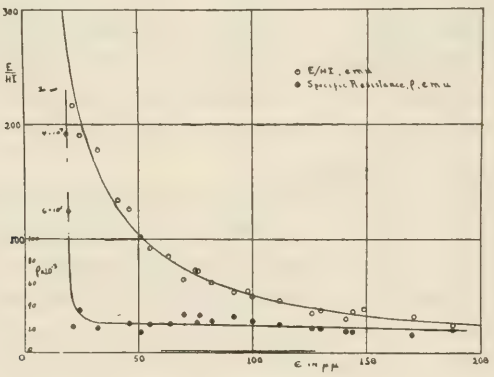

Fig. 2.

The specific resistance ρ as a function of thickness is also shown in Fig. 2. Its behavior is similar to that found in films obtained by other methods. The average value, taken from films whose thicknesses are greater than the critical thickness, *i.e.*, the thickness at which ρ becomes infinite, is given in Table I. It is to be noted that we have here a large increase in ρ as compared with bulk silver, about 1,000 per cent., and a relatively small change in the Hall coefficient. The straight line in

[1] PHYS. REV., 30, p. 1, 1910.

Fig. 2, near the axis of abscissas, indicates the value of ρ for bulk silver. The resistances of the films remained sensibly constant with time.

The x-ray analysis was only qualitative, it being desired merely to determine whether or not the metal was crystalline. From data published by Hull,[1] the angular deviations of the most intense lines were computed, and found to coincide within the error of the experiment, to the lines observed with evaporated silver. The existence of the lines in their computed positions was taken as sufficient evidence that the metal was crystalline, and of the type found in bulk silver, that is, with the face-centered cubic lattice, of elementary side 4.06 A.U.

The films obtained were hard and very uniform in thickness. They possessed an excellent reflecting surface, and did not deteriorate readily with age. Repeated attempts to observe granular structure under a microscope failed. The films appeared blue by transmitted light, which is the characteristic color of silver.

Evaporated Copper Films.

Evaporated copper was found to behave in a manner similar to that of evaporated silver. The average values of R and ρ are given in Table I. The values of E/HI against ϵ, and ρ against ϵ, are plotted in Fig. 3. As in the the case of silver, evaporated copper has a large specific resist-

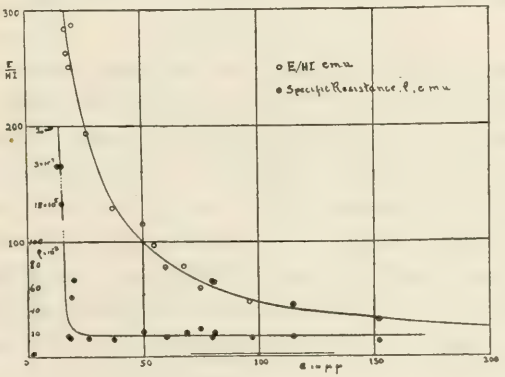

Fig. 3.

ance, although the Hall coefficient does not differ appreciably from the bulk value.

The copper films like silver were very good reflectors, although they reflect slightly more to the red than does silver. They appear green by transmitted light. Structure analysis was not made for the copper films.

[1] Hull, loc. cit.

Evaporated Iron Films.

Evaporated iron films behave in a manner similar to bulk iron in that they have a positive Hall coefficient which is not constant with magnetic field. Fig. 4 shows the relation between the Hall e.m.f. and the magnetic field for several films of different thicknesses. It will be seen that E is proportional to H up to fields of about 10,000 gausses. For bulk iron this proportionality holds for fields up to about 20,000 gausses. The bend in the curves is spoken of as the saturation of the Hall e.m.f. The average value of the Hall coefficient given in Table I., is computed for fields below 10,000 gausses by means of the relation

$$E = \frac{RHI}{\epsilon} .$$

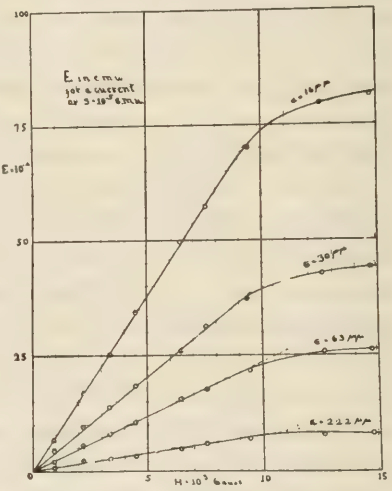

Fig. 4.

In contrast to its behavior in copper and silver, the Hall coefficient of evaporated iron shows an increase of about 600 per cent. over that of the bulk metal.

Wire containing 99.85 per cent. iron was used, so that the films obtained were relatively pure. The films appeared silver white by reflected light, and rather brownish by transmitted light. No trace of structure was visible under the microscope. The films reflect very well, were hard, and did not oxidize readily in air.

Evaporated iron was found to be crystalline, the lines occurring at the angular deviations computed from Hull's data.[1] As in the case of silver, it is inferred from the correspondence of these lines that the type of lattice is that found by Hull, which in iron is the centered cubic, of elementary side 2.86 A.U.

Discussion.

Let us consider in more detail the nature of evaporation in the sense that we use it. The wires were run at temperatures[2] that correspond to a vapor pressure of 10^{-3} mm. of mercury. At this pressure, the distance of the wire from the microscope slide was less than the mean free path. It has been found that metallic vapors are monatomic.[3] Then if the

[1] Hull, loc. cit.

[2] Johnston, Journ. Ind. Eng. Chem., 9, p. 873, 1917.

[3] Meyer, Ber., 12, p. 1426, 1879.

atoms are not reflected [1] upon striking the slide, the film must be deposited an atom at a time, the atoms reaching the slide without collision with each other. Since the evaporated metals are crystalline, some of the atoms evidently do not take random positions, but take definite places in a lattice, probably under the influence of the atoms already there. It is thought that rapid evaporation with a large temperature difference between the slide and the wire would tend to diminish crystalline growth.

The term crystalline grain is used in the sense employed in metallurgy,[2] that is, to designate a crystal of metal, in which the elementary crystals all have the same orientation. Its properties are supposed independent of the manner of obtaining it, as long as the same type of elementary crystal is obtained. Any specimen of metal is, in general, made up of an aggregate of crystalline grains separated by boundaries. The properties of the specimen are supposed to depend upon the size of the crystalline grains, and upon the contacts between them.

We conclude that in evaporated films, the crystalline grains are much smaller than in bulk metals, and that they are not in the intimate contact obtaining in bulk form. This view is supported by the fact that the metals have been found to be crystalline, that the crystalline grains were not visible under a microscope, that the surfaces of the films appear to have a very high polish, and that the essential nature of the process of obtaining them is not conducive to crystalline growth.

The large resistivity of evaporated metals leads us to believe that the resistivity of a specimen of metal will be smallest at a given temperature and pressure, when the specimen is a pure metallic crystal. The effect of the boundaries that separate adjacent crystalline grains is to increase the resistivity of the specimen. This increase is very pronounced when impurities are present that freeze out in the process of solidification. An idea of the effect upon the resistivity of a change in the size of the crystalline grains alone can be obtained by comparing the resistivity of two specimens of pure metal, the one obtained by sudden quenching, the other by slow cooling, during solidification.

The results on silver and copper indicate that the Hall coefficients of these substances do not change appreciably when the structure is changed. This might be expected, since the supposition that the impressed magnetic field produces the transverse e.m.f. accounts well for the observed effects. In the case of iron, however, for which the Hall coefficient is positive and therefore intimately associated with the molecular fields, one might expect structure to have a pronounced influence.

[1] Langmuir, PHYS. REV., 8, p. 149, 1916.

[2] See Sauveur, "The Metallography of Iron and Steel," and Rosenhain, "The Study of Physical Metallurgy."

A. W. Smith[1] has found that as temperature is increased, the Hall coefficient of iron increases, and the value of the magnetic field at which the Hall e.m.f. becomes saturated shifts to smaller fields. He points out that the saturation of the Hall e.m.f. should occur when $H = 4\pi I_m'$, where I_m' is the maximum value of the intensity of magnetization, and that the decrease of I_m' as temperature is increased accounts for the observed shifts. Now our proportionality between E and H holds only up to one half the value of H for pure bulk iron. Furthermore the directional change in R is the same in the two cases. Thus it appears that if the Hall effect is essentially the same phenomenon in the two cases, I_m' for evaporated iron is less than that for bulk iron.

The results indicate, then, that the effect of decreasing the size of the crystalline grains has been to decrease the maximum value of the intensity of magnetization that can be attained in the iron. This is not so surprising if we suppose that the permeability of the boundaries is different from that of the crystalline grains. Then each crystalline grain would have poles at the boundaries, and as the grains become smaller, the poles would exert a greater demagnetizing force. It does not seem improbable that a perfect crystal of iron would have the greatest I_m', and that the difference between I_m' for a perfect crystal and for a specimen of like size and shape, but made up of crystalline grains, would be a measure of the demagnetizing effect of the poles. Thus it appears that new importance is attached to the experiments in that they bear upon the nature of ferromagnetism.

In conclusion, I wish to express my appreciation to the members of the Department of Physics of the State University of Iowa for their assistance and interest, and especially to Dr. G. W. Stewart, under whose direction the work was carried on.

Physical Laboratory,
State University of Iowa,
August 20, 1922.

[1] Phys. Rev., 30, p. 1, 1910.

Reprinted from the Journal of the Optical Society of America and Review of Scientific Instruments
Vol. VII, No. 2, February, 1923

NOTE ON THE PRINCIPAL REFLECTING POWERS OF TELLURIUM

By L. P. Sieg

In a recent paper, Van Dyke[1] has published data giving the principal optical constants of isolated tellurium crystals. These data were obtained by reflecting plane polarized light from one of the six panel faces of an hexagonal crystal at azimuth 45°, with various angles of incidence, and determining by analysis of the reflected elliptically polarized light, the principal optical constants. In his experiments the crystal was placed successively in the first and second principal positions, the former with the principal crystalline axis perpendicular, and the second with the axis parallel to the plane of incidence. With results from these two principal positions, employing various angles of incidence, the disentangling of the various optical constants becomes simply a matter of carrying through the solutions of numbers of pairs of complex equations. Just as has been pointed out[2] for the analogous selenium crystals the results thus obtained are apparently satisfactory, but the computations are so detailed, and so many assumptions are made throughout the discussion leading to the final working equations, that one feels that direct experimental evidence ought to be obtained to check, as far as possible, the data indirectly calculated. The task of checking directly the principal indices and the principal absorption constants seems well nigh insuperable, but the reflecting powers, on the other hand, are quite easily determinable by direct means.

By the use of the same apparatus[3] employed for testing selenium crystals, a direct determination has been made of the principal reflecting

[1] Van Dyke, J. O. S. A. & R. S. I., *6*, p. *917*, *1922*.
[2] Sieg, J. O. S. A. & R. S. I., *6*, p. *448*, *1922*.
[3] Sieg, *loc. cit.*, p. *457*.

powers of a number of tellurium crystals for a range of wavelengths in the visible spectrum. The results, together with VanDyke's similar data are shown graphically in Fig. 1. The principal reflecting powers refer to the action of the crystal to normally incident plane polarized light with the electric vector parallel and perpendicular respectively to the principal crystalline axis. As was pointed out in discussing the results for selenium, there is present in these experiments a rather large experimental error due largely to the necessity of matching fields of light of very low intensity. Many independent

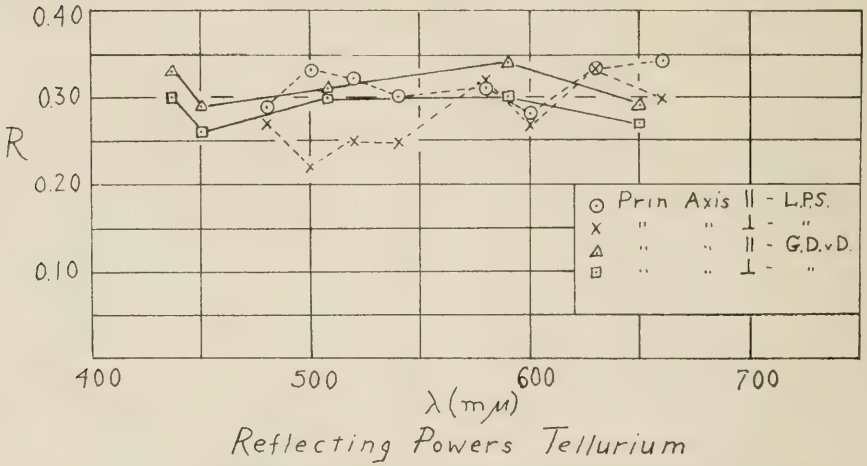

FIG. 1. *The principal reflecting powers of tellurium. Those obtained by direct experiment are indicated by the dotted lines; those obtained by an indirect method, by full lines.*

experiments, however, give average results that are fairly satisfactory. It will be noted in the figure, that my data in general agree very well with those of VanDyke,[4] and further, that the two reflecting powers are very close together. These data compare as to their average values very closely with those from selenium, but the latter are separated by a considerably wider interval.

It is now felt as a result of these direct experiments on selenium and tellurium, that in future the results of the indirect method may be relied upon, without the necessity of direct checking. These direct experiments are very tedious, and yield only the reflecting powers, while the polarimetric method yields all three sets of optical constants.

[4] The data of the present experiments are indicated in the legend on the figure by the initials L. P. S. VanDyke's data are indicated by G.D.v.D.

For exploration in the ultra violet (which investigation is now under way) there is no simple way of making direct tests. It is hoped to carry through a rather extensive program of determinations of optical constants of as many elementary substances as possible, these substances to be in the form of isolated crystals.

UNIVERSITY OF IOWA,
NOVEMBER, 1922.

Reprinted from the Journal of the Optical Society of America and Review of Scientific Instruments
Vol. VII, No. 2, February, 1923

A SIMPLE PRISM SPECTROGRAPH

By E. O. Hulburt

A spectrograph which satisfied in some degree the antagonistic requirements of high dispersion, ample light gathering power, small cost and simplicity of construction was obtained by mounting a glass prism in the Littrow manner. A diagram of the spectrograph is given in Fig. 1. The beam of light from the slit S, which is at the principle focus of the lens L, is directed to the lens by the small right angle prism R. The beam is rendered parallel by the lens and passes through the large 60° prism P. It is then reflected from the plane mirror M back again through the prism and lens. The spectrum is formed at T and may be viewed with an eye-piece or recorded on a photographic plate.

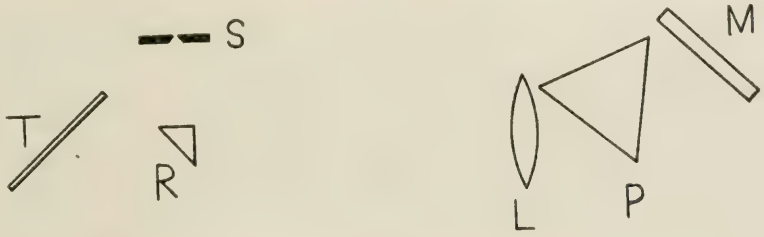

Fig. 1.

The lens was made of a single piece of glass 63 mm in diameter and of focal length 1 meter. The faces of the 60° glass prism were 50 mm square and those of the small right angle prism were 18 mm square. The lens and the two prisms were supplied from stock by the Bausch and Lomb Optical Company at a total cost of about thirty dollars. The mirror M, 80 mm square, was cut from a selected portion of ordinary plate glass and was plane within a wave-length of light as indicated by test with an optical flat. A reflecting layer of platinum was sputtered on to the glass.

The photographic performance of the spectrograph is demonstrated in Fig. 2. This shows spectrograms of the iron arc and of a condensed discharge through hydrogen at a pressure of 100 mm of mercury. The time of exposure to the hydrogen tube was about 5 seconds, with a slit width of about 0.02 mm, and to the iron arc a fraction of a second. Flat plates were used, curved ones would probably have given sharper lines at the ends of the spectrum. The visible spectrum was 65 mm in

length. The dispersion at 5000, 4000 and 3600 A.U. was approximately 40, 20, and 15 A.U. per mm, respectively.

Elaborate mountings of the optical parts of a Littrow spectrograph are described in the literature (see "Spectroscopy," E.C.C. Baly). In the present instance a modest design was carried out and was found to give every satisfaction. A wooden plank $60'' \times 11'' \times 2''$ served as the base. The slit S and the prism R were clamped to the base with adjustments in a vertical line and about a vertical axis. The parts L, P and M were firmly mounted on a wooden board $12'' \times 8'' \times 2''$ which could be moved by a screw adjustment along the base for the purpose of focussing. The lens L was clamped in place being tilted slightly to throw out of the field of observation the light reflected directly from its surfaces. The prism P was set at minimum deviation for wavelengths in the center of the spectrum and was clamped firmly with

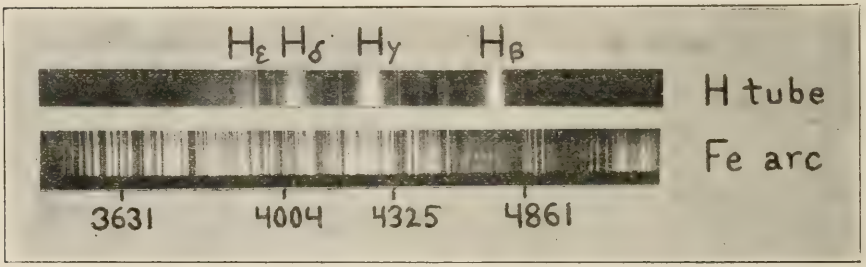

FIG. 2.

no subsequent readjustment for the other regions of the spectrum. The mirror M was held in a ball-and-socket type of adjustment so that any desired portion of the spectrum could be directed into the field of view of the eye piece or on to the photographic plate. Although a metal frame work is in general preferable, the wooden mounting was found to possess sufficient rigidity and permanence of adjustment. An achromatic lens at L instead of the singlet lens would enable greater ease of focussing but the advantage gained would often not be worth the greater expenditure. Higher dispersion could be attained by the use of a longer focus lens or by the introduction of a second 60° prism, the second method giving a spectrum of greater brilliancy than the first.

PHYSICAL LABORATORY,
UNIVERSITY OF IOWA,
NOVEMBER, 1922.

[Reprinted from The Physical Review, Vol. 21, No. 6, June, 1923.]

THE DEFLECTION OF A STREAM OF ELECTRONS BY ELECTROMAGNETIC RADIATION.

By E. O. Hulburt.

Abstract.

Deflection of a stream of electrons by electromagnetic radiation.—*A theoretical calculation*, based on classical electrodynamics, gives for the maximum angular deflection, when certain approximations are made, $He/m\omega$, where $\omega/2\pi$ is the frequency of the radiation, and H is the field due to it. For sunlight ($H = .04$) the value is only 4×10^{-10}, far too small to detect experimentally, while for intense x-rays, the value is of the order of 10^{-13}. Recently C. J. Lapp reported having obtained an observable deflection with x-rays. If further research should confirm this result, it would appear to be in direct conflict with the classical theory.

SOME time ago the writer determined from the classical equations of electrodynamics the path of an electron which moved in an alternating electromagnetic field. Renewed interest arose in the problem as the result of an experiment performed by C. J. Lapp[1] on "the effect of short electromagnetic waves on a beam of electrons," in which a strong beam of x-rays appeared to produce a deflection of a stream of electrons traversing the beam. The outcome of the theoretical calculation indicated, however, that no observable deflection would be expected unless a very sensitive method of detection were used. The details of the calculation follow.

A rigid electron of mass m and charge e moves initially along X with a velocity v in the midst of a plane polarized electromagnetic wave of frequency $\omega/2\pi$. The wave is propagated in the direction of X and the magnetic and electric vectors are $H_z = H \cos \omega t$ and $E_y = E \sin \omega t$, respectively, where H and E are the amplitudes. The reaction on the motion due to radiation from the electron is neglected. If x, y, and z are the positional coördinates of the electron at time t and electromagnetic units are used, the equations of motion of the electron are, in Newtonian notation,

$$\begin{aligned} \frac{m}{e}\ddot{x} &= -H\dot{y} \cos \omega t, \\ \frac{m}{e}\ddot{y} &= H\dot{x} \cos \omega t + E \sin \omega t, \\ \frac{m}{e}\ddot{z} &= 0. \end{aligned} \tag{1}$$

[1] Physical Review, **20**, 104, 1922.

Suppose initially $t = x = y = z = \dot{y} = \dot{z} = 0$ and $\dot{x} = v$. We see from (1) that z always remains zero and therefore we may concern ourselves only with the motion in the XY plane. The direct elimination of t from (1) leads to a differential equation in x and y which is difficult to integrate. We thereupon content ourselves with an approximate solution. Letting $\theta = \omega t$, (1) becomes

$$\begin{aligned} \frac{d^2x}{d\theta^2} &= -\frac{He}{m\omega}\frac{dy}{d\theta}\cos\theta, \\ \frac{d^2y}{d\theta^2} &= \frac{He}{m\omega}\frac{dx}{d\theta}\cos\theta + \frac{Ee}{m\omega^2}\sin\theta. \end{aligned} \tag{2}$$

It is assumed that ω is such a large quantity that the last term of the second equation of (2) may be neglected. This term is of the nature of a perturbing term and our assumption amounts to the omission of a small perturbation from the motion. Equations (2) then become, approximately,

$$\begin{aligned} \frac{d^2x}{d\theta^2} &= -\frac{He}{m\omega}\frac{dy}{d\theta}\cos\theta; \\ \frac{d^2y}{d\theta^2} &= \frac{He}{m\omega}\frac{dx}{d\theta}\cos\theta. \end{aligned} \tag{3}$$

Multiplying the first equation of (3) by $dx/d\theta$ and the second by $dy/d\theta$ and then adding leads to

$$\frac{d}{d\theta}\left[\left(\frac{dx}{d\theta}\right)^2 + \left(\frac{dy}{d\theta}\right)^2\right] = 0.$$

From this it follows that the speed of the electron in its path is constant.

When equations (3) are solved by expanding x and y as power series and by introducing the initial conditions, it is found that

$$x = \frac{v}{\omega}\theta; \qquad y = \frac{Hev}{m\omega^2}(1 - \cos\theta). \tag{4}$$

This is an approximate solution, obtained by neglecting terms in $He/m\omega^n$, where n is greater than 2. Remembering that $\theta = \omega t$, equations (4) become

$$x = vt, \qquad y = \frac{Hev}{m\omega^2}(1 - \cos\omega t), \tag{5}$$

which show that the electron pursues a sine curve in the XY plane, of small amplitude $He/2m\omega^2$ and of frequency $\omega/2\pi$. The direction in which the electron is moving is given by $dy/dx = He/m\omega \sin \omega t$, and

when $\omega t = \pi/2$, this has the maximum value

$$\left[\frac{dy}{dx}\right]_{\max} = \frac{He}{m\omega}. \tag{5}$$

We proceed to estimate the energy density of the x-radiation from a Coolidge tube. The energy of the cathode rays in a Coolidge tube under normal operation is about 200 watts. According to R. T. Beatty[1] perhaps the fraction 5×10^{-4} of the cathode ray energy goes into the general x-ray spectrum. If the characteristic radiation of the target is excited, a larger fraction of the energy passes into the emitted x-rays. The x-ray beam from the Coolidge tube of course diverges, but let us assume that all the x-ray energy is confined to a beam of a uniform cross section of 1 cm^2. The energy density of the x-radiation is then 3×10^{-5} ergs/cm^3.

Poynting's theorem states that the energy density of a plane sine wave is $\mu H^2/8\pi$, where H is the amplitude of the magnetic vector. If the conditions of Poynting's expression apply to the foregoing x-radiation we find, when the magnetic permeability μ is placed equal to unity, that $H = 0.03$ gauss. If the x-radiation is assumed to have a wave-length 10 A. U., ω is of the order of 10^{18}. Introducing these values into (5) and taking e/m to be 1.7×10^7 we find $[dy/dx]_{\max}$ to be of the order of 10^{-13}. This is a small quantity, so small in fact that although our estimates may be considerably in error and although the conditions of Lapp's experiment were more complex than those imagined in our calculation, we feel justified in concluding that the observed deflection of the electron beam seems to be at variance with the result to be anticipated from the classical equations.

It may be noted that even in the case of sunlight, since the maximum value of H is 0.04 gauss and ω is 1.6×10^{15}, $[dy/dx]_{\max}$ is only about 4×10^{-10}.

UNIVERSITY OF IOWA,
November 23, 1922.

[1] Royal Society Proceedings, *A*, 89, 314, 1913.

THE DISTRIBUTION OF INTENSITY IN THE BROADENED BALMER LINES OF HYDROGEN

BY

E. O. HULBURT

Reprinted from PHYSICAL REVIEW, pp 24 36, No 1, July, 1923

THE DISTRIBUTION OF INTENSITY IN THE BROADENED BALMER LINES OF HYDROGEN

By E. O. Hulburt

Abstract

Broadening of the Balmer lines of hydrogen by condensed discharges.—(1) At various pressures, 48 to 250 mm, the intensity distribution was determined for $H\beta$, $H\gamma$ and $H\delta$ by photographing the spectra through a neutral wedge. In each case the broadening was symmetrical, amounting to about 60A for each line at 250 mm, but the curves gave evidences of structure characteristic of each line. The effect of a quenched gap in series with the tube was to increase the broadening, while inductance decreased it. (2) *In mixtures with He or* N_2, the broadening was the same as in hydrogen alone at the same total pressure. (3) *Stark theory of broadening* which relates it to the Stark effect of the electrical fields of the ionized atoms or the radiating atoms, *is given mathematical formulation* by assuming a probability law for the distribution of the atoms and ions and an inverse square law for the strength of the field, and introducing Sommerfeld's quantum expression for the Stark displacement. This gives $\log I_\lambda = \log [a/(\lambda_0-\lambda)] - b/(\lambda_0-\lambda)$, where $a = A\lambda\lambda_0 p^2 f$ and $b = B\lambda\lambda_0 p^{2/3} f$, where f is a known function of the quantum numbers. Comparison with experiment shows agreement as to the general form of the distribution curves. The great broadening produced by the condensed discharge is then due to the momentary high current density and corresponding large proportion of ionized atoms.

Neutral wedge cell, filled with an aqueous solution of a black dye, was found more convenient to adjust than the ordinary neutral glass wedge.

Introduction

UNDER usual excitation by a transformer or induction coil the lines of the Balmer series of hydrogen at low pressure are sharply defined although weak in intensity. When the gas pressure is increased to several hundred mm of mercury and when condensed discharges are employed, the Balmer lines increase in intensity and widen until almost unrecognizable. This broadening has received unusual attention from investigators because of the large magnitude and because of the importance of the hydrogen atom in theories of atomic structure. However, Rossi[1] seems to have been the first to indicate what now appears to be the true cause of the enhancement of the lines. As a result of his observations he stated, "It would seem that current density is a very important, if not the only,

[1] Rossi, Astrophysical Journal **40**, 232, 1914

factor in the phenomenon." The work of Stark on the modifications of radiations when the source of the radiations was subjected to an electric field, led to the suggestion that the broadening of spectrum lines might in some instances be attributed to the presence of electric charges in the vicinity of luminous atoms. This suggestion was given definite form by Merton[2] and by Nicholson and Merton[3] in an investigation of the intensity distribution across $H\alpha$, $H\beta$ and $H\gamma$ radiated from hydrogen at atmospheric pressure when excited by condensed discharges A detailed analysis of the intensity curve of $H\alpha$ enabled them to conclude that the broadening was in close agreement with the results to be expected from Stark's observations of the electrical resolution of the line.

It seemed that an application of the recent theoretical work on the Stark effect of the Bohr hydrogen atom to the broadening problem would lead to a clearer understanding of the phenomenon. This has been attempted in the present investigation. After the intensity distribution had been measured across the hydrogen lines $H\beta$, $H\gamma$ and $H\delta$, stimulated by condensed discharges, for a pressure range from 48 to 250 mm of mercury, theoretical consideration of the radiations to be expected from a gaseous system of hydrogen atoms of the Bohr design mingled with charged particles, yielded a formula which gave substantial agreement with the observed intensity curves.

Experimental Details

Pure dry hydrogen, prepared from hydrochloric acid and zinc, was passed into the end-on discharge tube *d*, Fig. 1, made of glass with

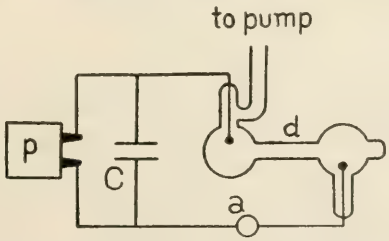

Fig. 1. Discharge tube and connections.

aluminum electrodes arranged out of line with the capillary, which was 4 cm long and 5 mm in diameter. The gas was excited by the discharges from a condenser *C* of capacity 0.0084 microfarads which received its power from a 1 kw, 25 kv, transformer *P*. The current through the tube was read by the thermo-galvanometer *a*. The current was in all cases

[2] Merton, Proc. Roy. Soc., **92**, 322, 1915
[3] Nicholson and Merton, Phil. Trans. Roy. Soc., **216**, 458, 1916

oscillatory, of frequency about 0.67×10^6 per second as measured by a wave-meter. The spectra were photographed with a glass prism spectroscope of the Littrow type, the dispersion at 5000, 4000, and 3600A being about 40, 20, and 15A per mm, respectively.

To obtain the distribution of intensity across the line a neutral wedge was placed before the slit of the spectrograph. A complete description of the neutral wedge method and a discussion of the theory is found in the papers by Merton, already referred to, in which the advantages and possibilities of the method and the precautions to be observed are clearly set forth. In the present instance a wedge was constructed by cementing glass plates together with sealing wax to form a cell with two wedge shaped compartments, Fig. 2. The angle α of the wedge was 17°, and the external dimensions of the cell were $1.5 \times 2.5 \times 3.5$ cm. One compartment

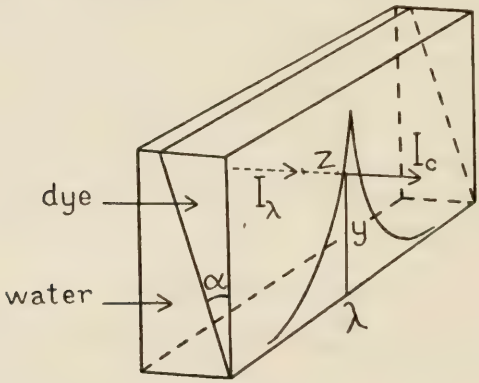

Fig. 2. Wedge cell.

was filled with water and the other with an aqueous solution of a black dye ("Erie Black, G×OO," National Anilene and Chemical Co., New York). The concentration of the solution was varied until the photographs had the best appearance. The advantage which this type of wedge had over a neutral glass wedge lay in the ease of construction and the freedom of adjustment to the experimental conditions.

The neutral wedge method. When the neutral wedge is interposed between a spectral line of finite width and the photographic plate, let us suppose that the plate records an image of the line of the form shown, for illustration, in Fig. 2. This figure indicates that the wedge was contiguous to the plate, whereas in reality the wedge was in front of the slit of the spectrograph, but the two cases are of course identical so far as the present discussion is concerned. We now seek the determination of the true intensity distribution curve of the line from the photographic

image found by means of the wedge. At all points on the edge of the image the intensity of the light has a constant value I_c, since under the condition of the exposure, light of less intensity does not produce a perceptible effect on the photographic plate. Let the coordinates of a point on the contour of the image be (λ, y), where y is measured from the thin edge of the wedge. Let z be the thickness of the wedge at this point. If I_λ is the undiminished intensity of the light of wave-length λ at this point, $I_c = I_\lambda e^{-kz}$, or

$$I_c = I_\lambda e^{ky \tan \alpha}, \qquad (1)$$

where k is the absorption coefficient of the material of the wedge for radiation of wave-length λ. I_c is a constant, and we shall assume k is a constant throughout the range of wave-lengths of the broadened line. Therefore from (1) the values of I_λ in arbitrary units may be determined for each value of λ merely by measuring y for each λ, and in this way the true intensity distribution curve may be obtained. Actually in the present experiment a variation of this procedure has been adopted; namely, I_λ was determined as a function of λ throughout the line from a theoretical consideration. From this function the form of the intensity distribution curve to be expected after the spectral line had passed through the wedge was calculated by means of (1) and a comparison was then effected between the theoretical and the experimental intensity curves.

Experimental Results

Spectra of hydrogen were photographed through the neutral wedge for pressures 48, 112, 160 and 250 mm of mercury. These are shown in Plate 1, *a*, *b*, *c* and *d*, respectively. The currents through the gas for each pressure were 1.2, 2.3, 2.8 and 4.1 amperes, respectively. The time of exposure was 20 minutes in each case. The contour of the image of the lines was in general convex to the wave-length axis for all the lines, the curves as seen in the reproduction being fairly smooth. On the original plates, however, the contours gave unmistakable evidences of structure in the line. $H\beta$ was noticeably a close hazy doublet at the apex; $H\gamma$ and $H\delta$ gave evidences of slight wings symmetrically placed on either side; and $H\gamma$ exhibited a bright central core which was lacking in the case of $H\delta$. These details are indicated more clearly in the heavy line drawings in Fig. 3 of the images for a pressure of 250 mm reduced to a uniform scale of wave-lengths. The facts concerning the structure of $H\beta$ and $H\gamma$ when broadened have been mentioned before.[1,2] If the images of $H\beta$ and $H\lambda$ were enlarged until their highest ordinates were equal to the maximum ordinate of $H\alpha$ it would be seen that the widening for a specified pressure increases with the series term number of the line.

Theoretical

We proceed to a consideration of the simple theory of the general form of the curves and reserve for a later paragraph a suggestion for a more detailed explanation.

Intermingled with the radiating hydrogen atoms in the discharge tube are charged particles. These charged particles may be electrons, ions or even the component charges of a neutral atom. As a result the radiating atom finds itself in an electric field and therefore, in agreement with the observations of Stark, instead of emitting a single line it gives forth a group of lines whose displacement from the parent line is directly

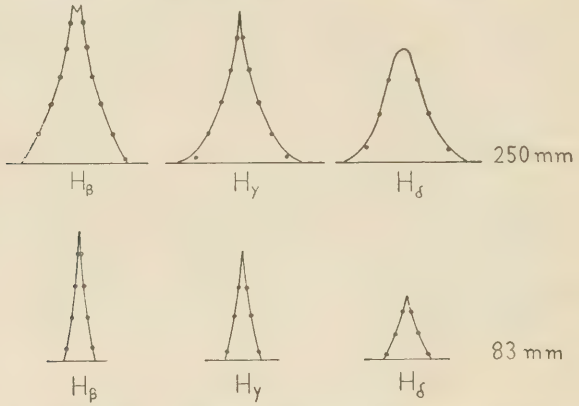

Fig. 3. Broadening curves; observed (full lines) and computed (dots).

proportional to the strength of the electric field. Throughout a finite interval of time a radiating atom may be expected to be subjected to fields of a wide range of intensities and in spite of the many complexities of the case it seems reasonable to suppose that the average over a considerable length of time of the influence of the electric fields on a large number of radiating atoms will be in accordance with a probability law. In the following paragraphs these ideas are couched in mathematical terms.

The hydrogen gas in the path of the condensed discharges is largely atomic and is composed of electrons and of charged and neutral, luminous and quiescent atoms. Since ionization is probably essential to luminosity under the conditions of the discharge we cannot be far wrong in assuming that the number of luminous atoms and the number of the charged particles are of about the same order of magnitude. J. J. Thomson[4] has estimated the ratio of the number of ions to the total num-

[4] Thomson, "Conduction of Electricity Through Gases," 1906, p. 83

ber of molecules in a gas during the passage of an electric current to be about 10^{-14} in a certain instance. In the present experiment this ratio was probably much greater, because condensed discharges were used, but we may estimate with safety that the ratio was not greater than, say, 10^{-6}. The conclusion is that the number of both luminous atoms and charged particles was small compared to the total number of atoms present.

Let the total number of atoms per unit volume be ν, of which a fraction q contribute to the radiation. Let the distance from a luminous atom to a charged particle be denoted by δ. It is assumed that the number of luminous atoms ν_1 per unit volume which are at a distance δ from a neighboring charged particle, is given by the probability relation[5]

$$\nu_1 = A\nu\delta^2 e^{-B\delta^2}. \tag{2}$$

In order to avoid needless complication we simplify matters by assuming that the luminous atoms are the charged particles. This does not materially affect the argument because we are interested in the orders of magnitude of the numerical constants and not in their precise values. On this assumption we may write $\int_0^\infty \nu_1 d\delta = q\nu$; hence, $A = 4q\sqrt{B^3/\pi}$. If δ_m is the average distance between luminous atoms, then

$$\delta_m = 4\sqrt{\frac{B^3}{\pi}}\int_0^\infty e^{-B\delta^2}\delta^3 d\delta = \frac{2}{\sqrt{\pi B}}.$$

Also $\delta_m{}^3 = 1/q\nu$. Therefore $A = 2^5 q\nu/\pi^2$ and $B = 4q^{2/3}\nu^{2/3}/\pi$. ν depends on the pressure and may be written $\nu = 4\times 10^{19} p/760$, where p is the pressure in mm of mercury. Introducing these values into (2) leads to

$$\nu_1 = \alpha p^2\delta^2 e^{-\beta p^{2/3}\delta^2}, \tag{3}$$

where $\alpha = 2^5/\pi^2 \left(\frac{4\times 10^{19}}{760}\right)^2 q$ and $\beta = 4/\pi\left(\frac{4\times 10^{19}}{760}\right)^{2/3} q^{2/3} = 5\times 10^{11} q^{2/3}$.

Making use of the estimated maximum value of q, i.e. 10^{-6}, the maximum value of β does not exceed 10^7.

The experiments of Stark[6] have demonstrated that in the case of the Balmer lines of hydrogen the displacements of the Stark components are closely proportional to the strength of the electric field. In his theoretical treatment of the electrical resolution of the radiations from the Bohr model of the hydrogen atom Sommerfeld[7] has derived a general

[5] Jeans, "Dynamical Theory of Gases," 1904, p. 28
[6] Stark, Ann. der Phys. **48**, 193, 1915
[7] Sommerfeld, "Atombau und Spektrallinien," 1922, p. 357

relation for the displacement of any component, which is in agreement with Stark's data, namely,

$$\lambda_o - \lambda = \frac{3hF}{8\pi^2 mE} \frac{\lambda\lambda_o}{c} f, \tag{4}$$

where f is a function of the quantum numbers. The exact value of f is known; it differs for each component. λ_o is the wave-length of the parent line; λ is the wave-length of the component when the intensity of the electric field is F; h is the Planck constant; m the electronic mass; E the nuclear charge, and c is the velocity of light in vacuum. Since the Stark components are symmetrically placed and equally displaced on either side of the parent line the absolute value of $\lambda_o - \lambda$ is used in (4). In the problem under discussion the luminous atom is conceived to be subjected to the electric field of the charge e on the neighboring atom a distance δ away. The strength of the electric field is e/δ^2, the dielectric constant of the medium being unity, and if δ is large compared to the diameter of the atom the field is approximately uniform over the luminous atom. We thereupon replace F by e/δ^2 in (4) and solve for δ^2. This yields $\delta^2 = \alpha'/(\lambda_o - \lambda)$, where $\alpha' = 3he\lambda\lambda_o f/8\pi^2 mEc$. Taking f to be of the order of 10 and putting $\lambda = \lambda_o = 5000$A, we find α' to be of the order of 10^{-11}. Upon substitution of the expression for δ^2 in (3) we obtain

$$\nu_1 = \frac{a\alpha' p^2}{(\lambda_o - \lambda)} e^{-[\beta\alpha' p^{2/3}/(\lambda_o - \lambda)]}. \tag{5}$$

It must be noted that in equating F to e/δ^2 we have tacitly assumed that the field was due to a single charge. Actually the electric field at any point in the gas was the resultant of the fields of a swarm of charged particles of both signs in the vicinity of the point. This indicates that the right hand side of (5) and the exponent should each be multiplied by some fraction.

We may now assume that the intensity I_λ of the radiations of wave-length λ is proportional to ν_1, and write $I_\lambda = \alpha''\nu_1$. Hence from (5)

$$I_\lambda = \frac{a\alpha'\alpha'' p^2}{(\lambda_o - \lambda)} e^{-[\beta\alpha' p^{2/3}/(\lambda_o - \lambda)]}. \tag{6}$$

The quantity $\beta\alpha' p^{2/3}$, according to our numerical estimates of β and α', is a small quantity, certainly never greater than 1/10 for pressures of the order of one atmosphere, and probably much less. We may therefore replace the exponential term of (6) by unity without appreciable error unless the absolute value of $\lambda_o - \lambda$ expressed in angstrom units be less than 1/10. Eq. (6) then becomes, to a close approximation,

$$I_\lambda = gp^2/(\lambda_o - \lambda), \tag{7}$$

where $g = \alpha\alpha'\alpha''$ and is approximately a constant across the broadened line. From (7) the line may be expected to widen with pressure. When I from (6) is plotted in arbitrary units against λ a curve of the form given by the heavy line of Fig. 4 is obtained. The curve is obviously not drawn to scale. At λ_o, I_λ is zero and the distance apart of the maxima is less than 0.1 A. This crevice in the intensity curve is perhaps beyond the reach of detection by experiment, and probably is of no physical significance. It merely results from the refusal of Eq. (6) to admit the possibility of there being any atom at all which emits the unaffected wave-length λ_o. In regard to the approximate formula (7), the intensity curve conforms closely to that of formula (6) except n the small interval

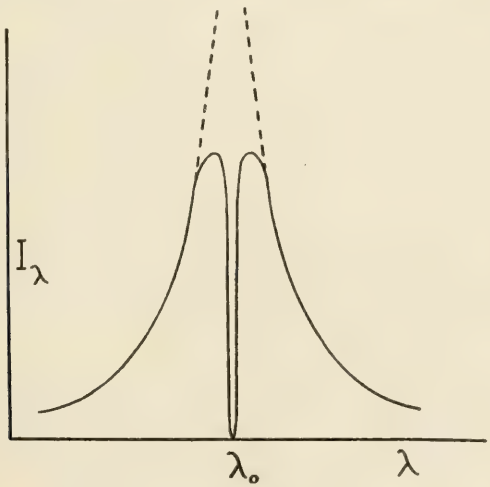

Fig. 4. Theoretical broadening curve.

between the two maxima in which the approximate formula is invalid. Ignorance of the exact physical conditions renders it difficult to attempt to derive an expression for the intensity at wave-length λ in terms of the intensity at the center of the parent line. We content ourselves therefore with formula (7) which affords relative values of I_λ for regions neither too near nor too remote from λ_o.

It remains to determine the equation of the intensity curve after the light has traversed the neutral wedge. This is obtained by eliminating I_λ between (1) and (7). There results

$$\lambda_o - \lambda = (gp^2/I_c)e^{-ky \tan \alpha}. \tag{8}$$

Comparison Between Theory and Experiment

Drawings of the enlarged images of the lines were made and reduced to a uniform wave-length scale. These are shown by the full lines of Fig. 3

for $H\beta$, $H\lambda$, and $H\delta$ at pressures 250 and 83 mm, which were plotted with values of y in arbitrary units as ordinates against values of $\lambda_0 - \lambda$ in angstrom units as abscissas. The constants g/I_e and $k \tan \alpha$ of Eq. (8) were determined from two observed points on the contour of $H\beta$ at a pressure 250 mm, and points on the intensity curve were then calculated. To obtain the theoretical curves for the other lines and pressures it was only necessary to readjust the quantity g/I_e of Eq. (8). This was permissible because the intensities were in arbitrary units. The calculated points are shown by the dots of Fig. 3. Similar comparisons were affected for all the other lines, and in all instances good agreement was found between the general forms of the observed and theoretical intensity curves.

Structural detail in the broadened line. The theoretical ideas thus far advanced in explanation of the general form of the intensity curve will not suffice to account for the evidences of structure observed in the broadened lines. A more detailed consideration is necessary. Merton[2] has supplied this by drawing attention to the close correspondence between the Stark components of a line and the form of the intensity distribution curve. To show this the p and s components of the electrical resolution of $H\beta$, $H\lambda$ and $H\delta$ as determined by Stark[8] are given in Fig. 5. It needs only a glance at these components to see that the $H\beta$ radiations

Fig. 5. Stark effect components.

from a large number of hydrogen atoms subjected to a wide range of electric fields will result in a widened line with perhaps a weak minimum at the center. In the cases of $H\lambda$ and $H\delta$ we should expect a widened line with more or less prominent wings, the center of $H\lambda$ being more brilliant than the center of $H\delta$. As far as can be judged these conclusions are in agreement with the appearance of the photographic images of the lines.

The role of the condensed discharge. As an outcome of the views set forth in explanation of the broadening, we are led to an understanding of the role played by the condensed discharge. In the condensed discharge the current density is very great for a short interval of time at the commencement of the discharge. It may easily amount to several hundred amperes. A gas which is stimulated by such a discharge emits

[8] Sommerfeld, loc. cit., p. 357

radiations characteristic of those caused by the passage of heavy currents. The luminous atoms in such a case are in the midst of a vast number of charged particles and a relatively large number may be expected to be subjected to strong electric fields. This results in the widening of the lines. On the other hand if a steady current, either direct or alternating, traverses the gas the current density never attains very high values and the charges present in the gas are never very numerous. Therefore the luminous atoms rarely experience strong electrical fields and no marked broadening of the lines occurs.

The effect of the quenched gap. The photographs *e* and *f* of Plate I indicate the increase in width of $H\beta$ occasioned by the introduction of a quenched gap in series with the tube. The pressure of the hydrogen was 130 mm, the current 2.1 amperes and the time of exposure 20 minutes in each case. For *e* the quenched gap was used, for *f* the discharge took place directly through the tube without the gap. The effect of the gap in producing widening was more marked at the lower than at the higher gas pressures. The insertion of the gap enabled the charges to accumulate on the condenser plates to higher potentials, so that when the discharge occurred a greater current than otherwise passed through the tube. The current was rapidly damped by the quenching action of the gap. As a consequence the gas was stimulated at each discharge by abrupt pulses of current more intense than those which occurred without the gap, even though the currents read by the thermogalvanometer were the same in the two cases. The stronger current pulses produced the greater broadening. The reason that the gap produced less effect for high gas pressures was simply that in those cases the tube itself quenched the discharge to a greater extent.

The effect of inductance. A coil of inductance 2.2×10^{-5} henries in series with the discharge tube reduced the widths of the broadened lines. An illustration of this is afforded by the photographs *g* and *h* of $H\beta$, *g* taken with the coil and *h* without the coil. The current was 3.0 amperes, the gas pressure 140 mm, and the time of exposure 11 minutes in each case. The frequency of the oscillatory discharge with the inductance was 1.2×10^{5} and without it was 6.7×10^{5}; these were measured with a wavemeter, the tuning being of course very broad because of the resistance of the tube. The inductance served to distribute the discharge over a longer interval of time so that the pulses of current were of less intensity and therefore the spectrum lines were narrower than when the inductance was absent. The fact that an inductance will reduce or suppress entirely certain lines excited by spark discharges, has been known for a long time, but it appears that in some instances the electrical conditions of the

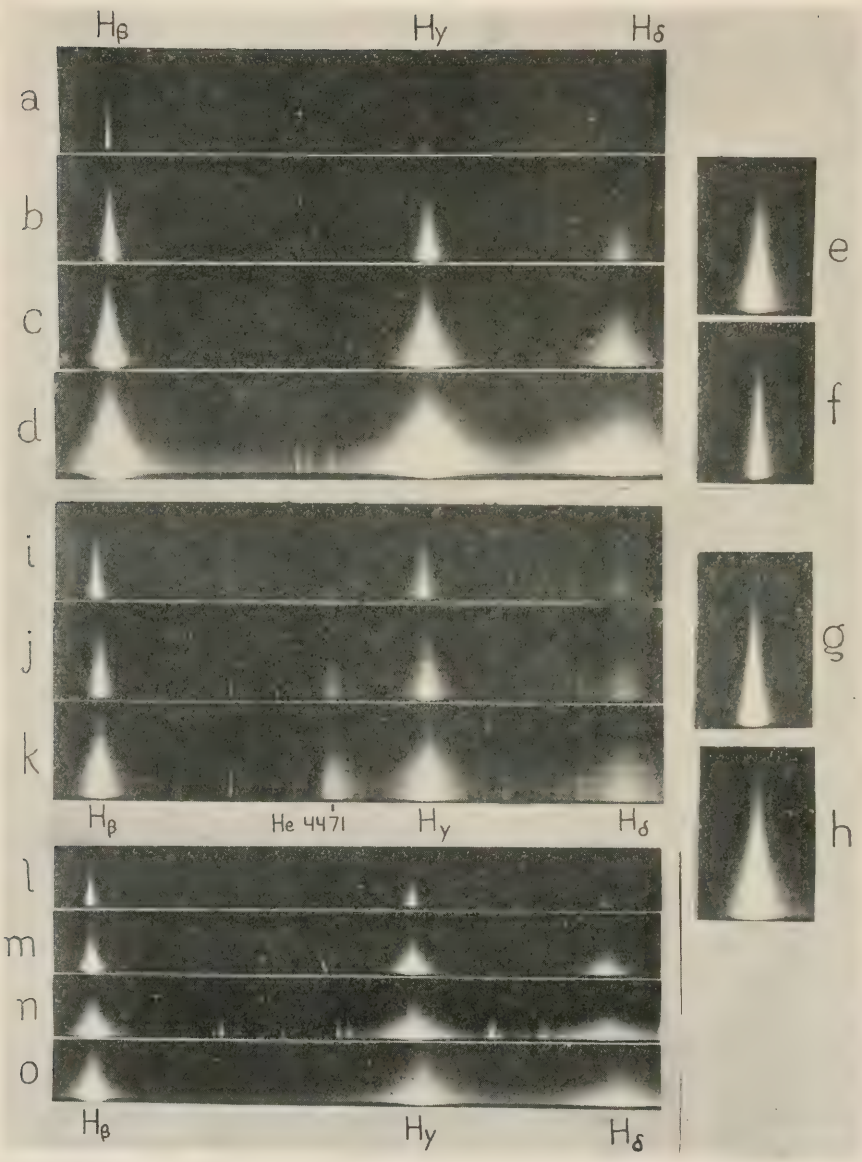

Plate I. Broadening of the Hydrogen lines by condensed discharges.

experiments have not been described in sufficient detail to enable possible explanations to be advanced.

Mixtures of Hydrogen with Helium and Nitrogen

Mixtures with helium. It was found that the Balmer lines of hydrogen at a relatively low pressure were broadened when the pressure was increased by the addition of an inert gas such as helium or nitrogen, in the same manner as by the addition of more hydrogen. Photographs *i*, *j* and *k* show the effect of helium. The data for these photographs are given in Table I. The helium contained a trace of nitrogen but this probably

Table I

Data for photographs i, j, and k

	Pressure of hydrogen	Pressure of helium	Current	Time of exposure
i	29 mm	79 mm	1.2 amp.	20 min.
j	29	188	3.0	20
k	29	380	4.2	20

had no effect in the present experiment. The enhancement of the hydrogen lines caused by the helium was to be expected from the views already outlined. Several factors, however, must be considered. The introduction of the inert gas increased the break-down potential of the discharge tube. A violent discharge thereupon ensued and a great number of charged particles were produced in the luminous gas with consequent enhancement of the Balmer lines. The charged particles came apparently from ionized hydrogen rather than from helium, since even with partial pressures of 380 mm of helium and only 29 mm of hydrogen the helium lines were of less intensity than the hydrogen lines. This of course was to be ascribed to the high resonance and ionization potentials of helium as compared with those of hydrogen, and to the fact that the higher the ionization potential of an element the greater is the difficulty with which it can be excited to emit its line spectrum.[9]

Mixtures with nitrogen. The enhancement of the Balmer lines from hydrogen mixed with nitrogen is shown by photographs *l*, *m*, *n* and *o*. The flatness of the contours of these lines resulted from the use of a neutral wedge of greater optical density than the one used for the other photographs. The conditions under which these were taken are given in Table II. It is interesting to notice the striking similarity of photographs *n* and *o* which were taken with the same total pressures but with quite different partial pressures of the component gases. The ionization potential of nitrogen is somewhat above that of hydrogen. Some of the

[9] Saha, Phil. Mag. **41**, 268, 1921

resonance potentials, however, are slightly lower than those of hydrogen and therefore it might be supposed that the nitrogen lines would appear nearly as prominently as the hydrogen lines. This does not seem to be the case in this experiment as indicated by spectrogram *k*. However, little can be said with certainty on this point because there is no criterion for the relative intensities of the spectrum lines of different elements.

Of the possible causes of broadening of spectrum lines recognized at the present time only two seem to be of sufficient potency to effect the relatively large widening noticeable in many enhanced lines. These two causes are the electric and magnetic fields. In the present experiments

TABLE II

Data for photographs l, m, n, o

	Pressure of hydrogen	Pressure of nitrogen	Current	Time of exposure
l	85 mm	0 mm	2.3 amp.	20 min.
m	85	55	2.5	20
n	85	115	3.0	20
o	200	0	3.0	20

as well as in all usual cases of broadened lines the Zeeman effect may be ruled out, although it may be possible to devise conditions in which the Zeeman effect is operative. This suggests that the Stark effect is the cause of most cases of broadening of spectrum lines, or more precisely, that the broadening is due to the electric fields of the charged particles which are produced by the same vigorous stimulation which brings into existence the broadened line. The results of many experiments, among which may be mentioned those of Hemsalech and de Gramont,[10] point to this conclusion.

I take pleasure in thanking Dr L. I. Shaw of the Bureau of Mines for a gift of helium.

PHYSICAL LABORATORY,
UNIVERSITY OF IOWA,
January 14, 1923[11]

[10] Hemsalech and Gramont, Phil. Mag. **43**, 287 and 834, 1922

[11] The paragraphs dealing with the effects of a quenched gap and of inductance were added February 7, 1923.

Reprinted from PHYSICAL REVIEW, pp. 193-197, No. 2, August, 1923

THE TORQUES AND FORCES BETWEEN SHORT CYLINDRICAL COILS CARRYING ALTERNATING CURRENTS OF RADIO FREQUENCY

BY W. A. PARLIN

ABSTRACT

Forces between two short cylindrical coils carrying alternating currents of frequency 60 to 1.5 x 10^6 cycles.—(1) Coils with a common diameter, mounted like a dynamometer, the outer coil being suspended and free to turn about the fixed inner one, were connected in series with the current in the same sense for zero angle. The torque was found proportional to the square of the current for all frequencies, but for a constant angle began to increase with the frequency at 3×10^5 cycles. The ratio of the torque for 15×10^5 cycles to that at 3×10^5 cycles decreased from two at 10° to one for 90° and remained one for all angles for which the currents were in opposite sense. In the case of 60 cycles, the variation of the torque with angle corresponded roughly with that computed from Maxwell's equations. (2) *Coils with planes parallel* showed a similar increase of force with frequency for frequencies above 3×10^5 cycles, when the currents were in the same sense, but not when they were in opposite sense. It is suggested that these variations with frequency may be due to the reactions caused by the radiation of energy from the coils in the form of electromagnetic waves.

INTRODUCTION

THE FORCES between circular currents have been the subject of considerable investigation both experimental and theoretical. Maxwell[1] has derived formulas which give the torques and forces between coils in various positions carrying electric currents. His formulas are valid for direct and slowly varying alternating currents. As far as is known no experimental work has been done to determine the torques and forces between coils carrying radio frequency currents, that is, frequencies of 10^4 to 10^7 alternations per second.

In the present work measurements have been made of the forces between circular coils in various positions, which carried direct current, 60 cycle alternating current, and currents of radio frequency. For the low frequency currents the torques and forces were found to conform to the usual formulas given by Maxwell and others, but in certain cases where radio-frequency currents traversed the coils, the measurements are not in agreement with the theoretical formulas.

[1] Maxwell, Electricity and Magnetism, Vol. II, 1873

Apparatus

To measure the torque between the two coils, a sensitive dynamometer arrangement was used which consisted of a fixed coil of 11 turns, 10 inches in diameter, and a movable coil of 11 turns, 12 inches in diameter, suspended outside of and free to turn about the fixed coil. Contact with the movable coil was made by mercury contacts. The suspension was a bronze wire 8.38 inches long and 0.005 inch in diameter. The upper end of the bronze wire was fastened to a dial which could be turned about the axis of suspension. To measure the torque, the dial was set so that the coils made a certain angle with no current flowing. With current through the coils a torque was produced which changed the angle between the coils. The dial was then turned so that the coils returned to the original angle. The difference in the readings denoted the torque between the coils. The two coils were in series with a carefully calibrated hot wire ammeter. For the radio-frequency currents a small coil was introduced in series with the dynamometer coils for coupling purposes. An electron tube oscillating circuit was the

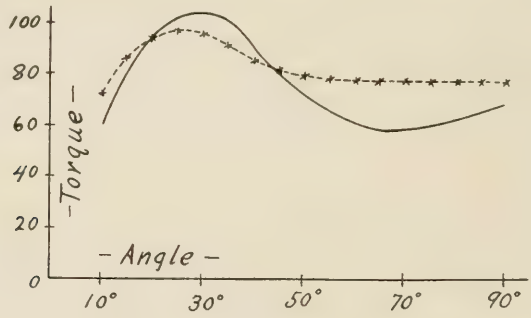

Fig. 1. Torque as function of angle, for 60-cycle current.

source of the undamped radio-frequency currents, and a one-half kilowatt transformer with a condenser and quenched spark gap, provided the damped radio-frequency currents.

Tests with slowly varying currents. Tests were made to see to what extent agreement between a theoretical formula and measurement might be expected. It was found that for a given angle between the coils the torque increased very closely as the square of the current, in accord with theory. For a constant 60 cycle current of 0.60 amperes the torque was measured for a series of angles between the coils, from 10° to 90°. The measurements are shown by the crosses and dotted curve of Fig. 1. The theoretical curve for this case, plotted from six terms of Maxwell's formulas (page 303, loc. cit.[1]), is given by the full line curve of Fig. 1. The agreement between the two curves is perhaps as close as could be ex-

pected because the formula refers to coils of a single turn whereas the coils in the present experiment were of finite length and had several turns of wire.

In all the figures the torques have been expressed in arbitrary units, actually in degrees. These values may be changed to dyne-centimeters by multiplying by 20.7.

The torque between coils carrying radio-frequency currents. In agreement with simple theory the torque between the coils for a constant angle

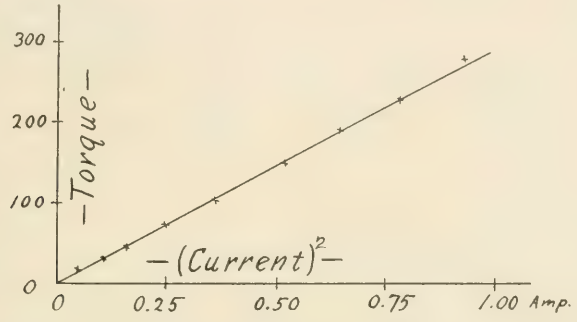

Fig. 2. Torque as a function of (current)^2, for frequency of 4×10^5 cycles.

of 30° traversed by a current of frequency 0.4×10^6 cycles (750 meters) varied directly as the square of the current. Fig. 2 gives the results of these measurements.

With the current through the coils in the same sense and the angle between the coils maintained constant, it was found that *the torque in-*

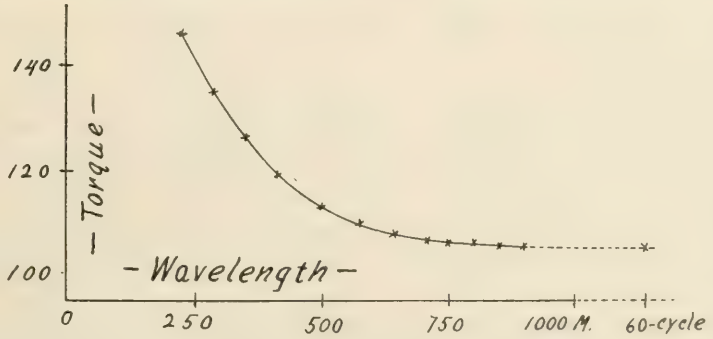

Fig. 3. Variation of torque with wave-length, for 22.5° angle.

creased with the frequency of the current. This is shown by Fig. 3 which was taken for a current of 0.60 amperes and an angle between the coils of 22.5°. The curve indicates that for the region between 60 cycles and about 700 meters no changes in torque with frequency of the current occurred, but that for the wave-lengths below 700 meters the torque

increased in a marked manner with the frequency. This increase in the torque with the frequency was not to be expected from the classical formulas of Maxwell, which contain no frequency term.

When the currents through the two coils were in the same sense, the change in torque with frequency was found to increase as the angle between the coils decreased. For angles between the coils from 90° to 270°, i.e., the currents being in the opposite sense, the torque did not change with the frequency of the current. These results are shown in Fig. 4 in which the percentage change in torque between wave-lengths 235 and 908 meters are plotted as ordinates against angles between the coils as abscissas. Similar results were obtained for damped radio frequency currents as for undamped currents.

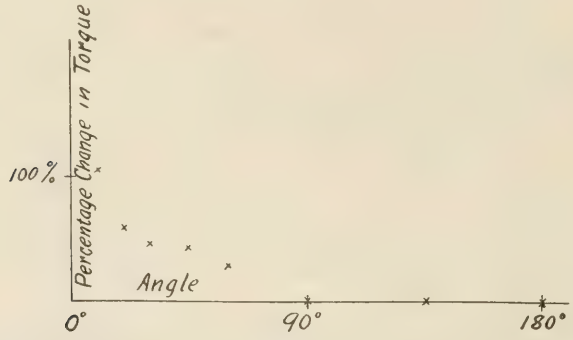

Fig. 4. Percentage excess torque for 235 meters as functions of angle.

The forces between parallel coils carrying radio frequency currents. The movable coil was arranged at the end of the bar of a torsion pendulum and the force between the two coils observed by means of a torsion head on the supporting wire of the pendulum. In the figures the forces are given in arbitrary degrees; these numbers may be reduced to dynes by multiplying by 1.16. For a constant distance between the two coils and with current of constant frequency, the force was found to increase directly as the square of the current, in agreement with simple theory.

With currents in the same direction in the two coils the force was found to increase with the frequency, the rate of increase of force with frequency depending upon the distance between the coils. Fig. 5 shows the force vs. wave-length curves for distance between the coils of 2, 4, 6, and 8 inches respectively, the current being 0.60 amperes in all cases. These results, as in the case of the torques, are at variance with the formulas for slowly varying currents. The percentage change in force

from wave-lengths 235 to 908 meters appeared to increase with the distance between the coils, as given in Fig. 6. Conclusions similar to those for the undamped currents were found to be true for damped radio frequency currents.

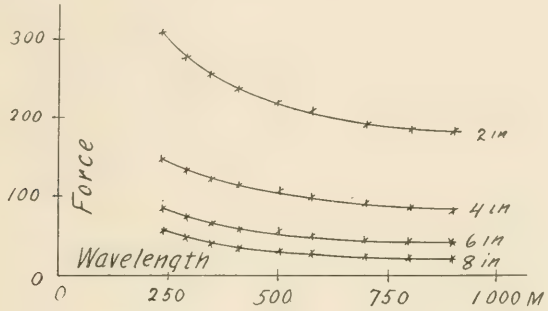

Fig. 5. Force between parallel coils as function of wave-length.

Discussion. From a consideration of the various phenomena of radio-frequency currents not taken into account by the classical theory it would seem that an explanation of the foregoing discrepancies between existing formulas and the present measurements is to be sought in the

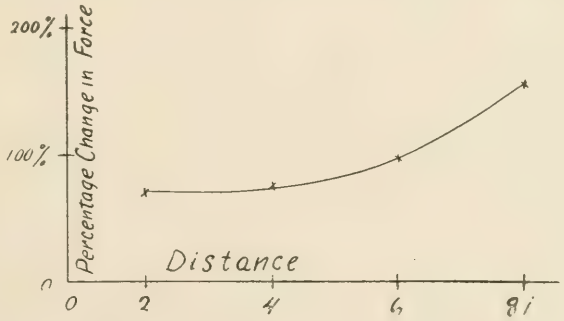

Fig. 6. Percentage excess force for 235 meters as function of distance apart of coils.

reactions caused by the radiation of energy from the coils in the form of electromagnetic waves.

In conclusion I wish to thank Dr. E. O. Hulburt for suggesting the problem and for his advice during the course of the work.

PHYSICAL LABORATORY,
STATE UNIVERSITY OF IOWA.
February 6, 1923

Reprinted from PHYSICAL REVIEW, pp. 180-187, No. 2, August, 1913

MAGNETIC AND NATURAL ROTATORY DISPERSION IN ABSORBING MEDIA

By E. O. Hulburt

Abstract

Electron Theory of Magnetic and Natural Rotatory Dispersion in Absorbing Media.—On the basis of the electron theory of Lorentz, theoretical formulas have previously been derived for rotatory dispersion in perfectly transparent liquids, but on comparison with experimental results, a discrepancy was found which seemed to be due to the absorption. In the present paper, the theory has been extended to take account of absorption, and by making certain approximations, simplified formulas are obtained which give the rotation for wave-lengths sufficiently removed from the critical wave-length, provided the refractive index and extinction coefficient conform to the Lorentz dispersion equations with one resonance frequency. The equation of magnetic rotation in isotropic media agrees closely with experimental results for CS_2 and α-monobrom-naphthalene. It is suggested that the theoretical equation for natural rotation: $\theta/l = r_1 + (2\pi^2\gamma_1/\lambda^2)\,[\mu_0^2 - 1/(1+\kappa_0^2)]$, (where μ_0 and κ_0 are refractive index and extinction coefficient, respectively, and r_1 and γ_1 are constants), may be assumed to describe the phenomenon in any medium, whether μ_0 and κ_0 satisfy the Lorentz dispersion equations or not, but this has not yet been tested experimentally.

Introduction

IN TWO recent communications[1] formulas for the natural and magnetic rotatory dispersion in transparent liquids were developed from the electron theory of H. A. Lorentz and were submitted to experimental test by means of data obtained for the purpose. It was found that the values of the magnetic rotation angles calculated from the theoretical formulas increased with decrease of wave-length more rapidly than the observed angles and it was pointed out that the discrepancy might be attributed, in part at least, to the neglect in the theory of the effect of absorption. In the present paper absorption of the radiation in the medium has been considered from a theoretical standpoint and more complete rotatory dispersion formulas have been derived.

The theory of magnetic rotatory dispersion, i.e., the Faraday effect, and of natural rotatory dispersion, i.e., the Biot effect, has been excellently stated by Drude[2] and Voigt.[3] H. A. Lorentz[4] has further con-

[1] Hulburt, Astrophysical Journal, **54**, 45 and 116, 1921.

[2] Drude, Lehrbuch der Optik, 1906.

[3] Voigt, Magneto- und Electrooptik, 1908.

[4] H. A. Lorentz, Theory of Electrons 1916 p. 132.

tributed to the electron theory of the Faraday phenomenon, obtaining formulas similar to those of Drude and of Voigt but with a different interpretation of the constants of the equations. The formulas when reduced by simplifying assumptions were found to be in accord with the observed magnetic rotation in the case of the sodium flame and other experiments.[5] It seems, however, that the general formulas have not been sufficiently developed to be useful for the consideration of absorbing media.

Magnetic Rotatory Dispersion

We use the electron theory of dispersion as given by H. A. Lorentz and restrict the discussion to isotropic media in which the temperature remains constant. Let ξ and E_x be the X-components of the displacement of the electron from its equilibrium position and the electric force, respectively, and η, ζ, E_y, and E_z be the Y and Z components of the quantities. The components of the "restoring force" and of the "frictional force" with which the medium acts upon the electron are $f\xi$, $f\eta$, $f\zeta$ and $\beta\dot{\xi}$, $\beta\dot{\eta}$, $\beta\dot{\zeta}$, respectively, where f and β are positive constants. The charge on the electron is denoted by e, its mass by m; N is the number of such electrons per unit volume. σ is a constant which Lorentz has shown to be approximately one-third for isotropic media. We shall denote the external magnetic field by H and shall suppose it to have the direction of the axis of Z, which is also the direction of the propagation of the light. The magnetic permeability of the medium is taken to be unity. All quantities are expressed in c.g.s. e.m. units. In Newtonian notation the equations of motion of the dispersion electrons of a single type are, then,

$$\left.\begin{aligned} m\ddot{\xi} &= e(E_x+4\pi c^2\sigma Ne\xi)-f\xi-\beta\dot{\xi}+He\eta, \\ m\ddot{\eta} &= e(E_y+4\pi c^2\sigma Ne\eta)-f\eta-\beta\dot{\eta}-He\dot{\xi}, \\ m\ddot{\zeta} &= e(E_z+4\pi c^2\sigma Ne\zeta)-f\zeta-\beta\dot{\zeta} \end{aligned}\right\} \qquad (1)$$

Let e be the base of natural logarithms, and let all dependent variables of (1) contain the time only in the factor $e^{i2\pi tc/\lambda}$, where c/λ is the frequency, λ the wave-length of the vibration in vacuum, c is the velocity of light in vacuum, and i is $\sqrt{-1}$. The solution of (1) yields two vibrations, circularly polarized in opposite directions, whose refractive indices μ_1 and μ_2 and extinction coefficients κ_1 and κ_2 are given by the relations

$$\frac{1}{\sigma+\dfrac{1}{[\mu(1-i\kappa)]^2-1}}=\frac{C_s}{1/\lambda^2{}_s-1/\lambda^2+ib_s/\lambda\pm Hh_s/\lambda}, \qquad (2)$$

where $C_s=N_se^2/\pi m_s$, $b_s=\beta_s/2\pi cm_s$, $h_s=e/2\pi cm_s$.

[5] Lorentz, loc. cit., p. 164.

The details of this solution are here omitted for they are essentially the same as those given by Lorentz. The subscript s is used to denote the s'th type of electron. c/λ_s is the frequency of the natural undamped vibration of the electron, and is equal to $1/2\pi\sqrt{f_s/m_s}$. When the plus sign is used in the right hand term of (2), μ is μ_1 and κ is κ_1. When the minus sign is used μ is μ_2 and κ is κ_2. We see that under the influence of the magnetic field the medium is doubly refracting and possesses two different degrees of transparency.

The *absorption coefficient* K of the nonmagnetized medium is defined by the relation

$$K=(1/2l)\ \log_e I_0/I, \tag{3}$$

where I_0 is the intensity of the incident radiation and I is the intensity, after passing through a layer of the medium of thickness l. In obtaining (2) from (1) we have made the substitution

$$\kappa=\lambda K/2\pi\mu. \tag{4}$$

From (3) and (4) the extinction coefficient κ is expressed by

$$\kappa=(\lambda/4\pi\mu l)\ \log_e I_0/I. \tag{5}$$

By means of (5), κ may be determined from measurements of the transmitted radiation.

Eq. (2) describes the refractive indices and extinction coefficients in terms of the constants of a single type of dispersion electron. There may be other types of dispersion electrons in the medium with constants peculiar to the type, so that in the more general case the right hand member of (2) may be assumed to be a summation of similar terms, one term for each type. For this case the complete dispersion formula is

$$\frac{1}{\sigma+\dfrac{1}{[\mu(1-i\kappa)]^2-1}}=\sum\frac{C_s}{1/\lambda_s^2-1/\lambda^2+ib_s/\lambda\pm Hh_s/\lambda}. \tag{6}$$

We assume we are dealing with a region of the spectrum in which the change of the refractive index with wave-length is determined by the electrons of a single type, denoted by the subscript 1, so that in the summation of (6) all the terms except one may be replaced by a quantity q_1, which is independent of λ and H. Then (6) becomes

$$\frac{1}{\sigma+\dfrac{1}{[\mu(1-i\kappa)]^2-1}}=q_1+\frac{C_1}{1/\lambda_1^2-1/\lambda^2+i\,b_1/\lambda\pm Hh_1/\lambda}. \tag{7}$$

Separating the real and imaginary parts of (7) by a transformation similar to one used by Havelock,[6] gives

[6] Havelock, Proc. Roy. Soc., **86**, 1, 1912.

$$\mu^2(1-\kappa^2)/q_1' = 1+g\lambda^2(\lambda^2-\lambda_2'^2)/[(\lambda^2-\lambda_2'^2)^2+g'^2\lambda^2],$$
$$2\mu^2\kappa/q_1' = gg'\lambda^3/[(\lambda^2-\lambda_2'^2)^2+g'^2\lambda^2], \quad (8)$$

where q_1', λ_2', g and g' are defined by the following equations;

$$q_1' = [1+q_1(1-\sigma)]/(1-q_1\sigma), \quad \lambda_2'^2 = \lambda_1'^2(1\mp Hh_1\lambda),$$
$$1/\lambda_1'^2 = 1/\lambda_1^2 - C_1\sigma/(1-q_1\sigma), \quad g = C_1\lambda_1'^2/(1-q_1\sigma)^2q_1', \; g' = b_1\lambda_1'^2. \quad (9)$$

Again, just as in the case of Eq. (2), Eqs. (8) are each two formulas, giving μ_1 and κ_1 when the minus sign is used in the expression for λ_2' in (9), and μ_2 and κ_2 when the plus sign is used. It will abbreviate our expressions to replace the right hand terms of (8) by A_1, A_2, B_1 and B_2, obtaining

$$\mu_1^2(1-\kappa_1^2)/q_1' = A_1, \quad \mu_2^2(1-\kappa_2^2)/q_1' = A_2,$$
$$2\mu_1^2\kappa_1/q_1' = B_1, \quad 2\mu_2^2\kappa^2/q_1' = B_2. \quad (10)$$

We shall be concerned with the dispersion formulas for the nonmagnetized medium. These are obtained by placing $H=0$ in Eqs. (8), which leads to

$$\mu^2(1-\kappa^2)/q_1' = 1+g\lambda^2(\lambda^2-\lambda_1'^2)/[(\lambda^2-\lambda_1'^2)^2+g'^2\lambda^2],$$
$$2\mu^2\kappa/q_1' = gg'\lambda^3/[(\lambda^2-\lambda_1'^2)^2+g'^2\lambda^2], \quad (11)$$

where q_1', λ_1', g and g' are defined by (9) and μ and κ, now physically single valued, refer to the nonmagnetized medium.

Let θ be the angle in radians of the rotation of the plane of polarization produced by a thickness l of the magnetized, doubly refracting, medium. It may be shown[7] that

$$\theta = (\pi l/\lambda)\,(\mu_2-\mu_1). \quad (12)$$

Solving (10) for μ_1 and μ_2 and substituting these values in (12) gives

$$\theta = (\pi l/\lambda)\sqrt{q_1'/2}\left\{\sqrt{A_2+\sqrt{A_2^2+B_2^2}}-\sqrt{A_1+\sqrt{A_1^2+B_1^2}}\right\} \quad (13)$$

This expression is rather cumbersome, so we change it into a more convenient form by availing ourselves of the fact that in most instances $Hh_1\lambda$ is small compared to unity. When the terms containing the square and higher powers of $Hh_1\lambda$ are neglected, (13) becomes

$$\theta = \pi lHh_1\lambda_1'^2\left\{[q_1'g\lambda^2/\mu(1+\kappa^2)]\,[(\lambda^2-\lambda_1'^2)^2-g'^2\lambda^2]/[(\lambda^2-\lambda_1'^2)^2+g'^2\lambda^2]^2\right.$$
$$\left.+[8\mu^3\kappa^3/(1+\kappa^2)q_1']\,[(\lambda^2-\lambda_1'^2)/gg'\lambda^3]\right\}. \quad (14)$$

We may obtain a less expansive value for θ by assuming that the changes in κ occasioned by the magnetic field produce negligibly small changes in θ, or in other words, by assuming that $\kappa=\kappa_1=\kappa_2$. Making use of this assumption as well as of the smallness of $Hh_1\lambda$ the approximate values of μ_1 and μ_2 were obtained from the two Eqs. (10) and were introduced into (12). This gave

$$\theta = [\pi lHh,\; q_1'\; g\lambda^2\lambda_1'^2/\mu(1-\kappa^2)]\,[(\lambda^2-\lambda_1'^2)^2-g'^2\lambda^2]/[(\lambda^2-\lambda_1'^2)^2+g'^2\lambda^2]^2 \quad (15)$$

[7] Drude, loc. cit., p. 396.

Because of the approximations, formulas (14) and (15) are in close accord with the exact formula (13) for wave-lengths sufficiently removed from the critical wave-length λ_1' but are invalid for wave lengths in the region of λ_1'. Furthermore, all the formulas are permissible only when the refractive index and the extinction coefficient of the medium conform to the dispersion equations (11).

For zero absorption (14) and (15) each reduce to

$$\theta = \pi l H h_1 [q_1' g/\mu] [\lambda_1'^2 \lambda^2/(\lambda^2 - \lambda_1'^2)^2], \tag{16}$$

and this in turn is changed by means of (9) to

$$\theta = \pi l H h_1 C_1 \{[\sigma(\mu^2 - 1) + 1]^2/\mu\} \{\lambda_1^4 \lambda^2/(\lambda^2 - \lambda_1^2)^2\}. \tag{17}$$

This is the same as formula (12) of a former paper,[8] and if σ is placed equal to zero, (17) agrees with a formula of Voigt when his quantities are expressed in c.g.s. e.m. units.

In the paper just cited the measured magnetic rotation angles of a number of liquids for wave-lengths of light in the visible region of the spectrum were found to be less than the angles calculated by means of (17) for the shorter wave-lengths. In order to apply the more complete formulas (14) or (15) the extinction coefficients must be known. These have not been measured directly for the substances concerned, but in the cases of carbon disulphide and α-monobromnaphthalene, values of g' are available which were derived from measurements of the ultraviolet reflecting powers[9] of the liquids. With these values of g', formula (15) gave close agreement with the observations throughout the visible spectrum. For illustration, the approximate calculations for carbon disulphide are given in Table I. From refractive index data in the visible spectrum, considering absorption negligible, it is found that $q_1' = 1.7544$, $g = 0.434$, and $\lambda_1' = 228.4\mu\mu$. From ultraviolet reflection data $g' = 0.5136 \times 10^{-5}$.

TABLE I

Wave-length	θ Magnetic Rotation Angles		
	from observation	from (16)	from (15)
$430\mu\mu$	22.1°	23.4°	22.0°
500	15.3	15.6	15.3
640	8.3	8.3	8.3

NATURAL ROTATORY DISPERSION

We postulate an optically active medium in which the temperature remains constant, free from the influence of an external magnetic field.

[8] Astrophysical Journal, 54, 45, 1921.
[9] Astrophysical Journal, 44, 1, 1917.

If the axis of Z be the direction of propagation of the light we find for the equations of motion of the dispersion electrons of a single type in Newtonian notation and c.g.s. e.m. units,

$$\left.\begin{aligned} m\ddot{\xi} &= e[E_x + 4\pi c^2\sigma N e\xi + \gamma\ \mathrm{curl}_x \bar{E}] - f\xi - \beta\dot{\xi}, \\ m\ddot{\eta} &= e[E_y + 4\pi c^2\sigma N e\eta + \gamma\ \mathrm{curl}_y \bar{E}] - f\eta - \beta\dot{\eta}, \\ m\ddot{\zeta} &= e[E_z + 4\pi c^2\sigma N e\zeta + \gamma\ \mathrm{curl}_z \bar{E}] - f\zeta - \beta\dot{\zeta}. \end{aligned}\right\} \tag{18}$$

All the quantities in the expressions except γ have been defined in the preceding section. γ is a constant which depends upon the anisotropy of of the medium and may be positive or negative. The explanation of the formation of these equations is given in the communication referred to in the introduction.[1]

The solution of (18) is carried out in the same way as in the case of equations (1) and is found to yield two vibrations circularly polarized in opposite directions, whose refractive indices μ_1 and μ_2 and extinction coefficients κ_1 and κ_2 are expressed by the relations

$$\frac{1}{\sigma + \dfrac{1 - [2\pi\gamma/\lambda][\mu_1(1 - i\kappa_1)]}{[\mu_1(1 - i\kappa_1)]^2 - 1}} = \frac{C_s}{1/\lambda_s^2 - 1/\lambda^2 + i\, b_s/\lambda}, \tag{19}$$

$$\frac{1}{\sigma + \dfrac{1 + [2\pi\gamma/\lambda][\mu_2(1 - i\kappa_2)]}{[\mu_2(1 - i\kappa_2)]^2 - 1}} = \frac{C_s}{1/\lambda_s^2 - 1/\lambda^2 + i\, b_s/\lambda}, \tag{20}$$

where C_s, b_s, and λ_s have the same meanings as before. Equations (19) and (20) describe the refractive indices and extinction coefficients in terms of the constants of a single type of dispersion electron. Since there may be other types of dispersion electrons in the medium, in the more general case the right hand members of (19) and (20) may be assumed to be summations of similar terms, one term for each type. However, if we deal with a region of the spectrum in which the changes of the refractive index and extinction coefficient with wave-length are determined by the electrons of a single type, denoted by the subscript 1, in the summations just mentioned all the terms except one may be replaced by a quantity q_1 which is independent of λ. Then (19) and (20) become, respectively,

$$\frac{1}{\sigma + \dfrac{1 - [2\pi\gamma/\lambda][\mu_1(1 - i\kappa_1)]}{[\mu_1(1 - i\kappa_1)]^2 - 1}} = q_1 + \frac{C_1}{1/\lambda_1^2 - 1/\lambda^2 + ib_1/\lambda}, \tag{21}$$

$$\frac{1}{\sigma + \dfrac{1 + [2\pi\gamma/\lambda][\mu_2(1 - i\kappa_2)]}{[\mu_2(1 - i\kappa_2)]^2 - 1}} = q_1 + \frac{C_1}{1/\lambda_1^2 - 1/\lambda^2 + i\, b_1/\lambda}. \tag{22}$$

If γ is zero in (21) or (22) we obtain quantities μ_0 and κ_0 defined by the expression

$$\frac{1}{\sigma+\dfrac{1}{[\mu_0(1-i\kappa_0)]^2-1}}=q_1+\frac{C_1}{1/\lambda_1^2-1/\lambda^2+ib_1/\lambda}. \tag{23}$$

Comparing (21), (22), and (23) we find

$$[\mu_0(1-i\kappa_0)]^2=\mu_1(1-i\kappa_1).\mu_2(1-i\kappa_2). \tag{24}$$

The real and imaginary parts of (21) and (22) may be separated, κ_1 and κ_2 may be eliminated, and μ_1 and μ_2 determined in terms of the dispersion constants. These values of μ_1 and μ_2 may be then introduced into equation (12) to determine θ. The expressions are unwieldy and in the present instance we choose to avoid such a straight-forward procedure and to simplify the equations by means of an approximation. We leave out of consideration the difference in transparency of the anistropic medium for the two kinds of circularly polarized light and assume that $\kappa_0=\kappa_1=\kappa_2$. This assumption is not permissible for wave-lengths near the critical region λ_1, but is closely valid for spectral regions removed from this. Eq. (24) then reduces to $\mu_0^2=\mu_1\mu_2$, which shows that μ_0 is the geometrical mean of μ_1 and μ_2. If the refractive index of the optically active medium be determined directly by a refractometer, the value obtained may be interpreted to be almost exactly μ_0. In like manner a measurement of the absorption coefficient by the usual transmission methods gives a number which may be taken to be K_0. The extinction coefficient κ_0 is obtained from this by means of the relation $\kappa_0=\lambda K_0/2\pi\mu_0$.

Introducing (21) and (22) into (12) and making use of the above assumption, we obtain

$$\theta=(2\pi^2\gamma l/\lambda^2)\ \{[\mu_0(1-i\kappa_0)]^2-1\}/(1-i\kappa_0), \tag{25}$$

where θ is now a complex quantity. The real part of θ is given by

$$\theta=(2\pi^2\gamma l/\lambda^2)\ [\mu_0^2(1+\kappa_0^2)-1]/(1+\kappa_0^2). \tag{26}$$

By the same reasoning as before we note that several types of electrons may contribute to the rotation and therefore (26) may be written in the general case,

$$\theta=\Sigma(2\pi^2\gamma l/\lambda^2)\ [\mu_0^2(1+\kappa_0^2)-1]/(1+\kappa_0^2). \tag{27}$$

When κ is zero formula (27) agrees with one obtained by Drude. Again, considering that only a single type of electron is important in determining the variation of θ with λ for the region of the spectrum under investigation, (27) simplifies to

$$\theta=r_1 l+(2\pi^2\gamma_1 l/\lambda^2)\ [\mu_0^2(1+\kappa_0^2)-1]/(1+\kappa_0^2). \tag{28}$$

The quantity r_1 is independent of λ and may be positive or negative.

Because the refractive index μ_0 and the extinction coefficient κ_0 occur explicitly in (28) and the constants of the Lorentz dispersion equation (23) do not occur therein, we may proceed as is often done in theoretical physics. We may discard the scaffolding by means of which the equation (28) has been built up and, without troubling ourselves any more about the theory of electrons we may postulate equation (28) as a concise description of the phenomenon in any medium, no matter whether the refractive index and extinction coefficient of the medium do or do not satisfy the Lorentz dispersion equation. It remains to substantiate this by experiment.

University of Iowa,
Iowa City,
November, 1922

This material must not be reprinted without the permission of The Institute of Radio Engineers

ON SUPER-REGENERATION*

By

E. O. Hulburt

(University of Iowa, Iowa City, Iowa)

The Armstrong super-regenerative circuit consists of the usual regenerative system, obtained by coupling the plate and grid circuits, with the addition of a local variation of relatively low frequency which is impressed either directly or indirectly on the grid. The explanation of the action of this system, set forth clearly by Armstrong,[1] may be given briefly as follows: In the absence of the low frequency variation the circuit would oscillate spontaneously at a radio frequency which is tuned to be either exactly or closely that of the incoming signal. The low frequency variation, however, introduces periodically a negative and a positive resistance into the radio oscillatory circuit and is found either to prevent the radio frequency oscillation entirely or to reduce it to a negligible value. In the presence of a signal the radio oscillation begins when the resistance arrives at a negative value, and during the interval that the resistance is negative builds up rapidly by regenerative action until a relatively great amplitude is attained. It is only prevented from reaching amplitudes sufficient to defeat the action of the circuit by the reversal of sign of the resistance. During the interval that the resistance is positive the radio frequency oscillation is reduced rapidly to zero, and then when the resistance becomes negative once more the amplifying action is repeated.

It has been pointed out by others that the expressions "negative resistance" and "positive resistance" do not perhaps afford a clear idea of the action in the circuit altho their general meaning is unquestionably correct. A more precise description of the action might be obtained by considering that the effect of the low frequency variation is to shift periodically the operating value of the grid potential so that the characteristics of the tube change periodically, at one moment the characteristics being such that the circuit is free to oscillate, corresponding to the negative resistance case, and at another moment being such as to prevent oscillation, corresponding to the positive resistance case.

A simple mathematical analysis brings out some essential

* Received by the Editor, February 21, 1923.

[1] Proceedings of The Institute of Radio Engineers, volume 10, page 244, 1922.

features of the super-regenerative action.

Let f be the frequency of the signal and of the radio frequency renegerative circuit, and let F be the frequency of the low frequency variation. For simplicity we shall assume that the variable resistance drops sharply to a finite negative value and remains there for an interval of time $1/\beta F$, where β is a number greater than 2. This assumption, of course, is not a statement of the actual case, for in reality the resistance both descends to the negative region and ascends therefrom as a continuous function. However, by the introduction of the multiplying factor β, the rather complicated action which really takes place may be represented in the theoretical way just mentioned. We denote by e_1, the grid voltage caused by the signal at the beginning of the time interval $1/\beta F$. Because of regenerative action, the grid voltage will increase rapidly according to an exponential law, which is the usual expression for this type of cumulative action. We may then write

$$e = e_1 \varepsilon^{kft},$$

where e is the value of the grid voltage at the time t and k is the constant of regeneration. k also contains the factor 2π resulting from defining f as a frequency. The average value E_1 of e over the interval $1/\beta F$ is given by

$$E_1 = \beta F \int_0^{\frac{1}{\beta F}} e_1 \varepsilon^{kft}\, dt = e_1 \frac{\beta F}{kf}\left(\varepsilon^{\frac{kf}{\beta F}} - 1\right). \qquad (1)$$

For a second signal which produces a grid voltage e_2, and which differs from the signal corresponding to e_1 only in intensity, the average value E_2 of the amplified grid voltage is such that

$$E_2 = e_2 \frac{\beta F}{kf}\left(\varepsilon^{\frac{kf}{\beta F}} - 1\right).$$

Then

$$\frac{E_1}{E_2} = \frac{e_1}{e_2}.$$

This shows that the amplification produces no distortion. This is in agreement with observation, for it is known that the super-regenerative system amplifies radio telephone signals without distortion.

The influence of the frequency of the resistance variation also appears from equation (1). Suppose that the same signal is amplified by super-regeneration using resistance variation frequencies F' and F'', which give rise to amplified average grid voltages E' and E'', respectively. Then, if other factors are considered constant in the two cases,

$$\frac{E'}{E''} = \frac{F'}{F''} \frac{\varepsilon^{\frac{kf}{\beta F'}} - 1}{\varepsilon^{\frac{kf}{\beta F''}} - 1}.$$

Since $kf/\beta F$ is a quantity much greater than unity, for if it were not the super-regenerative circuit would not amplify, this expression reduces approximately to

$$\frac{E'}{E''} = \frac{F'}{F''} \varepsilon^{\frac{kf}{\beta}\left(\frac{1}{F'} - \frac{1}{F''}\right)}. \qquad (2)$$

In the usual detector action the rectified component of the plate current corresponding to an impressed grid voltage is, to a first approximation, directly proportional to the square of the impressed grid voltage. The intensity of the sound heard in the telephones is directly proportional to the square of the rectified plate current. Therefore, the intensity of the sound is directly proportional to the fourth power of the impressed grid voltage. Denoting the sound intensity by I' and I'' for the two cases under consideration we have from (2)

$$\frac{I'}{I''} = \left\{ \frac{F'}{F''} \varepsilon^{\frac{kf}{\beta}\left(\frac{1}{F'} - \frac{1}{F''}\right)} \right\}^4.$$

From this we may expect the intensity of the signal heard in the telephones to increase very rapidly as the frequency of the resistance variation is decreased. A similar argument may be followed out in the case of the signal frequency, and the conclusion reached that, other things being equal, the intensity of the signal heard in the telephones increases in a marked manner as the signal frequency is increased. These conclusions are in accord with qualitative observation.

In spite of the numerous simplifications and variations of Armstrong's super-regenerative circuits which have been published (see, for example, recent numbers of "QST"), the author ventures to draw attention to the circuits of Figures 1 and 2. These systems were found very useful for a laboratory or class demonstration, being simple to assemble and operate and appearing to retain the amplification and selectivity characteristic of the more elaborate super-regenerative systems. The circuit of Figure 1 was the usual radio frequency regenerative receiver circuit with the addition of the low frequency circuit $L_4\,C_4$. The air condensers C_2, C_3, and C_4 were each variable from 20 to 1,000 $\mu\mu$f. The cylindrical coils L_2 and L_3, 17 cm. (6.7 inches) in diameter, each consisted of 22 turns of wire. L_4 was a honeycomb coil of 1,250 turns and of inductance about 0.1 henry. This arrangement was effective in receiving outside signals. The circuit of Figure 2 was a simple oscillatory circuit with the low frequency circuit $L_3\,C_3$ introduced into the filament connection. C_2 and C_3 were air condensers variable from 20 to 1,000 $\mu\mu$f, and the coils L_1 and L_2 were each of 15 turns of wire on a cylindrical

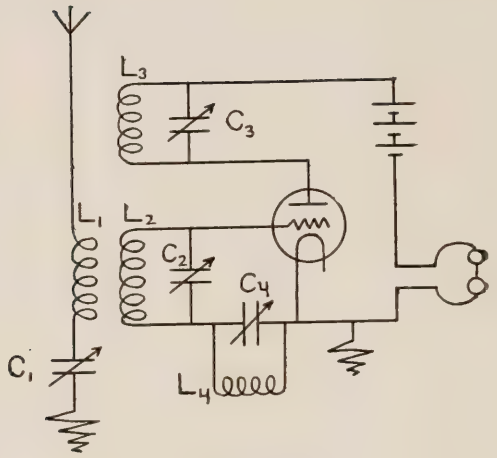

FIGURE 1

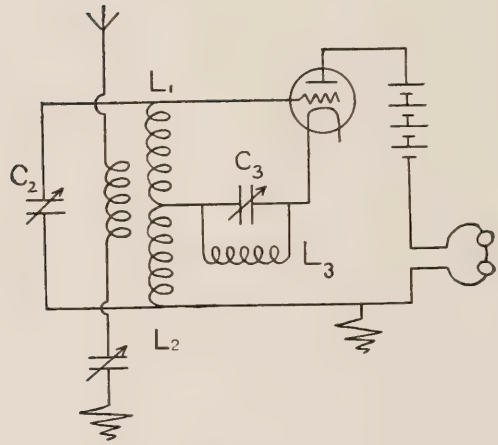

FIGURE 2

form 17 cm. (6.7 inches) in diameter. L_3 was the honeycomb coil of Figure 1. This circuit was interesting rather for its simplicity than for its usefulness as a receiver of signals.

Physical Laboratory,
University of Iowa,
February, 1923

SUMMARY: A simple mathematical analysis of super-regeneration yields conclusions, in accordance with observation, that the super-regenerative system amplifies without distortion and that the amplification increases with increase of signal frequency and with decrease of variation frequency.

Two single tube super-regenerative circuits, interesting because of their simplicity, are described.

STANDARDS OF CAPACITY PARTICULARLY FOR RADIO FREQUENCY CURRENTS*

By

J. B. Dempster and E. O. Hulburt

(Department of Physics, University of Iowa, Iowa City)

An investigation has been made of condensers which may be used for currents of radio frequency (as well as of other frequencies), and the capacity of which may be calculated with precision from the dimensions. In 1906, the late Lord Rayleigh[1] suggested a method of making and using a condenser which would enable all errors due to end and lead-wire capacities to be avoided. The principle was essentially that of the variable condenser of Maxwell[2] and required an adjustable condenser so constructed that altho its total capacity was unknown the increase in capacity was accurately known.

In the present instance, Rayleigh's suggestion has been adopted with some slight modification for measurements with radio frequency currents. A condenser of two coaxial cylinders was made according to the diagram of Figure 1. The two end pieces A consisted of cylindrical cups of brass about 7 cm. (2.76 in.) in length, each with an interior cup of brass held rigidly and accurately centered in the external cup by means of the insulating ring b and post d of hard rubber. The brass collars a and discs c served to keep the cylinders circular in cross section. The ends A fitted on to the section B which consisted of an interior and exterior cylinder of brass. The cylinders were held in place only by the ends A. The mean inner radius of the outer cylinder was 4.9232 cm. (1.93 in.) and the mean outer radius of the inner cylinder was 4.1326 cm. (1.63 in.). Connection was made to the inner cylinder by means of a brass rod e insulated from the outer cylinder. The capacity of the condenser with section B in place was measured in arbitrary units on the scale of a variable air condenser. Section B was then removed, the ends A were fitted together and the capacity of the condenser, which was composed

* Received by the Editor, May 28, 1923.

[1] "Philosophical Magazine," 12, 97, 1906.

[2] "Electricity and Magnetism," section 127.

only of the ends A, was recorded on the variable condenser. The difference in the two readings was exactly the capacity of section B given by the formula.

$$C = \frac{k\,l}{2\,log_{\epsilon}\frac{r_2}{r_1}},$$

where r_2 and r_1 are the radii of the external and internal cylinders, respectively, k is the dielectric constant of the medium, and l is the length of the section. In the present case k was unity, for air was between the condenser plates. Three sections were made to be placed at B, their lengths being 31.560, 15,780, and 7.890 cm. (12.4, 6.2, and 3.1 in.), so that the respective capacities were 100, 50, and 25 micromicrofarads. Any of these, either alone or in combination with the others, could be fitted between the ends A.

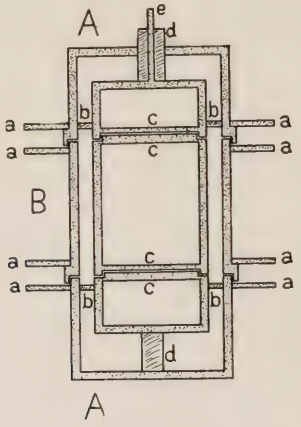

IGURE 1

No standard condensers were at hand with which these could be compared. Measurements of the capacities by means of resonant circuits supplied with undamped radio frequency current showed that the 100 $\mu\mu$f. section was equal to four times the 25 $\mu\mu$f. section and to twice the 50 $\mu\mu$f. section within the error of observation which was less than 0.2 $\mu\mu$f. Currents of frequencies corresponding to wave-lengths of 600 meters and 300 meters gave the same results. This was considered to be a decisive and complete verification that the absolute values of the capacities of the sections were what they were designed to be and that the condensers could be used with confidence with alternating current measurements. A photograph of the standard condenser is shown in Figure 2.

Lord Rayleigh recorded no measurements with this type of condenser. We should perhaps remark that a condenser of the form of that of Figure 1, in which the section B was insulated from the ends A was used by Rosa and Dorsey[3] in their determination of the ratio of the electrical units. Such a condenser, however, was of the guard type due to Lord Kelvin, and, therefore, was quite different from the one used here. It would be unsuited to measurements with alternating currents.

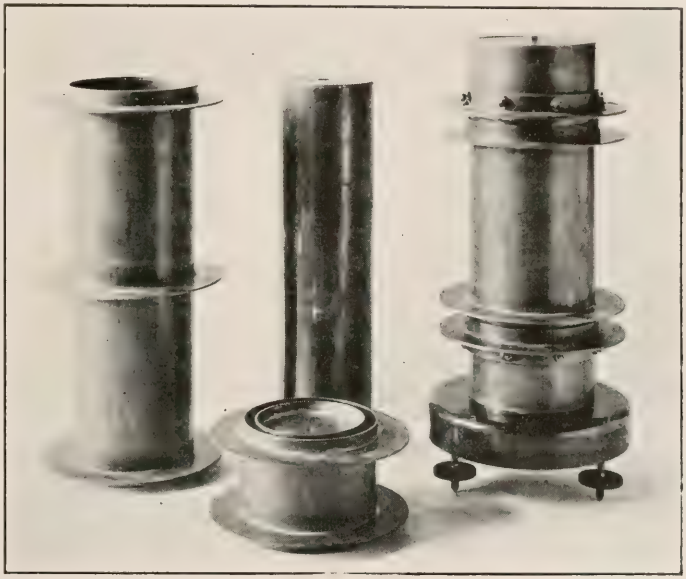

FIGURE 2

A semi-circular plate variable air condenser of forty-three plates was accurately calibrated and was used thereafter as a secondary standard. The dial of this condenser had 100 scale divisions and was turned by a worm-screw which had a head graduated into 100 parts. Measurements showed that each of these parts corresponded to a capacity change of 0.0676 $\mu\mu$f. This condenser was calibrated by means of the circuit of Figure 3. C_1 was the standard condenser of Figure 1, C_2 was the secondary standard, and C_3 was a variable air condenser. Current of frequency about 10^6 was induced in the circuit by coupling L loosely to an electron tube continuous wave generator. The central section B was removed from C_1 so that its capacity was formed

[3] "Bulletin of the Bureau of Standards," 3, 433, 1907.

only by two end sections A, condenser C_2 was set at a specified reading and the circuit was tuned to resonance by C_3. Section B was inserted into C_1, and C_2 was reduced untll resonance again occurred. The difference in the two readings of C_2 was equal to the capacity of section B. In this manner the secondary standard was calibrated step by step thruout its range. The calibration curve obtained in this way gave only the capacity corresponding to the difference in two scale readings. To fix the absolute value of the capacity corresponding to a scale reading a single direct comparison of the primary and secondary standards was carried out by the method of substitution.

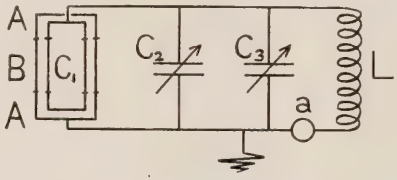

FIGURE 3

The resonance indicating instrument a, Figure 3, consisted of a thermo-couple of resistance 4.5 ohms and a d'Arsonal galvanometer. The galvanometer had a resistance of 121.5 ohms and a sensibility of 6×10^{-8} amperes per millimeter deflection at a scale distance of one meter. A marine type of suspension was used, the period being about one second. This system was quick in action and well adapted to measurements of resonance. Resonance points could be determined with an accuracy of about 0.5 $\mu\mu$f., as may be seen from a typical resonance curve, curve 1, Figure 4. The curve was obtained by plotting the variable capacity in micromicrofarads as abscissas against the current thru the thermo-couple in milliamperes as ordinates. In order to increase the sharpness of the resonance curve, and thereby the accuracy of the capacity measurement, advantage was taken of the fact that the thermo-couple galvanometer system is one in which the deflections are proportional to the square of the current, that is, $i^2=a\,r$ where i is the current, r the deflection, and a a factor of proportionality. The derivative, or sensibility, $d\,i/d\,r=2\,i/a$, and is seen to increase in direct proportion to the current i. Therefore, by increasing the coupling between L and the generating circuit to produce a stronger current, a sharper resonance curve was obtained. When stronger currents were used the galvanometer moved off the scale. To avoid this the

suspending fiber of the galvanometer was twisted slightly to depress the zero point. Curve 2, Figure 4, illustrates the resonance curve in this case, the sharpness of the curve being such as to enable the determination of the resonance point to within 0.2 $\mu\mu$f., or less. Of course there are many methods of determining resonance which are more sensitive than the one just described. These methods are for the most part more difficult of control and do not lend themselves to rapid observations.

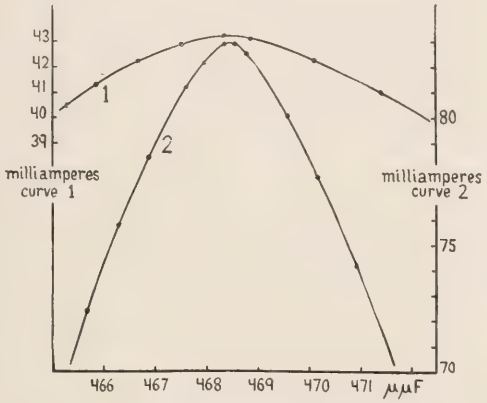

FIGURE 4

It was found that thin metallic discs and small metallic spheres suspended in the air could not in general be used as standards, for their calculated capacities (from the lengths of the radii) and observed capacities were not in agreement, due to unavoidable modification of the electric field caused by the connecting wire. In the case of small spheres the calculated capacities were 4.18, 7.07, and 8.35 $\mu\mu$f. and the measured values were 2.2, 4.2, and 5.0 $\mu\mu$f., respectively, after the observed capacities of the lead-wires had been subtracted. In the case of discs, the calculated capacities were 8.85, 17.7, and 35.4 $\mu\mu$f. When the lead-wire was connected to the centre and normal to the plane of the disc, the observed capacities were 5.7, 13.4, and 32.2 $\mu\mu$f., respectively. If the wire were attached to the edge of the disc the measured capacities became 5.9, 13.6, and 32.8 $\mu\mu$f., respectively.

The capacities of small parallel plate variable condensers were found to be in close agreement with the values calculated from the dimensions and the distance apart of the plates, using the usual formula for the capacity of a parallel plate condenser

with the edge effect correction. Figure 5 shows a photograph of one of these condensers. Thick brass plates were used, circular in shape, and beveled until the edges were thin.

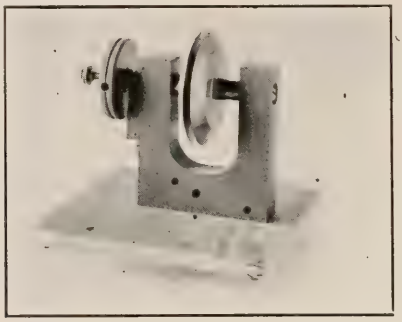

FIGURE 5

We take pleasure in thanking Mr. E. G. Linder for valuable help in making the observations.

Physical Laboratory,
University of Iowa,
May, 1923

SUMMARY: Standards of capacity for use with radio frequency currents, made according to a suggestion of the former Lord Rayleigh, are described. A simple method of increasing the sensitivity of the thermo-couple galvanometer system for indicating resonance is mentioned. Metallic discs and small spheres were found to be erratic standards, because of unavoidable effects of the connecting wires. The measured capacities of small parallel plate condensers were in agreement with the capacities calculated from the dimensions.

A VARIABLE SINGLE BAND ACOUSTIC WAVE FILTER

BY

G. W. STEWART

Reprinted from PHYSICAL REVIEW, pp. 502–505, No. 5, November, 1923

A VARIABLE SINGLE BAND ACOUSTIC WAVE FILTER

By G. W. Stewart

Abstract

Single band acoustic filter; simple method of varying the width of the transmitted band.—An extension of the earlier theory indicates that if the size of the orifice leading into the side tube is altered, the upper limiting frequency should change while the lower limiting frequency remains constant, thus changing the width of the band. The orifice is readily changed by introducing a cylinder of paper with punched holes of the proper size and position. Experimental results confirm the prediction as to the lower limit and give for three different orifices upper limiting frequencies of 455, 390 and 340 per sec., in fair agreement with the corresponding theoretical values 510, 440 and 385, respectively.

THE acoustic wave filter to be described is presented to illustrate the possibility of varying the width of the transmission band with but a slight alteration in the filter itself. It is not to be regarded as highly developed in form, for as yet little effort in that direction has been made.

Theory

For the sake of brevity reference will be made to a former paper[1] on the general theory, for equations and for the meaning of *impedance*, *inertance* and *capacitance*. The filter and its transmission curve are shown in Fig. 1 which is the same as Fig. 8 of that paper. The filter is drawn to scale, the length over all being 10 cm. In the previous article it was found that formula K gave the best agreement with experimental values. We will therefore make the assumptions involved in K', viz., that the orifice into the surrounding chamber has the inertance M_2', the conduit between two adjacent branches the inertance M_1, the chamber the capacitance C_2 and the branch tube leading to the outside, the inertance M_2. In addition, however, we will use a variable orifice at the opening from the conduit to the side tube and note the resulting change made in the transmission curve. The inertance of this orifice will be designated by M_2''.

According to Eq. (27)[1] the impedance of the side branch with the orifice represented by M_2'' omitted, is

$$(Z_2)_A = i\frac{M_2\omega(M_2C_2\omega^2-1)}{M_2C_2\omega^2+M_2'C_2\omega^2-1} \qquad (1)$$

[1] Stewart, Phys. Rev. **20**, 528, 1922

If we now introduce the orifice M_2'' in series, we have, since its impedance is $i\omega M_2''$,

$$(Z_2)_B = i\ M_2''\ \omega + i\frac{M_2\omega(M_2'C_2\omega^2-1)}{M_2C_2\omega^2+M_2'C_2\omega^2-1}$$

$$= i\frac{M_2''\omega(M_2C_2\omega^2+M_2'C_2\omega^2-1)+M_2\omega(M_2'C_2\omega^2-1)}{M_2C_2\ \omega^2+M_2'C_2\omega^2-1} \qquad (2)$$

If the conduit has an inertance between the branch openings of M_1, its impedance Z_1 is $iM_1\ \omega$. The limiting frequencies of no attenuation can

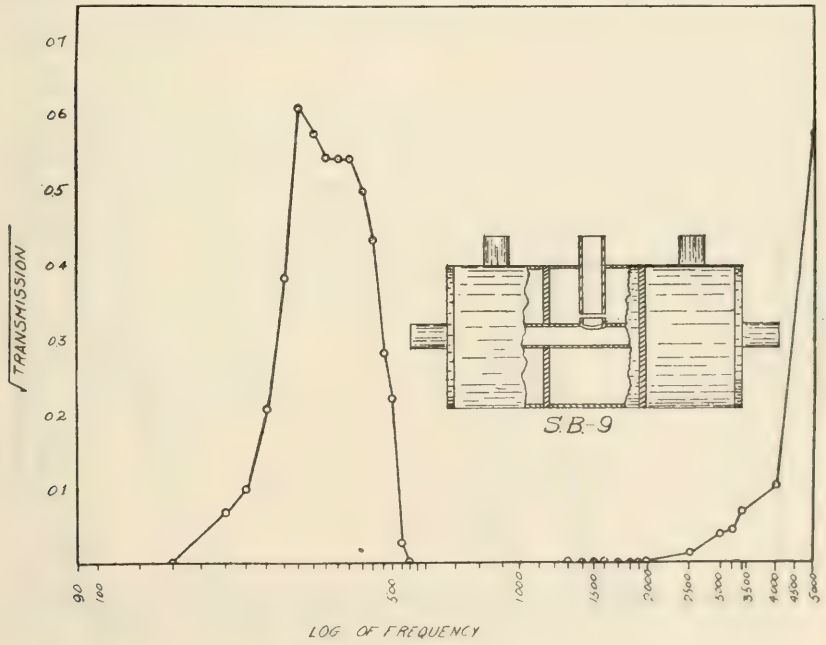

Fig. 1

now be ascertained by using $Z_1/Z_2=0$ and $Z_1/Z_2=-4$. If this is done, we find for the frequency $\omega/2\pi$ the following values:

$$f_1 = \frac{1}{2\pi}\sqrt{\frac{1}{C_2(M_2+M_2')}} \qquad (3)$$

and

$$f_2 = \frac{1}{2\pi}\sqrt{\frac{M_1+4\ (M_2+M_2'')}{C_2[4M_2(M_2'+M_2'')+M_2'(M_1+4M_2'')\ M_1M_2]}} \qquad (4)$$

Eqs. (3) and (4) show the interesting fact that the lower limiting frequency f_1 is independent of M_2'', whereas the upper limiting frequency f_2 is dependent upon M_2''. Thus, if the theory be substantially correct, the width of the band may be changed by altering the size of the orifice

represented by M_2''. In applying (3) and (4) the following measurements of the filter are substituted:

$M_1 = \rho l_1/S_1$, $M_2 = \rho l_2/S_2$, $M_2' = \rho/c'$, $M_2'' = \rho/c''$ and $C_2 = V_2/\rho a^2$.

In these, l and S refer to the length and area respectively, the subscripts having the same significance as already adopted; ρ is the density of the fluid, a is the velocity of sound, c' is the conductivity of the orifice into the volume M_2 computed approximately as an elliptical channel, and c'' is the conductivity of the circular orifice into M_2, numerically equal to twice the radius. The value of M_2' was $\rho/.455$.

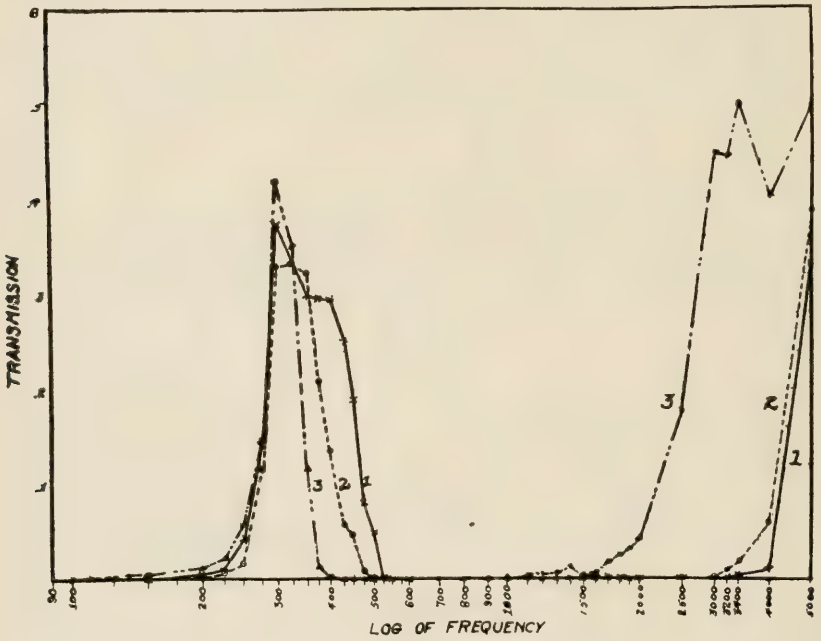

Fig. 2

Experiment

In order to introduce and to modify the orifice, a tightly fitting roll of heavy writing paper with holes of selected sizes was introduced into the conduit, the holes being centered in the branch tubes.

The transmission curves are shown in Fig. 2. Curve 1 is with the orifice 0.486 cm in diameter, the curve being the same as in Fig. 1. This orifice is really the end of the tube M_2, and is considered as part of it. Hence it does not give any value to M_2'' and $M_2'' = 0$. Curves 2 and 3 are for orifices with diameters of 0.3 cm and of 0.1 cm, respectively. As is clearly shown, the lower limiting frequency, taken as the

frequency for one-half of the maximum transmission, remains unchanged, as indicated by the theory. For the upper limiting frequency, we have the following experimental and corresponding theoretical values. The latter were obtained by Eq. (4) and are placed in parentheses. Curve 1, 455 (510); curve 2, 390 (440); and curve 3, 350 (385).

Discussion

The agreement between experiment and theory is satisfactory since it covers both points, viz., the constancy of the lower limiting frequency and the decrease of the upper limiting frequency with decrease in the size of the orifice.

The fact that the transmission increases appreciably at 3,200 per sec. in curve 1, and at lower frequencies in curves 2 and 3, is not anticipated in the present theory, which gives attenuation for all frequencies higher than those of the band. The extension of the theory which explains this increase of transmission has been made and will be presented in a later paper. As will be shown in later contributions, there are at least two ways in which this transmission at higher frequencies may be practically eliminated.

Physical Laboratory,
University of Iowa
March 17 1923

Reprinted from the JOURNAL OF THE OPTICAL SOCIETY OF AMERICA AND REVIEW OF SCIENTIFIC INSTRUMENTS
Vol. VII, No. 12, December, 1923

THE EFFECT OF THE MATERIAL COMPOSING THE SIDES OF DEEP SLITS ON THE INTRINSIC INTENSITY OF LIGHT TRANSMITTED THROUGH THE SLITS

BY CLARENCE R. SMITH

INTRODUCTION

The phenomena occurring when light is passed through a narrow, deep slit appear to be very interesting and more complicated than one might at first suppose. There is not only strong polarization but also marked absorption. Moreover this absorption bears an interesting relationship to the wave length of the light, the depth of the slit, the width of the slit and also the material of which the walls of the slit are composed.

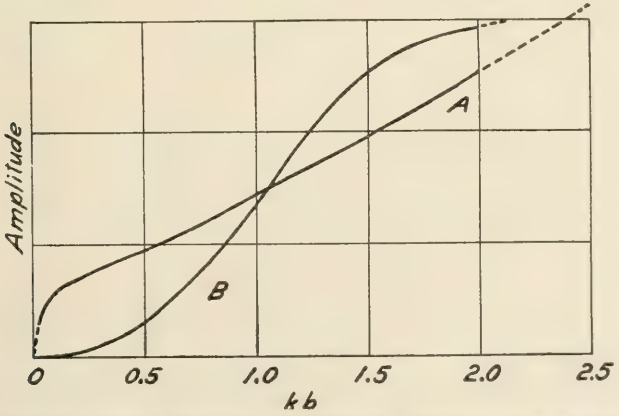

FIG. 1. *Rayleigh's curves showing the amplitude as a function of a number proportional to the width of the slit. A—electric vector perpendicular to direction of slit. B—electric vector parallel to direction of slit.* $k=2\pi/\lambda$. $b=\frac{1}{2}$ *width of slit.*

Lord Rayleigh[1] has treated theoretically the polarization of light by a narrow slit though he assumed the slit to be in an infinitely thin

[1] Lord Rayleigh. Roy. Soc. Lond. Proc. A, *89*, p. 194; 1913–14.

screen. Nevertheless his curves (Fig. 1) show a close resemblance in general shape to the experimental curves obtained by Sieg and Fant[2] (Fig. 2) with "deep" slits, and also to the curves shown in this paper.

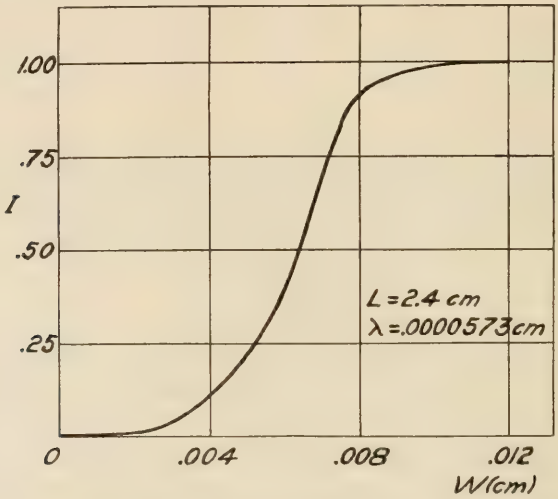

FIG. 2. *One of Sieg and Fant's curves showing the intensity as a function of the width of slit.*

Stewart[3] in some experiments performed in another connection noticed that "a narrow slit, in a thick screen, can . . . by being made sufficiently narrow, extinguish all transmitted light, though the slit still have a width of 5 to 8 wave lengths." Sieg and Fant[4] investigated the intensity of light transmitted by a deep slit as a function of the width and depth of the slit. It was their work which suggested the problem of this present paper which is to consider the effect of the variation of the material constituting the walls of the slit.

DESCRIPTION OF APPARATUS

The arrangement of the various parts of the apparatus is shown diagrammatically in Fig. 3. The general arrangement and principles of operation are similar to those of Sieg and Fant[5] except in regard to several details, the more prominent of which will subsequently be pointed out.

From the slit S_1, of a monochromatic illuminator, light was received by the lens L_1 and sent forward in a parallel beam. The lower portion

[2] L. P. Sieg and A. T. Fant. J. Op. Soc. Am., *5*, p. 218; 1921.
[3] G. W. Stewart. Abstract. Phys. Rev. *5*, p. 73; 1915.
[4] Sieg and Fant. loc. cit.
[5] Sieg and Fant. loc. cit.

of this beam was interrupted by mirror M_1 and projected over to mirror M_2 while the upper portion passed on to the slit S_2. The horizontal position of the edge of the mirror was considered to be better than the vertical position used by Sieg and Fant not only because of greater ease in adjustment but also in offering less opportunity for slight differences in wave length between the two divided portions of the light beam.

The light passing over the upper edge of M_1 reached S_2 which was the slit under investigation. Between S_2 and P only one lens was used instead of two as in Sieg and Fant's arrangement, and the light

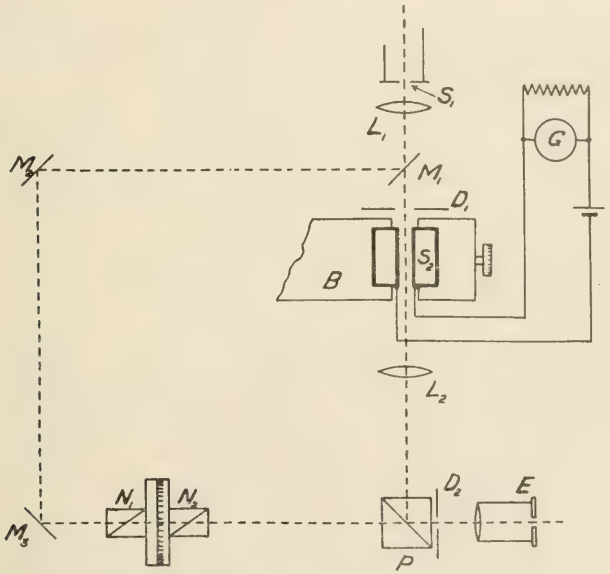

FIG. 3. *Diagram of Apparatus.*

instead of being sharply focused upon the silver strips in P, was slightly diffused into a spot of appreciable size. This was thought to be of advantage since the eye is more reliable in matching areas of larger size and lower intensity than areas of smaller size and higher intensity.

The cube P was made of two right-angled glass prisms with silver strips cemented between. The use of the diaphragms D_1 and D_2, and also the mirrors M_2 and M_3 will be readily understood from the diagram. One of the blocks used to form the slit was rigidly attached to the bed of a Michelson interferometer B; the other was set in wax on the movable carriage of the interferometer. The galvanometer G was used to register contact between the blocks, or zero width of the slit.

By rotating the nicol N_2 with reference to the stationary nicol N_1, the intensities of the two images in P could be made to match when viewed by means of the eyepiece E.

For the measurements made with steel, the slit was formed by two of the plane surfaces of two similar blocks which had been made by cutting in two a Hoke Precision Gauge. Thus the original surface of the gauge was used. For the other metals employed, the surfaces were especially prepared by the method described below. The depth of the slit in every case was 2.31 cm.

EXPERIMENTAL

The preparation of the various metallic surfaces composing the walls of the slits under investigation comprised a prominent feature of the work and will be described specifically.

First two blocks of steel about $10\times75\times75$ mm were ground together with successively finer grades of emery and finally with rouge until the surfaces gave interference bands which were fairly straight. Finally the surfaces were carefully inspected and from the best areas were cut smaller blocks each having a part of the original surface measuring about 7×23 mm.

Four pairs of these small blocks were selected and the flat surfaces of each pair then plated electrolytically with one of the four metals, nickel, copper, silver and gold. In each case it was found that the flatness of the new surface was fairly well preserved after this deposit. A slight amount of polishing was done upon these new surfaces with French chalk on a piece of chamois skin. It was found, however, that this sort of polishing tended to wear away the surface faster near the edges and thus destroy the flatness, hence it had to be discontinued before a very highly reflecting surface was obtained. The nickel came from the plating bath with the brightest surface of any of the four metals tried while the silver had the dull appearance which is characteristic of electrolytic silver. Enough polishing was done upon the silver surface to render what might be termed a bright appearance though not a brilliant mirror. When in the condition finally used all the surfaces were flat to within about 0.0001 cm.

With a given pair of surfaces set face to face, the slit was adjusted for a wide opening and then the light transmitted was matched in P with that coming by way of the path through the nicols when N_2 was set for a certain position chosen as a maximum. This was accomplished by means of a neutral tint photographic wedge placed before S_2.

The actual maximum position of 90° for N_2 was not used but rather an angle of about 60° as observations were more easily made near this angle.

Starting with the slit at zero opening it was gradually widened at intervals of 0.001 cm. Three independent adjustments of N_2 were made for each value of W thus chosen. These were recorded as 1st, 2nd, and 3rd trial as illustrated in Table 1.

The intensity I for any position is given by

$$I = k \sin^2\theta \tag{1}$$

where θ is the angle through which N_2 has been rotated from the dark position and k is a constant so chosen that for the width at which the intensity became constant, I was unity.

In the table one typical series of observations is given as a sample. In Figures 5, 6 and 7 are compared the results of the five metals used for each wave length λ. The depth of slit L was 2.31 cm in every case. Throughout the work it is intrinsic intensities which are obtained and not total transmitted light.

CONCLUSIONS

Sieg and Fant[6] have given a theoretical discussion of the relationship between the intensity of light transmitted by a slit and the width and depth of the slit. For the diffracted light within any angle θ, they give the following expression for the resultant intensity of light passing through a slit of given depth, assuming unit intensity for a slit which is infinitely thin:

$$I = \frac{1}{0.45\pi \cdot m} \cdot \frac{\pi}{2} \left[\sum_{i=o}^{i=m} \frac{\sin^2\alpha_i}{\alpha_i^2} R_s^{\,i} + \sum_{i=o}^{i=m} \frac{\sin^2\alpha_i}{\alpha_i^2} R_p^{\,i} \right] \tag{2}$$

In this expression α is an auxiliary angle defined by the relation

$$\alpha = \frac{\pi w}{\lambda} \sin\theta$$

where w is the width of the slit and λ the wave length of the light. In (2) α_i represents the value of α for i reflections, and m the number of reflections when $\alpha = \pi$. R_s and R_p represent the reflection constants for the electric vector parallel and perpendicular respectively to the plane of incidence. R_s and R_p are assumed in the above expression to be constant, though as pointed out by the authors themselves, the R's are in reality not constant but are complicated functions of the angle α. A more rigorous expression than (2) might be formulated as a definite integral but its evaluation would be well-nigh impossible owing to the complicated relations between the R's and α.

[6] Sieg and Fant. loc. cit., p. 221.

TABLE 1. *One Series of Observations Shown as a Sample*

$L = 2.31$ cm $\lambda = .0000650$ cm Material = copper

W cm	Scale readings for θ				θ deg.	$\sin^2\theta$	$I = k \sin^2\theta$
	1st trial	2nd trial	3rd trial	Av.			
.00000	329.9	332.0	331.8	331.2	0.0	.000	.000
.00100	327.4	328.3	327.7	327.8	3.4	.004	.006
.00200	326.0	325.9	326.6	326.2	5.0	.008	.013
.00300	324.8	324.8	325.0	324.9	6.3	.012	.019
.00400	321.1	321.0	321.7	321.3	9.9	.030	.048
.00500	318.7	319.1	320.9	319.6	11.6	.040	.064
.00600	313.7	311.9	312.4	312.7	18.5	.101	.163
.00700	313.8	312.9	312.7	313.1	18.1	.097	.156
.00800	314.4	313.8	314.0	314.1	17.1	.086	.138
.00900	305.3	306.8	304.8	305.6	25.6	.187	.301
.01000	300.7	301.8	302.3	301.6	29.6	.244	.391
.01100	297.5	300.9	297.5	298.6	32.6	.290	.467
.01200	301.6	300.7	301.0	301.1	30.1	.252	.405
.01300	305.7	301.2	300.9	302.6	28.6	.229	.369
.01400	300.8	300.4	303.0	301.4	29.8	.247	.398
.01500	299.8	300.3	299.6	299.9	31.3	.270	.435
.01600	299.6	301.8	301.2	300.9	30.3	.255	.410
.01700	294.9	298.4	297.3	296.9	34.3	.318	.512
.01800	297.0	299.4	299.0	298.4	32.8	.294	.474
.01900	295.2	295.7	299.0	296.6	34.6	.322	.518
.02000	294.6	297.9	296.4	296.3	34.9	.327	.526
.02100	294.6	294.9	296.3	295.3	35.9	.344	.554
.02200	292.6	290.6	289.5	290.9	40.3	.418	.674
.02300	292.6	293.5	290.6	292.2	39.0	.396	.638
.02400	289.3	289.2	289.5	289.3	41.9	.446	.718
.02500	291.0	288.5	287.9	289.1	42.1	.450	.725
.02600	286.9	289.0	287.9	287.9	43.3	.470	.757
.02700	285.5	285.5	285.9	285.6	45.6	.511	.823
.02800	285.0	283.8	285.0	284.6	46.6	.528	.850
.02900	284.0	282.3	286.5	284.3	46.9	.533	.858
.03000	283.9	285.6	282.5	284.0	47.2	.538	.867
.03100	283.0	283.9	284.3	283.7	47.5	.544	875
.03200	285.8	277.5	279.2	280.8	50.4	.594	.956
.03300	283.5	284.1	280.3	282.6	48.6	.563	.907
.03400	280.0	283.4	284.6	282.7	48.5	.561	.903
.03500	279.9	281.2	279.0	280.0	51.2	.607	.977
.03600	278.3	285.7	283.0	282.3	48.9	.568	.915
.03700	277.5	278.0	283.0	279.5	51.7	.616	.992
.03800	277.9	280.8	281.0	279.9	51.3	.609	.981
.03900	283.3	278.0	276.4	279.2	52.0	.621	1.000

That the reflection constants play a prominent part in such an expression as the above is evidenced experimentally by the results of the present work, in which for the same values of λ, L and W,

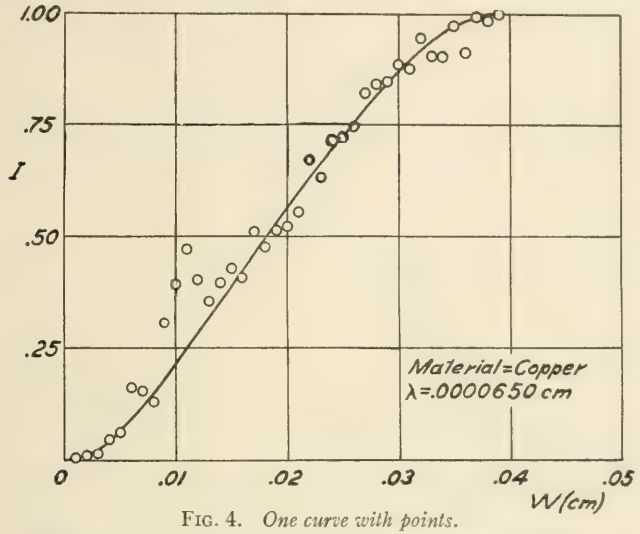

FIG. 4. *One curve with points.*

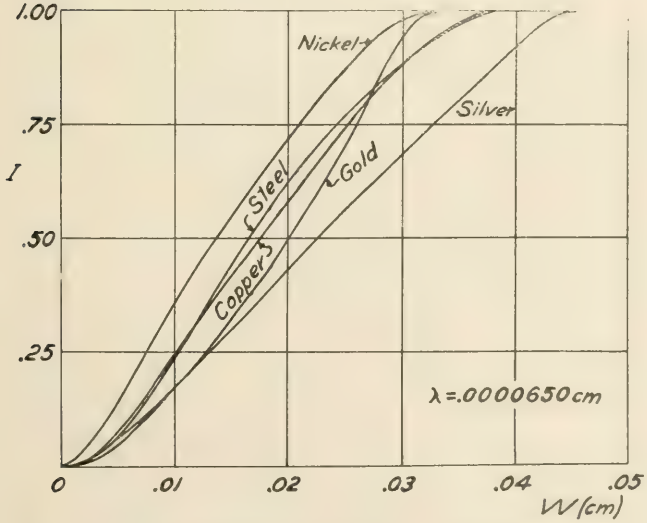

FIG. 5. *Comparison of results for* $\lambda = .0000650$ *cm.*

different materials were used to make up the walls of the slit. The results obtained are somewhat irregular but a comparison of the curves shows at once that differences in intensity of the light transmitted by a deep slit, are produced by changing the material though the other conditions mentioned above are kept constant.

It will be noticed that the curves for the various metals agree fairly well for small and for large openings of the slit while the greatest differences occur in an intermediate region. For large openings a

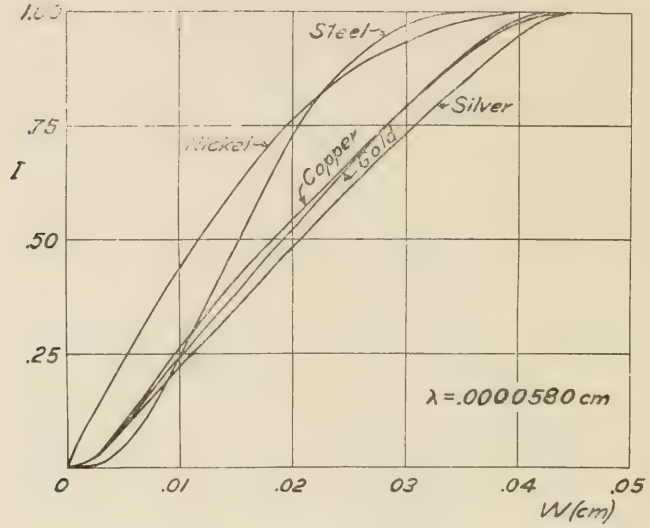

FIG. 6. *Comparison of results for* $\lambda = .0000580$ *cm.*

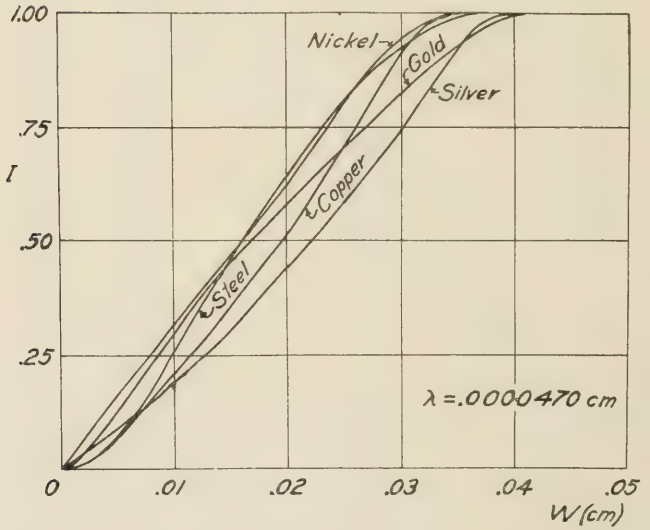

FIG. 7. *Comparison of results for* $\lambda = .0000470$ *cm.*

greater portion of the light is directly transmitted and not subject to reflection at the walls of the slit, hence would not be influenced by the material and we should expect the curves to be similar. This

situation is represented in Fig. 8 (a) where *o* is any point on the incident wave front *ab*. However as the opening is made less, the light which is directly transmitted becomes less in proportion to that which is diffracted and reflected as shown in Fig. 8 (b). Here the material composing the sides of the slit will play a more prominent part and greater differences in the curves would be expected. As the slit becomes still narrower a relatively greater portion of the transmitted light will have been subject, not merely to one or a few reflections, but many reflections from side to side before emergence. Since absorption

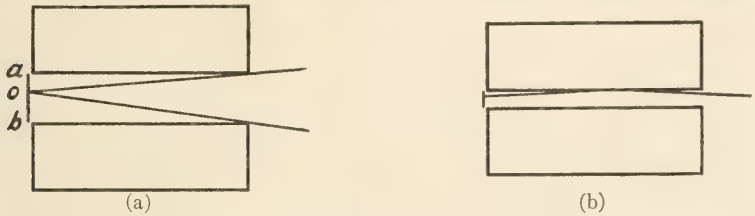

FIG. 8. *Illustrating effect of width of slit.*

occurs at each reflection, the intensity of the light will gradually approach zero for zero width of the slit. Hence the curves approach each other near the zero point.

The probable error was calculated for several values of I chosen at equal intervals from a typical series of data. The results obtained showed the probable error to average about 5%. The chief source of error throughout the work is in the inability of the eye to match accurately the light areas. Compared with this, other sources of error involved are considered to be insignificant.

In the present work no account has been taken of the condition of the light with respect to polarization. The light incident upon the slit under investigation was doubtless slightly polarized by the slits of the monochromatic illuminator. Further work should be done to determine the effect of using completely polarized incident light and varying the direction of the electric vector from parallel to perpendicular with respect to the plane of incidence.

The writer wishes in conclusion to acknowledge his indebtedness to the staff of the Physics Laboratory of the University of Iowa and especially to Prof. L. P. Sieg, who suggested the problem, and whose advice and continued interest were of invaluable aid throughout the work.

UNIVERSITY OF IOWA,
IOWA CITY, IOWA,
JULY, 1923.

ACOUSTIC WAVE FILTERS: ATTENUATION AND PHASE FACTORS

BY

G. W. STEWART

Reprinted from PHYSICAL REVIEW, pp. 520-524, No. 4, April, 1924

ACOUSTIC WAVE FILTERS: ATTENUATION AND PHASE FACTORS

By G. W. Stewart

Abstract

Acoustic wave filters; attenuation and phase factors.—*Theoretical discussion.* The ratio of the rate of volume displacements in successive sections e^{Y} is equal to $e^{-\alpha}\, e^{-i\varphi}$ where α is the attenuation constant and φ the decrease in phase from section to section. If Z_1 and Z_2 are the impedances in the conduit and branch respectively, it is shown that in the region of no attenuation, $\cos \varphi = 1 + \frac{1}{2} Z_1/Z_2$ and φ changes from 0 to π, while in the attenuated region φ is either 0 or π and $\cosh \alpha = |(1 + \frac{1}{2} Z_1/Z_2)|$, becoming infinite for the natural frequency of the side branch while φ passes discontinuously from 0 to π or π to 0. *Experimental values of phase change* φ. Sound from various points along the filter was transmitted to one ear and the relative phase was determined from the apparent direction of the phantom source. For a low-pass filter the values of the total change per section agree well with the theory except that the change occurs gradually instead of suddenly, but agreement was not found in the cases of the other two types.

I. Theoretical

IN a recent discussion of acoustic wave filters[1] the theory and experimental results as to frequency limits of transmission without attenuation were presented. The present article is a continuation of the theory, with acknowledgement of the suggestions received from discussions of electric wave filters by Campbell,[2] Pierce[3] and Zobel.[4] The acoustic filters discussed in the previous article[1] were shown diagrammatically in Fig. 2. If Z_1 and Z_2 refer to acoustic impedances, I_n to the rate of volume displacement in the n^{th} section, and $AGEG$ to the conduit through which transmission is desired, it was shown that

$$I_{n+1}/I_n = e^{Y} \tag{1}$$

where

$$\cosh\ Y = 1 + \tfrac{1}{2}\, Z_1/Z_2. \tag{2}$$

If

$$e^{Y} = e^{-\alpha}\, e^{-i\varphi} \tag{3}$$

α is the attenuation constant and φ is the decrease in phase from section to section.

For the practical filters previously discussed[1] the different approximate assumptions made led to different expressions for Z_1 and Z_2 but in all

[1] G. W. Stewart, Phys. Rev. **20**, 528, December, 1922
[2] Campbell, U. S. Patent 1, 227, 113.
[3] Pierce, Chap. XVI, Electrical Oscillations and Electric Waves, 1920
[4] Zobel, Bell Sys. Tech. J. **2**, 1, Jan., 1923

cases the ratio between them was real and therefore cosh Γ was real. Hence (cosh $\alpha \cos\varphi + i \sinh \alpha \sin\varphi$) is real, and

$$\sinh \alpha \sin \varphi = 0. \tag{4}$$

Therefore cosh $\Gamma = \cosh \alpha \cos \varphi$. Then when $\alpha = 0$, or *in the region of no attenuation*,

$$\cosh \Gamma = \cos \varphi = 1 + \tfrac{1}{2} Z_1/Z_2. \tag{5}$$

But the former discussion[1] shows that the limits between which $\alpha = 0$, are determined from the relationships, $Z_1/Z_2 = 0$ and $Z_1/Z_2 = -4$. These two ratios, when substituted in (5) give respectively, $\cos \varphi = 1$ and $\cos \varphi = -1$.

It is clear from these that φ changes from zero to π when the frequency is varied from one limit of no attenuation to the other. Since functions of Z_1 and Z_2 employed in our theory are continuous, φ must vary continuously between these frequency limits. *In the attenuated region*, since α is not zero, Eq. (4) shows that $\sin \varphi = 0$, and $\varphi = 0$ or π. These two possible values of φ are the same as those just found at the limits of no attenuation, as they must be for φ is single valued.

Since,

$$\cosh \alpha \cos \varphi = \cosh \Gamma = 1 + \tfrac{1}{2} Z_1 Z_2, \tag{6}$$

we have throughout the attenuated region, the positive quantity

$$\cosh \alpha = (1 + \tfrac{1}{2} Z_1/Z_2)/(\pm 1) > 0 \tag{7}$$

The sign of the sum in the parenthesis (7) is therefore determined by that of $\cos \varphi$. Consequently if it changes sign, $\cos \varphi$ must also, and this means an alteration by π.

The above discussion is identical with the reasoning in the case of electric filters and shows that φ can be obtained from (5) in the unattenuated region and from (6) in the attenuated region, and that in the latter region, α is given by (7).

In discussing the three types of filters previously considered,[1] the same semi-empirical values of Z_1 and Z_2 are adopted. These give for the low-pass, high-pass and single-band filters respectively, the following values of the quantity in Eq. (6):

$$1 + \frac{\tfrac{1}{2} M_1 C_2 \omega^2}{M_2 C_2 \omega^2 - 1};\quad 1 + \frac{\tfrac{1}{2} M_1}{M_2 (1 - M_1 C_1 \omega^2)};\quad 1 + \frac{M_1 (M_2 C_2 \omega^2 + M_2' C_2 \omega^2 - 1)}{2 M_2 (M_2' C_2 \omega^2 - 1)}.$$

If Eqs (5), (6) and (7) are utilized, substituting the values just cited for the right hand member, one can readily ascertain the following:

1. In the region of no attenuation, φ changes with increasing frequency from 0 to π (low-pass), π to 0 (high-pass), 0 to π (single-band-pass); and for all cosh $\alpha = 1$.

2. With each filter there is in an attenuation region an infinite value of α for a frequency at which φ passes discontinuously, with frequency increasing, from π to 0 (low-pass), 0 to π (high-pass), and π to 0 (single-band-pass). In the last named filter, $\alpha = \infty$ occurs in the upper of the two regions of attenuation.

3. The value of cosh α at zero frequency is $(1+M_1/2M_2)$ for the high-pass and single-band-pass filters. The low-pass has this value at infinite frequency.

4. In the cases of the low-pass and the single-band-pass filters, at the frequency for which $\alpha = \infty$, each filter reduces to the well-known case in acoustics wherein, if the frequency is that causing resonance in the side branch, the transmission through the conduit past the branch is zero.

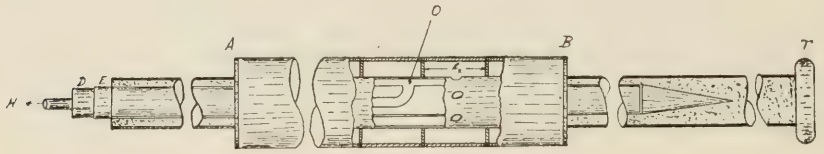

Fig. 1. Low-frequency-pass filter.

II. Experimental

Values of α. A comparison of theoretical and experimental values of α has been made by H. B. Peacock and is published in an accompanying article.

Values of φ. The accompanying diagram shows the low-frequency-pass filter AB and the apparatus for measuring the change in φ. The sound from the telephone T passes through a tube partially filled with hair felt which is continuous with the inner tube of the filter AB. The sound, after leaving the filter, continues to pass through a similar tube containing hair felt and finally either into the atmosphere or, by reflection from the opening, back into the tube. The quantity and distribution of the hair felt were such as to prevent noticeable resonance. The distance from B to T is 100 cm and from A to E is 46 cm. The filter AB is similar in principle to those already described[1] and is, in fact an extension of H13 from 5 sections to 10 sections. The inner case was made of two telescoping tubes, the outer one containing a slot and the inner one a tube with the opening in the slot. By sliding the inner tube D back and forth, the opening of the hearing tube at O could be moved without modifying the phase conditions in the tube other than through the influence of the opening. The sound transmitted into this "feeler" tube was led to one ear of the observer. The current passing through the telephone T passed

also through another telephone T', not shown. T'' was shunted by a resistance which remained constant throughout a trial. A tube was presented to the telephone T' and the sound from it was transmitted to the other ear of the observer. The opening of the tube could be moved a small distance nearer to or further from T', thus altering intensity values without an appreciable change in phase. The relative phases in the two tubes were compared by the binaural difference of phase effects.[5] In this effect, at a phase difference zero the phantom source of sound passes

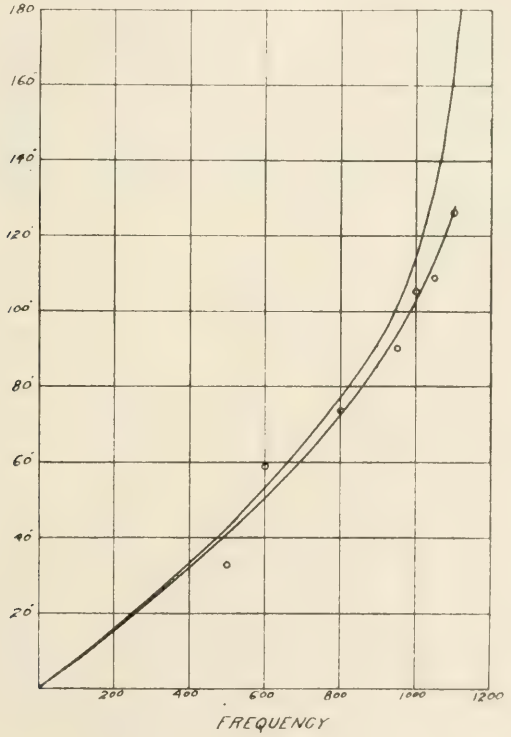

Fig. 2

across directly in front, and at a difference of π it passes quickly from one side to the other. By observing the position of the tube D at these two phase differences, care being taken to keep the intensities approximately constant, the change of phase along the filter could be ascertained. Since each section was 4 cm in length, the results are expressed in Fig. 2 as the change in φ per section, as a function of the frequency. The upper full line curve represents the values computed from (5). The agreement of

[5] The effect is described fully by Stewart, Phys. Rev. **15**, 432, 1920

theory and experiment is satisfactory, excepting in one respect. The theory asserts that φ changes discontinuously at the junction. In point of fact there is strictly no junction "point" and experimentally φ does not change discontinuously. The agreement, even with this exception, is remarkable. In fact, the nature of the assumptions made in the derivation of the theory does not permit one to anticipate that our somewhat empirical expressions for Z_1 and Z_2 would lead to correct theoretical values of φ.

A high-frequency-pass and a single-band filter were constructed and the same exploring tube as shown in Fig. 1 was used in them. The observations, however, failed to disclose any such variation in φ as that determined by (5). At the present time there is offered no explanation for this failure other than the semi-empirical nature of the formulas. A careful investigation as to the actual change in φ will need to be made.

PHYSICAL LABORATORY,
UNIVERSITY OF IOWA,
August 25, 1923.

Reprinted from PHYSICAL REVIEW, pp. 525-527, No. 4, April, 1924

PREDICTED TRANSMISSION CURVES OF ACOUSTIC WAVE FILTERS

BY H. B. PEACOCK

ABSTRACT

Transmission curves for three acoustic wave filters.—Using the experimental procedure of G. W. Stewart, the energy transmitted as a function of the frequency was determined for a low-frequency-pass, a high-frequency-pass, and a single-band-pass filter. Corrected for dissipation, the results agree well with theoretical curves computed from Stewart's equation for a filter of n sections $I_n/I_0=e^{-n\alpha}$, where α, the attenuation factor, is computed from the impedances.

ACCORDING to the theory developed in the preceding paper by G. W. Stewart to account for the action of certain acoustic wave filters, it should be possible to predict transmission curves from computation. It is the purpose of this investigation to test this theory by comparing the theoretical and experimental transmission curves.

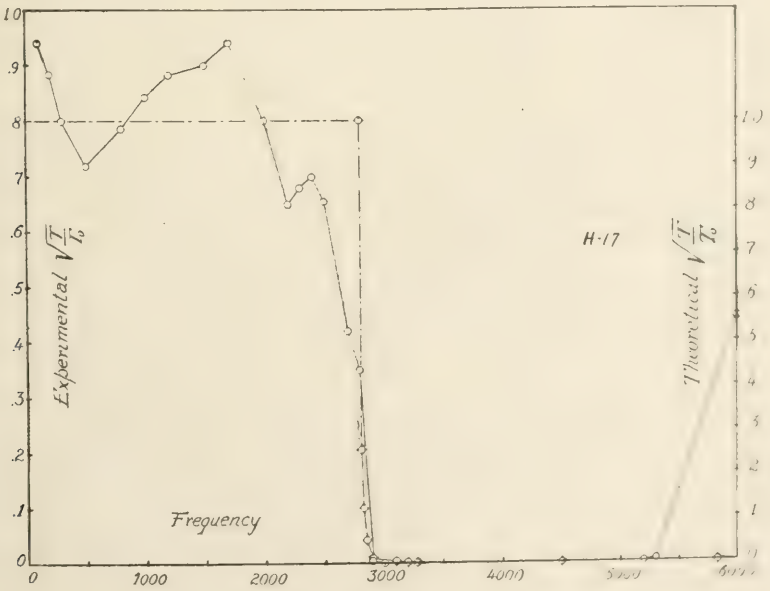

Fig. 1

The experimental procedure was similar to that previously used by G. W. Stewart.[1] Three types of filter were investigated, H-17 being a low-frequency-pass filter, L-50 a high-frequency-pass filter, and SB-9,

[1] Stewart, Phys. Rev. **20**, 528, Dec., 1922

a single-band-pass filter. The experimental curves are the full-line curves shown in Figs. 1, 2, and 3, in which the square-root of the percentage transmission is plotted as a function of the frequency.

The theoretical transmission curves can be determined from the equations,

$$e^{-\alpha} = I_{n+1}/I_n, \tag{1}$$

which becomes $e^{-n\alpha} = I_n/I_0$ for a filter of n sections, where

$$\cosh \alpha = \pm(1+\tfrac{1}{2}\, Z_1/Z_2). \tag{2}$$

In these equations α is the attenuation factor; the I's are the rates of change of volume displacement and are proportional to the square-root

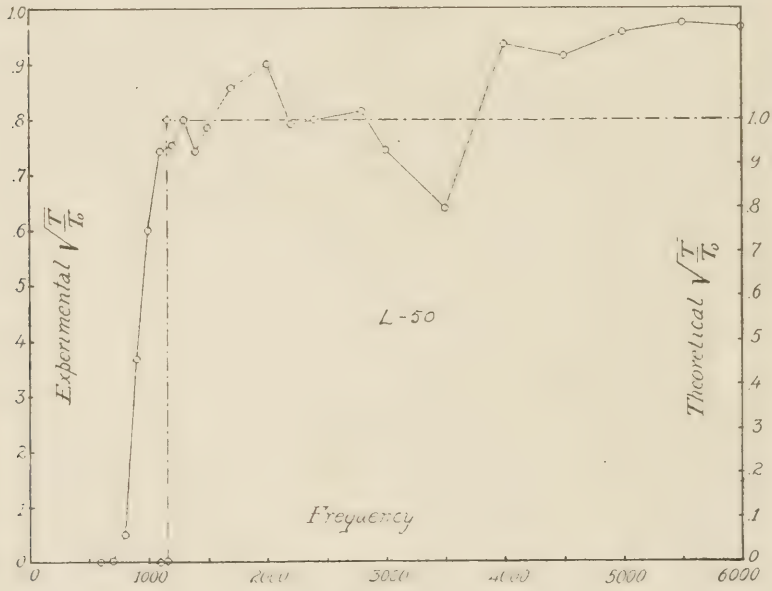

Fig. 2

of the transmitted energy; the Z's are acoustic impedances and can be calculated from the dimensions of the filter and the frequency. The values of Z_1 and Z_2 are those selected by Stewart. The computed transmission curves are shown by the dotted lines in Figs. 1, 2, and 3.

In comparing the two sets of curves, it will be observed that the ordinates of the theoretical and experimental curves are not the same. The reason for this is that these filters do not transmit all of the energy outside of the attenuated region, and this is explained by unavoidable dissipation. However, at a certain frequency for each filter, a sharp diminution of intensity occurs. Since we are chiefly concerned with the comparison with theory within the region of attenuation, the transmitted

energy at the beginning of attenuation is taken as 100 per cent for the theoretical transmission. With the exception of the difference caused by dissipation, the experimental values are in fair agreement with those computed from the formulas.

Considering the necessary approximations in the theory and the inexactness of its application, a perfect correspondence between theory and experiment cannot be expected. The chief approximations are the assumption of infinitely long wave-length and somewhat arbitrary

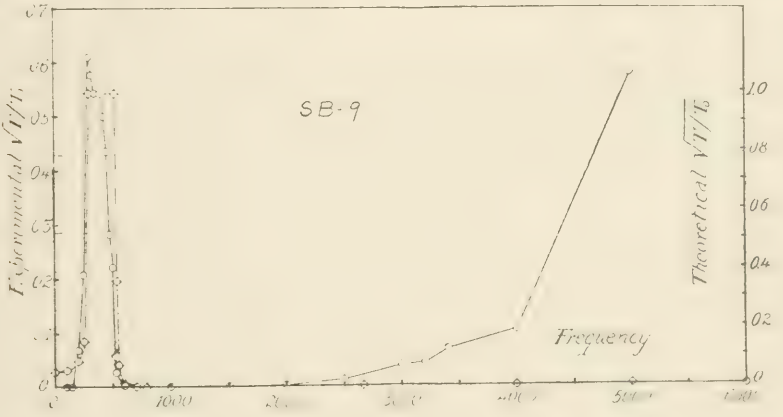

Fig. 3

limiting values for Z_1 and Z_2. Under the circumstances the agreement between theory and experiment is surprisingly good.

In conclusion the writer wishes to express his appreciation of the courtesies extended by the staff of the Department of Physics and to acknowledge especially the assistance received from Dr. G. W. Stewart, under whose direction the experiments were conducted.

PHYSICAL LABORATORY,
UNIVERSITY OF IOWA,
August 25 1923.

Reprinted for private circulation from
THE ASTROPHYSICAL JOURNAL, Vol. LIX, No. 3, April, 1924

ON THE BREADTH OF THE HYDROGEN LINES IN STELLAR SPECTRA

BY E. O. HULBURT

ABSTRACT

The effect of pressure according to modern theories.—When the Stark theory of the broadening of the Balmer lines of hydrogen is combined with the Saha theory of high-temperature ionization, it is found that in order to account for the broad Balmer lines observed in many stellar spectra, the pressure in the stellar envelope must be as great as several atmospheres. This seems to contradict evidence from other sources which points to much lower pressures. The assumption of a considerable number of free electrons in the atmosphere might explain the discrepancy.

From a consideration of the breadth of the Balmer lines in stellar spectra, it would seem possible to estimate the conditions of the atmosphere of the hydrogen stars. To this end the theory of high-temperature ionization developed by Saha[1] has been combined with the Stark theory of the broadening of the hydrogen lines. Saha's theory has been successful in accounting for many of the important features of stellar spectra, and the view that the broadening of the Balmer lines of hydrogen with pressure or current density is a manifestation of the Stark effect has received additional confirmation from recent work of the author.[2]

Assume pure atomic hydrogen gas ionized by its temperature. Let ν be the total number of hydrogen atoms per cc. If a fraction χ of these are ionized, there are $2\chi\nu$ charged particles per cc. The average distance between the ions is $(2\chi\nu)^{-\frac{1}{3}}$ cm. The positive ions are assumed to be the radiating atoms. Therefore from Coulomb's law of force, each radiating atom finds in an electric field of mean value $e(2\chi\nu)^{\frac{2}{3}}$ electrostatic units, where e is the electronic charge. This result is obtained by assuming that the field is due to a single charge. Actually the field at a point in the gas is the resultant of the effects of a swarm of charged particles of both signs in the vicinity of the point. This indicates that the mean value of the field should be multiplied by a factor σ, which we take to be one-third. The Balmer line radiated by the atom is separated into its Stark

[1] *Philosophical Magazine*, **40**, 472, 1920.

[2] *Physical Review*, **22**, 24, 1923.

components, the separation being proportional to the intensity of the electric field. According to Stark[1] in the case of Hβ the extreme components are displaced 20 A to either side of the parent line by a field of 1.04×10^5 volts, a maximum widening of 40 A. Since the broadened line emanating from the gas is composed of contributions from all the electrical components of a large number of radiating atoms, the average widening may be taken to be a half of this or 20 A. This amounts to a width of 0.06 A per unit c.g.s.e.s. field for Hβ. If w is the width of the line in angstrom units

$$w=0.06\sigma e(2\chi\nu)^{\frac{2}{3}}. \tag{1}$$

This calculation is of course not precise; the methods of averaging employed are of the roughest. A more elaborate analysis could be resorted to if necessary, but this would seem hardly advantageous at present because, in the very nature of the problem, orders of magnitude only can be considered significant. We therefore permit this result and those that follow to stand without further qualification. The discussion has borne upon the emission of radiation, but may refer equally well to the absorption of radiation.

Taking ν to be 2.7×10^{19} at 0° C. and atmospheric pressure and replacing e by the value 4.77×10^{-10}, equation (1) becomes

$$w=6000(\chi PT^{-1})^{\frac{2}{3}}, \tag{2}$$

where P is the pressure in atmospheres and T is the temperature on the Kelvin scale.

The reaction isobar of ionized hydrogen atoms in the original form stated by Saha (*op. cit.*, p. 486) is

$$\log_{10}\chi^2(1-\chi^2)^{-1}P=6.851\times10^4\,T^{-1}+2.5\log_{10}T-6.5. \tag{3}$$

Eliminating χ between (2) and (3) yielded an equation in w, P, and T. From this equation values of P in atmospheres were calculated for a series of values of w and T. These are given in Table I. The table refers to the Hβ line. The calculations for Hα and Hγ are slightly different, but the orders of magnitude of the pressures are the same as those for Hβ.

[1] *Annalen der Physik*, **48**, 202, 1915.

Although the width of a spectrum line cannot be judged with great accuracy from a reproduction, an examination of certain pictures of stellar spectra published by Sir William Huggins and by the Yerkes Observatory indicated that the widths of the hydrogen lines, either of absorption or emission, were in many cases greater than 20 A and sometimes nearly 30 A, as for example the Balmer absorption lines of α Lyrae. From Table I we see that to produce lines as broad as these would necessitate high pressures or temperatures. Recent evidence, reviewed in a paper by Fowler and

TABLE I

PRESSURES IN ATMOSPHERES

T	w IN ANGSTROMS	
	10 A	40 A
5000° K	10^{10} atm.	10^{12} atm.
10,000	10^{3}	10^{5}
15,000	10	10^{2}
20,000	1.3	24
25,000	1.6	14
30,000	1.9	15
35,000	2.2	16

Milne,[1] points unmistakably to the conclusion that the pressures in the reversing layers are low, of the order of 10^{-3} or 10^{-4} atmospheres. This is in serious disagreement with the present calculations. As a further illustration, for 10,000° K and a pressure of 10^{-3} atmospheres, formulae (2) and (3) give a width of 0.07 A for Hβ. To obtain a width of 20 A would require a number of charged particles which is 2200 times the number permitted by the Saha formula, or about 1800 times the number of the atoms of hydrogen.

The cause of this discrepancy is not evident. If it is admitted that the pressures in the stellar envelopes are low, we must look for errors in the theory or in the statement of the theory outlined in the foregoing paragraphs. Although equation (1) is not exact, it is difficult to see how it can be in error by several orders of magnitude. The assumption of other and perhaps more potent causes of ionization, such as the absorption of radiation, ionization by

[1] *Monthly Notices of the Royal Astronomical Society*. **83**, 415, 1923.

collision, etc., would not be of much help as long as the pressure is low. The calculation has been made for pure hydrogen. If the easily ionized metal atoms were present, they would supply a large number of charged particles, but even in this case to have a sufficient number the total pressure of the gas would have to be several atmospheres. A possible explanation would be to assume a large number of free electrons. These would produce the broadening without increasing the pressure.

UNIVERSITY OF IOWA
December 1923

Reprinted from the Journal of the Optical Society of America and Review of Scientific Instruments
Vol. VIII, No. 5, May, 1924

A SIMPLE AUDIOFREQUENCY MECHANICAL ALTERNATOR

By C. J. Lapp

Since the advent of the vacuum tube, high frequency mechanical alternators have received little attention. A small alternating current, say sufficient to energize a telephone receiver, with a frequency range from 20 to 40,000 cycles, has many uses. It is desirable in some cases for such a current to be produced by a simple mechanical alternator with a wide range of frequency. Such a generator has been designed.

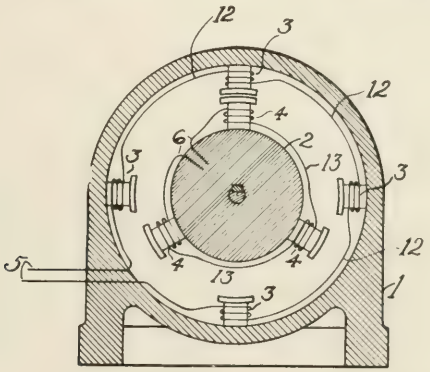

Fig. 1

By making use of the Vernier principle it has been possible to make the number of cycles generated per revolution equal to the product of the number of poles on the stator by the number of armatures on the rotor. A drawing has been made, Fig. 1, and is reproduced simply to show clearly the basic principle used in design. A machine built similar to Fig. 1 would give 12 cycles per revolution.

A photograph has been reproduced (Fig. 2) of the actual alternator as constructed. Each pole made from soft iron has an outside diameter of 2.5 inches and an inside diameter of 2 inches. The field windings are in series and contain twenty turns of No. 22 copper wire on each pole. The armatures each 0.375 inch long and 0.25 inch on each side are set into a brass disk 0.25 inch thick and 3 inches in diameter. This can be rotated at any desired speed by a belt on a pulley at the end of the shaft. The air gap at each end of the armature is 0.005 inch.

The current is induced in coils wound on the poles by the changing

flux in the poles. All coils are therefore stationary. These coils contain 2000 turns of No. 34 D. S. C. copper wire.

The design of the alternator can be greatly changed and still retain the Vernier principle of action. The number of turns on either of the coils can be changed at will. The number of armatures on the rotor may be any multiple of $(n-1)$ or $(n+1)$ where n is the number of poles.

FIG. 2

The armature as described above can be rotated at any speed up to 12,000 R. P. M. This gives 4000 cycles per second. A machine with 15 poles and 14 armatures at this speed would give more than 40,000 cycles per second.

PHYSICS LABORATORY,
UNIVERSITY OF IOWA,
IOWA CITY, IOWA.
NOVEMBER, 1923.

Reprinted from the Journal of the Optical Society of America and Review of Scientific Instruments
Vol. VIII, No. 5, May, 1924

A QUARTZ SPECTROGRAPH FOR WAVE LENGTHS TO 1850 A

By E. O. Hulburt

A spectrograph which was effective in the ultra-violet region of the spectrum to wavelength 1850 A was constructed by mounting a 30° quartz prism in the Littrow manner. The parts were arranged as shown in Fig. 1. The light from slit S, which was at the ultra-violet focus of the quartz lens L, was rendered approximately parallel by the lens and passed through the quartz prism P. It was then reflected from the back surface of the prism by a layer of mercury in contact with the quartz and returned through the prism and the lens, being brought to a focus on the photographic plate T, or fluorescent screen. The plate

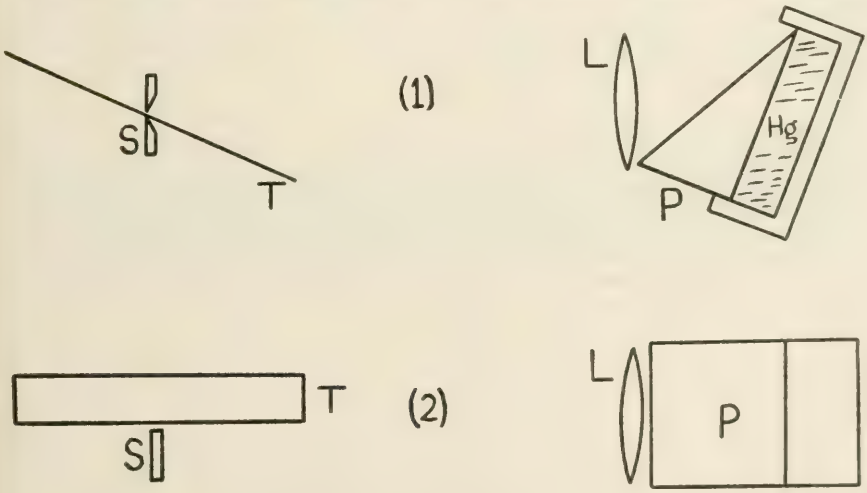

Fig. 1. *Quartz spectrograph; (1) plan, (2) elevation.*

was placed immediately above the slit and was tilted at an angle of about 25° with the axis of the spectrograph. Those wave-lengths which came to a focus above the slit automatically passed through the prism at minimum deviation. Since the prism was traversed by the light in both a forward and backward direction the prism behaved exactly as a Cornu prism. The quartz lens was 32 mm in the diameter and of focal length about 27 cm for visible light and 21 cm for light of wave-length 2100 A. The small angle of the prism was 30°, the other angles

were 60° and 90°, respectively, and the face of the prism was sufficiently large to cover the beam of light from the lens. The lens and prism were received a few months ago from Steeg and Reuter, Germany, (through the J. G. Biddle Co., Philadelphia) at a total cost of about forty dollars. Clean mercury was poured into a small tank fastened to the prism. The tank was sealed with beeswax and rosin mixture and the reflecting surface has remained without appreciable deterioration for several months.

The photographic performance of the spectrograph is demonstrated by the spectrograms of Fig. 2. This gives the spectra taken on Seed L Ortho plates of the condensed spark between aluminum and zinc terminals, respectively, with a current of about eight amperes. The time of exposure was thirty seconds for the zinc spectrum and for the aluminum spectrum down to the point marked *a*. For the shorter wavelength aluminum lines below *a* the exposure was three minutes. The extreme cadmium lines 1856 and 1873 appeared on these plates with an exposure of six minutes. The length of the spectrum from 2800 to 1850

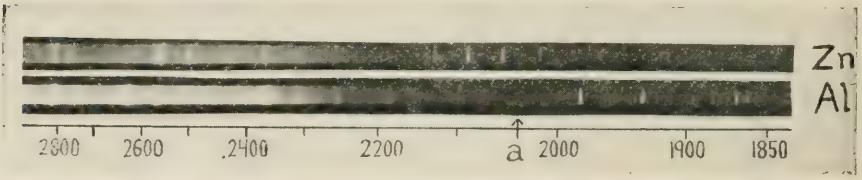

FIG. 2

A was about 77 mm. The dispersion at 2700, 2500, 2300, 2100, and 1900 A was 24, 18, 13, 9, and 6 A per mm, respectively. The reflecting power of quartz backed by mercury was measured[1] sometime ago and was found to be about 55% for the region 3500 to 2100 A. Comparison between spectrograms taken with the present instrument and those taken with a 60° prism, two lens, quartz spectrograph of the usual type indicated that the reflecting power of mercury against quartz does not diminish rapidly, if at all, from wavelength 2100 to 1850 A. The falling off in intensity of spectra from a quartz spectrograph in the region below 2000 A is due in large part to the absorption of quartz and to a lesser extent to that of air. Therefore, improvement in intensity as well as in dispersion and clearness of spectrum is gained by the use of thin lenses, not too short in focal length, and of thin, small angled, prisms.

[1] Astrophysical Journal, *44*, p. 1; 1917.

The lens L and prism P were mounted on a metal carriage which could be moved by a screw adjustment along the base of the spectrograph for the purpose of focussing. Both the lens and prism were provided with adjustments for tilting and rotating about a vertical axis. The slit S could be rotated slightly in its own plane. Just as in any short focus spectrograph, this is a sensitive and important adjustment, being used to obtain lines perpendicular to the march of the spectrum. The plate holder T, which was mounted above the slit S and as close to it as possible, could be rotated about an axis in line with the slit. Flat plates were used and gave fair sharpness of focus over the region of the spectrograms of Fig. 2. For wider spectral ranges curved plates would perhaps be better. All adjustments were greatly facilitated by being equipped with some simple form of arbitrary scale.

The lens is tilted slightly to prevent the light reflected from its surfaces from falling on the plate. The prism is also tilted to throw the spectrum above the slit. As a result a distortion of the spectrum occurs, evident in Fig. 2, such that if the lines above the slit, i.e. in the central portion of the spectrum, are perpendicular to the march of the spectrum, the lines remote from this region are not so, but show a small obliquity and curvature which increase with the distance from the slit. This distortion would usually be inconsiderable; it could, if necessary, be corrected by the use of a lens or prism with properly curved surfaces.

PHYSICAL LABORATORY,
UNIVERSITY OF IOWA.
JANUARY, 1924

Reprinted from PHYSICAL REVIEW, pp. 593-597, No. 5, May, 1924

THE BALMER ABSORPTION SERIES OF HYDROGEN

BY E. O. HULBURT

ABSTRACT

Laboratory method of obtaining ten Balmer lines in absorption.—Condensed discharges were passed through an under water spark in series with a tube, 75 cm in length, of moist hydrogen at a pressure of 0.5 mm of mercury. The light from the spark traversed the glowing hydrogen, and the Balmer lines appeared as narrow dark absorption lines against the continuous spectrum of the spark, the absorption series extending to the tenth Balmer line. By adjusting the relative intensities of the light of the spark and of the glowing hydrogen, spectra were obtained with $H\alpha$ and $H\beta$ either bright or dark while the higher members of the series remained always dark. Spectra were produced showing $H\beta$ and $H\gamma$ dark but with a bright central core. These phenomena are well known in stellar spectra, to which reference is made.

IN an investigation of unusual interest R. W. Wood[1] by means of long vacuum tubes has extended the Balmer emission spectrum of hydrogen to the twentieth member. Recently Whiddington[2] has described a different method of accomplishing this. The Balmer absorption spectrum, on the other hand, although well known in stellar spectra to the thirty-second line, has never been produced in the laboratory beyond $H\beta$. Several years ago Ladenburg and Loria[3] succeeded in reversing $H\alpha$ and $H\beta$ by passing the light from a short tube filled with hydrogen at considerable pressure through a long tube of hydrogen at a low pressure. The two tubes were connected in series and were excited by condensed discharges. The absorption lines appeared as fine dark lines against the broadened emission lines of $H\alpha$ and $H\beta$. Attempts[4] which have been made to extend the absorption to the other members of the series have met with but little success. It is not obvious why these attempts have failed. In the present experiments by a slight variation of Ladenburg's method the absorption series has been extended to the seventh line using dry hydrogen, and to the tenth line using moist hydrogen.

The experimental arrangements are indicated in Fig. 1. The 30 kv, 1 kw, transformer P charged the condenser C, of capacity 0.015 microfarads, which discharged through the quenched gap Q, the long hydrogen

[1] R. W. Wood, Roy. Soc. Proc. **97,** 455 (1920); Phil. Mag. **44,** 538 (1922)
[2] Whiddington, Phil. Mag. **46,** 605 (1923)
[3] Ladenburg and Loria, Verh. Deut. Phys. Ges. **10,** 858 (1908)
[4] Foote and Mohler, Origin of Spectra, p. 98 (1922)

tube T, the underwater spark S, and the ammeter A. The auxiliary gap Q was necessary to insure abrupt discharges. The tube was of glass, 75 cm in length between the electrodes and 2.3 cm in diameter, with aluminum electrodes. The electrodes of the underwater spark S were of phosphor bronze, for this metal disintegrated slowly and the spark emitted a very intense continuous spectrum in the region under investigation. The light from the spark S, rendered slowly converging by the lens L, passed through the glowing hydrogen tube and came to a focus on the slit H of a concave grating spectrograph of dispersion 8.8 A per mm.

Spectrograms taken with dry hydrogen in the tube showed the Balmer lines as fine dark absorption lines against the continuous emission from the under water spark. The series was recorded to the seventh Balmer

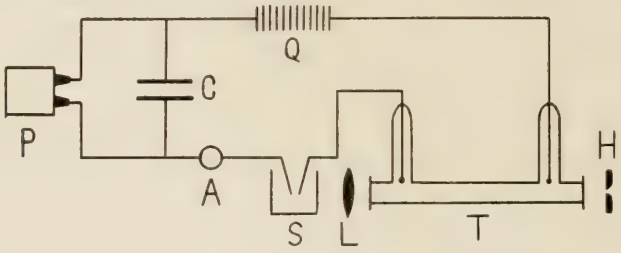

Fig. 1

line. To extend the series farther, use was made of the fact, long known,[5] that the presence of a slight amount of water vapor in a hydrogen discharge tube suppresses the secondary spectrum and intensifies the Balmer spectrum. Moist hydrogen was admitted into the tube through a slender capillary tube in the manner described by Wood.[1] The best absorption spectrograms, which recorded the reversed Balmer lines to H_{10}, shown in *a*, Plate 1, were obtained with a pressure of about 0.6 mm of mercury (dark space 5 mm) and with a current of about five amperes through the tube. The time of exposure was five minutes. In the emission spectrum of the hydrogen tube taken with an exposure of 15 minutes, the series lines could be traced only to H_6. With a five minute exposure the emission spectrum barely included H_4. It is evident that under these conditions the absorption brings out many more lines than the emission. Apparently the stimulated atoms are very effective absorbers for the Balmer radiations. This is in keeping with the theory of absorption discussed mathematically by Lamb[6] who pointed out that a single resonator can exert enormous checking power upon advancing

[5] Merton and Nicholson, Roy. Soc. Proc. **96**, 116 (1919)
[6] Lamb, Cambridge Phil. Soc. Trans. **18** (1900)

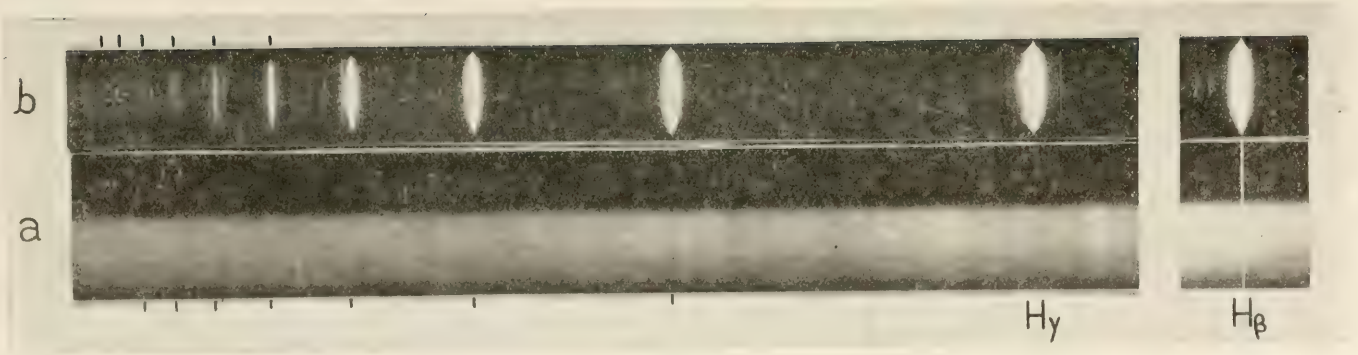

Plate 1

(a) Absorptions spectrogram, showing reversed Balmer lines to H_{10}.
(b) Emission spectrum of hydrogen tube, showing lines to H_{12}.

radiation of a frequency very nearly, but not quite, that of its own period. A similar instance is the high opacity of mercury vapor for the mercury line 2536.[7]

In an attempt to extend the absorption series farther into the ultraviolet a long tube was made with a straight portion 40 cm in length, 7 mm internal diameter, and with long side branches leading to the electrodes, such as described by Wood.[1] The present experiment necessitated a departure from Wood's method in that powerful condensed discharges were required instead of sixty cycle currents. With the condensed discharges the Balmer emission lines from the long tube became somewhat diffuse because of the Stark broadening, and with an exposure of ten minutes only twelve lines could be traced under the best conditions which were obtained. Spectrogram *b* of the Plate illustrates this. When the absorption was attempted with this tube the Balmer lines remained bright because the small bore of the tube effectually prevented the passage of the continuous spectrum in sufficient intensity. To overcome this difficulty a long tube was constructed with an internal diameter of 2.3 cm instead of 7 mm. Although various types of electrical excitation were tried, all attempts failed to bring this tube completely into the "black stage," as Wood has called it, i.e., the Balmer lines strong and the secondary weak, so that only eight Balmer absorption lines were recorded. The walls of the tube were perhaps not close enough to all parts of the gas to catalyze effectively the molecules to the atomic state. A more intense electrical excitation of some sort might have been necessary.

It is seen that all the Balmer lines of spectrogram *a* were reversed except Hβ which was bright. A visual observation at the time showed that Hα also was bright against the continuous background. Decreasing the brilliancy of the glowing hydrogen by admitting a small amount of hydrogen into the tube, brought out Hβ dark, instead of bright, against the continuous spectrum. Increasing the brightness of the glowing hydrogen gave a spectrum with Hα, Hβ and Hγ appearing as emission lines and the other lines as absorption lines. The explanation of these observations is to be found in the conclusions of Ladenburg[8] as a result of an investigation of the absorption of Hα. By means of Nicol prisms the relative brightness of Hα and the back-ground illumination were varied at will. It was established that in the region of wave-lengths covered by the Balmer line the light from the background was completely absorbed, and that the light which did appear in this region was emitted from the long column of stimulated hydrogen. Therefore the appearance

[7] Wood, Researches in Physical Optics, Part 1.

[8] Ladenburg, Verh. Deut. Phys. Ges. **12**, 54 and 549 (1910)

of the Balmer line as bright or dark depended primarily upon the relative brightness of the two sources.

The spectrograms of the present experiments find interesting counterparts in certain stellar spectra,[9] some stars giving spectra with all the hydrogen lines bright, others with all the hydrogen lines dark, and still others, such γ *Argus* and η *Tauri*, with the earlier members of the Balmer series bright and the shorter wave-length hydrogen lines dark.

Spectrograms were obtained in which Hα and Hβ were bright, Hγ was dark with a bright centre, and the other lines were entirely dark. The complex character of Hγ, although unmistakable on the negative, did not lend itself successfully to an enlarged reproduction, for the extreme width of Hγ on the plate was only about 0.2 mm and the edges of the bright core were hazy. Other spectrograms under slightly different conditions showed Hα bright, Hβ dark with a bright centre and the remaining lines dark. That the dark absorption line may have a bright core was observed by Ladenburg[8] in the case of Hα who proved that the dark edges of the line resulted from an absorption by the long layer of glowing hydrogen, greater than the emission, whereas in the bright centre the reverse was true. Again these facts are well known in the spectra of the stars. For instance, the quasi-permanent stars μ *Centauri* and *J Velorum*[10] at one time exhibited Hβ and Hγ as absorption lines with well marked emission centres. In the spectrum of II *Camelopardalis*[11] Hγ and at least seven of the Balmer lines which follow it are dark with bright centres of emission.

In this connection we may mention a complexity of certain stellar hydrogen lines which as yet has not been imitated in the laboratory, as for example Hγ, Hδ and Hϵ in the spectrum of φ *Persei* and Hβ and Hγ in the spectrum of β *Monocerotis*.[12] These lines are broad dark absorption bands with a narrow bright centre band which in turn is divided by a yet narrower line of absorption. Such a complex line would perhaps result if the following conditions existed: (1) a hot dense stellar interior yielding a continuous spectrum, (2) an absorbing envelope of hydrogen, relatively dense, giving a wide absorption line, (3) above this a region of less pressure and greater ionization which emitted somewhat narrower lines, and (4) above this yet another region of cooler, more rarified hydrogen causing the still narrower center of absorption.

PHYSICAL LABORATORY,
UNIVERSITY OF IOWA,
January 5, 1924

[9] Campbell, Astrophys. J. **2**, 177 (1895)
[10] R. H. Curtiss, Observatory Pub., U. of Michigan, **3**, 21 (1923)
[11] Curtiss, l.c.[10] p. 27
[12] Curtiss, l. c.[10] p. 23

Reprinted from PHYSICAL REVIEW, pp. 9–15, No. 1, July, 1924

THE K AND L ABSORPTION AND EMISSION SPECTRA OF TUNGSTEN

BY C. B. CROFUTT

ABSTRACT

Both the absorption and emission spectra were photographed simultaneously on the same plate, using a special float-operated mechanism to turn the crystal very slowly so as to obtain the faint lines between β_2 and β_5. The *absorption wave-lengths* were found to be: LA_1, 1.2122A; LA_2, 1.0716A; LA_3, 1.0217A; KA, .17802A. Table I gives the *emission wave-lengths* of 28 L emission lines including the four new lines β_{15} (1.2432), β_{16} (1.2166), γ_{12} (1.0748) and n (1.0699), and of the $K\beta_3$ line (.18525) which is the line found by DeBroglie. *Comparison with the Bohr theory.* The agreement of the emission frequencies computed from the energy levels with the measured wave-lengths is better than 1/10 per cent, except for β_{15} and β_{16}. The lines β_{10}, β_9,γ_{12}, and γ_{11}, however, correspond to transitions between energy levels which are not predicted by the selection principle, and lines β_8 and n are not in agreement with the accepted energy levels. While Ln may be due to an impurity, β_8 is probably a tungsten line.

THIS work is an investigation of the absorption and emission spectra of tungsten under the same experimental conditions. Both spectra were obtained simultaneously on the same photographic plate in order to make certain the relative positions of the absorption limits and the emission lines.

EXPERIMENTAL METHOD

A medium focus tungsten target Coolidge tube was used as a source of x-rays. The x-rays were analyzed by means of a rock salt crystal and the spectra were recorded on photographic plates. The apparatus is essentially that used by Dershem[1] with the substitution of an accurately constructed crystal table, a narrow slit of 0.005 cm width, and a new rotator for the crystal.

The crystal table is shown in Fig. 1 and consists of a spindle fitted in bearings as shown. This spindle is removable and additional spindles make it possible to change crystals without remounting each time.

The crystal was rotated through a small angle by means of levers attached to a float in a tank of water, the level of which was raised by means of a small stream of water and lowered by the use of an intermittent syphon. The advantage of this method is that the crystal can be set for a particular line and a prolonged exposure taken with the as-

[1] Dershem, Phys. Rev. **11**, 461 (1918)

surance that the crystal will not rotate too far. The rotation can be made as slow as desired and the angle kept as small as a quarter of a degree. The fine slit greatly prolongs the time of exposure but enables greater resolving power to be obtained. The fine slit and the rotator made it possible to obtain the group of faint lines between β_2 and β_5.

While working with the L series it was necessary to keep the voltage so low that no appreciable second order continuous radiation would affect the plate at the same point.

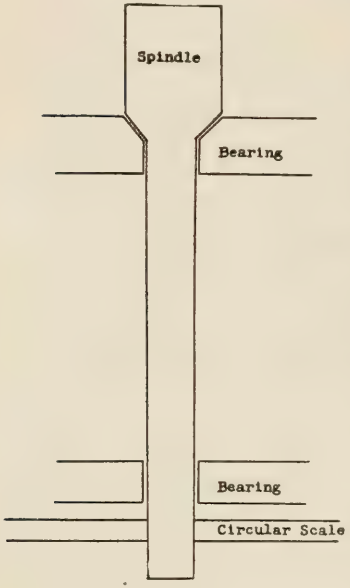

Fig. 1. Crystal table.

The work on the K series was done in the third order using 110,000 volts, effective value. The first and second order radiations were removed by absorbing screens.

The absorption bands were obtained by placing a screen of tungsten oxide in the path of the beam before it entered the spectrometer. This in no way interferes with the production of the emission spectra but does interfere with the analysis as emission lines are close to the absorption bands.

The method of measuring the plates is that developed by Dershem[1] in which a correction is made for the width of the slit. Measurements of faint emission lines and absorption bands were always made relative to strong emission lines.

Corrections

With the method employed there are two chief sources of error.

(a) If the plate is not perpendicular to the line of collimation it can be shown from geometrical considerations that θ is given by the following formula

$$D \tan 2\theta = d\sqrt{(1+m^2)} \pm \sqrt{d^2(1+m^2)+D^2m^2},$$

where θ is the glancing angle, d the distance from the crystal to the plate, D the distance between the lines as photographed on both sides of the line of collimation, and m the tangent of the angular displacement of the normal to the plate from the line of collimation. Since this correction is small, m may be determined with sufficient accuracy by means

of two known lines. In a manner similar to the above it can be shown that

$$2(1-p)m=(1+p)(m_1+m_2)\pm\sqrt{(1+p)^2(m_1+m_2)-4(1-p)^2m_1m_2}$$

where p is the ratio of the distances between the two lines on opposite sides of the line of collimation, m_1 and m_2 the value of $\tan\theta$ for the two known lines.

(b) If the face of the crystal is not in the axis of rotation an amount equal to $\delta/\sin\theta$ must be added to or subtracted from the distance from the axis of rotation to the plate in order to obtain the distance from the crystal to the plate, where δ is the displacement of the face of the crystal from the axis of rotation. Since for small values of θ, $\sin\theta$ is small this correction is important.

TABLE I

Wave-lengths in Angstroms

L SERIES

α_2	1.4844	β_{15}	1.2432	β_{10}	1.2099	A_2	1.0716
α_1	1.4733	β_2	1.2421	β_9	1.2027	n	1.0699
η	1.418	β_8	1.2364	γ_5	1.1299	γ_2	1.0659
β_4	1.2988	β_7	1.2217	γ_1	1.0964	γ_3	1.0599
β_6	1.2875	β_{16}	1.2166	γ_8	1.0786	γ_{11}	1.0444
β_1	1.2793	β_5	1.2133	γ_{12}	1.0748	γ_4	1.0266
β_3	1.2602	A_1	1.2122	γ_6	1.0723	A_3	1.0217

K SERIES

Comparison lines				Measured			
α_2	.21352	β	.18436	β_3	.18525	A	.17802
α_1	.20885	γ	.17940				

Using Dershem's method for locating the lines, the penetration into the crystal does not introduce an error for the method depends on locating the edge of the line as reflected from the face of the crystal.

EXPERIMENTAL RESULTS

Table I shows the experimental results on the emission and absorption in the L and K series. The absorption limits are indicated by the letter A with appropriate subscript. In the L series the following lines were measured carefully and the results taken as standards for the measurements of all other lines: α_1, β_1, β_2, γ_1, γ_3, and γ_4. The comparison lines in the K spectrum are indicated in Table I. Because of the presence of the reference lines the results obtained on two or more plates varied only in the last significant figure shown. The line l does not appear because of the absorption in the glass walls of the tube. The lines β_{15}, β_{16}, γ_{12}, and n are new lines for the L series of tungsten.

Discussion of Results

Fig. 2 presents the results in the well known form of energy levels as recently published by Bohr and Coster.[2] Table II gives the corresponding frequencies of the energy levels. The K and L frequencies were obtained directly from the measurements made on the wave-lengths. The other

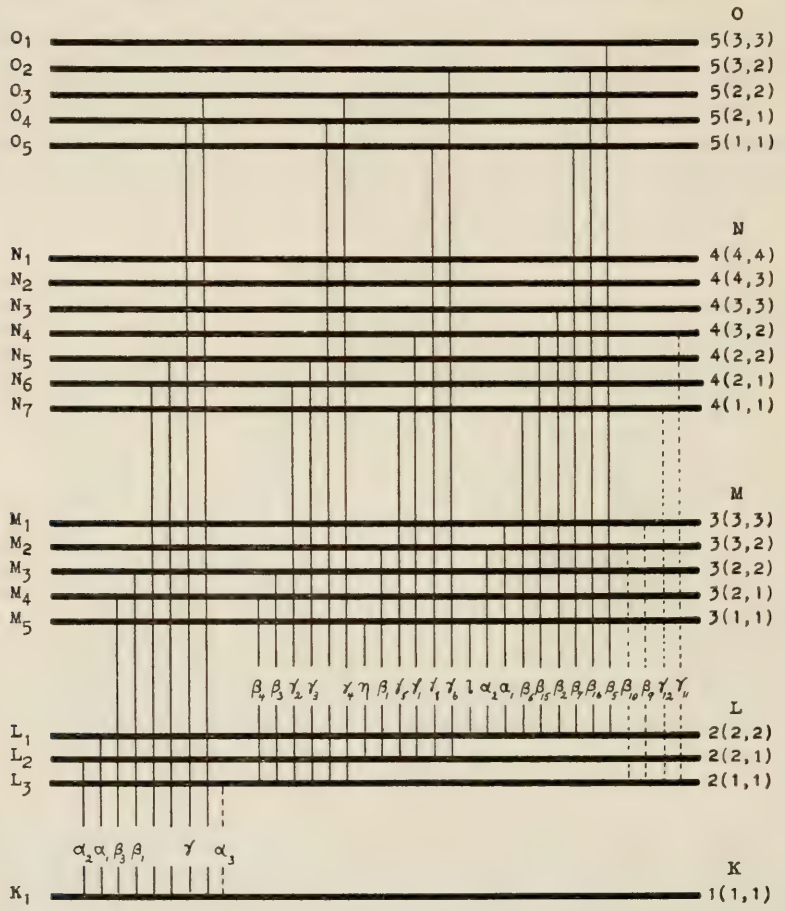

Fig. 2. Energy level diagram for tungsten showing the K and L series. Solid lines are transitions predicted by the selection principle. Broken lines are other transitions.

frequencies were calculated from the K and L absorption frequencies and the frequencies of the emission lines. The solid lines between the energy levels of Fig. 2 represent transitions predicted by the selection principle.[3]

[2] Bohr and Caster, Zeits. f. Phys. **12**, No. 6 (1923)

[3] Bohr, Phil. Mag. June 1922

The broken lines represent other transitions found. The notation is that of the line produced by the transition. If there is no symbol the line has not been found. The symbols at the left of the horizontal lines are the usual notations of the energy levels; those at the right are the notations of Bohr and Coster [the symbol 4(2,1) corresponds to the energy level having the total quantum number 4, the "grund" quantum number 2 and the azimuth quantum number 1].

The selection principle states that the azimuth quantum number must change by ± 1 or 0 and that the "grund" quantum number must change by ± 1.[2]

TABLE II

Absorption frequencies $\times 10^{-18}$

K and L measured; M, N and O calculated

K_1	16.844	M_1	.4401	N_3	.0579	O_1	.0022
L_1	2.4738	M_2	.4548	N_4	.0629	O_2	.0053
L_2	2.7982	M_3	.5554	N_5	.1058	O_3	.0140
L_3	2.9349	M_4	.6261	N_6	.1220	O_4	.017
		M_5	.6814	N_7	.1448	O_5	.0189

A comparison of Table I with Fig. 2 shows that all but the β_8 and n lines are represented on the diagram. The n line is a new line and may be due to some impurity, although a comparison with tables failed to reveal its identity. The β_8 line has been found by Overn[4] and Siegbahn[5] and should be accepted as a line of tungsten. This line is hard to measure being very indistinct. Coster[6] has shown that it appears as β_{11} and β_{12} in elements of atomic numbers 47 to 51. Of the four lines of the L series β_9, β_{10}, γ_{11}, and γ_{12} not given by the selection principle, γ_{12} is a new line. A careful investigation failed to reveal the $K\alpha_3$ line of which Duane and Shimizu[7] found some indication. The results indicate that if it does exist it does not differ in wave-length from the α_2 line by more than .04 per cent, or else its intensity is so low that it is concealed by the general radiation. It is not predicted by the selection principle. The two other new lines are given by the selection principle.

β_{15} is so close to β_2 that it could not be completely resolved, but because of the difference in intensity the edges of both lines could be located and measured. The other new lines are very faint and close to lines already known. $K\beta_3$ is the line previously found by DeBroglie.[8] The wave-lengths obtained for the absorption bands are shorter than those

[4] Overn, Phys. Rev. **14**, 137 (1919)
[5] Siegbahn, Phil. Mag. Nov. 1919
[6] Coster, Phil. Mag. Sept. (1922)
[7] Duane and Shimizu, Phys. Rev. **14**, 67 (1919)
[8] De Broglie, Comptes Rendus, 1920

obtained by Duane, which are usually accepted as standard. These changes in wave-length are sufficient to alter the relative positions of the LA_1 and the LA_2 with respect to β_5 and γ_6, as is shown in Table III and of course visually on the plates themselves.

It is seen from Fig. 2 that all lines found as transitions between energy levels but not predicted by the selection principle involve (1,1) energy levels. This may be a coincidence but it may have significance.

No special attempt was made to obtain the relative intensities of the lines. The β_{15} is of medium intensity while the other new lines are very faint.

The fact that the lines β_{15}, β_{16}, and γ_{12} fit into the energy level diagram makes it seem reasonable that they are tungsten lines.

Since the absorption and emission spectra appear on the same plates it is impossible to say much regarding the structure of the absorption bands, some of the emission lines being very close to the absorption edges. However the edges were sharp and easily measured.

TABLE III

The shift in absorption wave-lengths

A_1	1.2140*	A_2	1.0730*	γ_4	1.0266
β_2	1.2133	γ_6	1.0723	A_3	1.024*
A_1	1.2122	A_2	1.0716	A_3	1.0217

The differences between the frequencies of the emission lines as computed (1) from the energy levels and (2) from the measured results are about .13 per cent for β_{15} and β_{16} and less than .10 per cent for the remainder with an average difference of .03 per cent.

CONCLUSIONS

The selection principle reduces the possible number of lines from fifty-one to twenty-one for the L series and from twenty to eight for the K series. Two of the new lines found agree with the selection principle, thus increasing the total number in agreement from eighteen to twenty for the L series, leaving one more line to be found. All lines in the K series are in agreement with the principle.

In addition to the lines given by the selection principle four were found in the L series which are not in agreement but which quantitatively correspond to transitions between energy levels. The $K\alpha_3$ line, found by Duane but not observed by the present photographic method, is not in agreement with the selection principle and is yet somewhat in doubt.

As an indication that the present energy levels are not sufficient there appear to be two lines in the L series which are not in agreement. One

*Values given by Duane and Shimizu[7]

of these is a new line and may be due to an impurity; the other is the β_8 line.

It is seen from the above that the energy levels as drawn do not satisfy all the measurements of what are undoubtedly tungsten lines, and that Bohr's selection principle would eliminate four lines which have been found. These disagreements emphasize the need for further experimental and theoretical work.

I wish to acknowledge indebtedness to the members of the staff of the physical laboratory at the University of Iowa for their interest in the work and especially to Professor G. W. Stewart who suggested the problem.

UNIVERSITY OF IOWA.
February 27, 1924.

Reprinted from PHYSICAL REVIEW, pp. 129-133, No. 2, August 1924

THE ABSORPTION LINES IN THE SPECTRUM OF THE METALLIC SPARK IN WATER

BY E. O. HULBURT

ABSTRACT

Absorption spectra of twenty elements, 4500 to 2000 A, obtained with condensed spark in water.—These spectra, seven of which are reproduced, consist of a continuous background crossed by bright and dark lines characteristic of the metal. For Al, Bi, Cd, Au, Ir, Pb, Mg, Pt, Rd, Ag, Sn and Zn, the absorption lines are those which are reversed in the arc. For Sb, Co, Cr, Cu, Fe, Mo, Ni and W, the water spark shows as absorption lines all the lines reversed in the arc and in addition about four hundred absorption lines, in all, which are not listed as reversed in the arc. Some of these are mentioned.

INTRODUCTION

EXPERIMENTS by Hale,[1] Bloch[2] and others[3] have shown that the spectrum of the condensed spark under water between metallic electrodes exhibits a continuous spectrum crossed by bright and dark lines characteristic of the metal. Although many metals have been considered in these investigations throughout various regions of the spectrum, no complete record of the absorption lines has been reported and in only a few instances have the observations been extended below 2500 A. It appeared of interest, therefore, to investigate these spectral phenomena more extensively. The earlier experimenters found that in many cases the number of lines which appeared as absorption lines depended upon the type of electrical excitation and perhaps upon such circumstances as the size of the electrodes, the depth of the spark in the water, the purity of the water, the temperature, etc. They found further that many kinds of absorption lines occurred, the different lines being intense, weak, narrow, broad, asymmetric, bright on one edge, displaced, etc., and that the character of the absorption line sometimes varied with the circumstances of the experiment.

Examination of these details has not been attempted in the present investigation. Attention has been directed to the presence or absence of an absorption line rather than to its behavior and character. Spectra were photographed throughout the region 4500 to 2000 A of the con-

[1] Hale, Publications of the Yerkes Observatory, **3**, Part 2 (1907)
[2] Bloch, Journ. de Phys., **3**, 309 (1922)
[3] See Baly, Spectroscopy, p. 413 (1912)

densed spark under water between electrodes of twenty different metallic elements. Guided by preliminary experiments, conditions of electrical excitation were chosen to bring out as many absorption lines as possible. In the main the purpose of this paper has been to present experimental results and to leave possible discussion of their bearing upon spectral series to others.

Experimental Details

The arrangement of apparatus is indicated in Fig. 1. The condenser C of capacity 0.01 microfarad was charged by the 25 kv, 1 kw, transformer T, and discharged through the quenched gap Q and the water spark S. S was placed in a jar of distilled water, at all times about four centimeters below the surface of the water. The electrodes of S, which were usually about a millimeter apart, could be approached to each other

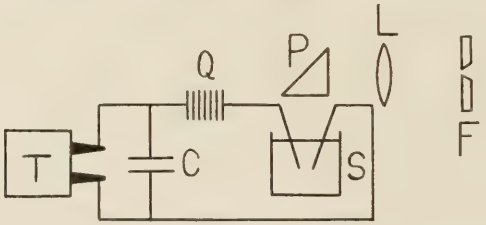

Fig. 1. Diagram of apparatus.

by a screw adjustment as they splintered away during the passage of the spark. In case very rapid disintegration of the electrodes occurred the water was changed continually. The quenched gap served to ensure an abrupt discharge. The current through the spark was between 5 and 10 amp. as measured by a hot wire ammeter, and was oscillatory, heavily damped, of a frequency about 10^5. The light from the spark S passed upward across the surface of the water, was directed by the quartz prism P through the quartz lens L, and came to a focus on the slit F of the spectrograph. A grating spectrograph of dispersion 8.8 A per mm served for the region from 4500 to 2400 A and a small quartz spectrograph for the region from 2400 to 1850 A. The water spark spectra usually extended nearly to 2000 A but rarely below this. The times of exposure were from 2 to 15 minutes. Seed plates, L Ortho, were used for the photography of the longer wave-length region and Schumann plates for the shorter wave-length region. On the same plate with each water spark spectrum an air spark spectrum was taken for comparison. Wave-lengths are from Kayser's Handbook and from the later tables of Watts.

The condensed spark under water takes place with explosive violence, the light being brilliant and the sound intense. Upon the passage of the

spark, vapor of the metal is thrown off, probably in an excited or partially excited condition. It is this envelope of metallic vapor which produces the line absorption in the continuous spectrum from the core of the spark. On all the spectrograms there appeared a group of fine absorption lines near 3100 A which is attributed to water vapor.[4] This group may be seen superimposed on the doublet $1\pi - 2\delta$ of the aluminum spectrogram of Plate I.

General Conclusions

The following statements may be made for the spectral region 4500 to about 2000 A and for the conditions of the present experiments:

(1) The absorption lines which appeared in the water spark spectra of the metals Al, Bi, Cd, Au, Ir, Pb, Mg, Pt, Rd, Ag, Sn, and Zn were those which were reversed in the arc, no more and no less. The identification of about one hundred and fifty lines contributed to this conclusion.

(2) For the metals Sb, Co, Cr, Cu, Fe, Mo, Ni and W all the lines reversed in the arc appeared as absorption lines in the water spark spectra. This conclusion resulted from the identification of over two hundred lines. In addition, the water spark spectra of these metals exhibited altogether more than four hundred absorption lines which were not listed as reversed in the arc. The actual numbers were: Sb, 7; Cu, 8; Mo, 3; W, 6; and Co, Cr, Fe, and Ni more than 100 each.

There were a few doubtful instances where it was uncertain whether a line which was reversed in the arc, actually appeared as an absorption line in the water spark. These instances, about twenty in number, occurred when the line was of low intensity, or was over-shadowed by a neighboring stronger line, or was one of a complex group of lines.

Further Details

Aluminum. In the aluminum spectrogram of Plate I the first four members of the $1\pi - m\delta$ diffuse doublet series[5] and the first two members of the $1\pi - m\sigma$ sharp doublet series were brought out as absorption lines in very pretty fashion.

Antimony. The water spark reversals included the arc reversals throughout the range of observation which extended to 2070 A. In addition there were seven water spark absorption lines which were not reversed in the arc, namely, 2224.98, 2220.80, 2207.7, 2145.03, 2141.8, 2139.76, and 2127.55. This last line is reversed in the spark but not in the arc.

[4] Konen, Ann. der Phys. **9**, 779 (1902)

[5] Fowler's notation.

Cobalt, chromium, iron and nickel. The water spark spectra of these metals were extremely complex, possessing many emission and absorption lines. As has been said, besides showing as absorption lines all the arc reversals the water spark spectra of these metals exhibited hundreds of other absorption lines. These were especially numerous in the extreme ultraviolet. Spectrograms with higher dispersion would be necessary to obtain more exact data. The chromium triplets 4289.98, 4274.95, 4254.50 and 3605.48, 3593.63, 3578.81 were strongly reversed. Some of the absorption groups of cobalt and nickel are given in Plate I.

Copper. The important pair of lines 3274.08 and 3247.66 appeared prominently reversed in the water spark. All the water spark absorption lines, including the line 2104.73, were arc reversals with the exception of the eight ultraviolet lines 2135.92, 2130.87, 2125.97, 2122.91, 2112.02, 2054.92, 2043.74, and 2037.06. These were not reversed in the arc. Some of these lines may be seen in the copper spectrogram of Plate I. This spectrogram was chosen because it was more suitable for reproduction than a number of others which extended farther into the ultraviolet.

Lead. The water spark absorption lines matched the arc reversals throughout the region of observation, which extended to 2190 A. Grotrian[6] has observed about fifteen absorption lines in a continuous spectrum passed through lead vapor heated above 1200°C. All of these lines were included in the water spark reversals.

Magnesium. The water spark and arc reversals were in agreement. The magnesium spectrogram of Plate I illustrates various types of absorption lines. In the upper portion, which is of the water spark, the quintette group around 2780 is strikingly reversed. The two lines 2802.80 and 2795.62 of the quadruplet are strongly absorbed and overshadow their weaker neighbors 2798.17 and 2790.99 to such an extent that the reversals of these are seen with difficulty. The $1S-1P$ line, 2852.29, is very diffusely reversed. The lower portion of the spectrogram gives for comparison the condensed magnesium spark in air.

McLennan[7] found absorption in magnesium vapor at 2852.22 and 2026.46. The first of these lines is reversed in both the arc and water spark and the second in neither. The $1S-1p_2$ line 4571.24 is of interest. McLennan did not observe its absorption in magnesium vapor whereas Barratt[8] did very readily. This line is not reversed in the arc or water spark.

[6] Grotrian, Zeit. f. Phys. **18,** 169 (1923)
[7] McLennan, Roy. Soc. Proc. **A 92,** 574 (1916)
[8] Barratt, Roy. Soc. Proc. **A 105,** 221 (1924)

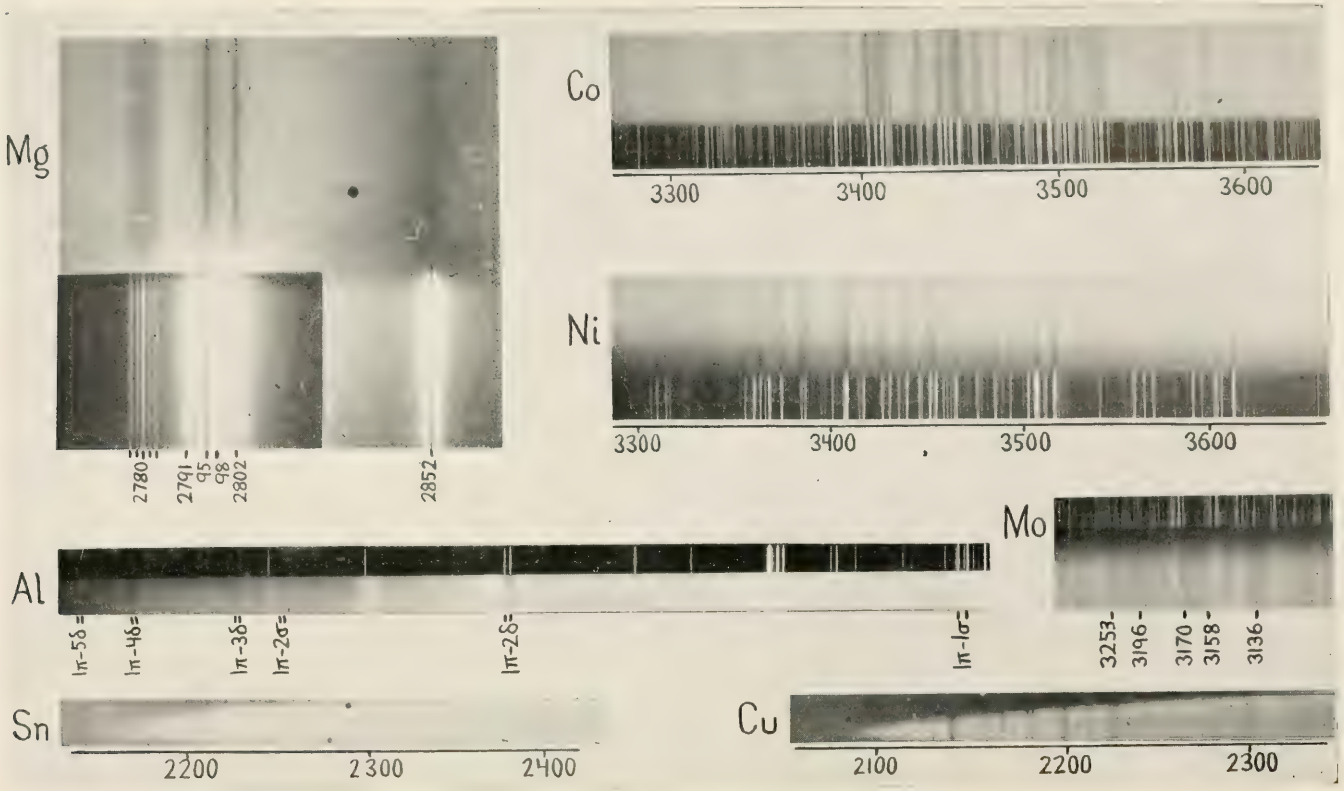

Plate 1 Water spark spectra of various metals

Molybdenum. The seven arc reversals listed by Kayser are included in the water spark reversals as well as three more lines, 3253.89, 2816.22, and 2775.74. The spectrogram of Plate I shows the character of the molybdenum water spark spectrum.

Tungsten. There are no arc reversals reported by Kayser for tungsten. In the water spark we find six lines appearing as absorption lines, namely, (2947.50, 2947.10), 2944.50, 2896.56, (2879.51, 2879.21), 2852.21 and 2830.24. The first and fourth of these lines are doublets and it was not possible to say whether the absorption line referred to one member or to both.

Concluding Remarks

It seems that all the investigations of water spark spectra, including the present one, have been concerned primarily with accumulating data for a large number of metals. These data are often conflicting, which is no doubt to be ascribed to differing experimental conditions. In only one instance has a thorough consideration of a single metal been attempted. Hale[1] has dealt with iron under a great variety of circumstances and found important changes in the character of the water spark spectrum with experimental conditions. It might not be fruitless to study other metals as he has done The difference in the water spark spectra from a high potential source, as a Tesla coil, and from a relatively low potential transformer, as used in the present work, might be examined. Those lines which appear as emission and those which disappear altogether in the water spark perhaps deserve as much scrutiny as the absorption lines.

University of Iowa,
April 5, 1924

Reprinted from Physical Review, pp. 152-157, No. 2, August, 1924

EFFECT OF TEMPERATURE ON THE REGULAR REFLECTION OF X-RAYS FROM ALUMINUM FOIL

By E. H. Collins

Abstract

Effect of temperature on the reflection of x-rays from rolled Al foil.— The powder method of analysis was used, a coil of the foil being placed at the center of the spectrometer in an electric furnace provided with openings for the x-rays. Intensity measurements for the scattered rays, wave-length .710 A, were obtained with an ionization chamber, for temperatures 80°, 310° and 600°C. The scattering curve for 80°C shows peaks at 17.4°, 20°, 28.7° and 33.8° (for planes 111, 100, 110 and 311). These are displaced for the higher temperatures because of the expansion, and are also decreased in intensity, the ratios for I_{600} to I_{80} being respectively .86, .815, .56 and .71. These ratios are considerably less than those predicted by the Debye theory, .94 to .81.

Relative spacing of crystal planes in aluminum rod and foil.— The angles of the peaks are from 0.4° to 0.7° less for the foil than for the rod, showing that the planes in the foil are about 1.5 per cent farther apart as a result of the rolling. This difference is not decreased by heating to 600°C.

1. Introduction

A THEORETICAL study of the change in intensity of general scattered and regularly reflected x-rays with a change in temperature of the scattering material has been made by Debye[1] and by Darwin.[2] Experimentally this effect has been investigated by Bragg,[3] Jauncey[4] and Blackhurst.[5]

This paper is a report of an experimental study of the change of intensity of x-rays regularly reflected from a cylinder of aluminum foil at temperatures 80°, 310° and 600°C.

2. Apparatus and Method

The x-ray spectrometer used was the instrument described by Hewlett.[6] It employed the powder method of x-ray analysis, the relative intensities of the scattered x-rays being measured by an ionization

[1] Debye, Ann. der Physik **43,** 49-95 (1914)
[2] Darwin, Phil. Mag. **27,** 325 (1914)
[3] Bragg, Phil. Mag. **27,** 881 (1914)
[4] Jauncey, Phys. Rev. **20,** 421 (1922)
[5] Blackhurst, Proc. Roy. Soc. **102,** 341 (1922-23)
[6] Hewlett, Phys. Rev. **20,** 690 (1922)

chamber and electrometer. The scattering material was a cylinder. diameter 8 mm, made by a roll of aluminum foil, the amount used being the optimum for maximum reflection.

A furnace of special design, shown by the diagram Fig. 1, was constructed for heating the aluminum. The rotating aluminum cylinder *A* was enclosed in a pocket made from asbestos board with heating strips wound in spiral form at the top and bottom of the pocket. An open space all around the furnace was left for the entrance and exit of the x-rays. The dimensions of the furnace were such tha' the secondary scattering and tert ary radiation reaching the ionization chamber from the materials of the furnace were reduced to a minimum.

To determine the temperature of the aluminum a preliminary experiment was first performed to measure the difference in temperature between a point *T*, Fig. 1, just above and outside the cylinder and a

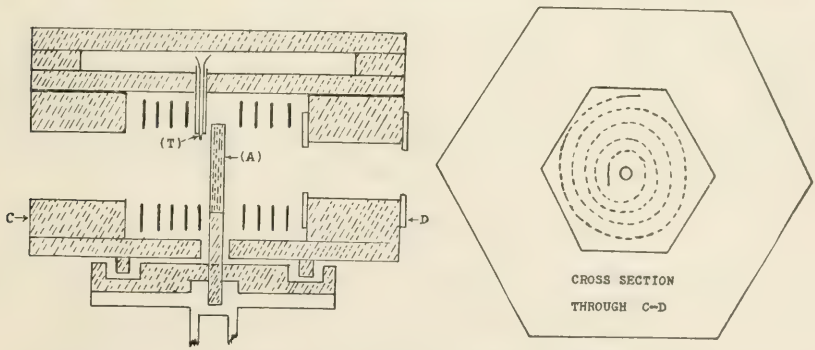

Fig. 1. Vertical and horizontal sections through furnace.

point within the cylinder itself. When observations were in progress it was only necessary to measure the temperature at that point *T* and subtract the difference observed in the preliminary experiment to obtain a very close approximation to the actual temperature of the aluminum. Hoskins chromel-alumel thermocouples and a sensitive millivoltmeter were used in the temperature measurements. The low temperatures were checked with a mercury thermometer.

The intensity of the scattered x-rays was taken as proportional to the rate of deflection of the electrometer. From this rate taken with the aluminum in place was subtracted the rate with the aluminum removed. The latter reading represented the drift of the electrometer plus any scattering of x-rays from the furnace and surrounding objects reaching the ionization chamber.

In obtaining the data for the scattering curves the following method was used: The intensity of the scattered x-rays from the aluminum

cylinder was determined at 80°C over the angular region desired, then the aluminum was heated to the higher temperature (310°C or 600°C) and the observations of intensities again taken over the same angular region; finally the procedure was repeated for aluminum at 80°C. The average of the two intensities at 80°C was plotted on the same set of axes as the intensity for the scattered x-rays at the higher temperature. This procedure was necessary because in the interval of time (about four hours) necessary to take the data for one of these curves the density of methyl bromide gas in the ionization chamber changes slightly. The temperature 80°C was used to save time because a relatively much longer time was required for the aluminum cylinder to cool from 80°C to room temperature due to the presence of the furnace than for the aluminum to cool from 310°C or 600°C to 80°C.

3. Experimental Results

The experimental results are shown graphically by curves I, II, III, IV, Fig. 2 and curve V, Fig. 3 which represent the intensity of the scattered radiation plotted against angle from the incident beam. The arbitrary unit of intensity is not the same in the curves I, II, III, IV because of changes in the density of the methyl bromide gas.

4. Comparison with the Debye Theory

For the purposes of comparison of the experimental results with Debye's theory, Debye's formulas are put in the following form:

$$\log\left(\frac{I_1}{I_2}\right) = 418.\left[\left(1-\cos\phi_1\right)\frac{\varphi\,(x_1)}{\Theta\,x_1} - \left(1-\cos\phi_2\right)\frac{\varphi\,(x_2)}{\Theta\,x_2}\right]$$

for no zero point energy; and a similar formula with $\varphi(x_1)/x_1$ replaced by $(\varphi(x_1)/x_1+1/4)$, and $\varphi(x_2)/x_2$ replaced by $(\varphi(x_2)/x_2+1/4)$ for zero point energy.

Where I_1 = intensity of reflected x-ray at a high temperature;

φ_1 = angle of observation at a high temperature;

x_1 = ratio of the characteristic temperature Θ of the substance to the absolute temperature T.

$\varphi(x_1)$ is a function of Θ/T which Debye evaluates. The letters with the subscripts 2 have a similar meaning for a lower temperature.

A comparison of the observed and calculated ratios of the intensity of regularly reflected radiation at high temperatures to the intensity of the regularly reflected radiation at low temperatures is shown by Table I. The "observed" intensity of the regular reflection is proportional to the length of the ordinate at the crest of the peak minus the length of a

portion due to the general scattered radiation. The value of the portion subtracted is found by plotting the intensities at each side of the peaks as shown, then interpolating graphically for the value of the intensities

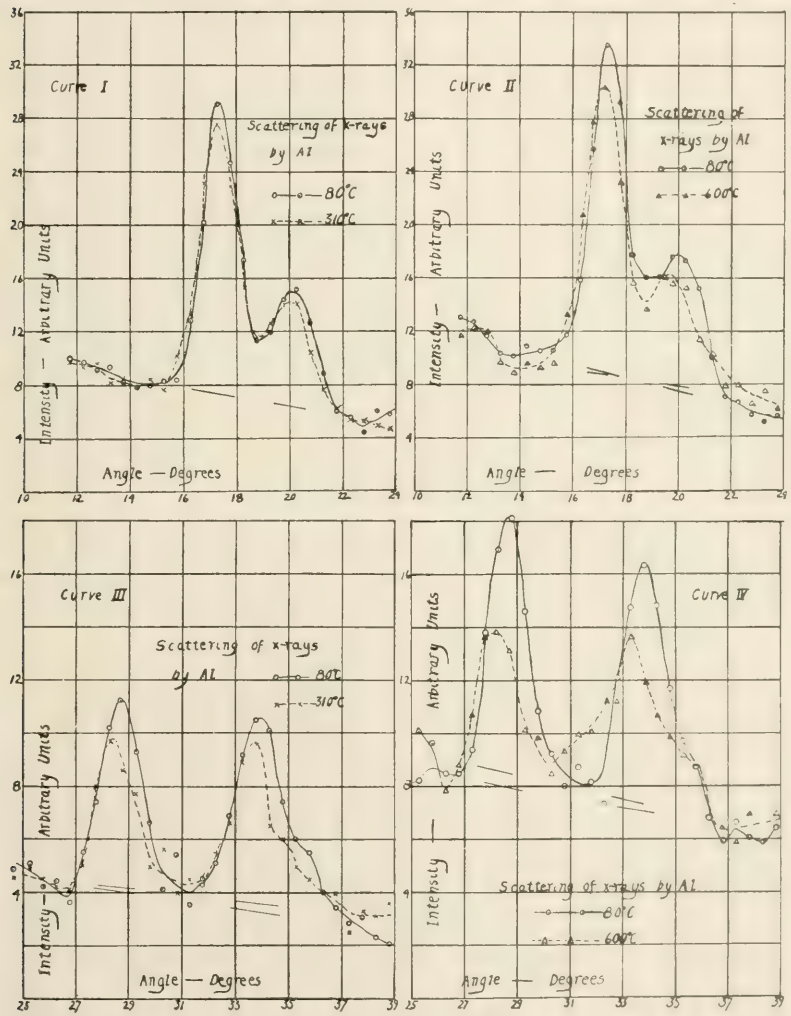

Fig. 2. The temperature effect on the regular reflection of x-rays from aluminum foil.

of the general scattered radiation just under the peaks (see the straight lines directly under the peaks).

In Table I the subscripts indicate the temperature, I the intensity and φ the angle of regular reflection. This table and the scattering curves of Fig. 2 show that there is not satisfactory quantitative agreement with

Debye's theory. The decrease in intensity ratio with increase in temperature is markedly larger than that predicted by Debye's theory. Again the decrease in intensity ratio with increase in angle is larger than that predicted by Debye's theory, and the increase in ratio with angle is contradicted. Debye's theory is therefore inadequate.

TABLE I

Comparison of experimental and theoretical results

φ_{80}	Crystal planes	I_{310}/I_{80} obs.	calc.*	calc.†	I_{600}/I_{80} obs.	calc.*	calc.†
17.4	111	.92	.973	.976	.86	.936	.942
20.	100	.88	.966	.967	.815	.926	.928
28.7	110	.77	.935	.936	.56	.857	.857
33.8	311	.84	.913	.914	.709	.809	.809

* Assuming zero point energy.
† Assuming no zero point energy.

5. Discussion of Details

It is difficult to draw a definite conclusion in regard to the general scattered radiation, because its intensity is too small in comparison with other sources such as the regular reflection of other wave-lengths which get through the zirconium oxide filter.

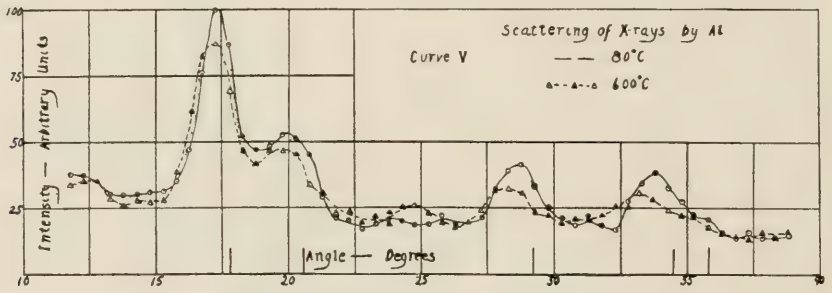

Fig. 3. The relative height and positions of the interference maxima at 80° and 600°C.

Due to the expansion of the crystal, and the resulting change in grating space, the maxima at high temperatures are shifted toward the small angle side. The observed shifts of the maxima are in good agreement with the calculated values.

Curve V, Fig. 3 is a composite of curves II and IV, Fig. 2. This shows the relative heights of the interference maxima.

A discrepancy exists between the angles of the regularly reflected x-ray beams obtained by A. W. Hull[7] and the angles obtained in this experiment. The angles obtained by Hull are indicated by the short lines ruled on the angle axis of curve V. This means that the crystal structure of aluminum was changed, the distance between the planes being increased, by rolling the aluminum into foil. The scattering from an aluminum rod gave results which were in agreement with Hull's values; this shows that the difference between the values here obtained and those of Hull is not due to experimental error. This effect has been noticed by J. Czochralski.[8]

In conclusion the writer wishes to express his appreciation to the Physics Department of the State University of Iowa for valuable assistance, especially to Professor G. W. Stewart under whose direction the work was carried on, and also to acknowledge indebtedness to Dr. C. W. Hewlett, now of the General Electric Company, whose x-ray spectrometer was used.

University of Iowa,
Iowa City, Iowa,
April 12, 1924.

[7] Hull, Phys. Rev. **10**, 661 (1917)
[8] Czochralski, Science Abstracts, No. 2035, 1923.

Reprinted from the Journal of the Optical Society of America and Review of Scientific Instruments, Vol. 9, No. 3, September, 1924

THE INTRINSIC INTENSITY AND POLARIZATION OF LIGHT AFTER PASSAGE THROUGH DEEP SLITS

By L. P. Sieg

Some three years ago A. T. Fant and myself[1] made a brief investigation of the intrinsic intensity possessed by light after passage through deep slits or channels between polished steel walls. A rough calculation indicated that our results agreed fairly well with theory. Later Mr. C. R. Smith[2] under my direction undertook a similar problem in which work he used, in addition to steel, Cu, Ag, Au, and Ni for the walls of the deep channels, applying these latter substances to the original steel by successive electrodeposition. He obtained distinct variations among the different metals used, which at the time of performing the experiments had not been checked by any theory. In order to obtain a check on Smith's results, and in order to investigate the phenomenon of polarization arising from the passage of light through these deep channels, I have somewhat revised and extended the simple theory given previously.[3]

The only similar work that I can discover, and which only remotely resembles the present problem, is found in two papers by the late Lord Rayleigh.[4] In these papers the passage of waves through perfectly conducting, infinitely thin slits, whose breadth, $2b$, is of the order of, or less than, the wave-length of light, was discussed. That problem, as Rayleigh states, is extremely difficult, so difficult in fact that he had to resort to rather laborious numerical calculations in order to arrive at his results. The present problem is even less amenable to exact rigorous calculation. However, a fairly rough, though apparently physically sound method, that agrees fairly well with experiment, where there have been experiments to test the matter, is here discussed. In addition the theory enables one to predict the per cent of polarization of the transmitted light. It is hoped in the near future to test this latter aspect by direct experiment.

Referring to Fig. 1, L denotes the depth of the channel, w its width, θ an angle of diffraction of a pencil of light from a random point in the

[1] Sieg, L. P. and A. T. Fant, J. O. S. A., *5*, p. 218; 1921.
[2] Smith, C. R., J. O. S. A. and R. S. I., *7*, p. 1069; 1923.
[3] Sieg and Fant. Loc. cit.
[4] Rayleigh. Roy. Soc. Lond. Proc., A, *89*, p. 194; 1913-14. Phil. Mag., *43*, p. 259; 1897.

opening of the slit, and m the number of reflections of this pencil before emergence. It is fairly obvious that with a given angle of diffraction not all the light over the width of the slit will suffer the same number of reflections. However, in any given case, a certain portion of the wave will have m reflections, while the remainder will have $m+1$ reflec-

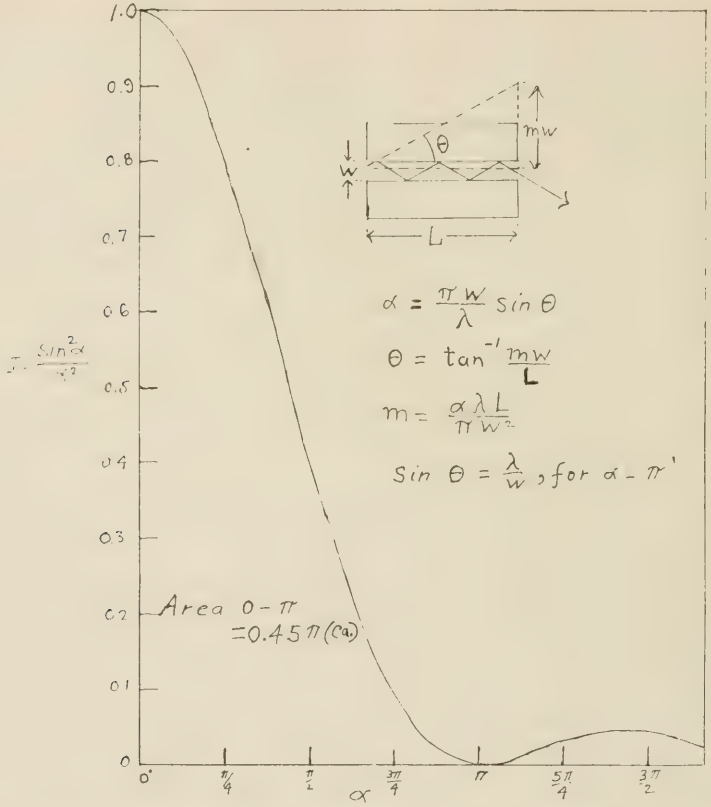

FIG. 1. *Intensity of light diffracted from a narrow slit. Diagram of deep slit, showing relations among width and depth of slit, the angle of diffraction, and the number of reflections.*

tions. The relative intensity of light diffracted in a certain direction is given by the well-known expression, $\sin^2 a/a^2$, where a is an auxiliary angle given by

$$a = \frac{\pi w}{\lambda} \sin \theta \tag{1}$$

where λ is the wave-length of the light. It is easily seen that

$$\theta = \tan^{-1}\frac{mw}{L} \tag{2}$$

since θ is usually small one can substitute tan θ for sin θ and we have from equations (1) and (2),

$$m = \frac{a\lambda L}{\pi w^2} \tag{3}$$

In the same Fig. 1, we have the usual curve where the relative intensity I is plotted against the angle α. The area under the curve from 0 to ∞ is 0.5π, and from 0 to π is approximately $.45\pi$. Hence if we let α vary merely from 0 to π we shall be accounting for most of the total intensity of the diffracted light. The limiting angle θ corresponding to $\alpha = \pi$ is easily seen from (1) to be given by

$$\sin\theta = \frac{\lambda}{w} \tag{4}$$

At this point, the solution of the problem of finding the intrinsic intensity and the state of polarization of light passing through a typical deep slit can best be explained by considering two typical examples. Suppose we are dealing with a slit between steel jaws. $w = 0.0001$ cm, $\lambda = .00006$ cm and $L = 0.1$ cm. From (3) we find, for $\alpha = \pi$, that $m = 600$. The extreme diffracted light thus suffers 600 reflections. It would appear at first thought that no light could suffer 600 reflections and still possess any intensity, but we must remember that we are dealing with angles of incidence approaching grazing incidence, and that for such angles the reflecting power of even ordinary reflectors is nearly unity. To be sure, in this case we easily see that we cannot go as far as 600 reflections but we shall use as many as 96. The results are arranged as shown in Table 1.

TABLE 1

$\frac{\alpha}{\pi}$	m	$\theta°$	$\phi° = 90 + \theta°$	h	$R_\perp$	R_{II}	$I_\perp = h.R_\perp$	$I_{II} = h.R_{II}$
0	0	0	90	0.5	1.00°	1.00°	.500	.500
.02	12	0.75	89.25	0.49	$.99^{12}$	$.883^{12}$	.441	.111
.04	24	1.50	88.50	0.48	$.983^{24}$	$.772^{24}$	.329	.001
.06	36	2.25	87.75	0.48	$.98^{36}$	$.685^{36}$	.226	
.08	48	3.00	87.00	0.47	$.97^{48}$	$.613^{48}$	.111	
.10	60	3.69	86.31	0.46	$.966^{60}$	$.553^{60}$	.058	
.12	72	4.43	85.57	0.45	$.96^{72}$	....	.023	
.14	84	5.17	84.83	0.44	$.95^{84}$	....	.006	
.16	96	5.91	84.09	0.44	$.942^{96}$	....	.001	

The column headed α contains certain values of α from 0 to such a value (in this case $.16\pi$) that will not yield too large a value for m. Under m we have the number of reflections corresponding to the various

values of α. ϕ is the angle of incidence corresponding to the angle of diffraction, θ. h is 1/2 the mean ordinate of the curve of Fig. 1. It is a measure of the intensity of the light diffracted through the angle θ. The half ordinate is selected, because it is assumed that half the incident intensity is due to light with the electric vector parallel to the length of the slit, and half perpendicular to the length. On viewing it in another way, half the light has its electric vector perpendicular to the plane of incidence, and half parallel to it. The columns headed R and $R_{\parallel}$ represent the reflecting powers of steel at the given angles of incidence for the electric vector perpendicular and parallel respectively to the plane of incidence. These values for R are obtained from the well-known expressions[5]

$$R_{\perp}=\frac{n^2(1+\kappa^2)-2n\cos\phi+\cos^2\phi}{n^2(1+\kappa^2)+2n\cos\phi+\cos^2\phi} \tag{5}$$

$$R_{\parallel}=\frac{n^2(1+\kappa^2)\cos^2\phi-2n\cos\phi+1}{n^2(1+\kappa^2)\cos^2\phi+2n\cos\phi+1} \tag{6}$$

These values of R for steel for three wave lengths, 0.325μ, 0.600μ, and 1.5μ are plotted in Fig. 2, for certain angles of incidence. In equations (5) and (6), n represents the index of refraction, κ the coefficient of absorption, and ϕ the angle of incidence. The columns of Table 1 headed $I_{\perp}$ and $I_{\parallel}$ are formed by multiplying together the appropriate values of h and R. Specifically, the number .329 in the column under $R_{\perp}$ means that for this particular pencil, diffracted at 1.5°, there were 24 reflections; the coefficient of reflection is .983, and the half ordinate of the curve of Fig. 1 is 0.48. Thus this particular pencil of light emerges with an intensity given by $0.48\times.983^{24}$, or .329. The corresponding emergent intensity of the pencil vibrating in the plane of incidence is only .001. Thus the relatively strong polarization of this particular pencil is accounted for. Now we can look upon the numbers in the columns headed $I_{\perp}$ and $I_{\parallel}$ as ordinates of two curves, the abscissas being given by the values of α. The ratio of the sum of the areas under these two curves from $\alpha=0$ to the highest value of α used to the area under the curve of Fig. 1 will give the intensity of the transmitted light relative to that of the incident light. Again the ratio of the difference of the areas under the two I curves to their sum will give the fraction of polarization of the transmitted light. Resorting to our example in Table 1, we can get the areas under the I curves sufficiently well by

[5] Winkelmann, Handb. d. Phys. 1st Ed. p. 824.

taking the means of the ordinates in pairs, multiplying each mean by the base (in this case $.02\pi$) and summing the products; or what amounts to the same thing, summing the means, and multiplying the sum by $.02\pi$. Performing this operation we have $\Sigma[I_\perp] = 1.454$ and $\Sigma[I_\parallel] = 0.366$, where the brackets indicate that means are used. Multiplying each of these by $.02\pi$ we have the two relative intensities

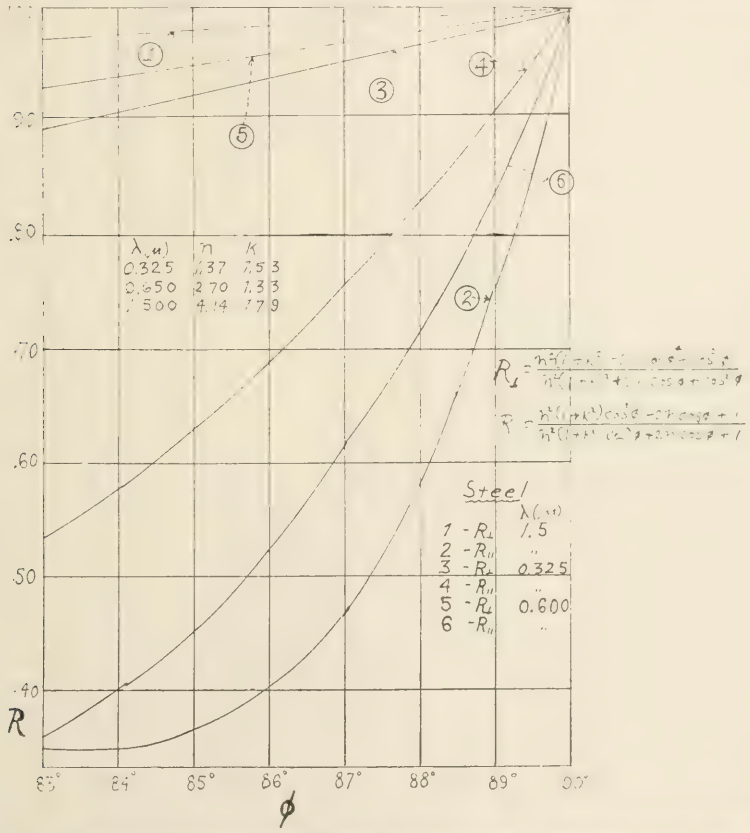

FIG. 2. *The coefficients of reflection of steel for large angles of incidence, for the electric vector both perpendicular, and parallel to the plane of incidence. List of optical constants for which these reflection coefficients are calculated.*

$.0291\pi$ and $.0072\pi$ respectively. Adding these and dividing by 0.45π, the area under the curve of Fig. 1 from $\alpha = 0$ to $\alpha = \pi$, we get .081 or a transmission of 8.1% of the incident intrinsic intensity. Dividing the difference of $.0291\pi$ and $.0072\pi$ by their sum, and expressing in per cent, we get a percentage of polarization of 60.3. This same method is followed for all cases where m is large. Where m is small the procedure

is somewhat different, as will be illustrated by the following case, the details of which are given in Table 2.

Again dealing with steel, let $L = 0.0025$ cm, $w = 0.0001$ cm, and $\lambda = 0.00006$ cm. We find, as shown above, that m for $\alpha = \pi$ is 15, and θ for this value of α is 36.9°.

TABLE 2.

α/π	m	$\theta°$	$\varphi°$	h	$R_\perp$	$R_{\shortparallel}$
0	0	0	90	0.5	(1.000)°	(1.000)°
0.1	1.5	3.69	86.31	0.46	$.5(.968)^1+.5(.968)^2$	$.5(.550)^1+.5(550)^2$
0.2	3.0	7.38	83.62	0.43	$(.926)^3$	$(.340)^3$
0.3	4.5	11.07	78.93	0.36	$.5(.890)^4+.5(.890)^5$	$.5(.280)^4+.5(280)^5$
0.4	6.0	14.76	75.24	0.28	$(.863)^6$	.....
0.5	7.5	18.45	71.55	0.20	$.5(.833)^7+.5(.833)^8$	.....
0.6	9.0	22.14	67.86	0.13	$(.805)^9$	.....
0.7	10.5	25.83	64.17	0.07	$.5(.780)^{10}+.5(.780)^{11}$	.....
0.8	12.0	29.52	60.48	0.03	(.755)12	.....
0.9	13.5	33.21	56.79	0.005	$.5(.730)^{13}+.5(.730)^{14}$	.....
1.0	15.0	36.90	53.10	0	0	.....

Table 2 is not complete for it is intended to illustrate merely the variation in procedure from that discussed in connection with Table 1. For example under the column headed "$R_\perp$", the second line, we note that we have to deal with $m = 1.5$, i.e., one and one-half reflections. This is equivalent to saying that 0.5 of the incident wave front suffers one reflection, and 0.5 of it two reflections. Had m been 2.37 we should have had 0.63 of the wave front reflecting two times and 0.37 of it reflecting three times. The remainder of the procedure is now clear. We obtain the value as listed under the R columns, multiply each by the proper h, and form the $I_\perp$ and $I_{\shortparallel}$ columns (not shown in the table). Then the areas are found under these two I curves as before. The result for this case gives a transmitted intensity of 43.2%, and a percentage of polarization of 51.2. The reflecting coefficients for the various angles of incidence, ϕ, are calculated by formulas (5) and (6). The reflecting coefficients for certain large values of ϕ for the metals Cu, Au, Ag, Ni, Fe, and Si are plotted in Fig. 3. On this same figure are listed the per cent transmission and per cent polarization for all these substances where in each case the wave-length is 0.6μ, $L = 1$ cm, and $w = .001$ cm. It will be noted what appears as obvious, that the greater the difference between the $R_\perp$ and $R_{\shortparallel}$ coefficients, the greater the percentage of polarization, whereas the percentage of transmission is proportional to the absolute magnitudes of $R_\perp$ and $R_{\shortparallel}$. Thus a slit

having silicon jaws would produce the greatest polarization, gold the least; and silver and silicon, of the substances tested, would represent the extremes of transmission.

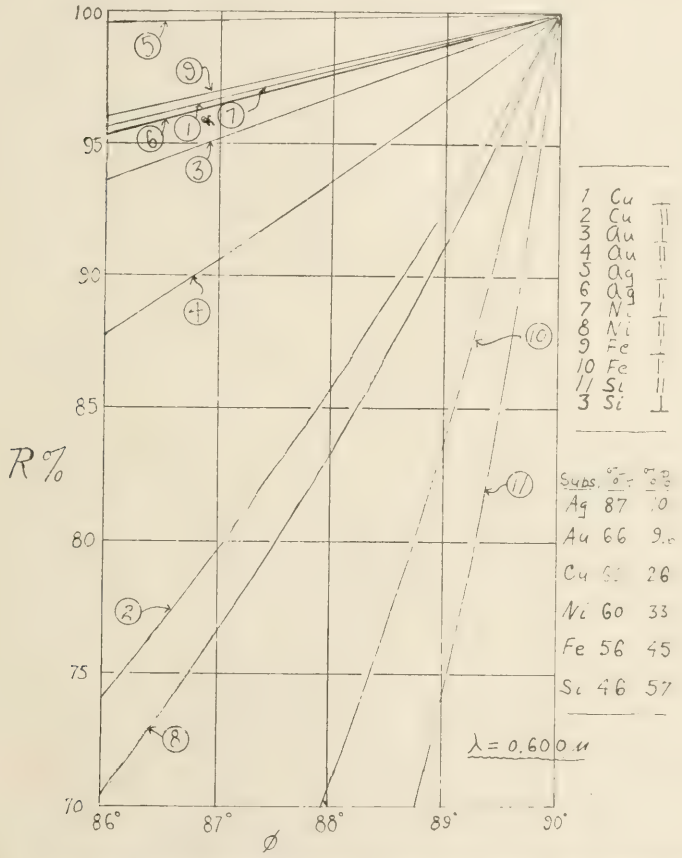

FIG. 3. *Coefficients of reflection with the electric vector both parallel and perpendicular to the plane of incidence for the substances Cu, Au, Ag, Ni, Fe, and Si. Also table of per cent transmission and polarization for these substances for a given deep slit.*

It is interesting to compare the variation of polarization and transmission, with the separate variation of the three variables, λ, L, and w. These variations for steel are shown respectively in Figs. 4, 5, and 6. In Fig. 4, we note that the polarization increases with the increase of wave-length in the range chosen, whereas the transmission decreases. We note (Fig. 5) a similar variation in these two quantities when L is the variable. If one wanted, for example, to design a deep slit for large polarization coupled with a fairly large transmission, he would have

to choose some intermediate length. Large intensity and high per cent of polarization are not simultaneously consistent. In Fig. 6 we note that the polarization decreases rapidly with increasing width, whereas the transmission increases from 0 to its final constant value of unity, only after a certain relatively large width of jaws.

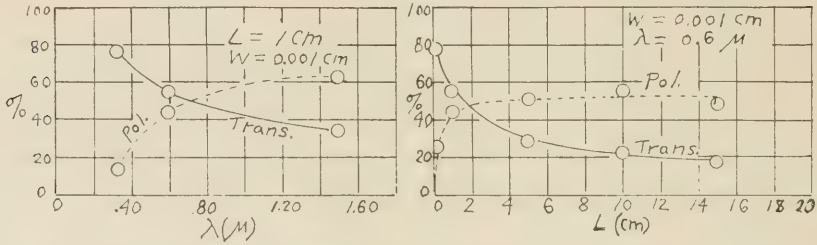

FIG. 4. *The transmission and polarization with a given deep slit, as the wave-length λ is varied.*
FIG. 5. *The transmission and polarization with a given deep slit, as the depth L of the slit is varied.*

The results for transmission as indicated in Figs. 5 and 6 have been well verified[6]; those of Fig. 4 for transmission are not in agreement with experiment. No experimental results for polarization have been obtained. It is hoped to try these soon to see if they will check the above calculations. Recently Smith[7] performed some experiments in this laboratory, the results of which should, if our theory is correct, be com-

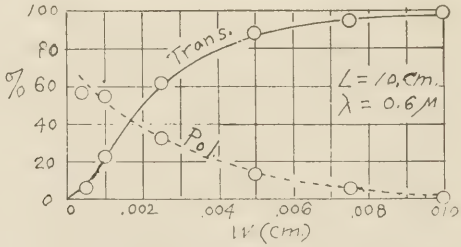

FIG. 6. *The transmission and polarization with a given deep slit, as the width W of the slit is varied.*

parable with the results for transmission listed in the table shown in Fig. 3. The agreement between these is not very satisfactory. It must be noted, however, that the calculated results are all based on certain optical constants for these various metals. Our tables of optical constants show wide variations in these constants among the results of different observers. Dealing as we do with large angles of incidence,

[6] Sieg and Fant. Loc. cit.
[7] Smith. Loc. cit.

the reflecting coefficients must be very sensitive to conditions as they are no doubt very much dependent upon the state of the reflecting surface—its polish, contamination, scratches, etc.

This problem has probably but little practical importance. It does lend us a bit of caution in measuring polarization and intensity of a source of light by means of any apparatus by which the light is made to pass at any point through a fine or a deep slit, as this slit itself introduces its own selective changes in both intensity and polarization.

THE UNIVERSITY OF IOWA,
MAY, 1924.

Reprinted from PHYSICAL REVIEW, pp. 658-665, No. 6, December, 1924

MAGNETIC PROPERTIES OF THIN FILMS OF FERROMAGNETIC METALS PRODUCED BY THE EVAPORATION METHOD

By A. J. Sorensen

Abstract

Magnetic properties of thin films of iron, nickel and cobalt.—The films were deposited by the evaporation method on tin or aluminum foil, and the magnetic properties studied by an induction method for fields up to 139 gauss. The thickness of the films varied from 20 to 300 millimicrons (mμ). The results are as follows. (1) The maximum value of the intensity of magnetization is of the same order of magnitude as for bulk metal. In the case of cobalt, however, it is evident from the curve that with higher fields values higher than any heretofore attained might be secured. The magnetization is independent of the crystal size and the thickness of the film. (2) The remanence is high for iron and cobalt. For nickel a low value was obtained, perhaps due to oxidation. The remanence depends on the crystal size but not on the thickness. (3) The coercive force is high for all three metals and changes abruptly to lower values as the thickness is increased beyond a critical value, which for iron, cobalt and nickel is about 55, 70 and 200 mμ respectively. The high values of the coercive force may be due to the minute size of the crystals in the films. (4) The results combined with Steinberg's curves for the Hall effect in films, tend to contradict Kundt's conclusion that the Hall e.m.f. is proportional to the intensity of magnetization.

THE present work is an investigation of the magnetic properties of thin films of iron, nickel and cobalt, similar to those which were investigated in regard to Hall effect by J. C. Steinberg[1] and which in some respects gave remarkable results.

Method and Apparatus

The method used was similar in principle to one used by Kaufmann and Meier,[2] in which the intensity of magnetization was obtained by measuring the change of flux through a search coil, which was situated in a constant magnetic field, when the magnetized specimen was removed from the search coil. The arrangement of the instruments is shown in Fig. 1.

To obtain the sensitiveness required by the very small amount of metal available (one continuous operation of the evaporating device

[1] Steinberg, Phys. Rev. **21**, 22 (1923)
[2] Kaufmann and Meier, Phys. Zeit. **12**, 513 (1911)

yielding only about one milligram of metal), the scheme illustrated in Fig. 2 was adopted.

In Fig. 2, the switches S_1 and S_2 are both in series with the galvanometer and search coil. The rubber band R is under considerable tension

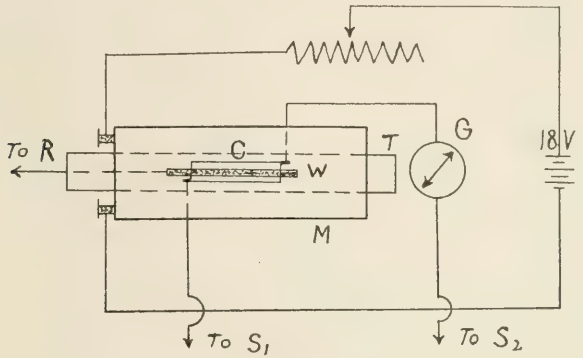

Fig. 1. Experimental arrangement.

and can be held in the position shown in Fig. 2 by the rod A which has a little metal ring slipped loosely over it, through which R passes. Before a reading is to be taken, the switches are set as shown in the figure and R is connected by a string to the specimen in the search coil. Then the

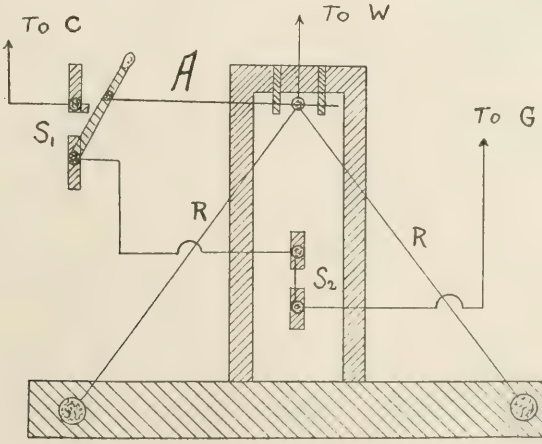

Fig. 2. Circuit controlling device.

operator closes S_1, A slides ahead and releases the ring retaining R in place, and R moves back toward S_2 and pulls the specimen out of the search coil. When R reaches S_2 it catches the handle (not shown in the figure) and opens the switch so that the circuit is again open. The length

of the time interval during which the circuit is closed can be varied by varying the position of S_2. Devices of a similar nature have been used by Wwedensky,[3] Gildemeister[4] and Wilson.[5]

In order to test the validity of the method and at the same time calibrate the set-up, the rod A in Fig. 2 was connected to the handle of a switch which was inserted in the circuit containing the magnetizing coil, so that small changes in the field through the search coil could be made and the corresponding deflections read. The deflections proved to be proportional to the deflecting currents and to be independent, within reasonable limits, of the tension on R and the position of S_2.

The deposits were made in a device described by Steinberg,[6] provided with a few minor changes, on tin or aluminum foil approximately 7.5 by 2.5 cm. The weights of the deposits were determined by weighing the foil before and after deposit, and the thicknesses were computed assuming the value of density in bulk. After this had been done, the foil was rolled upon a thin thread so as to form a uniform cylinder, 7.5 cm long and thin enough to be inserted in the search coil.

The iron used in this investigation was a sample of Armco iron, which, according to an analysis furnished by the makers (Page Steel and Wire Co., Bridgeport, Conn.) is 99.874 per cent pure. The nickel was furnished by Baker & Co. and contained, according to an accompanying analysis, 0.27 per cent iron, 0.05 per cent copper, and 0.004 per cent manganese. Cobalt wire was made by electrolytic deposition on a one mil tungsten wire by a method described by Langbein and Brannt in "Electrodeposition of Metals." These deposits presented a very bright surface but were exceedingly brittle so that great care had to be taken not to put any strain on them in inserting them in the evaporation device.

Experimental Results

In Table I the results obtained for the three metals will be found. The following symbols are used:

δ = thickness of film in millimicrons ($m\mu$);
d_m = deflection for $H = 139$ gauss;
B_m = magnetic induction for $H = 139$ gauss;
B_r = remanence;
H_c = coercive force for a cycle in which the maximum value of the field was 139 gauss.

[3] Wwedensky, Ann. der Phys. **66,** 110 (1921)
[4] Gildemeister, Ann. der Phys. **23,** 401 (1907)
[5] Wilson, Phys. Soc. Proc. **34,** 55 (1922)
[6] Steinberg, loc. cit.[1]

TABLE I. Experimental data.

Experimental data for iron, nickel and cobalt films.

	δ	d_m	B_m	B_r	H_c
Iron	14	16	16800	87 per cent	111
	26	34	19000	88	116
	32	45	20400	88	91
	39	66	23800	91	96
	40	63	22900		114
	55	78	22100	83	99
	59	108	26000	89	39
	74	125	24400	88	45
	98	148	22000	93	53
	150	222	21500	90	43
Nickel	51	6	1725	33 per cent	
	61	6	1460		105
	93	16	2530	55	77
	194	37	2710	54	75
	207	51	3280	59	56
	215	43	2830	53	61
	268	57	3070	56	62
	295	60	2890	58	55
Cobalt	18	22	16100	74 per cent	89
	22	32	19200	83	75
	25	33	17900	76	83
	36	40	14400	88	73
	63	78	16200	76	83
	77	91	16100	62	34

It will be seen that for each metal the films can be divided into two groups according to the coercive force. Fig. 3 represents the hysteresis curves obtained for one specimen from each group of iron films.

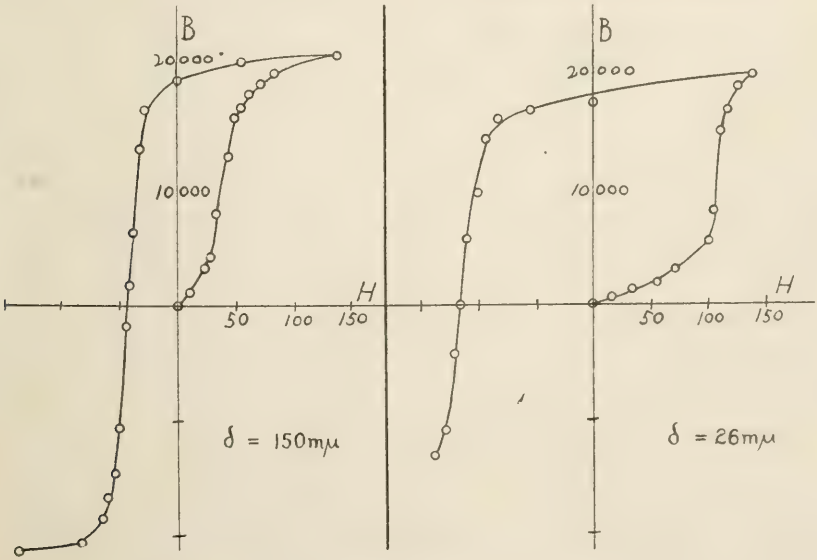

Fig. 3. Hysteresis curves for iron films.

It will be noticed that the thinner of the two films does not give a symmetric hysteresis curve. This is due to the fact that the maximum value of the field was not far enough beyond the coercive force to produce symmetry.

The lapse of time had very little influence on the magnetic properties of the films. While a slight decrease in permeability could be detected in the iron films four weeks after the first test was made, no change was detected in the remanence or coercive force of any of the three metals.

All of the cobalt films and some of the iron films acquired a magnetic moment during the process of deposition, which in some of the films amounted to as much as one-fourth of the moment due to the maximum field used in the tests, $H = 139$ gauss.

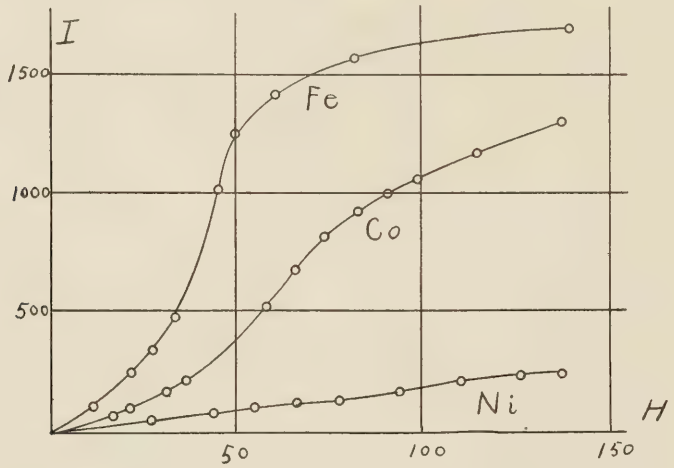

Fig. 4. Magnetization curves for films of iron, nickel and cobalt.

Discussion of the Results

In Table II and Fig. 4 are exhibited the most important results obtained.

Table II

Collected results for all metals.

	I_m	I_r	H_c
Fe.....	1700	90 per cent	43
Ni.....	234	56	62
Co.....	1300	62	34

The values in the table are taken from the thicker groups of films in Table I. I_m and I_r are the maximum and the remanent values, respectively, of the intensity of magnetization.

In regard to the maximum value of I_m, the iron films appear not to be different from bulk iron. In the case of nickel I_m falls considerably below the accepted value for bulk metal (400, according to the Landolt-Börnstein tables). This is probably due, at least in part, to the very slow increase of I with the field. It may also be due, in part, to oxidation of the metal at the high temperature, which manifested itself during the process of deposition in a dull surface without metallic luster and which is largely responsible for the all too great irregularities in the B_m column of Table I.

In the cobalt films I_m reaches considerably higher values than are ordinarily given for bulk metal. Thus, Ewing[7] gives $I=800$ for $H=140$; Fleming, Ashton and Tomlinson[8] give 650 for $H=114$; Rowland[9] gives a still lower value. The samples used in these cases, however, contained considerable amounts of impurities. It therefore appears that cobalt is capable of a higher intensity of magnetization than has been heretofore attained. Moreover, the curve for cobalt in Fig. 4 indicates that still higher values might be obtained if stronger fields were applied.

In connection with the above results it should be noted that in work on thin films of electrolytic iron I_m has in all cases been found lower than for bulk iron.[10] Leick[10] investigated nickel and cobalt as well as iron and found for both approximately the same value as given for nickel in Table II. This low value for cobalt Leick explains as due to sponginess of the deposits.

The most remarkable result in Table II is the high value of the coercive force for all three metals. An explanation of this may perhaps be looked for in the crystalline structure of the films. It has been shown[11] that the size of the crystal granules in the metal has great influence on the specific resistance and the coercive force of iron but that the remanence and the maximum value of the magnetization are practically unaffected by changes in crystal size. Over a considerable range of crystal size the resistivity and the coercive force were both found to be linear functions of the number of crystals per unit length.

There is evidence[1] that the films are crystalline, but that the crystal granules are very small. Thus, Steinberg found evidence of crystal structure in iron films by an x-ray method, but failed to find any such

[7] Ewing, Magnetic Induction in Iron and Other Metals.
[8] Fleming, Ashton and Tomlinson, Phil. Mag. **48,** 271 (1899)
[9] Rowland, Phil. Mag. **48,** 271 (1874)
[10] Kaufmann and Meier, loc. cit.[2];
Leick, Ann. der Phys. **58,** 691 (1896);
Schild, Ann. der Phys. **25,** 586 (1908)
[11] Thompson, Phil. Mag. **31,** 357 (1916)

structure under the microscope. This fact, together with the very high specific resistance of the films,[1] indicates that the crystal granules are very small. Therefore, according to the investigation of Thompson cited above, we should expect to find a high value for the coercive force.

The abrupt change in the coercive force at a certain thickness of film recalls the work of Maurain,[12] who found that when iron was deposited in a constant magnetic field, the magnetic moment of the deposit did not increase in proportion to the amount deposited until the thickness of the deposit was about 80 mμ. For nickel the same was found to be true, only in this case the critical thickness was 200 mμ. On the molecular field theory this is taken to mean that at those thicknesses the molecular field reaches a constant value, or, in other words, at those thicknesses the magnetic properties of the metal become definite. The present results may be taken to be in support of this theory in so far as a definite change is here found at a certain thickness, in one of the magnetic properties, namely,the coercivity. Since, however, the other magnetic properties do not change, the evidence is far from conclusive.

Assuming that the size of the crystals in the films is different from the size of those in bulk metal, the conclusions to be drawn are

(1) The maximum intensity of magnetization is independent of the size of the crystals and also of the thickness.

(2) The remanence depends on the crystal size but not on the thickness.

(3) The coercive force depends on the crystal size and also, in the way indicated above, on the thickness.

The above conclusions agree with the work of Thompson cited above, except in the case of the remanence, in which Thompson found no variation. This may have been due to the facts (1) that the crystals in his samples were very much larger than those in the films, and (2) that the range of sizes that he investigated was relatively small. It is interesting to note that the recent work on permalloy[13] and silicon steel[14] bears out the above conclusions.

On the basis of the results of an investigation[15] in which Kundt proved the Hall e.m.f. in ferromagnetic metals to be proportional to the rotation of the plane of polarization, and the results of an investigation by Du Bois,[16] in which the magnetic rotation of thin films of ferromagnetic metals was shown to be proportional to the intensity of magnetization

[12] Maurain, Jour. de Phys. **10,** 123 (1901)
[13] Arnold and Elmen, Bell Technical Journal, July 1923.
[14] Yensen, Am. Inst. Elec. Eng., May and June, 1924.
[15] Kundt, Ann. der Phys. **49,** 257 (1893)
[16] Du Bois, Ann. der Phys. **31,** 941 (1887)

of the metals in bulk, Kundt drew the conclusion that the Hall e.m.f. is also proportional to the intensity of magnetization. If the Hall e.m.f. is plotted against the external field into which the experimental material is introduced, the curve rises rapidly at first as the field increases to a value roughly equal to 4π times the maximum value of the intensity of magnetization of the bulk metal. From this point on the curve rises only slightly as the field is further increased.

A. W. Smith[17] confirmed Kundt's results; however, in extending the investigation to higher temperatures he found the permeability and the Hall e.m.f. to vary in different ways with the temperature. Hence, the Hall e.m.f. cannot be expressed at various temperatures in terms of the permeability alone.

Steinberg[1] studied the Hall effect in thin films of evaporated iron and, in plotting the Hall e.m.f. against the external field, obtained a curve of the same general shape as those obtained by Kundt and Smith. However, the bend in the curve occurred when the external field had reached a value of 10,000 gauss, and the curve rose only slightly as the field was further increased. It was therefore inferred that the maximum value of the intensity of magnetization in the films was given, approximately, by

$$4\pi I_m = 10{,}000$$

so that I_m would be only about one-half of the value for bulk iron.

It will be seen that the present results do not support this conclusion. However, it must be borne in mind that in the study of the Hall effect the field is at right angles to the plane of the film, while the magnetic properties were measured in a direction parallel to it. Until the magnetic properties of the films have been studied at right angles to the film, the question can hardly be regarded as settled. However, until then the present results at least leave a doubt as to the proportionality between the Hall e.m.f. and the intensity of magnetization, even at room temperature.

In conclusion, the writer wishes to thank the members of the Department of Physics at the State University of Iowa for their assistance and interest, and especially Professor G. W. Stewart, under whose direction the work was carried on.

STATE UNIVERSITY OF IOWA,
August 7, 1924.

[17] A. W. Smith, Phys. Rev. 30, 1 (1910)

Obtainable from the University
Editor; Price $0.75